Vol. 51 • No. 3

March 2008

Microwave Journal

www.mwjournal.com

MICROWAVE JOURNAL 50 years 1958 2008 as the Industry Standard

Test, Measurement and CAD

Parametric Diode Q Measurements

Measuring Scattering Parameters

Radiated Performance of Mobile WiMAX Devices

horizon house®
Founded in 1958

VCOs

10 to 6740 MHz from $11.95 ea. (qty. 5)

RoHS COMPLIANT
RoHS models available, consult factory.

Want a miniature surface mount, shielded plug-in, or rugged connectorized voltage controlled oscillator with the right stuff for your project ? Contact Mini-Circuits! From custom designs to standard catalog models ***always in stock***, we'll supply extra robust, 100% tested VCO solutions you need at a price you can afford. Choose from narrow, to broad, to octave bandwidths. Select from models with low phase noise, linear tuning, load insensitivity, dual output, wide modulation bandwidths, or 5V models optimized for PLL ICs and synthesizers. And pick from an innovative array of miniature surface mount packages as small as 0.25" square, all featuring our exclusive glue-down process on each circuit component to give you ultimate reliability during reflow soldering. You can quickly find the model you need using our online catalog or "The YONI2 Search Engine" at the Mini-Circuits web site. Just enter your specs into YONI2…click…and immediately start evaluating suggested VCO solutions using the actual measured performance data displayed. But perhaps you need a custom design. Not a problem! Contact us for our fast response, low prices, and quick turnaround. For your commercial, industrial, and military applications, choose Mini-Circuits VCOs!

Mini-Circuits ...we're redefining what VALUE is all about!


Mini-Circuits


THE HEART
OF YOUR
SWITCHING NETWORK
IN A COMPLETE RF SOLUTION
DowKey Microwave
From Start To Finish, Dow-Key Adds Experience to Your Signal Routing Needs With Our Relays, Matrices, and Custom Full Switch Networks with Integrated Components.
CONTACT DOW-KEY TODAY
(805) 650-0260
email: askdk@dowkey.com
www.dowkey.com
Visit http://mwj.hotims.com/16339-40 or use RS# 40 at www.mwjournal.com/info
Who's at the heart of your system?
microwave products group
Join Us at the NAB Show in Las Vegas, NV (April 14-17) at Booth #C5945
Dow-Key® Microwave
CORPORATION
A DOVER COMPANY


Helping Customers Innovate, Improve & Grow
VI VECTRON INTERNATIONAL
A DOVER COMPANY
Our Markets
Medical
Industrial
Wireline
Military
Space
Wireless
Products for
Wireless Applications
Today and tomorrow's network requires precise timing. Our Disciplined Oscillator Modules help you meet your stringent timing requirements. We can work with you to design a custom solution that fits your applications needs and get your end product to market quickly with unparalelled quality.
Signal in
Signal out
Disciplined Oscillator Module
SAW
VCSO
VCXO
FX
OCXO
TCXO
CDR
Timing
XO
Vectron International is both a product manufacturer and a solutions provider, leading with our advanced packaging and established crystal and SAW technology. These innovations and capabilities reflect the trend towards higher frequencies, lower cost designs and unique integrated solutions. Our goal is to help you innovate, improve and grow your business.
• In-house ASIC Design Team
• Crystal Design Capabilities
• HFF Crystal Capabilities
• SAW Fabrications
• QRM™ Low G Sensitivity Solutions
• High Temperature Modules
• Leading Edge Packaging
• Integrated Solutions
Complete
Fully Tested
Solution
To Your
Requirements
Visit http://mwj.hotims.com/16339-149 or use RS# 149 at www.mwjournal.com/info
for more product information,visit...... www.vectron.com

MARCH 2008 VOL. 51 • NO. 3

FEATURES

NOTE FROM THE EDITOR

COVER FEATURE: THEN AND NOW

TECHNICAL FEATURES

51 Years of Publishing Excellence

Microwave Journal (USPS 396-250) (ISSN 0192-6225) is published monthly by Horizon House Publications Inc., 685 Canton St., Norwood, MA 02062. Periodicals postage paid at Norwood, MA 02062 and additional mailing offices.

POSTMASTER: Send address corrections to *Microwave Journal*, PO Box 3256, Northbrook, IL 60065-3256 or e-mail mwj@omeda.com. Subscription information: (847) 291-5216. This journal is issued without charge upon written request to qualified persons working in that part of the electronics industry, including governmental and university installation, that deal with VHF through light frequencies. Other subscriptions are: domestic, $120.00 per year, two-year subscriptions, $185.00; foreign, $200.00 per year, two-year subscriptions, $370.00; back issues (if available) and single copies, $10.00 domestic and $20.00 foreign. Claims for missing issues must be filed within 90 days of date of issue for complimentary replacement.

Posted under Canadian international publications mail agreement #0738654


www.awrcorp.com
Catch design flaws before they burn you.
AWR
Half solutions can wreak havoc on product development. Visual System Simulator™ not only does system budget analysis and identifies sources of IM products, including the effects of conversions, harmonics and noise. It also has a powerful simulator for developing and analyzing complex communication systems, including radio and circuit designs, baseband signal processing, algorithmic development and digital fixed-point implementations. It's the complete system tool. Visit www.awrcorp.com/vss for more.
Visual System VSS Simulator
Advancing the wireless revolution™
Visit http://mwj.hotims.com/16339-21 or use RS# 21 at www.mwjournal.com/info
© 2008 AWR All rights reserved.

Microwave Journal

FEATURES

TECHNICAL FEATURES

PRODUCT FEATURES

DEPARTMENTS

STAFF

Publisher: Carl Sheffres
Associate Publisher: Edward Johnson
Editor: David Vye
Managing Editor: Keith W. Moore
Technical Editor: Frank M. Bashore
Associate Technical Editor: Dan Massé
Staff Editor: Jennifer DiMarco
Editorial Assistant: Barbara Walsh
Consulting Editor: Howard I. Ellowitz
Consulting Editor: Harlan Howe, Jr.
Consulting Editor: Peter Staecker
Consulting Editor: Dan Swanson
Web Editor: Samantha Bookman
Traffic Manager: Edward Kiessling
Traffic Administrator: Ken Hernandez
Director of Production & Distribution: Robert Bass
Multimedia Designer: Greg Lamb
Web Site Production Designer: Michael O'Brien
DTP Coordinator: Janet A. MacDonald

EUROPE

European Editor: Richard Mumford
Office Manager: Eugenie Hardy

CORPORATE STAFF

Chairman: William Bazzy
CEO: William M. Bazzy
President: Ivar Bazzy
Vice President: Jared Bazzy

Executive Editorial Office:

685 Canton Street, Norwood, MA 02062
Tel: (781) 769-9750
FAX: (781) 769-5037
e-mail: mwj@mwjournal.com

European Editorial Office:

46 Gillingham Street, London SW1V 1HH, England
Tel: Editorial: +44 207 596 8730 Sales: +44 207 596 8740
FAX: +44 207 596 8749

www.mwjournal.com

Printed in the USA

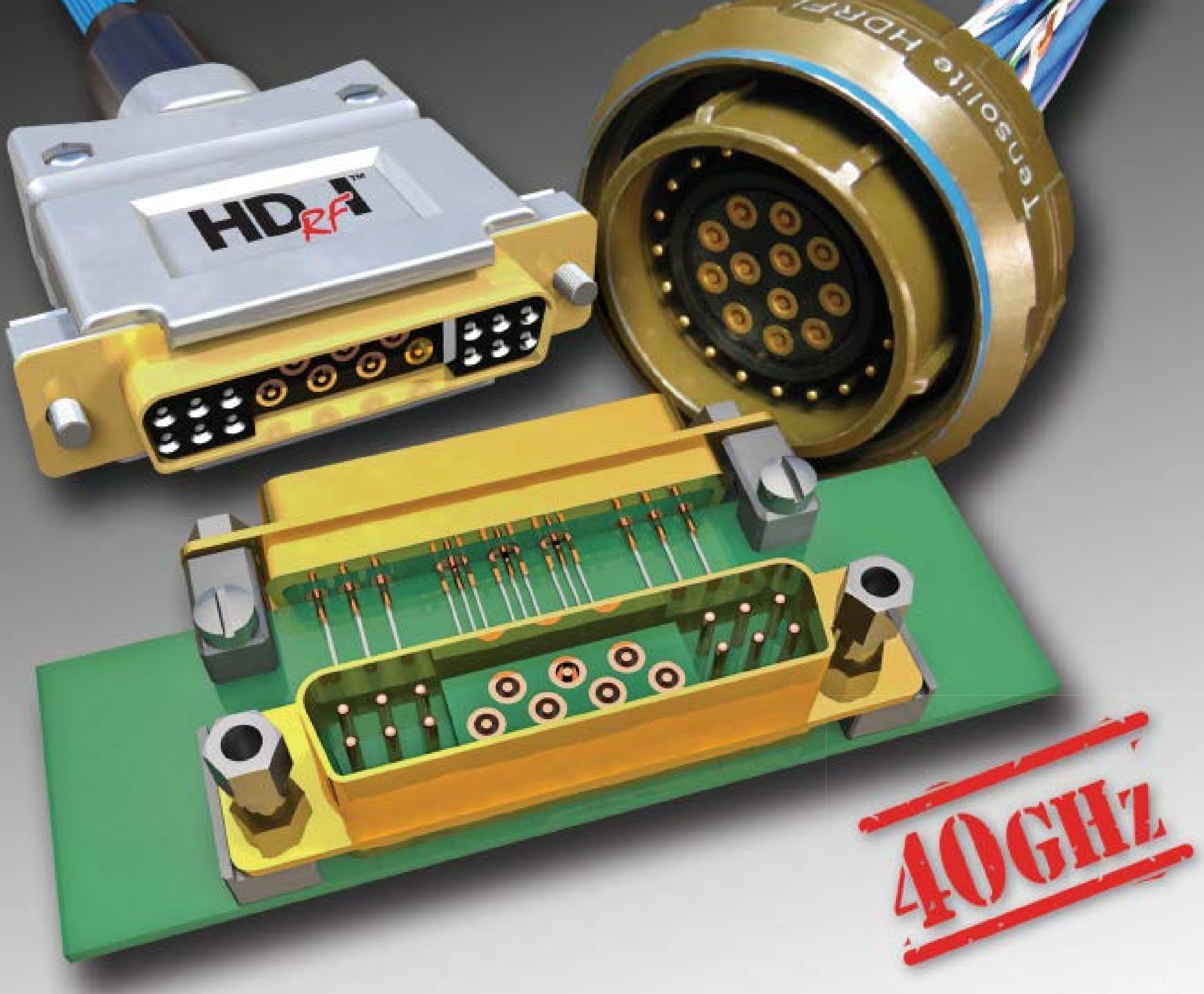

Not Enough Space?

Tensolite Has The Solution!

Introducing HDRFI™ Mixed Signal D-Sub and Circular:

Tensolite's HDRFI™ Assemblies use High Frequency Low Loss Coax and a unique patented interconnect system to transfer high frequency/data through a planar connection system, using a z-axis elastomer. This allows for very high frequencies to transfer with minimal loss through the connector interface.

Features include:

- *Standard Pin and Socket Power Contacts*
- *40 GHz RF Contacts*
- *High Bandwidth*
- *Small Form Factor*
- *Scalable*
- *No Moving Parts*
- *Frictionless*
- *Low Compression Mating Force*
- *Zero Extraction Force*
- *Customizable For Multiple Configurations*

RoHS COMPLIANT AVAILABLE

AS 9100 CERTIFIED

Tensolite

A CARLISLE Company

(800) 458-9960 phone • (904) 829-3447 fax • For more information go to www.HDRFI.com

SEE OUR WEBSITE FOR CAREER OPPORTUNITIES

HDRFI™ products are covered by patent number 7,074,047 and others. HDRFI™ is a trademark of the Tensolite Company.

Microwave Journal Online

Go to www.mwjournal.com

The latest industry news, product updates, resources and web exclusives from the editors of *Microwave Journal*

Free Webinar

MWJ/Besser Associates Webinar Series

Tune-up your skills. Join the thousands of engineers and managers who have participated in this monthly series on RF/microwave theory and practical applications.

Systems: WiMAX, 802.11, Bluetooth and More

This month's webinar examines communication systems and the engineering concepts underlying today's leading wireless/networking technologies. Standards such as WiMAX, IEEE 802.11 a/b/g, Bluetooth and others will be discussed.

Presented by **Besser Associates** and *Microwave Journal*.

Live webcast: 3/18/2008, 11:00 AM (EST)
Sponsored by **AWR** and **Tyco Electronics**

Online Technical Papers

Design of Four Feeding Microstrip Patch Antennas
M.F. Ain, J.S.Mandeep, C.T. Chin, Hassan M.A. Othman and B.M. Nawang

Recent Advances in Fresnel Zone Plate Antenna Technology
S.M. Stout-Grandy, A. Petosa, I.V. Minin, O.V. Minin and J.S. Wight

Design of a Miniaturized Quarter-circular Slot UWB Antenna
Joon-Won Jang and Hee-Yong Hwang

Performance Analysis of OFDM
S.S. Riaz Ahamed

Events

MWJ editors will report on our industry news from the World Mobile Congress exhibition halls, Barcelona, Spain, February 11–14.

Expert Advice

Microwave Journal asks a noted industry expert to provide commentary related to the month's editorial theme. Respond with comments and win a complimentary copy of *Electrical Engineering: A Pocket Reference* from Artech House (see www.mwjournal.com for details).

March: Joel Dunsmore, senior R&D engineer/scientist with Agilent Technologies, discusses the enhancements and trade-offs that enable VNAs to move beyond S-parameters, and the improvements brought about by extending the calibration capabilities of VNAs into other measurement classes.

Retrospective

Michael Hiebel, author of *Fundamentals of Vector Network Analysis,* gives a European perspective of the development of VNAs from the days of the slotted line, to the present day and beyond as he identifies potential future developments.

Executive Interviews

In this month's executive interview, MWJ talks with **Bryan Sayler**, senior vice president and general manager at ETS-Lindgren, about being a member of the WiMAX Forum and its new WiMAX™ RPT Test System designed to provide detailed information on the radiated transmit and receive performance of wireless devices in an over-the-air environment.

Also, from our European Office, MWJ talks with **Peter Krauss**, managing director of Mician. He outlines fast and efficient methods for the simulation and optimization of passive microwave systems and components to meet 21st century demands. He focuses on horn antenna synthesis and stresses the importance of pan-European collaboration.

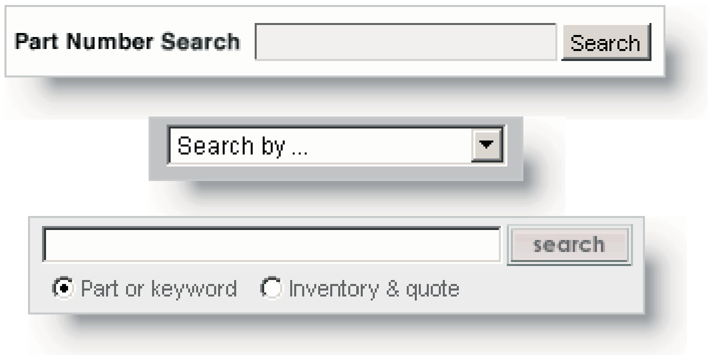

Their sites have search engines. Ours has a find engine.

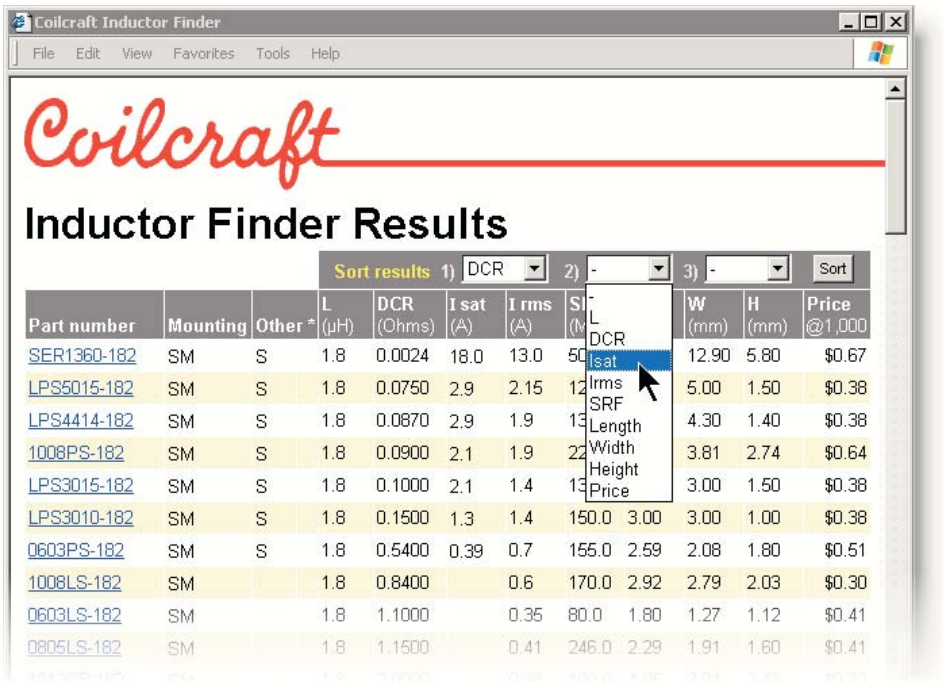

On most inductor web sites, their search engine results in more aggravation than answers.

But Coilcraft's web site is different.

In seconds, our Inductor Finder will show you all the parts that meet your electrical and size requirements. You can sort the results by your most important parameters. Compare pricing. Even analyze the core and winding losses of up to four different power inductors!

You'll find lots of other design tools to help you choose the perfect part. And then request free samples with just a few clicks.

So quit searching for magnetics and start finding them at **www.coilcraft.com**!

ORDER DIRECT
BUY.COILCRAFT.COM
800-322-2645
OVERNIGHT DELIVERY ORDER BY 5
RoHS COMPLIANT

Coilcraft®

www.coilcraft.com 800/322-2645

PUBLISH... AND PROSPER

DAVID VYE, *Microwave Journal* Editor

Welcome to March, another special month in our 50-year celebration of *Microwave Journal* and the microwave industry. This is the month we publish our annual Test & Measurement/CAD issue along with our Cables and Connectors supplement. As in previous years, we dedicate this month to measurement and simulation, two engineering tools that guide us in our quest to understand how technology works and how to advance it. Undoubtedly, studying device behavior is a critical step in developing the next generation of design and therefore deserves our attention.

Keeping with our anniversary year theme, this "special" issue of *Microwave Journal* includes side-by-side articles on the state-of-the-art in measurements today and a classic from our earlier days. Our reprint article captures both the measurement and device technology of 50 years ago. The extent of the industry's progress is clearly evident by this comparison of past and present. If your career spans back that far, I think you'll enjoy this nostalgic journey. If your career is less long in the tooth, you should be amused at how devices were measured back then and appreciate today's tools even more.

Looking back at my own start in the industry, I remember the VSWR meter and its peripherals as a dusty collection of equipment piled up in the test lab's supply graveyard, mothballed unless you were among the unfortunate without a replacement budget for aging instruments. In the mid-1980s, fresh out of school, I witnessed a great deal of engineering attention focused on gallium arsenide and MMIC development. As a relatively new piece of test equipment, the automatic network analyzer (ANA) was making a big impact on most of the novel device development occurring at that time.

The ANA (now referred to as the VNA) helped us accurately extract S-parameters, impedances, loss (insertion and reflective) and group delay. It truly was breakthrough technology, spawning such test-lab social phenomena as the sign-up sheet, the measurement guru and the calibration kit with precision torque wrench kept under lock and key by the calibration guru (multiple gurus being budget-dependent). Over time, changing job responsibilities meant less and less contact with the VNA, but in microwave engineering, one never gets too far away from S-parameters. So when it is time to commemorate 50 years of measurements in our industry, I could not think of a better candidate for the spotlight than the network analyzer.

The job of an editor for *Microwave Journal* is an interesting one. While many individuals who work and study in our industry submit content to the *Journal* unsolicited, editors must often seek out the help of microwave engineers, managers and marketing folks to get the materials we need for special reports. We rely on these people who are closest to their respective technologies to provide us articles or information on what is happening in their areas of expertise (beware the pestering editor with a deadline). For our cover story, various sources on the web and personal experience made the early days of the VNA relatively easy to write. I found the continuing evolution of the VNA since my days in the test lab to be truly remarkable and considerably beyond what I had been aware of. Detailing all the recent advances in VNA measurements would not have been possible without the timely help from the folks at Agilent, Anritsu and Rohde & Schwarz. These people all know their stuff and I am extremely grateful. It is amazing how quickly technology changes and how quickly we come to adapt to these changes and expect more. VNAs today have much greater capability than just a couple of years ago. They are extremely fast (for acquisition of large data sets), have greater dynamic range, address differential circuit topologies and pulsed operations while providing calibrated measurements far beyond just S-parameters. If you haven't been keeping up with these advances, now is a great time to read up.

This brings me to a final thought concerning information. In engineering, it is vital that we stay up-to-date, which necessitates information sharing. While protecting intellectual property is vital, technical advances happen faster when we are informed and our achievements are allowed to leap frog one another. Working on something novel and you have some interesting results? Tell the industry and validate your findings while educating potential customers. Looking to find or share information? Attend our online webinars and the invaluable Q&A sessions afterwards, reply to our monthly online Expert Advice column, or send us an article.

We enjoy hearing from our readers and would like to share what you are working on with the rest of the industry. Recently retired *Microwave Journal* editor Harlan Howe addressed this need in a very popular editorial from several years back entitled "Publish or Perish." If it's been awhile since you've openly discussed your technical accomplishments, now may be the time to get the word out. To paraphrase Harlan's message, "Publish and Prosper." Here's to your success. ■

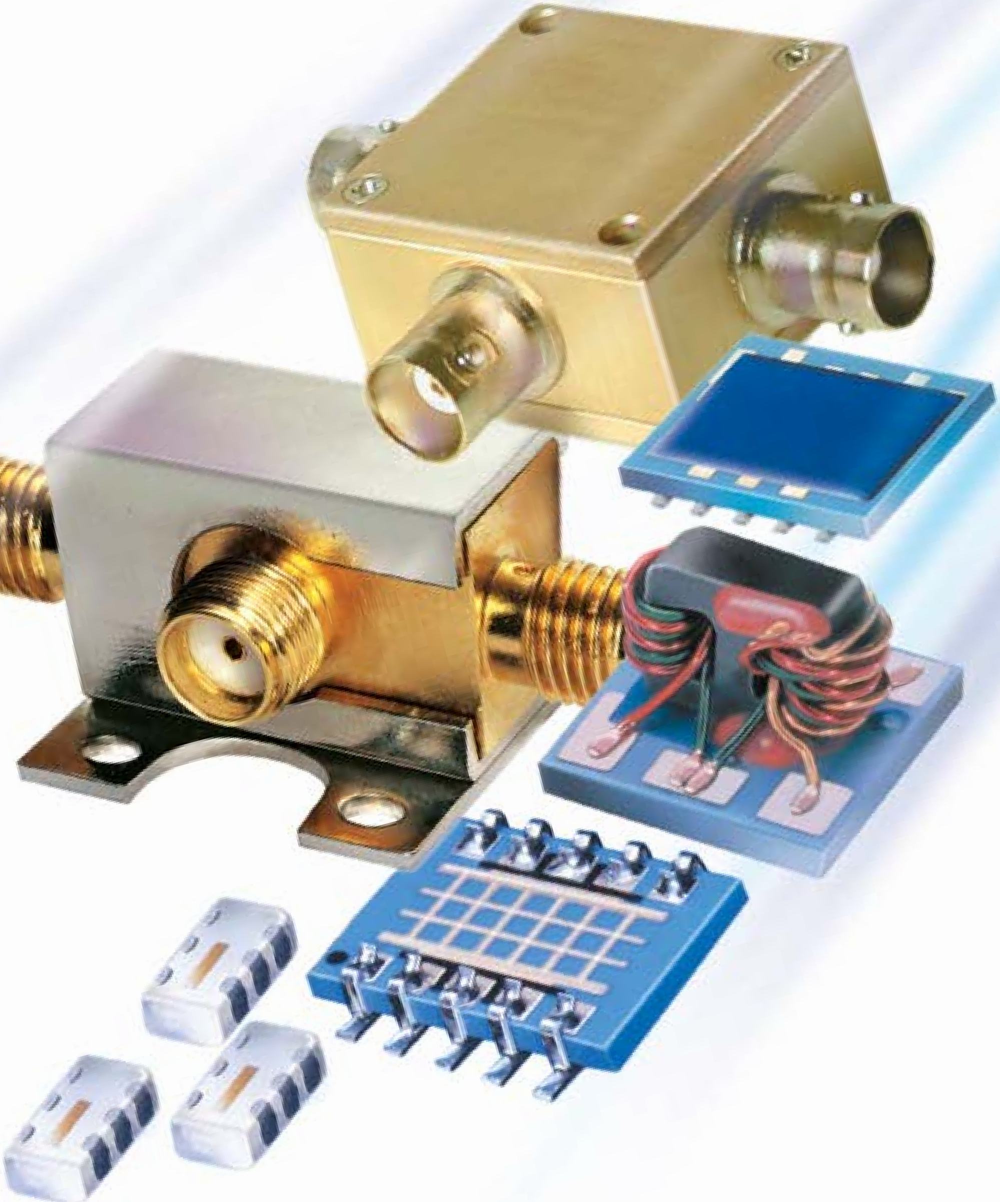

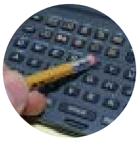

Coming Events

CALL FOR SPEAKERS

WCA International Symposium and Business Expo
www.wcai.com

APRIL

CTIA WIRELESS 2008
April 1–3, 2008 • Las Vegas, NV
www.ctiawireless.com

ARMMS RF AND MICROWAVE SOCIETY CONFERENCE
April 7–8, 2008 • Steventon, Oxfordshire, UK
www.armms.org

WCA 2008
April 21–23, 2008 • Washington, DC
www.wcai.com

MAY

IEEE COMCAS 2008
May 13–14, 2008 • Tel-Aviv, Israel
www.microwave.co.il

IEEE RADAR CONFERENCE 2008
May 26–30, 2008 • Rome, Italy
www.radarcon2008.org

JUNE

IEEE RADIO FREQUENCY INTEGRATED CIRCUITS SYMPOSIUM (RFIC 2008)
June 15–17, 2008 • Atlanta, GA
www.rfic2008.org

IEEE MTT-S INTERNATIONAL MICROWAVE SYMPOSIUM AND EXHIBITION (IMS 2008)
June 15–20, 2008 • Atlanta, GA
www.ims2008.org

71ST ARFTG CONFERENCE
June 19–20, 2008 • Atlanta, GA
www.arftg.org

AUGUST

IEEE EMC SYMPOSIUM
August 18–22, 2008 • Detroit, MI
www.emc2008.org

SEPTEMBER

IEEE INTERNATIONAL CONFERENCE ON ULTRA-WIDEBAND (ICUWB 2008)
September 10–12, 2008 • Hannover, Germany
www.icuwb2008.org

ANTENNA PARAMETER MEASUREMENTS BY NEAR-FIELD TECHNIQUES
September 16–18, 2008 • Boulder, CO
www.nist.gov

WIMAX WORLD AMERICAS
September 30–October 2, 2008 • Chicago, IL
www.wimaxworld.com

OCTOBER

EUROPEAN MICROWAVE WEEK
October 27–31, 2008
Amsterdam, The Netherlands
www.eumweek.com

NOVEMBER

WCA INTERNATIONAL SYMPOSIUM AND EXPO
November 4–7, 2008 • San Jose, CA
www.wcai.com

MILITARY COMMUNICATIONS CONFERENCE (MILCOM 2008)
November 17–19, 2008 • San Diego, CA
www.milcom.org

Workshops & Courses

Reverberation Chamber Theory and Experiment Short Course

■ **Topics:** This course is designed for engineers who will be involved in radiated emission of immunity testing of commercial or military systems using reverberation chambers. The theory portion will cover the statistical nature of reverberation chamber testing, characterization of the EM test conditions, and the tradeoff between uncertainty in test results and test time. The experiments include typical measurement techniques, chamber calibration, immunity, emission and pulse testing in reverberation chambers.

■ **Site:** Stillwater, OK

■ **Dates:** March 31–April 4, 2008

■ **Contact:** For more information, visit http://rc-course.okstate.edu.

Modern Wireless Data Communications

■ **Topics:** This course is tailored to end users, technology planners, decision makers and implementers who need an understanding of how wireless works and what the technology can do. The information starts with an introductory level, and progresses into coverage of the more technical material at an intermediate depth. For more information, visit http://epdweb.engr.wisc.edu.

■ **Site:** Madison, WI

■ **Dates:** April 8–10, 2008

■ **Contact:** University of Wisconsin-Madison, Department of Engineering Professional Development, 432 North Lake Street, Madison, WI 53706 (800) 462-0876.

Ansoft Designer Training

■ **Topics:** This one-day course uses examples and exercises to provide a comprehensive understanding of Designer. The course is intended for beginners and intermediate users and assumes no prior knowledge of Designer. Covers using the Ansoft Designer Desktop features, creating and manipulating Circuit/System/Planar EM models, and working with different data types. Includes basic sections on field visualization and high level and low level data manipulation.

■ **Site:** Irvine, CA

■ **Date:** April 10, 2008

■ **Contact:** For more information, visit www.ansoft.com.

Antenna Engineering

■ **Topics:** This course provides an overview of the theory and practice of antenna engineering, including a range of antenna types, applications and electromagnetic properties from basic to state-of-the-art. Explore a wide spectrum of frequencies from 550 kHz to 550 GHz, with primary emphasis in the VHF, UHF and microwave regions. Examine communications and radar, commercial and military applications.

■ **Site:** Atlanta, GA

■ **Dates:** April 21–25, 2008

■ **Contact:** Georgia Institute of Technology, Professional Education, PO Box 93686, Atlanta, GA 30377 (404) 385-3500.

IEEE COMCAS 2008

■ **Topics:** This two-day technical program covers a variety of complementary subjects and a technology exhibition. The idea is to create a very diverse and multidisciplinary conference where engineers and scientists from various complementary electronics disciplines can meet and discuss subjects of common interest. Emphasis will be on applications oriented research and development, from antennas and device engineering to circuit applications to systems and software.

■ **Site:** Tel-Aviv, Israel

■ **Dates:** May 13–14, 2008

■ **Contact:** ORTRA Ltd., 1 Nirim Street, P.O. Box 61092, Israel +972-3-6384455, www.microwave.co.il.

Printed Circuit Board Design for Real-world EMI Control

■ **Topics:** The primary focus of this seminar is to help working engineers understand the causes of EMC problems so this knowledge can be applied to real world product design immediately. Formulas and equations are not required and are minimized throughout the seminar. Understanding the causes of EMC problems will allow engineers to make difficult design trade-off decisions.

■ **Site:** Oxford, UK

■ **Date:** June 2008

■ **Contact:** University of Oxford Continuing Education, Rewley House, 1 Wellington Square, Oxford OX1 2JA +44 (0)1865 270360, or visit www.conted.ox.ac.uk.


when we say
free
of
charge,
we're talking about
the price.
sonnet® lite. $0.
www.sonnetsoftware.com/lite-mj
high frequency EM analysis,
free of charge with sonnet lite v11.
SONNET®
the world's most accurate 3D planar EM simulator.
Visit http://mwj.hotims.com/16339-135 or use RS# 135 at www.mwjournal.com/info

PARAMETRIC DIODE Q MEASUREMENTS

RICHARD I. HARRISON

GENERAL TELEPHONE and ELECTRONICS LABS, Inc.*
Bayside, New York

Introduction

The measurements of microwave impedance and the Q of solid-state diodes has become increasingly important since the advent of the parametric amplifier. A new method of measuring the Q of such a diode, Q_d, has recently come into rather general use; the purpose of this paper is to explain it and to show its validity.

Recent publications[1,2] have dealt with methods of measuring parametric diode impedance. The semiconductor diode with its cartridge is usually embedded in a transmission line which may be preceded by a microwave impedance transformer and followed by a short circuit or a matched load. Normalized impedances are measured by standard slotted line techniques. The problem is to find the absolute value of the impedance of the semi-conductor material itself, taking into account various impedance transformations occurring in the rest of the cartridge and connecting transmission line system. In order to establish an absolute impedance level, it is necessary to utilize resistive standards or TEM waveguides of known characteristic impedance. In the measurement of diode Q_d to be treated, the problems and equipment are similar except that it is not necessary to establish an impedance level. Since Q_d is essentially a ratio of reactance to resistance, it can be related to normalized impedance measurements made with a slotted line.

Before going into the specifics of this measurement, an alternative method of measuring Q_d based on the well known cavity Q measurements should be noted. This method essentially involves making measurements with and without the diode loading a cavity. It is believed that the method of measuring Q_d described in this paper is comparatively simple in the experimental procedure, has less involved equipment requirements, and detects diode series resistance changes in addition to Q_d.

*Formerly Sylvania Research Labs.

Diode Equivalent Circuit and Q_d

The usual circuit representation of a parametric diode is shown in Figure 1. It is assumed in obtaining this representation that the effective electric field lines are essentially in the axial cartridge direction and that the microwave environment outside the cartridge has negligible effect on the direction of these fields. In this figure, only the semiconductor material is considered and the impedance corresponding to the rest of the diode cartridge circuitry is omitted. It consists of a resistance R_d in series with a parallel combination of a voltage-sensitive small signal capacitive reactance X_d, and a shunting resistance R_p. In ordinary parametric amplifier operation, the diode is reversed or negatively biased and, for the range of applied voltages, R_p is so large compared

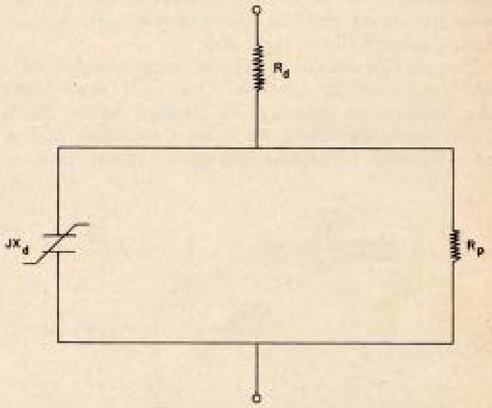

Figure 1 — Equivalent circuit of a parametric diode.

May, 1960 43

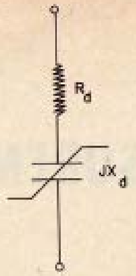

Figure 2 — Simplified equivalent circuit of a parametric diode for reversed bias.

to $|X_d|$ that the equivalent circuit can be simplified to that shown in Figure 2. It should be noted here that the series resistance R_d is substantially constant and independent of diode bias for all negative operating bias voltages and for a small range of positive bias voltages whereas X_d is a voltage-sensitive quantity. The diode Q_d is defined by

$$Q_d = \frac{-X_d}{R_d} = \frac{1}{\omega R_d C_d} \quad (1)$$

where

$\omega = 2\pi f =$ frequency in radians per second
$X_d =$ negative capacitative reactance

and is, for a given frequency, a function of bias.

Equipment Requirements

The equipment necessary for the measurement of Q_d consists of a signal generator, a slotted line (and standing wave detector), an ideally lossless variable transformer, and an ideally lossless diode cartridge holder. All these devices are connected in series as shown in Figure 3. The diode cartridge holder should be so constructed that the dc bias lead does not provide an r-f leakage path to the outside. The diode cartridge is ideally lossless except for the semiconductor material itself. As part of the procedure, the semiconductor material must be effectively replaced by a highly conductive material, thus effectively creating a required short circuit. One way to make this short circuit is to use a diode cartridge identical to that under test except that the semiconductor wafer is made highly conductive by a metal film.

One practical coaxial waveguide setup consisted of a double-stub tuner for the variable microwave transformer and a commercial coaxial diode cartridge holder altered so that the dc bias connection is not a microwave leakage path. Another rectangular waveguide system used an E.H. tuner for the microwave transformer and a commercial waveguide diode cartridge holder. Alterations were made to eliminate the r-f leakage path along the bias connection by shunting the BNC output connector with a large capacitor.

Measurement Procedure

The measurement procedure can be summarized as follows:

1. The input microwave power level is adjusted to such a level that the dynamic capacitance swing is small compared with the static capacitance at the particular diode bias used. One way to accomplish this in practice is to set the diode bias at zero, then adjust the microwave power so that the change in dc current is small when the r-f power is turned on.

2. The variable microwave transformer is adjusted so that a match is measured at a reference bias[3] of zero.

3. At various negative and positive biases[4] the corresponding normalized impedance is measured with respect to an arbitrarily chosen plane as the reference plane. These measurements plot on the Smith chart as a portion of a circle whose diameter is the same as that of the $R/R_o = 1$ circle as shown in Figure 4.

4. The semiconductor material in the diode is then replaced by an effective short circuit. The normalized impedance is measured using the same reference plane chosen earlier. This point is plotted on the Smith chart as shown in Figure 4. (Often it is convenient to choose the position of a standing wave minimum obtained with the short circuit as the reference plane). One way to achieve an effective short circuit is to substitute for the diode cartridge the short circuited cartridge mentioned earlier. Another way to accomplish this is to plot the normalized impedance of the diode for a range of positive biases. It has been found that, for silicon junction diodes, the semiconductor impedance tends to go to zero for positive

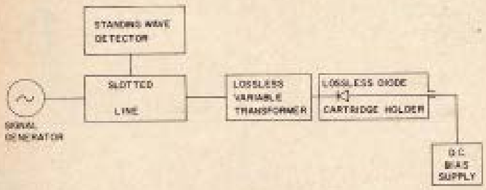

Figure 3 — Equipment Used for the Q_d measurement.

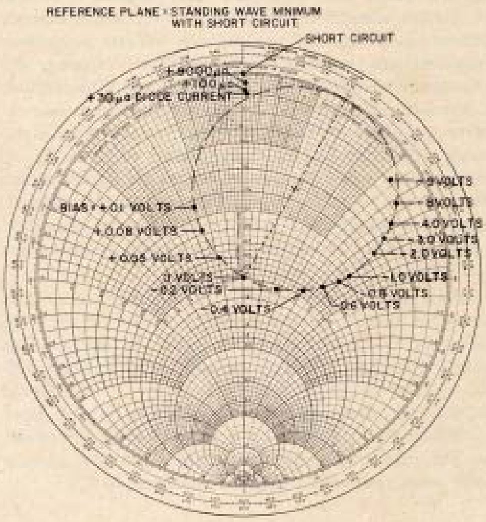

Figure 4 — Data plot on Smith chart.

44 *the microwave journal*

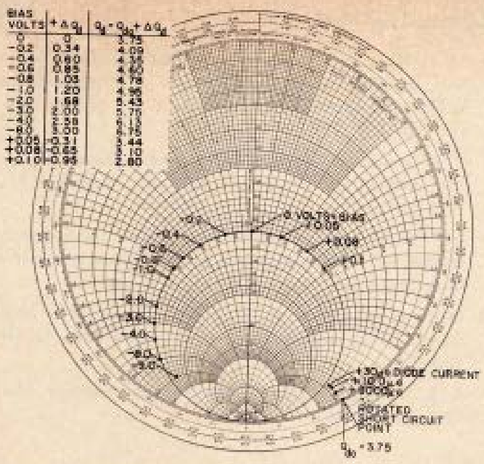

BIAS VOLTS	$+\Delta Q_d$	$Q_d = Q_{do} + \Delta Q_d$
0	0	3.75
−0.2	0.34	4.09
−0.4	0.60	4.35
−0.6	0.85	4.60
−0.8	1.03	4.78
−1.0	1.20	4.95
−2.0	1.68	5.43
−3.0	2.00	5.75
−4.0	2.38	6.13
−9.0	3.00	6.75
+0.05	−0.31	3.44
+0.08	−0.65	3.10
+0.10	−0.95	2.80

Figure 5 — Rotated data plot.

biases. Typical normalized impedance points, labeled with the dc diode current, are shown in Figure 4. In the case of point-contact gallium arsenide diodes, experience has shown that the diode dc currents exceed a permissible maximum much before an effective short circuit point is reached and the former shorted cartridge method is preferable.

5. The section of the circle plot around the center of the Smith chart is then graphically rotated so that it coincides with the $R/R_o = 1$ circle as shown in Figure 5. The short circuit point is similarly rotated through the same angle. (Note that the normalized impedance points taken to establish the short circuit point fall on a constant reactance line in this plot.)

6. The normalized reactance of the rotated short circuit point which is identically the Q_{do} of the diode at the zero bias point is then read. The Q_d for any bias point falling on the $R/R_o = 1$ circle can be found by adding to the zero-bias Q_{do} the negative of the normalized reactance,

$$\Delta Q_d = -X/R_o \tag{2}$$

read off the corresponding point on the $R/R_o = 1$ circle. Thus,

$$Q_d = Q_{do} + \Delta Q_d \tag{3}$$

A table illustrating results is given in Figure 5. For data points that do not fall on the $R/R_o = 1$ circle because R_d begins to vary, the Q_d may also be found. An example of such a point is the —9 volt bias point in Figures 4 and 5. To obtain Q_d for this point, first divide the Q_{do} by the normalized resistance corresponding to this point as plotted in the rotated data plot. Then,

$$Q'_{do} = \frac{Q_{do}}{R/R_o} \tag{4}$$

Next divide the negative of the normalized reactance by the normalized resistance of the point, giving

$$\Delta Q'_d = \frac{X/R_o}{R/R_o} \tag{5}$$

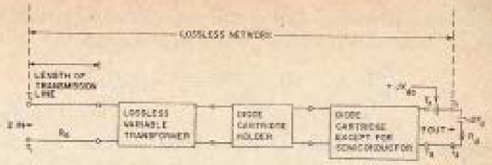

Figure 6 — Lossless network for measuring Q_d of a diode with a variable bias semiconductor reactance of $X_{do} + \Delta X_d$ where X_{do} is the zero bias reactance.

Then at this point

$$Q_d = Q'_{do} + \Delta Q'_d \tag{6}$$

Analysis of the Method of Measurement

The analysis of the Q_d measurement starts with a consideration of the input-output impedance relation for a lossless network. This relation is

$$Z_{in} = \frac{A\,Z_{out} + B}{C\,Z_{out} + D} \tag{7}$$

where A and D are real and B and C are imaginary.[5] For the Q_d measurement, the network is assumed to be as shown in Figure 6 between T_1 and T_2; that is, the lossless network includes a length of input transmission line of characteristic impedance R_o, a lossless variable transformer, a diode cartridge holder, and all of the reactive impedance of the diode cartridge including the zero-bias capacitive reactance of the semiconductor, but excluding the series resistance of the semiconductor. Under these conditions, step (2) in the measurement procedure requires that

$$R_o = \frac{A\,R_d + B}{C\,R_d + D} \tag{8}$$

In order to establish the length of input transmission line or the input reference plane for which the data points in step (3) of the measurement procedure would fall on the $R/R_o = 1$ circle of the Smith chart, consider the condition where $Z_{out} = 0$. It follows from (7) that

$$Z_{in} = B/D \tag{9}$$

and Z_{in} is purely reactive with a value between plus and minus infinity depending on the position of the input reference plane. For the length of transmission line that gives $Z_{in} = 0$ for $Z_{out} = 0$, it follows that

$$B = 0 \tag{10}$$

because D is normally finite. Since in (8) R_o, R_d, A and D are real, and C is imaginary, it is necessary that

$$C = 0 \tag{11}$$

Therefore, for this length of input transmission line, or at the input reference, plane T_1,

$$\frac{Z_{in}}{R_o} = \frac{Z_{out}}{R_d} \tag{12}$$

It's the accuracy that makes your ideas run faster.

CST MICROWAVE STUDIO® 2008. There's more behind it.

➤ Need to get a solution fast without slipping up on accuracy? CST puts 3D EM on the fast track with new software and hardware technology designed to fit your workflow groove.

Don't just judge the book by the cover though – the software has to perform. Check out the time taken to reach your accuracy requirement and we are convinced that our simulation technology will come out on top. All application have different needs. CST has the technology to cover them.

CST MICROWAVE STUDIO® [CST MWS] is the first commercial HF 3D EM code to offer the advantages of time and frequency domain, hexahedral and tetrahedral meshing, united in one interface, allowing you to choose the technology best suited to your application. Embedded in an advanced design environment, CST MWS can be coupled with all CST STUDIO SUITE™ solver technology including circuit and thermal simulation.

CST MICROWAVE STUDIO® is the market leading time domain tool for 3D EM simulation. It has benefited from over 30 years experience in the area of numerical field calculation, and is used by industry market leaders worldwide.

➤ Choose the accuracy and speed offered by CST MWS. There's more to performance than meets the eye.

CST

CHANGING THE STANDARDS

Visit http://mwj.hotims.com/16339-36 or use RS# 36 at www.mwjournal.com/info

CST of America®, Inc. | To request literature or a free demo CD ✆ (508) 665 4400 | info: www.cst.com

The input impedance seen at T_1 for a semiconductor diode in the range of bias voltages where R_d is constant is

$$\frac{Z_{in}}{R_o} = 1 + j\frac{\Delta X_d}{R_d} = 1 - j\Delta Q_d \tag{13}$$

Hence for this choice of input terminal plane the impedance points on a Smith chart plot on the $R/R_o = 1$ circle where $X/R_o = \Delta X_d/R_d = -\Delta Q_d$. The Q at zero bias, Q_{do}, can be determined from the input impedance at T_1 corresponding to a short circuit at port T_3 which, from Figure 6, means replacing the semiconductor by a short circuit. Mathematically, this is equivalent to an impedance $Z_{out} = -j\ X_{do}$ across port T_2 since this will just compensate for $+\ j\ X_{do}$ between T_2 and T_3.

Equation 12 can then be re-written in the form

$$\frac{Z_{in}}{R_o} = \frac{-j\,X_{do}}{R_d} = +\,j\,Q_{do} \tag{14}$$

Therefore, the total Q_d can be found from (3) of step 6 in the measurement procedure.

In similar manner, it can be shown that Equations (4), (5), and (6) follow from the same analysis. In practice it is not necessary to establish the reference plane T_1. A measurement is made with an arbitrary reference plane, and the circle plot is then rotated to establish T_1.

References and Notes

1. M. C. Waltz, "A Technique for the Measurement of Microwave Impedance in the Junction Region of a Semiconductor Device," *the microwave journal*, Vol. 2, No. 5, May 1959, pp. 23-27.
2. R. P. Garver and J. A. Rosado, "Microwave Diode Cartridge Impedance," Diamond Ordnance Fuze Labs., Document TR-721, July 6, 1959.
3. The choice of the reference bias where the transformer is adjusted for match is arbitrary as long as the bias is anywhere in the range where the series resistance is constant.
4. In the measurement at positive biases, care should be taken to limit the dc forward diode current to rated values for the diode.
5. E. L. Ginzton, "Microwave Measurements," McGraw Hill, 1957, pp. 278-280.

Acknowledgments

The author is indebted to Dr. G. E. Weibel for suggesting a simplified approach that led to the analysis described, and to Shirley W. Harrison for making the measurements.

providing optimal semiconductor solutions worldwide

MIMIX SMARTSETS... COMPLETE QFN CHIPSET SOLUTIONS!

	Description	Device	Frequency (GHz)	Gain (dB)	Gain Flatness (dB)	Noise Figure (dB)	Output P1dB (dBm)	OIP3 (dBm)	Bias (mA @V)	Package (mm)
5-10 GHz Mimix SmartSet	Buffer Amplifier	XB1007-QT	4.0-11.0	23.0	+/-1.5	4.5	+20.0	+30.0	100 @ 4.0	3x3
	Power Amplifier	XP1035-QH	5.9-9.5	26.0	+/-1.0	-	+29.0	+39.0	500 @ 6.0	4x4
	Power Amplifier	XP1039-QJ	5.9-8.5	15.0	+/-1.0	-	+34.5	+49.0	1150 @ 8.0	6x6
	Receiver	XR1011-QH	4.5-10.5	13.0	+/-1.0	1.8	+6.0	+16.0	130 @ 4.0	4x4
	Doubler	XX1002-QH	5.0-12.0 fout	16.0	+/-1.5	-	+16.0 Psat	-	125 @ 5.0	4x4
	Transmitter	XU1012-QH	5.0-10.0	-8.0	+/-1.0	-	+7.0	+17.0	120 @ 4.0	4x4
10-16 GHz Mimix SmartSet	Buffer Amplifier	XB1008-QT	10.0-21.0	17.0	+/-2.0	4.5	+19.0	+32.0	100 @ 4.0	3x3
	Power Amplifier	XP1042-QT	12.0-16.0	21.0	+/-1.0	-	+25.0	+38.0	500 @ 5.0	3x3
	Power Amplifier	XP1043-QH	12.0-16.0	20.0	+/-1.0	-	+30.0	+41.0	700 @ 7.0	4x4
	Receiver	XR1007-QD	10.0-18.0	13.5	+/-1.0	2.7	+5.0	+15.0	150 @ 5.0	7x7
	Doubler	XX1000-QT	15.0-45.0 fout	10.0	+/-2.0	-	+18.0 Psat	-	200 @ 5.0	3x3
	Doubler	XX1002-QH	5.0-12.0 fout	16.0	+/-1.5	-	+16.0 Psat	-	125 @ 5.0	4x4
	Transmitter	XU1014-QH	8.0-18.0	-10.0	+/-1.0	-	+2.0	+12.0	80 @ 4.0	4x4

Mimix SmartSets, our innovative QFN packaged chipset solutions, lower material and assembly costs and increase reliability and manufacturability of products, while also allowing engineers to simplify design and improve time-to-market.
Visit www.mimixbroadband.com/smartsets to learn more!

Mimix
BROADBAND™

Mimix Broadband, Inc., 10795 Rockley Rd., Houston, TX 77099 U.S. 281.988.4600 mimixbroadband.com

Visit http://mwj.hotims.com/16339-79 or use RS# 79 at www.mwjournal.com/info

MEASURING S-PARAMETERS: THE FIRST 50 YEARS

The past 50 years has witnessed a remarkable evolution in semiconductor technology. The devices that enable our wireless communication systems rely on sophisticated characterization. "Measuring the Q of a Parametric Diode" by Richard Harrison, the May 1960 *Microwave Journal* article reprinted in this month's "Then & Now" Cover Feature series, discussed a method for parametric measurements and quantifying the value of Q of a semiconductor device almost 50 years ago. While Q continues to dictate key RF specifications from bandwidth to phase noise, the evolution of semiconductor characterization is as impressive as the advances in the devices themselves. Today's semiconductors are measured in time and frequency domains, under small- and large-signal conditions, CW and pulsed excitations, and at measurement sweep rates that support high volume production. Device technology and test capability share a common history. In fact, the developments in test systems were made possible largely through the advances in semiconductors and vice versa. However, before any of this was possible, the microwave community relied on a powerful yet elegant duo: the S-parameter matrix and the network analyzer.

Vector network analyzers (VNA) measure the magnitude and phase characteristics of microwave devices, including passive (diplexers, couplers, filters, antennas, baluns and interconnects, for example) and active components (power amplifiers, LNAs, mixers and switches, for example) as well as multi-functional MMICs/RFICs. These test systems operate by comparing the incident signal supplied by the analyzer with either the signal transmitted through or reflected from the device terminals. With phase measurements come scattering, or S-parameters, which are a shorthand method for identifying these forward and reverse transmission and reflection characteristics. Phase data also adds vector error information, which permits error correction of the measurement system and minimizes measurement uncertainty. Phase measurements also allow for measuring group delay, which is the "rate of change of phase vs. frequency." Throughout many years of service, S-parameters and the network analyzer have provided microwave engineers with invaluable device information, transcending the role of test equipment and

DAVID VYE
Microwave Journal *Editor*

data to become vital components in the design process. This article looks back at the 50-year evolution and current state of the test equipment responsible for measuring S-parameters.

THE EARLY DAYS OF MICROWAVE DEVICE CHARACTERIZATION

At low frequencies, voltages and currents (and impedance) are used to represent the electrical properties of an electrical circuit at a certain instant in time. When the excitation frequency increases to the point where the physical size of the circuit has the same order of magnitude as the associated wavelength, wave propagation must be taken into account. Voltage and current can no longer be defined unambiguously. For this reason, microwave engineers are forced to replace voltages and currents with incident and reflected waves as a means to characterize devices. In 1965, an IEEE article entitled "Power Waves and the Scattering Matrix" by Kaneyuki Kurokawa of Bell Labs was among the first technical papers to popularize the concept of the scattering matrix, today referred to as S-parameters. This form put transmission, reflection and impedance into a single two-dimensional representation, which could be readily measured and easily visualized, thus revolutionizing high frequency measurement and design (see ***Figure 1***).

In the 1960s, the emergence of reflection, transmission and S-parameter measurements were critical to the engineers beginning to design with newly available high frequency semiconductors. These early microwave measurements were performed using test systems implemented with rudimentary signal generators, power detectors and impedance bridges. A similar system based on a signal generator, slotted line, standing wave meter and lossless variable transformer was described in the aforementioned "Measuring the Q of a Parametric Diode" article.

The standing wave detector or SWR meter (HP415E) used to measure diode Q in Harrison's 1960 article was actually an AC voltmeter with a narrow filter centered at 1.000 kHz. Many of the signal generators from that period had a built-in 1 kHz modulation to support the use of the "VSWR meter". Prior to the network analyzer, the procedure described in this article was fairly common. The method was both tedious and time-consuming. Hand-tuned measurements were taken one frequency point at a time using a swept scalar analyzer combined with painstaking, point-by-point reconstruction of the relative phase characteristics of devices. It was not uncommon to spend an entire day measuring enough data in order to construct a Smith chart with a reasonable band of frequencies. Before the network analyzer, microwave measurements also suffered from inadequate error-correction. Transistor measurements were especially problematic because they required either an open or short termination on the transistor often causing the device to break into oscillation.[1]

THE BIRTH OF THE NETWORK ANALYZER

Even back then, advances in semiconductor and measurement technology went hand-in-hand. For instance, samplers based on semiconductor diodes became the fundamental building blocks of instrumentation. These were used to sample waveforms and measure the signal's relative amplitude and phase. Agile signal sources based on backward-wave oscillators allowed measurements to be taken across a wide frequency range. Based on a vector voltmeter, the first network analyzer capable of swept amplitude and phase measurements was the HP8407 RF network analyzer from Hewlett-Packard (predecessor to Agilent Technologies). This early network analyzer allowed comparison of the amplitude and phase of two waveforms, but it operated only up to 110 MHz.

$$\begin{pmatrix} b_1 \\ b_2 \end{pmatrix} = \begin{pmatrix} S_{11} & S_{12} \\ S_{21} & S_{22} \end{pmatrix} \begin{pmatrix} a_1 \\ a_2 \end{pmatrix}$$

Expanding the matrices into equations gives:

$$b_1 = S_{11}a_1 + S_{12}a_2$$

and

$$b_2 = S_{21}a_1 + S_{22}a_2$$

(a)

(S_{11}) **(one-port)**

$\begin{pmatrix} S_{11} & S_{12} \\ S_{21} & S_{22} \end{pmatrix}$ **(two-port)**

$\begin{pmatrix} S_{11} & S_{12} & S_{13} \\ S_{21} & S_{22} & S_{23} \\ S_{31} & S_{32} & S_{33} \end{pmatrix}$ **(three-port)**

Etc.

(b)

▲ *Fig. 1 Reflected and incident power waves and the S-parameter matrix (a), and the general S matrix form (b) for networks with a different number of ports.*

In 1967, Hewlett-Packard (HP) introduced the model HP8410 network analyzer (see ***Figure 2***). This system extended swept frequency capability up to 12 GHz and revolutionized S-parameter measurements at microwave frequencies. The HP8410 could display data directly on a CRT screen, which allowed engineers to view the device response in real time and even permitted the tuning of a device under test. This bench-top system was composed of several instruments performing various functions integrated into a single unit. The source module or signal generator provided the stimulus to the device under test (DUT). The test set module routed the stimulus signal to the DUT and sampled the reflected and transmitted signals. The frequency range of the source and test set modules established the frequency range of the system. Frequency conversion occurred in the analyzer. The analyzer module down-converted, received, and interpreted the IF signal for phase and magnitude data. It then displayed the results.

The two main modules of the HP8410 RF section included a sampler, used to convert the RF signals into lower frequency signals suitable for digital signal processing, and a synthesizer to provide the necessary excitation to the device under test. The RF heart of the HP8410 system was the HP8411A "Harmonic Converter." Instead of using a sampling pulse generator, the samplers were driven by a harmonic generator (via a SRD driven by a VCO). The harmonic converter relied on a variable frequency oscillator to generate har-

▲ *Fig. 2 The HP8410 network analyzer mainframe and various plug-in modules.*

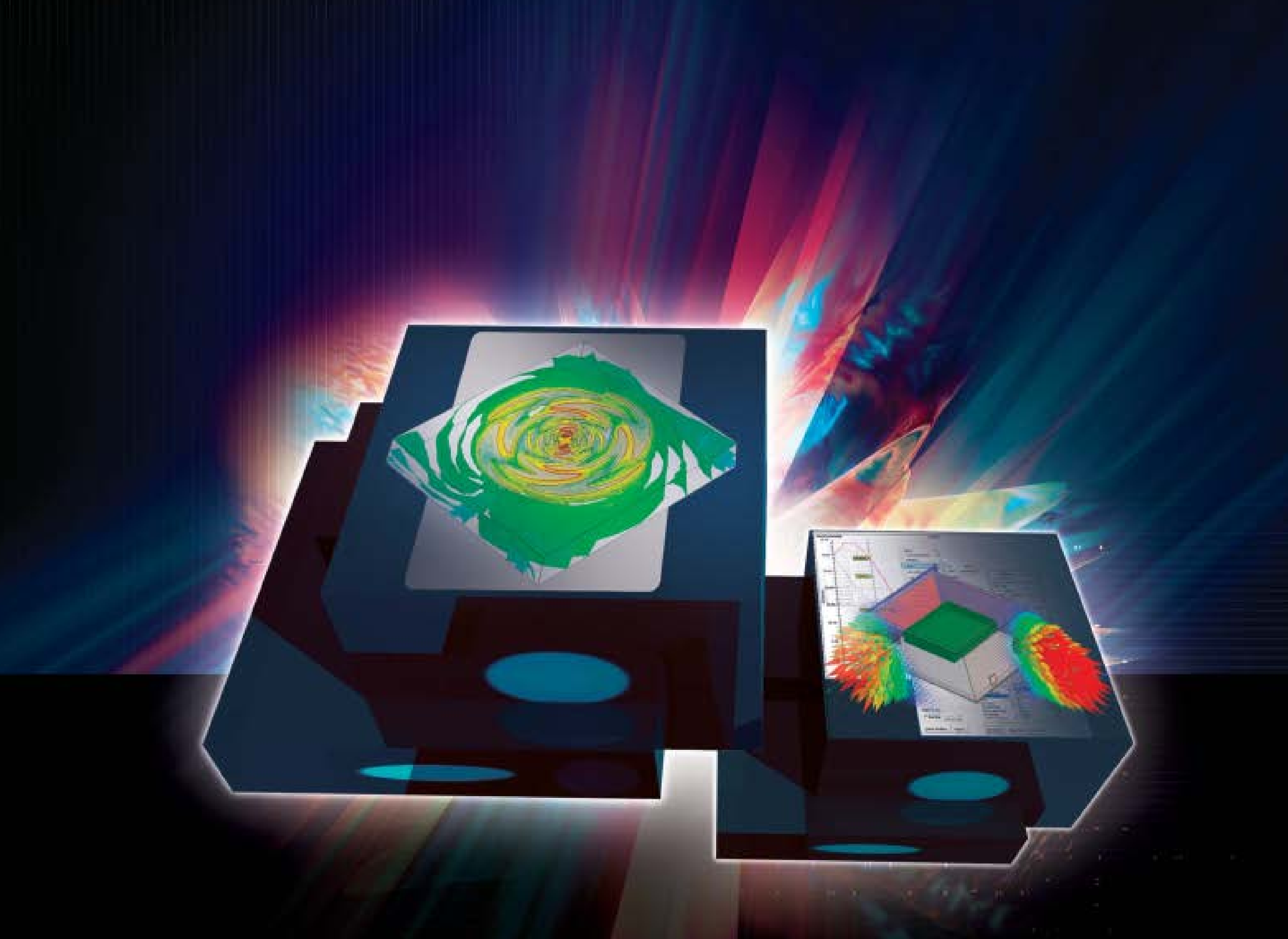

monics way up into the microwave region and act as the local oscillator to the reference and test mixers which in turn provided signal to the reference and test input ports. The down converted intermediate frequency was fed back into the HP8410 main frame. A socket on the front or rear panel of the network analyzer test set was available for adding a longer reference line to balance the phase (an important consideration for measuring phase linearity) associated with the electrical length of the DUT and the connecting coaxial test cable.

Octave band sweep oscillators using a backward wave oscillator (BWO) plug-in module drove the early test sets. The plug-in included a plastic ruler that snapped over the frequency pointers to give the user a rough idea of the frequency. A wave meter in series with the setup was often required to accurately know the frequency. A combiner box held the three plug-ins and a controller allowed sweeping across a frequency range covered by the three BWO modules. Solid-state sweepers would eventually be capable of sweeping greater frequency ranges.

▲ *Fig. 3 Faculty from the University of Washington, College of Electrical Engineering stands proudly by their newly donated HP8510 network analyzer, 1985.*

EARLY DISPLAYS

Unlike the sophisticated display technology of today, early data displays were rather crude and relied on various dedicated CRT hardware plug-ins. For instance, the Phase Magnitude Display was the display of choice for looking at gain or loss vs. frequency in real time. Grease pencils were often used to temporarily record a response during tuning or to indicate the pass/fail specification during production testing. The polar display CRT was useful for impedance measurements and matching. Smith chart overlays of different magnifications were available to translate trace position into impedance values. The Phase Gain Indicator meter was another popular display, allowing users to expand the meter scales for more resolution during manual measurements.

COMPUTERS: DISRUPTIVE TECHNOLOGY—1970s STYLE

S-parameters and the network analyzer led to more bench-top tuning and improved design efficiency via build and test prototyping. As the network analyzer became a design tool, greater accuracy (error-correction) and increased data collection was needed. By the late 1970s and early 1980s, computers (especially the PC) were often used to expand instrument capabilities. Computer-

controlled network analyzers such as the HP8542 introduced error correction mathematics, pulsed measurements, "large-scale" production testing and other capabilities to this test system. Many engineering groups developed their own computer-controlled systems based on need and desire to improve the software and/or calibration methods.

Due to the electrical characteristics of the cables and fixturing that supplies the signal to the DUT, there will be electrical delays and losses between the reference and test signals that are not contributed by the DUT. These effects must be calibrated out of the measurement before any accurate data can be retrieved. For phase vs. frequency measurements, early network analyzers used an extended coax reference line to equalize the signal with the length of the test arm. Software and computer-controlled network analyzers, however, provided a far superior approach to handling the path length differences and system losses.

Despite the improved accuracy and automation made possible by computer control, these early systems were large, containing up to three racks of equipment. Eventually, network analyzers would realize all of this capability in a single bench-top box including a synthesized source, receivers, test set and display thanks to solid-state sources, improved samplers and microprocessors. Network analyzers of the mid-1980s (see ***Figure 3***) fueled the microwave component development and manufacturing that coincided with the high-levels of avionics and radar activity taking place during the Reagan administration. The first fully error-corrected RF network analyzer offering lower cost and higher capability came to market just as the manufacturing demands for the first generation of cell phones was growing (see ***Figure 4***). Meanwhile the RF semiconductor technology that was made possible by the network analyzer was also being used to build the next generation of test equipment.

ADDRESSING THE WIRELESS MARKET

The early 1990s ushered in the wireless device boom and the first high frequency consumer market. Communication devices and their components (RFICs/MMICs, discrete and hybrid modules) would not only need to support complex performance brought on by digital modulation techniques, they would also be subject to cost pressures and high volume manufacturing. Many mobile communications systems would use time-domain duplexing leading to the need for pulsed measurements. Many devices also included frequency conversion devices, as well as balanced

Fig. 4 An early RFIC test station for high volume production.

inputs or outputs. Such devices required more than two excitation ports. Frequency conversion devices such as mixers required a network analyzer with a frequency-offset mode to allow the source stimulus and the response receivers in the analyzer to be independently tuned to different frequencies. All of these challenges had to be met without giving up fast measurement throughput and dynamic range. The network analyzer would evolve once again to meet these challenges.

By the late 1990s the nature of commercial RF components changed in several significant ways. Circuits started using balanced (differential) topologies in order to take advantage of lower power requirements and higher isolation. A key improvement for testing these devices came in 2001 with the introduction of Agilent's ENA (E5071A), the first four-port network analyzer designed for the mass production market (see **Figure 5**). In addition to differential I/Os, new and highly integrated devices at both the chip and package level resulted in a large number of input/output (I/O) ports. Measuring the performance of individual IC elements, particularly with respect to isolation became a challenge. As the number of required measurements grew by N-squared (N represents the numbers of ports), characterizing higher port devices with existing VNAs became impractical.

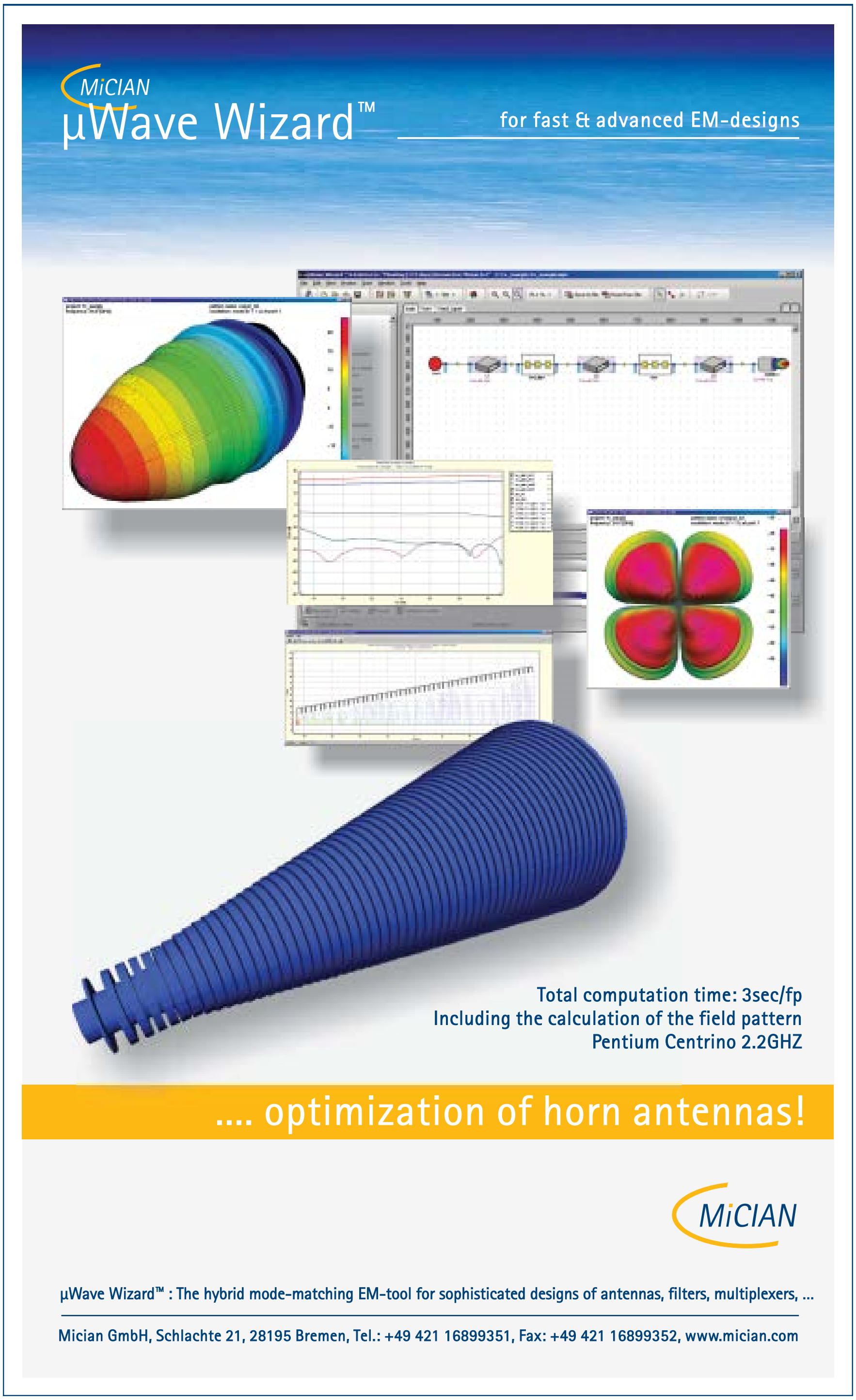

DIFFERENTIAL I/OS AND MULTI-PORT DEVICES

The next generation of test sets to be introduced extended the port count of the network analyzer even further. These N-port systems use internal switches and couplers to seamlessly integrate the test set with the analyzer giving the N-port test set a level of performance that is directly comparable to that of two- or four-port systems. There are eight- and 12-port versions of N-port network analyzers currently available, with 16- and 32-port systems soon to follow.

All major VNA manufacturers (Agilent, Anritsu, Rohde & Schwarz) today offer multi-port systems for characterizing devices such as diplexers, circulators, directional couplers, differential transmission lines and active components such as mixers. Calibrating a multi-port instrument can be time-consuming if done conventionally. Therefore, techniques have been developed to greatly shorten the calibration process, including the use of electronic calibration modules, which provide a full NxN matrix of calibrated measurements with only N-connection steps.

Auto-calibration modules provide fast, repeatable and high quality coax-

▲ *Fig. 5 Agilent's ENA (E5071A), the first four-port network analyzer designed for the mass production market.*

▲ *Fig. 6 On-wafer measurements to 500 GHz with the ME7808C from Anritsu.*

ial calibrations. Test port cable converter kits also allow a single module to calibrate insertable and non-insertable devices. However, most semiconductor measurements today are performed while the devices are still in wafer form. The development of the wafer probe from Cascade Microtech was instrumental in allowing VNA measurements to be performed at the chip level, eliminating the need to place a device in a package and test fixture. RF wafer probes allow the excitation and measurement of closely located device ports. Combined with the automated probe station, today's chip testing is quite sophisticated, supporting research and development as well as high-volume production testing (see ***Figure 6***).

COMBINING THE NETWORK ANALYZER WITH OTHER MEASUREMENT SYSTEMS

RF semiconductor devices must work over a wider range of operating conditions than 50 years ago. To keep pace with the device requirements, test systems are integrating more functionality, supporting multiple tests such as large-signal S-parameters, power and spectral measurements for CW and pulsed operations all with a single device connection. Because the network analyzer also corrects for mismatches between the DUT and test equipment, combining it with more complex stimulus-response test systems offers more accurate results. Network measurement systems can now also address large-signal and pulsed operations. In 2007, Rohde & Schwarz introduced the first measurement system to combine a full-featured vector network analyzer with a spectrum analyzer in a single portable instrument that can perform both reflection and spectral measurements such as adjacent-channel power or third-order intercept, as well as measurement of UMTS, WLAN, or WiMAX signals. The optional spectrum analysis capability also supports phase noise, noise figure and high-accuracy power measurements.

LARGE-SIGNAL MEASUREMENTS

Transistors used in RF and microwave applications must be characterized dynamically (large-signal operation) in order to determine compression characteristics, intermodulation and spectral re-growth. A nonlinear network measurement system is a stimulus/response system, similar to a vector network analyzer but used to characterize the large-signal device behavior completely under a periodic stimulus (see ***Figure 7***).

The system includes a test set to separate incident and reflected waves. A microwave source injects a signal into the DUT. If this component is nonlinear, it will generate har-

monics. These harmonics are reflected back by the mismatch created by the measurement system. A broadband acquisition system is able to take proper samples of the broadband incident and reflected waves. The systematic errors of the measurement system are eliminated using proper calibration techniques. The complete spectrum (amplitude and phase) of incident and reflected waves can be acquired and the time waveforms reconstructed.

These same network measurement systems can also be used to determine power performance while accounting for test system/DUT impedance mismatches. Many VNAs have built-in capabilities for analyzing specific device performance metrics. For example, the Anritsu 37000D VNA provides an automated power flatness calibration program for characterizing test port power. By providing flat output power from the analyzer test port over the frequency range, this system allows optimum swept frequency gain compression measurements. When calibrated with the Anritsu ML24XX series power meters, the calibration routine automatically stores a power correction table in the analyzer for later recall. The result is a vector network analyzer with high power at the test port and power meter accuracy. Capabilities such as this use to be the realm of custom built systems and software developed in-house.

BALANCED LARGE-SIGNAL MEASUREMENTS

Options available for the R&S ZVA and ZVT analyzers with three or more ports introduced "true" differential VNA measurements, providing accurate results for balanced active devices operating under large-signal conditions. The option also allows two signals to be generated, with 0° or 180° of phase shift, to produce true common-mode or differential mode measurements with a conventional single-ended VNA. The phase shift does not vary with time and temperature variations, a significant breakthrough in itself, since it is one of the primary reasons why this technique could not be achieved previously. The sources are controlled with a special algorithm and control circuitry that precisely maintains the magnitude/phase relationship. Traditionally, balanced devices measured in the nonlinear large-signal region almost invariably overstated device performance. As a result, manufacturers would specify their products inaccurately.

Using the true differential technique, gain compression may occur at lower drive levels than when measured using the conventional technique. The result is that amplifiers will produce unacceptable levels of intermodulation products under conditions that were previously thought to meet specifications. Testing with differential inputs under large-signal conditions allows manufacturers to specify their parts conservatively ensuring they will meet their rated performance under actual operating conditions. This nonlinear region is of vital interest to the device designers employing the orthogonal frequency division multiplex (OFDM) modulation technique, such as WiMAX, lightwave communications and cable systems in order to ensure extraordinarily high levels of linearity. In addition, when the Long Term Evolution (LTE) enhancement to UMTS wireless systems is deployed in a few years, it too will require the same level of linearity.

PULSED MEASUREMENTS

In many mobile communications systems and radar applications, devices must often be characterized with a pulsed RF signal or a pulsed control voltage. With pulsed stimulus signals, S-parameters can be measured at the correct drive without exceeding destructive power or temperature levels. By using an appropriate duty cycle, the average power can be reduced significantly while maintaining a high peak power. In addition, many components for radar systems only exhibit their desired performance and effectiveness under pulsed stimulus conditions. The VNA measures the effect that the DUT has on the pulsed stimulus. Since the VNA performs ratio measurements, any non-ideal behavior of the pulses themselves is removed from the measurement.

The point-in-pulse measurement enables accurate S-parameter and power measurements by shifting the moment of data acquisition within the pulse. This technique eliminates the dependency of dynamic range on duty cycle; however, it does require a VNA with a wide measurement bandwidth. Using the point-in-pulse measurement technique, the pulse is monitored only during the "on" phase of the RF bursts so the sampling time (T_{spl}) to acquire the raw data of a wave quantity or an S-parameter must be shorter than the pulse width, t_{on} (see ***Figure 8***).

By selecting a suitable trigger delay, the start of the sampling process can be shifted by the designer to the point of interest such as the quiet "pulse roof" of the active device. Dynamic range and sensitivity using the point-in-pulse method depends on sensitivity and the measurement bandwidth of the receivers, which are independent of the duty cycle of the RF pulse. Consequently, dynamic range depends on pulse width, which limits sampling time and thus the required measurement bandwidth. Averaging can be applied to increase dynamic range by maintaining the measurement bandwidth.

To analyze the time-dependent behavior of a device during a burst, the VNA must perform a so-called "pulse profile" measurement (see ***Figure 9***). The pulse profile method can be performed with most VNAs in conjunction with an external setup for pulse profile measurements. Disadvantages include the inability to analyze non-periodic pulses, double

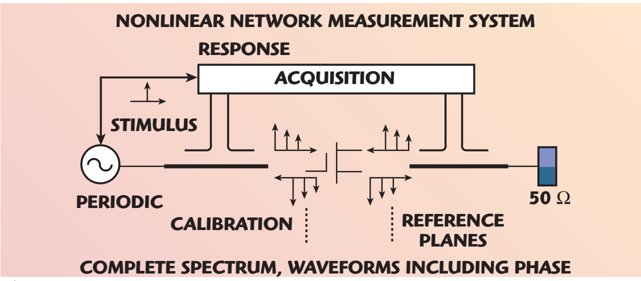

▲ *Fig. 7 Components of a single-port nonlinear network measurement system.*

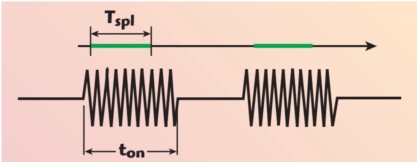

▲ *Fig. 8 Sampling time for point-in-pulse measurements.*

pulses, pulse trains, or complex modulated pulsed signals. The technique requires recalibration with a change of duty cycle, suffers from low dynamic range for low duty cycles and requires high resolution, which results in low measurement speed.

Rohde & Schwarz employs wideband detection and fast data recording to improve pulse profile measurements (see ***Figure 10***). Pulse profile analysis or S-parameter measurements with pulsed stimulus is limited by the sampling rate of the A/D converter, the processing time between two consecutive data points and the available bandwidth. Sampling rate and data processing time between two data points limit the time resolution, while the measurement bandwidth determines the minimum rise and fall time of the pulse that can be analyzed. Options for select VNAs reduce bottlenecks by uncoupling the data acquisition process from the data processing step in order to make pulse profile measurements with high resolution at high speed. The R&S approach is to sample the raw data and store it directly without filtering, allowing the instrument firmware to immediately perform the digital down-conversion and filtering. An A/D converter continuously samples and digitizes the data at 80 MHz and writes it into high-speed RAM. The technique produces fast yet detailed and accurate pulsed profiling. It combines fast throughput (more than 10 sweeps/s over 1001 test points) with time pulse resolution of 12.5 ns/point.

The PNA-X Series of VNAs from Agilent Technologies can supply either a CW or pulsed stimulus and accurately measure the CW or pulsed responses. The pulse-measurement timing is generated by an integrated pulse generator, which has four main output channels, each with independent delay and width. The output channels can be routed internally inside the PNA-X to drive the modulators and acquisition circuitry, and/or externally to drive external peripheral devices. Since these pulse generators are independent of the measurement channels, each measurement channel can have independent pulse generator setting. This allows the simultaneous measurement and display of a variety of measurements, including pulse-profiling, point-in-pulse and gain compression on a single display.

The PNA-X VNA can make pulse measurements in wideband and nar-

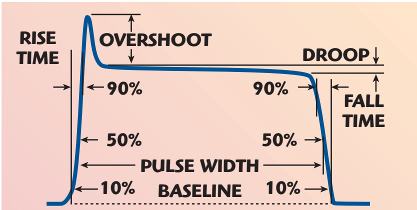

▲ *Fig. 9 A pulse waveform highlighting various time-dependent characteristics.*

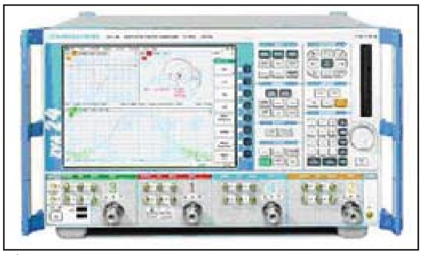

▲ *Fig. 10 The Rohde & Schwarz ZVA series VNA.*

rowband modes. The two modes have benefits and trade-offs. Modern VNAs such as the PNA-X include both detection modes so that operators have the flexibility to tailor their measurements to the characteristics of the DUT. Wideband detection is suitable for cases when the majority of the pulsed RF spectrum falls within the bandwidth of the VNA's receiver.

The advantage of the wideband mode is that there is no loss in dynamic range for low-duty-cycle pulses, with a relatively constant signal-to-noise ratio (SNR) versus duty cycle. The disadvantage is that there is a lower limit on measurable pulse widths. As a signal's pulse width becomes narrower, the spectral energy is spread over a wider bandwidth. When enough of the pulse's energy falls outside of the receiver's bandwidth, the receiver can no longer properly detect the pulse.

In narrowband detection mode, the pulse width is usually much less than the minimum time required to digitize and acquire one discrete data point. With this technique, the entire pulse spectrum is removed by filtering except the central frequency component, which represents the frequency of the RF carrier. After filtering, the pulsed RF signal appears as a sinusoid or CW signal. With narrowband detection, analyzer samples are not synchronized with the incoming pulses (therefore no synchronized measurement trigger is required), so the technique is also known as asynchronous acquisition mode. This approach is also called the "high PRF" mode because the PRF is usually high compared to the receiver's IF bandwidth.

CURRENT NETWORK ANALYZERS

What capabilities do today's network analyzers offer? Speedy measurements are paramount to collecting the vast amount of S-parameter data needed to represent high frequency semiconductors operating in the current generation of wireless devices. The latest VNAs offer impressive capabilities in the following areas:

- Performance—includes wide dynamic range, fast measurement speed (time for frequency sweep, switching times between channels and setups), high output power, wide power sweep range and accuracy
- Multi-port capability—includes two, four or more ports with direct access to all generator and receiver paths
- Versatility—includes advanced network measurement capabilities such as large-signal analyses, frequency converters, balanced circuit topologies, pulsed, intermodulation, hot S-parameters and integrated spectrum analysis
- Usability—powerful yet user-friendly interface for measurement control, custom automation and data visualization (post-processing functionality)
- Connectivity—and data acquisition via high speed data exchange (GPIB, USB and WLAN)
- Portability—vendors are now offering small, light, portable vector network analyzers suitable for field applications (calbe loss, distance-

to-fault, system frequency response, etc.)

CONCLUSION

For nearly 50 years, S-parameters and the network analyzer have been a fundamental source for characterizing component behavior. This measurement system made the evolution of the RF/microwave semiconductor possible to the extent that measurements played a critical role in component design. In turn, the VNA benefited directly from using the technology that it was responsible for measuring. This bootstrapping, which began 50 years ago, continues today. Wherever the need for stimulus/response characterization exists, the network analyzer will be there, measuring the attributes of new devices and materials, adapting to address the needs of new applications, operating conditions and parametric analyses. ■

For readers interested in keeping up with the latest advances in network analyzer technology, the manufacturers have excellent reading material on the current state of technology and measurement techniques. Some interesting material is listed below:

Agilent

Application Note 1408-12: Pulsed-RF S-parameter Measurements Using Wideband and Narrowband Detection, http://cp.literature.agilent.com/litweb/pdf/5989-4839EN.pdf.

Article reprint 5989-6353EN: http://cp.literature.agilent.com/litweb/pdf/5989-6353EN.pdf.

Anritsu

Application Note No. 11410-00387: Primer on Vector Network Analysis, http://www.us.anritsu.com/downloads/files/11410-00387.pdf.

Application Note No. 11410-00383: Power Measurements—Handheld Site Master™/VNA Master™/Spectrum Master™/ BTS Master™/Cell Master™ Products, http://www.us.anritsu.com/downloads/files/11410-00383.pdf.

Application Note No. 11410-00300: Pulsed S-parameter Measurements, http://www.us.anritsu.com/downloads/files/11410-00300.pdf.

Application Note No. 11410-00329: S-parameter Measurements with Multiport Balanced Test Sets, http://www.us.anritsu.com/downloads/files/11410-00329.pdf.

Application Note No. 11410-00197: Measuring Frequency Conversion Devices, http://www.us.anritsu.com/downloads/files/11410-00197.pdf.

Rohde & Schwarz

Application Note 1MA124_0E: Tackling the Challenges of Pulsed Signal Measurements, http://www.rohde-schwarz.com/appnote/1MA124.html.

Application Note 1EF48: Power Measurement on Pulsed Signals with Spectrum Analyzers, http://www.rohde-schwarz.com/appnote/1EF48.html.

Application Note 1EZ52: Antenna Measurements, RCS Measurements and Measurements on Pulsed Signals with Vector Network Analyzers R&S ZVM, R&S ZVK, http://www.rohde-schwarz.com/appnote/1EZ52.html.

Application Note 1MA32: Noise Figure Measurements on Amplifiers in Pulsed Mode, http://www.rohde-schwarz.com/appnote/1MA32.html.

Additional VNA Information Featured in March at www.mwjournal.com

Expert Advice

Dr. Joel Dunsmore, senior R&D engineer/scientist with Agilent Technologies, discusses the enhancements and trade-offs that enable VNAs to move beyond S-parameters, and the improvements in these measurements brought about by extending the calibration capabilities of VNAs into other measurement classes.

Retrospective

Michael Hiebel, from Rohde & Schwarz and author of *Fundamentals of Vector Network Analysis*, gives a European perspective of the development of VNAs from the days of the slotted line, to the present day and beyond as he identifies potential future developments.

Broadband Amplifiers by AML Communications

To Order Call: (805)388-1345 ext. 203

Model	Frequency (GHz)	Gain (dB)	Flatness (dB) max	NF (dB) max	P1dB (dBm) min	VSWR (In/Out)	DC Current @ +12/+15VDC
Broadband Low Noise Amplifiers							
AML016L2802	0.1 – 6.0	28	±1.25	1.3*	+7	2.0:1	190
AML48L3001	4.0 – 8.0	30	±1.0	1.2	+10	1.8:1	150
AML412L3002	4.0 – 12.0	30	±1.5	1.5	+10	1.8:1	150
AML218L0901	2.0 – 18.0	9	±1.0	2.2	+5	2.5:1	60
AML0518L1601-LN	0.5 – 18.0	16	±1.0	2.7	+8	2.2:1	100
AML0126L2202	0.1 – 26.5	22	±2.25	3.5*	+8	2.2:1	170
AML1226L3301	12.0 – 26.5	33	±2.0	2.8	+8	2.5:1	200
Broadband Medium Power Amplifiers							
AML0016P2001	0.01 – 6.0	21	±1.25	3.2*	+23*	2.0:1	480
AML26P3001-2W	2.0 – 6.0	28	±2.5	6	+33	1.8:1	1500
AML28P3002-2W	2.0 – 8.0	30	±2.0	5.5	+33	2.0:1	2000
AML218P3203	2.0 – 18.0	32	±2.5	4	+25	2.0:1	450
AML618P3502-2W	6.0 – 18.0	35	±2.5	4	+33	2.0:1	1850
Narrow Band Low Noise Amplifiers							
AML23L2801	2.8 – 3.1	28	±0.75	0.7	+10	1.8:1	150
AML1414L2401	14.0 – 14.5	24	±0.75	1.5	+10	1.5:1	130
AML1718L2401	17.0 – 18.0	24	±0.75	1.6	+10	1.8:1	150

Low Phase Noise Amplifiers — Phase noise (dBc/Hz) at offset

Part Number	Frequency (GHz)	Gain (dB)	Output Power (dBm)	100Hz	1KHz	10KHz	100KHz
AML811PN0908	8.5 – 11.0	9	17	-154	-159	-167	-170
AML811PN1808	8.5 – 11.0	18	18	-152.5	-157.5	-165.5	-168
AML811PN1508	8.5 – 11.0	15	28	-145.5	-153.5	-158.5	-164.5
AML26PN0904	2.0 – 6.0	9	20	-150	-165	-165	-178
AML26PN1201	2.0 – 6.0	11	15	-155	-160	-160	-175

High Dynamic Range Amplifiers

Part Number	Frequency (MHz)	Gain (dB)	P1dB (dBm)	OIP3 (dBm)	DC
AR01003251X	2 – 32	21	32	52	+28V @ 470mA
AFL30040125	50 – 500	23	28	53	+28V @ 700mA
BP60070024X	20 – 2000	32	30	43	+15V @ 1100mA

*Above 500MHz.

Power Amplifiers by Microwave Power

To Order Call: (408)727-6666 ext. 42

Model	Frequency (GHz)	Psat (dBm)	Psat (W)	P1dB (dBm)	Gain (dB)	DC Current(A) @ +12V or +15V
Broadband Microwave Power Amplifiers						
L0104-43	1 - 4	42.5	17.8	41.5	45	14
L0204-44	2 - 4	44	25	42.5	45	14
L0206-40	2 - 6	40	10	38.5	40	8.5
L0208-41	2 - 8	41	12	40	40	17
L0218-32	2 - 18	32	1.4	31	35	5
L0408-43	4 - 8	43	20	41.5	45	17
L0618-43	6 - 18	43	20	41.5	45	22
L0812-46	8 - 12	46	40	45	45	28
Millimeter-Wave Power Amplifiers						
L1826-34	18 - 26	34	2.5	33	35	4
L1840-27	18 - 40	27	0.5	26	30	2
L2240-28	22 - 40	28.5	0.7	27	30	3
L2630-39	26 - 30	39	8.0	38	40	15
L2632-37	26 - 32	37	5.0	36	38	10
L2640-31	26 - 40	31	1.2	30	30	5
L3040-33	30 - 40	33	2.0	32	33	9
L3337-36	33 - 37	36	4.0	35	40	12
L3640-36	36 - 40	36	4.0	35	40	10

High-Power Rack Mount Amplifiers

Model	Frequency (GHz)	Psat (dBm)	Psat (W)	P1dB (dBm)	Pac (kW)	Height (in)
C071077-52	7.1 - 7.7	52.5	170	51.5	1.8	10.25
C090105-50	9 - 10.5	50	100	49	1	8.75
C140145-50	14 - 14.5	50.5	110	49.5	2	10.25
C1416-46	14 - 16	46	40	45	0.35	5.25
C1820-43	18 - 20	43	20	41.5	0.25	5.25
C2326-40	23 - 26	40	10	39	0.25	5.25
C2630-45	26 - 30	45	30	44	0.45	5.25
C3236-40	32 - 36	40	10	39	0.25	5.25
C3640-39	36 - 40	39	8	38	0.24	5.25

AML Communications

Camarillo, CA (805)388-1345 ext. 203

Over 1000+ amplifiers at

www.amlj.com

Look for some serious power at

www.microwavepower.com

Microwave Power

An AML Communications Company

Santa Clara, CA (408)727-6666 ext. 42

Visit http://mwj.hotims.com/16339-12 or use RS# 12 at www.mwjournal.com/info

Delivery From Stock!

MIXERS

Model Number	RF/LO Frequency (GHz)	IF Frequency (GHz)	LO Power (dBm)	Conversion Loss (dB) Typ./Max.	LO-to-RF Isolation (dB) (Min.)
DOUBLE-BALANCED VERSIONS					
DM0052LA2	0.5 – 2	DC – 0.5	7 – 13	6.5/8.5	30
DM0104LA1	1 – 4	DC – 1	7 – 13	5.5/7.0	30
DM0208LW2	2 – 8	DC – 2	7 – 13	7.0/8.0	30
DM0416LW2	4 – 16	DC – 4	7 – 13	7.0/8.0	30
DB0218LW2	2 – 18	DC – 0.75	7 – 13	6.5/8.5	22
DB1826LW1	18 – 26	DC – 2	7 – 13	7.5/9.5	20
DB0226LA1	2 – 26	DC – 0.5	7 – 13	9.0/10	20
DB0440LW1	4 – 40	DC – 2	10 – 15	9.0/10	20
M1826W1	18 – 26	DC – 8	10 – 15	9.0/12	25
M2640W1	26 – 40	DC – 12	10 – 15	10/12	28
TRIPLE-BALANCED VERSIONS					
TB0218LW2	2 – 18	0.5 – 8	10 – 15	7.5/9.5	20
TB0426LW1	4 – 26	0.5 – 8	10 – 15	10/12	20
TB0440LW1	4 – 40	0.5 – 20	10 – 15	10/12	18

PASSIVE DOUBLERS

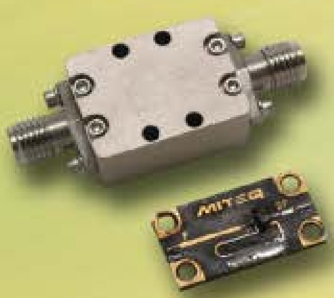

Model Number	Input Frequency (GHz)	Input Power (dBm)	Output Frequency (GHz)	Conversion Loss (dB) Typ./Max.	Rejection (dBc, Typ.) Fund.	Rejection (dBc, Typ.) Odd Harm.
DROP-IN VERSIONS						
SXS01M	0.5 – 3	8 – 12	1 – 6	13/16	-20	-25
SXS04M	2 – 9	8 – 12	4 – 18	13/15	-20	-25
SXS07M	3 – 13	8 – 12	6 – 26	13/17	-18	-25
CONNECTORIZED VERSIONS						
SXS2M010060	0.5 – 3	8 – 12	1 – 6	13/16	-20	-25
SXS2M040180	2 – 9	8 – 12	4 – 18	13/15	-20	-25
SXS2M060260	3 – 13	8 – 12	6 – 26	13/17	-18	-25

Additional models available with 60 day lead time, please contact MITEQ.
Above models also available with optional LO power ranges, please contact MITEQ.

Fastest Delivery Available! + 3 YEAR WARRANTY = MITEQ

30 Day Delivery!

IMAGE REJECTION MIXERS

Model Number	RF/LO Frequency (GHz)	Conversion Loss (dB) Max.	Image Rejection (dB) Min.	LO-to-RF Isolation (dB) Min.
IMAGE REJECTION MIXERS				
IRM0204(*)C2(**)	2 – 4	7.5	18	20
IRM0408(*)C2(**)	4 – 8	8	18	20
IRM0812(*)C2(**)	8 – 12	8	18	20
IRM1218(*)C2(**)	12 – 18	10	18	20
IRM0208(*)C2(**)	2 – 8	9	18	18
IRM0618(*)C2(**)	6 – 18	10	18	18
IR1826NI7(**)	18 – 26	10.5	15	20
IR2640NI7(**)	26 – 40	10.5	15	15

Model Number	RF/LO Frequency (GHz)	Conversion Loss (dB) Max.	Balance Phase (±Deg.) Typ./Max.	Balance Amplitude (±dB) Typ./Max.	LO-to-RF Isolation (dB) Min.
I/Q DEMODULATORS					
IRM0204(*)C2Q	2 – 4	10.5	7.5/10	1.0/1.5	20
IRM0408(*)C2Q	4 – 8	11	7.5/10	1.0/1.5	20
IRM0812(*)C2Q	8 – 12	11	5/7.5	.75/1.0	20
IRM1218(*)C2Q	12 – 18	13	10/15	1.0/1.5	20
IRM0208(*)C2Q	2 – 8	12	7.5/10	1.0/1.5	18
IRM0618(*)C2Q	6 – 18	13	10/15	1.0/1.5	18
IR1826NI7Q	18 – 26	13.5	10/15	1.0/1.5	20
IR2640NI7Q	26 – 40	13.5	10/15	1.0/1.5	15

SSB UPCONVERTERS OR I/Q MODULATORS

Model Number	RF Frequency (GHz)	Conversion Loss (dB) Max.	Carrier Suppression (dBc) Min.	Carrier Suppression Carrier - Fundamental IF (dBc) Min.
IF DRIVEN MODULATORS				
SSM0204(*)C2MD(**)	2 – 4	9	20	20
SSM0408(*)C2MD(**)	4 – 8	9	20	18
SSM0812(*)C2MD(**)	8 – 12	9	20	20
SSM1218(*)C2MD(**)	12 – 18	10	20	18
SSM0208(*)C2MD(**)	2 – 8	9	20	20
SSM0618(*)C2MD(**)	6 – 18	10	20	18

For full data sheets on the products shown, please visit www.miteq.com/adinfo

For Carrier Driven Modulators, please contact MITEQ.

MODEL NUMBER OPTION TABLE

(*) Add Letter	LO/IF Power Range	P1 dB C.P. (dBm) (Typ.)
L	10 – 13 dBm	+6
M	13 – 16 dBm	+10
H	17 – 20 dBm	+15

(**) Add Letter	IF FREQUENCY OPTION (MHz)
A	20 – 40
B	40 – 80
C	100 – 200
Q	DC – 500 (I/Q)

For additional information or technical support, please contact our Sales Department at (631) 439-9220 or e-mail components@miteq.com

MITEQ®

100 Davids Drive, Hauppauge, NY 11788
(631) 436-7400 FAX: (631) 436-7430
www.miteq.com

Northrop Grumman Demonstrates New Synthetic Aperture Radar

Northrop Grumman Corp. has successfully demonstrated the capability to generate high-resolution, in-flight synthetic aperture radar (SAR) maps using the AESA (active electronically scanned array) radar being produced for the US Air Force's F-22 Raptor fighter aircraft.

"The flight tests, on board a company BAC 1-11 test bed aircraft, have proved that the F-22 fighter's mission capabilities have expanded to include directly identifying and targeting enemy ground defenses and mobile forces," said Teri Marconi, vice president of Combat Avionics Systems at Northrop Grumman. "This is a hugely significant event for the F-22 program because it ensures that Raptor pilots will have access to critical detailed information about both air and ground threats before the enemy's radar ever detects the F-22."

The test flights are the first phase of a planned multi-year contract with the Boeing Co. to incorporate SAR capability into the existing fleet of F-22s and new production aircraft in support of future air-to-ground requirements. Northrop Grumman's Electronics Systems sector leads a joint venture with the Raytheon Co. to design, develop and produce the F-22 radar system. Northrop Grumman is responsible for the overall design of the AN/APG-77 and AN/APG-77(V) 1 ARSA radars, the latter of which features the new air-to-ground capabilities, including SAR. The company is also responsible for the control and signal processing software and radar system integration and test activities.

The Boeing Co., which is teamed with the prime contractor Lockheed Martin Corp. and Pratt & Whitney to design and build the F-22 Raptor, has responsibility for integrating the radar with the other avionics systems to produce an integrated suite that features sensor-fused target detection and tracking.

Harris Corp. Introduces First Multiband Radio for Federal Agencies

Harris Corp., an international communications and information technology company, introduced the first multiband land mobile radio that provides real-time interoperable communications for the growing federal public safety and homeland security market. Public safety communications interoperability has been identified by Congress, the National Governor's Association, the US Conference of Mayors and the 9/11 Commission as an urgent national priority and is a principal focus of the Department of Homeland Security.

"The Harris Land Mobile radio allows federal agency personnel to talk to first responders and homeland security personnel—whenever they need to—without having to carry multiple radios," said Dana Mehnert, president, Harris RF Communications. "By enabling communications interoperability, our customers are much better equipped to effectively coordinate emergency response and joint operations."

"The federal agency market for land mobile radios is a natural expansion into an adjacent market, a market we believe is more than $600 M and growing. Expanding into adjacent markets is one of our core strategies. We will continue to invest in new product development and apply our extensive experience with defense and government customers throughout the world to broaden our opportunities."

The new Harris RF-1033M land mobile radio is the first product to provide homeland security and other public safety officials with direct, secure multi-agency communications across multiple frequency bands. The radio covers VHF and UHF frequency bands, providing true multiband, multimission capabilities for public safety communications.

Land mobile radios today are limited to single frequency bands, making it difficult for federal agencies and local public safety officials to talk to each other—a problem highlighted during national emergencies such as the San Diego wild fires and Hurricane Katrina. Interoperability today is typically obtained only through an ancillary system of equipment.

The new radio is compliant with APCO Project 25, the technical standard for digital public safety radio communications developed by the Association of Public Safety Communications Officials. Because the new Harris Land Mobile Radio is software-defined, it is adaptable to evolving technical standards and changing mission requirements. The radio leverages Harris leadership in software-defined, multiband handheld communication products, which are used extensively around the world.

Saab Inks $310 M Deal for Thai Air Defense, Gripens

Following Thailand's purchase of an integrated air surveillance system from Sweden in a government to government deal, FMV, the Swedish Defense Material Administration, has placed a contract with Saab valued at $310 M for the development and production of the systems. Deliveries will take place during 2011.

The order comprises six Gripen fighters of the C/D version, two Saab 340 aircraft, of which one will be equipped with the company's radar surveillance system Erieye, and associated equipment and services. Also included in the agreement is a command and control system, which will be the link between the Erieye system and the Gripen fighters. The complete system will be used for air surveillance and protection of Thailand's territory.

Saab CEO, Åke Svensson, stated, "This further strengthens Gripen's position on the export market. There is a great interest for Gripen today and several important export deals will be settled within the next few years. This agreement also strengthens our position within the area of airborne surveillance and advanced command and control systems."

Lockheed Martin Receives $194 M Contract for Army Tactical Missile System

Lockheed Martin has received $194 M from the US Army Aviation & Missile Command for production of the combat-proven Army Tactical Missile System (ATACMS). Work will be conducted at the company's facilities in Dallas and Horizon City, TX, with completion expected by the second quarter of 2010.

The contract includes the ATACMS Quick Reaction Unitary and the Block IA Missiles. ATACMS is the world's premier long-range missile artillery round designed specifically for destroying high-priority targets at ranges up to 300 kilometers. Able to deliver a wide variety of warhead options, it can operate in all climate and light conditions while remaining beyond the range of most conventional weapons.

"Combat-proven ATACMS adds to the concept of 'joint fires interdependence' by offering the right munition to achieve the right effect at the right time, regardless of the color of the uniform you're wearing," said Col. Gary S. Kinne, Training and Doctrine Command Capabilities Manager for Rocket and Missile Systems at Fort Sill, OK. "The Army's first surface-to-surface, long-range, all-weather, precision attack capability used in combat, ATACMS provides the Joint Force Commander an immediately available, lethal asset to attack time-sensitive and high value stationary or fixed targets in both open and constrained environments (complex/urban terrain)."

During the first Operation Desert Storm, ATACMS became the first tactical surface-to-surface missile ever fired in combat by the US Army. ATACMS is an evolutionary family of missiles that scored numerous successes again in Operation Iraqi Freedom, during which 456 missiles were fired.

"ATACMS is performing excellently for our Warfighters," said Jim Gribschaw, director of Precision Fires at Lockheed Martin Missiles and Fire Control. "A veteran of many battles, ATACMS is indispensable to the present fight, and gives commanders the ability to accurately engage the enemy at depth on the battlefield. And ATACMS's pinpoint accuracy helps minimize collateral damage."

Each ATACMS missile is approximately 13 feet long, two feet in diameter and has a range of up to 300 kilometers. A single ATACMS missile can defeat company-size targets beyond the range of current Army cannons and rockets. The first launch of an ATACMS missile was April 26, 1988, at White Sands Missile Range, NM. ■


GPS FILTERS
www.reactel.com/gps
GPS Notch Filter
Ceramic
GPS Filters
GPS Diplexers
GPS Bandpass Filter
GPS Dual Filter
RoHS
Compliant
Reactel, Incorporated • Phone: (301) 519-3660 • Fax: (301) 519-2447 • reactel@reactel.com
Visit http://mwj.hotims.com/16339-112 or use RS# 112 at www.mwjournal.com/info

IET and IoN Create MNT Network

The Institution of Engineering and Technology (IET) and the Institute of Nanotechnology (IoN) are to create a joint Microsystems and Nanotechnology (MNT) Network to share knowledge and promote the understanding and application of nanotechnology. The Network will develop both virtual activities and live events, and will draw on the strengths and skills of both organisations and their members. A joint IET/IoN Executive Team consisting of experts in the field from both industry and academia has been established that will outline the scope of the MNT Network, set its objectives and develop the programme for the future.

The IET, which currently operates a Microsystems and Nanotechnology Network, is looking to revitalise its activities in the nanotechnology space. Similarly, the IoN firmly believes that by uniting the extensive network of members of both bodies, a substantial community of interest will be created, accelerating the progress of nano and micro technologies to the benefit of the UK.

Robin McGill, chief executive of the IET, commented: "This is an exciting joint initiative in a fast growing and very important area of technology. This is the latest of a series of collaborations designed to broaden the technological footprint of the IET."

Ottilia Saxl, chief executive officer of the IoN, said: "By bringing together the members of the IET and IoN that share a common interest in nano and micro technologies, we will create a group of highly qualified individuals who will not only learn about leading-edge developments in this fast growing field, but will also contribute to them."

EADS Has Designs on HAI Centre

EADS and Hellenic Aerospace Industry (HAI) have signed an agreement valued at €9.7 million for the development of HAI's design centre. HAI is generating the design centre programme with the support of the Greek Ministry of Defence and through this agreement with EADS the company will obtain all the essential technological infrastructure and know-how necessary to establish an essential facility.

The design capability that this new centre offers will facilitate the company's transformation from an air structure part builder to a company capable of designing, manufacturing and supporting aerostructure products. This new capability will offer HAI excellent prospects for future growth and will increase the company's competitiveness. Furthermore, HAI will have the opportunity to participate in collaborations and consortiums worldwide as a strategic partner in the designing and development sectors such as research and technology.

Bernhard Gerwert, CEO of Military Air Systems, an integrated business unit of EADS Defence & Security, said: "EADS will support HAI to acquire its own design capability in true partnership. This is a significant step forward for HAI and will not only improve its competitiveness but will also expand its potential for future business activities."

Ceragon Demonstrates PBB-TE Over Microwave

Ceragon Networks has joined forces with industry leaders to successfully demonstrate Provider Backbone Bridges-Traffic Engineering (PBB-TE) protection over an adaptive modulation packet microwave, thus setting a new milestone for enabling carrier-grade Ethernet services in mobile backhaul networks with high capacity microwave.

The demonstration centres on the advanced FibeAir IP-MAX2 platform with its adaptive modulation capabilities that offer multiple service profiles over a single radio link. By enabling carrier-grade services over microwave the company paves the way for migrating these networks to cost efficient carrier Ethernet.

Aviv Ronai, chief marketing officer at Ceragon, commented: "As more and more operators are looking to IP/Ethernet-based backhaul solutions, powering them with true carrier-grade quality solutions becomes a major competitive differentiator."

NextWave and EB Collaborate on Mobile WiMAX

Elektrobit (EB) and NextWave Wireless Inc. are collaborating to bring one of the first commercial mobile WiMAX handset reference designs to the global market for wide-scale deployment. Together, the partners will provide wireless device manufacturers the opportunity to bring mobile WiMAX products to market faster and with lower development costs.

Core to this cooperation are innovations such as cutting-edge 4G wireless silicon from NextWave, and compact handset form factor and unique reference design integration expertise from EB. This synergy enables rich capabilities, including carrier-grade VoIP and high-speed multimedia services on a consumer-friendly device.

The handset reference design has been developed to provide customers with an ultra-low-power, integrated mobile WiMAX solution for improved performance, reduced power consumption, advanced multimedia application usage, and seamless operation and roaming across major global WiMAX spectrum allocations, including 2.3 to 2.7 GHz and 3.4 to 3.8 GHz, and their local variations such as the Wireless Communications Service (WCS) and Educational Broadband Service/Broadband Radio Service (EBS/BRS) bands in the US.

As the main platform integrator, EB's role includes platform specification, hardware development, form factor mechanical design, antennae specification, software configuration and integration of third party components. The company will also call on its end-to-end expertise in mobile WiMAX, from network elements to handsets and air-interface testing.

Jewel in the Crown for Thales in UK

Thales UK has opened its new Joint Electronic Warfare Experimentation Laboratory (JEWEL) in Leicester, UK. The JEWEL features a fully operational Electronic Warfare Operation Centre (EWOC) to provide complete simulation of land electronic warfare scenarios, support tools, and mission planning and reporting. Its ability to simultaneously simulate up to nine sensors, including two live sensors, allows Thales to demonstrate the capability and flexibility of sensor remote control.

The laboratory adds to the company's EW capability in the UK where more than 400 people are dedicated to the research, development and delivery of its integrated EW systems. Long-term plans include the ability to link the JEWEL with Thales' existing Intelligence, Surveillance, Target Acquisition and Reconnaissance (ISTAR) Theatre in Crawley, UK, to conduct even more extensive modelling and simulation exercises.

"The JEWEL is an extremely powerful tool and a breakthrough in our research, development and testing capability," said Richard Deakin, managing director of Thales' aerospace business in the UK. "It allows us to work hand in hand with our customers to model, test and refine their land EW operational requirements."

Kevin Swales, director of Electronic Combat Systems activities for Thales in the UK, stated: "This is a major step forward in EW modelling in the UK. The possibilities for it to help our customers develop and test their EW strategies are extremely exciting—with the electromagnetic spectrum increasingly cluttered, our defence forces need to know how their equipment is going to cope in real combat environments." ■

VERY HIGH IP3...to +36 dBm

MIXERS

2 to 2500 MHz

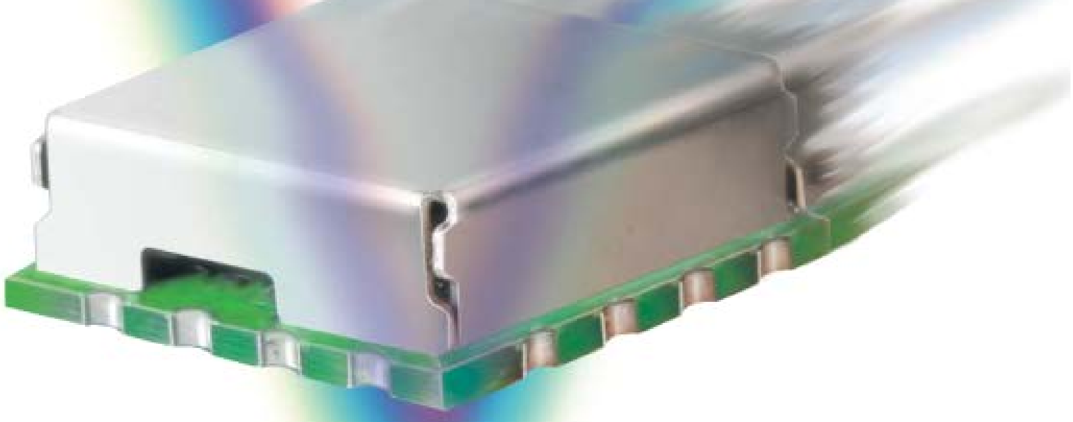

From $13.95 ea. Qty. (100) IN STOCK

- Very Wide Band, 2-2500 MHz
- Very High Isolation, up to 52 dB
- Very High 1 dB Compression, up to +23 dBm
- Very Low Conversion Loss, from 6.3 dB

It's an industry first...only from Mini-Circuits!

Mini-Circuits shielded RoHS LAVI frequency mixers deliver the breakthrough combination of very high IP3 up to +36 dBm, ultra-wideband operation, and outstanding electrical performance.

By combining our advanced ceramic, core & wire, and semi-conductor technologies, we've created these evolutionary broadband mixers that are specially designed to help improve overall dynamic range so you can realize lower distortion and combat interference in today's crowded spectrum. They're the very best, very low in cost, and immediately available off-the-shelf from the world leader in mixer technology, ***Mini-Circuits!***

TYPICAL SPECIFICATIONS

Model No.	Frequency (MHz) RF	LO	IF	LO Pwr. (dBm)	IP3 (dBm)	1dB Comp. (dBm)	Conv.Loss (dB)	Isolation (dB) L-R	L-I	Price $ ea. Qty.(1-9)
LAVI-9VH+	820-870	990-1040	120-220	+19	+36	+23	7.2	46	46	15.95
LAVI-10VH+	300-1000	525-1175	60-875	+21	+33	+20	6.3	50	45	22.95
LAVI-17VH+	470-1730	600-1800	70-1000	+21	+32	+20	6.8	52	50	22.95
LAVI-22VH+	425-2200	525-2400	100-700	+21	+31	+20	7.7	50	45	24.95
LAVI-2VH+	2-1100	2-1100	2-1000	+23	+34	+23	7.5	48	47	24.95
LAVI-25VH+	400-2500	650-2800	70-1500	+23	+32	+20	7.5	50	45	24.95

U.S. Patent Number 6,807,407

Pb RoHS COMPLIANT

Mini-Circuits®

ISO 9001 ISO 14001 CERTIFIED

ALL NEW minicircuits.com

P.O. Box 350166, Brooklyn, New York 11235-0003 (718) 934-4500 Fax (718) 332-4661 For detailed performance specs & shopping online see Mini-Circuits web site

YONI2™ Patent Pending ***The Design Engineers Search Engine*** *Provides ACTUAL Data Instantly From MINI-CIRCUITS At:* ***www.minicircuits.com***

RF/IF MICROWAVE COMPONENTS

412 RevC

Analysts Say Mobile Handset Merger a Good Start

Independent market research firm Strategy Analytics applauded Kyocera's recent acquisition of Sanyo Electronics' mobile handset division. Having gained important scale in the takeover, Kyocera will now face the formidable challenge of leveraging Sanyo's resources to drive growth in important 3G product segments.

Neil Mawston, associate director at Strategy Analytics, commented, "The combined entity of Sanyo Electric and Kyocera Corp. registered a global market share of 10 percent in CDMA handset shipments during the third quarter of 2007. This gives them greater scale-economies. Kyocera-Sanyo is now the clear number four vendor in this market and they are breathing down the necks of LG, Motorola and Samsung in the three places above."

Chris Ambrosio, director at Strategy Analytics, added, "This acquisition gives Kyocera important design resources and high-tier CDMA products that it failed to develop on its own. Whether Kyocera can integrate Sanyo's resources and churn out a compelling line of new products will be the acid test for 2008. In W-CDMA handsets, in particular, Sanyo has so far largely failed to penetrate the global market. Even with the acquisition, we expect it will be a monumental task for Kyocera to move into that fiercely-competitive 3G market in the future."

Semiconductor End-use: Market Diversity is a Good Thing

Noting that the semiconductor industry has been experiencing relatively balanced growth over the past few years, market research firm In-Stat expects that this will continue over the next five years. Although there will be some variation in growth rates among the end-use segments in terms of semiconductor consumption, these will all track close enough to the average that none can be said to be the driver in the sense that the computer and communications segments have been drivers in the not too distant past.

In-Stat expects worldwide semiconductor revenue to grow by 2.4 percent in 2008 to $261.9 B. The consumer segment will lead 2008 growth at 5.9 percent and the consumer and communications segments will gain share while the computer segment share declines. The computer segment, whose share has been trending downward since 2000, is expected to remain the largest segment by a wide margin, although, by 2012, its share is forecast to be 41.8 percent, well below the 50 percent+ levels of the 1990s.

The communications segment has stabilized at slightly over 20 percent of all semiconductor revenue and In-Stat expects that the trend toward wireless, in everything from computer networking to telephony, will allow the communications segment to maintain this level. The third ranked consumer segment has experienced the strongest growth over the past five years and it is expected that this growth will slow slightly, but will remain above the average and that the consumer segment share will break through the 20 percent level in 2008. However, it is not expected to surpass the communications segment before 2013.

The traditional industrial markets are increasingly seeing standard computer and communications hardware replace custom hardware, but any losses here are balanced by growth in medical products. Accordingly, the industrial segment share is expected to be more or less flat over the next five years.

The automotive segment's share is also forecast to remain essentially flat. There are many opportunities for semiconductors in high-end vehicles, but these are relatively low volume. The much-hyped impending growth of the automobile markets in China and India will be concentrated in low-priced vehicles with little semiconductor content. Overall, the innate caution and cost consciousness of the automobile industry will keep this growth in check.

Evolving ZigBee's Potential Still Unclear

ZigBee, the formal network, security, application-framework and application-profile layer overlay on top of the 802.15.4 PHY (physical) and MAC (media-access-control) layers used in low-power wireless mesh networks, continues to evolve with its potential still unclear, reports In-Stat. Currently, ZigBee technology targets building automation, industrial, medical, home automation, asset management, HVAC and other monitoring applications, the high-tech market research firm says. More applications will be invented as programmers acquire more understanding of the technology.

Within the market, there are different philosophies between chipset manufacturers and their approaches. A company like Jennic sees the technology as an application-enabler, focusing on giving their clients low-cost tool kits and providing their ZigBee software stack for free for customers who choose to build with their components. Ember allows their co-processor chipset, the EM-250, as an add-on for a customer that has application-specific MCUs.

Recent research by In-Stat found the following:

- Total ZigBee/802.15.4 node and chipset units will reach 120 million in 2011, up from 5 million in 2006.
- The ZigBee Pro feature set released to members in October 2007 includes: network scalability, fragmentation, frequency agility, automated device address management, group addressing, wireless commissioning and centralized data collection.
- There is a surge in interest in ZigBee technology for Automated Meter Infrastructure.
- Adoption in the consumer electronics is expected to be low because of competing technologies.

This information is drawn from the In-Stat research report, "ZigBee 2007: What it Iz and What it Iz Not," which covers the worldwide market for ZigBee technology.

Wholesale Prices of GPS-enabled Handsets to Fall Under $200 by 2010

Presently, most handsets with integrated GPS are smartphones or high-end feature phones, with wholesale price in the range of $250 to $500. However, chipset manufacturers now have solutions in place that will permit the integration of GPS in handsets at lower costs, and provide significant improvements in terms of accuracy, time-to-first-fix and reception in indoor environments. As a result, the wholesale ASP (Average Selling Price) of GPS-enabled handsets will fall under $200 by 2010.

"Recent industry developments, such as the announcement by CRS and Samsung of lower costs for GPS modules for mobile devices, will ensure that prices for GPS-enabled handsets quickly come down," says ABI Research industry analyst Shailendra Pandey. "Further, in coming years, it will become more cost-effective for manufacturers to have GPS in a large proportion of devices, rather than offering in fewer handsets; this will enable lower ASP for devices as well."

Until now, GPS chipset solutions for handsets have been costly ($5 to $10 per handset). However, GPS chipset vendors, such as CSR and SiRF have developed solutions that will bring down the cost of integrating GPS in handsets to under $2. Other vendors, including Broadcom, have plans to integrate GPS with Bluetooth and to offer a single-chip solution. Current GPS-enabled handsets typically are CDMA devices, but these solutions will also allow the integration of GPS in GSM and WCDMA handsets at much lower cost.

ABI Research expects the market for GPS-enabled handsets to grow strongly in the next five years, from around 140 million handsets in 2007 to more than 600 millions handsets shipments in 2012. In addition to major handset manufacturers such as Nokia, Motorola, RIM and Samsung, smaller Asian ODMs including HTC, Quanta and Inventec are introducing GPS-enabled devices. ABI Research's recent report, "GPS-enabled Mobile Devices," examines the market landscape and future potential for GPS-enabled mobile phones. It discusses critical business and marketing issues, as well as market opportunities and challenges for handset vendors, mobile operators, semiconductor vendors and other industry players who address the GPS-enabled handset market. ■

INDUSTRY NEWS

■ A report released by national non-profit **Connected Nation** suggests that the US could realize an impact of $134 B annually from a modest increase in broadband adoption. The report details the potential state-by-state impact of legislation to accelerate broadband access and use. The Connected Nation report measures the impact of its first state-based program, ConnectKentucky. Kentucky has experienced a rate of growth in broadband adoption (i.e. the number of households subscribing to high-speed broadband service) that is measurably higher than the nation. By surveying consumer savings in time, miles driven and healthcare and by calculating the impact on job creation/retention, the report projects the estimated annual economic benefit for Kentucky. From this data, Connected Nation extrapolated the economic impact of modest growth in broadband adoption for each state and the country as a whole.

■ As improvement projects continue in preparation for the 2008 Summer Olympics in Beijing, China, **Andrew Wireless Solutions** is helping ensure wireless coverage is at a gold medal standard in Beijing Metro's six rail lines. Andrew was chosen to supply and install wireless networking systems that will improve coverage and add network capacity in Beijing Metro's lines, which will see heavy use during the upcoming international event. The Beijing Organizing Committee for the 2008 Olympic Games has predicted that Beijing will receive 6.4 million visitors during the events, which would have put Beijing Metro's previous wireless network capacity under strain. "Andrew has a strong track record in supporting rail systems around the world, including 12 previous projects in Beijing," said Patrick Leung, managing director, Andrew Telecommunications (China) Co. Ltd., Andrew's China subsidiary. "In fact, Andrew has supported nearly 30 metro rail projects in Shanghai, Guangzhou and other major Chinese cities to ensure world-class wireless communications."

■ **Accellera**, an electronics industry organization focused on Electronic Design Automation (EDA) standards, announced that its members and board of directors have approved the VHDL 4.0 standard specification. VHDL 4.0 is a refinement of VHDL 3.0 (approved by Accellera in October 2006) based on feedback from trial implementations. Accellera has immediate plans to release VHDL 4.0 to the IEEE for balloting in 2008 and to support the IEEE 1076™-2008 balloting process. VHDL 4.0 addresses over 90 issues that were discovered during the trial implementation period for the VHDL 3.0 version. These encompass enhancements to major new areas introduced by VHDL 3.0 including generic types, intellectual property protection, property specification language integration, VHDL application programming interface integration, and the introduction of fixed and floating point types. "We have established an effective process for delivering standards in a timely manner and transferring them to the IEEE," said Shrenik Mehta, chairman of Accellera. "The IEEE gave us permission to revise the VHDL language and continue to improve it, thereby addressing the needs of the VHDL community."

■ **Park Electrochemical Corp.** announced the grand opening of its new advanced composite materials plant located on Pioneer Road in Jurong, Singapore. The new facility will focus on the development and manufacture of advanced composite materials for the aerospace industry in Asia. The new facility contains approximately 32,000 square feet of manufacturing, laboratory and office space. The Pioneer Plant will be operated by Park's wholly owned subsidiary, Nelco Products Pte. Ltd. (Nelco Singapore), which is also located in Jurong, Singapore. Nelco Singapore, which commenced operations in October 1986, develops and manufactures high-tech materials for the Asian electronics equipment industry. The grand opening of the Pioneer Plant coincides with the Singapore Air Show.

■ **Neptuny**, an IP network planning and capacity management specialist, has warned organizations offering Internet services to the public, as well as those firms using intranets, to prepare for a revolution in wireless technology that is coming in the next 12 months. In February, the Bluetooth Special Interest Group announced a major enhancement to the Bluetooth personal area network standard that allows compatible devices to hop on to WiFi networks whenever extra range and/or bandwidth is required. The enhancement, which essentially makes Bluetooth devices capable of handing off data calls to WiFi networks—and vice versa—is known as alternate MAC/PHY and will be seen in the Bluetooth 3.0 standard due out later this year. "Any organization offering user-facing Internet or intranet facilities can expect to see a surge in their WiFi bandwidth usage as hundreds of millions of mobile phone users start to come on-stream," said Fabio Violante, Neptuny's founder and CEO.

■ **Orbit**, a designer, developer and manufacturer of a wide range of stabilized satellite communication systems, announced Standard Intelsat Type Approval (GVF/IA 200FLT K2&G) for its OrSat (AL-7103 MK II) Ku-band Maritime Stabilized Antenna System. The approval comes on the heels of Eutelsat Type approval last year. "These type approvals from the leading satellite companies are a significant step forward for Orbit," said Ehud Netzer, Orbit's CEO.

■ **Litron**, a primary outsourcing partner for medical device and aerospace suppliers, now houses its glovebox units in a Class 100,000 Clean Room. This adds a new level of protection for mission-critical parts as they are handled on their way to and from the glovebox. "This is one of several investments we have made to ensure that the components we handle are returned in pristine condition," said Mark A. Plasse, Litron president. "While many outsourcing partners provide glovebox hermetic sealing, it is rare—maybe even unique—to find the same level of protection for components as they travel through a ven-

dor's plant. We see this as a valuable new contribution to the efficacy of our customers' medical and electronic devices."

■ **Allied Electronics**, a subsidiary of Electrocomponents plc, has been recognized with a Silver Award from Honeywell for revenue growth. Each year Honeywell Sensing and Control recognizes members within its sales channel for outstanding achievements. This year, Honeywell recognized Allied for 2007 Largest Organic Revenue Growth Year Over Year. "It is an honor for Allied to be recognized by Honeywell for our outstanding revenue growth," said Scott McLendon, vice president of marketing at Allied. "Our partnership with Honeywell has been mutually beneficial in helping both organizations grow."

■ **Strategy Analytics**, a market research firm, views the Experia Windows Mobile 6 device announcement from SonyEricsson as a win-win for both players in driving further gains in the European smart device market. Microsoft gains due to SonyEricsson's track record of innovation for European consumers, while SonyEricsson diversifies its struggling smart device lineup and becomes a valid smart device supplier to the picky European business user segment. "To date, SonyEricsson has been unable to leverage its innovation track record to drive smart device sales; and we are concerned that adding the Experia sub-brand will cause some consternation to users in terms of deciphering the primary value of the device and its various brands," said Neil Mawston, director at Strategy Analytics. "However, with Windows Mobile on Experia, SonyEricsson diversifies its aged Symbian line-up, and immediately establishes a choice for both media hungry consumers and business-minded professionals needing the productivity and messaging synergies that Microsoft offers."

■ **ABI Research** expects sales of mobile phone accessories are expected to generate over $40 B in revenue in 2008 and that the market for mobile phone accessories will grow steadily in the next five years, generating over $80 B in revenue in 2012. The firm's recent study "Mobile Phone Accessories" examines the market landscape and future potential for mobile phone accessory products. The growing popularity of mobile phones with large screens and touchscreens is resulting in strong sales of accessory products that offer handset protection, such as carry cases, covers, screen protectors and scratch removers. Audio-video playback capabilities in handsets are resulting in growing demand for earphones and headsets, as well as memory cards to enable storage of music, videos and images. Also, the need for connecting the mobile phone to the PC/laptop for transferring multimedia and data files means a greater need for accessory products such as data connection kits and USB chargers.

CONTRACTS

■ **Aeroflex** announced it has entered into a multi-year contract worth in excess of $10 M with a leading supplier of cellular mobile phones and communications devices. This contract selects Aeroflex as a leading supplier of manufacturing test solutions for mobile handsets worldwide. "Aeroflex's innovative RF PXI products have helped our customer realize a significant reduction in manufacturing test time. We are pleased to provide a flexible platform to accommodate the varied test demands for current cellular and emerging broadband wireless systems," said Bob Vogel, vice president/general manager, Aeroflex Test Solutions, Wireless Division. Customer deliveries have commenced and the first product lines using Aeroflex equipment are currently operational.

■ **Laser Energetics Inc.** announced it has received a contract worth $481,268 from **ITT Corp.** for a laser demonstration of an all solid state frequency tripled Alexandrite laser using the LEI proprietary BrightStar™ technology. This contract is in support of the US Army's initiative to develop an all solid-state laser for the next generation of chemical warfare agent sensor currently being developed by ITT. The contract follows the Army's selection of Laser Energetics' BrightStar™ as the laser technology of choice for this remote sensing of chemical warfare agents.

■ **RF Neulink's Telemetry Division** announced it has been awarded an initial $335,000 contract to support the United States Marine Corps' Integrated GPS Radio System (IGRS). The IGRS is an advanced personnel tracking system which will provide the USMC with GPS-based real-time tracking, position and status information for personnel engaged in battlefield activities. "We hope to announce further contracts for this project later this year," said Robert White, Neulink's sales and marketing director.

■ **Nextlink** has signed a master purchase agreement with **DragonWave** for the purchase of carrier grade radio solutions in support of Nextlink's portfolio of broadband wireless services. Nextlink will use DragonWave's Horizon and AirPair products to offer backhaul solutions that enable wireless service providers to more cost-effectively support next generation mobile applications, content and data across their networks as an alternative to conventional wireline networks. Nextlink owns licensed wireless spectrum covering 75 metropolitan US markets.

■ **AR Modular RF** has been awarded a contract to supply its new model KMW1040 multi-band amplifier to the US Special Operations Command. The KMW1040 is designed as a vehicle-mounted 50 W, 30 to 512 MHz self-tuning amplifier. It will be used as a booster amplifier in conjunction with hand-held and vehicle-mounted multi-band tactical radios such as the Harris AN/PRC-117F, the Harris AN/PRC-152, the Raytheon AN/PSC-5D, the Thales AN/PRC-148 MBITR and other similar tactical radios.

■ **Tampa Microwave**, a designer and manufacturer of RF and microwave communications and test equipment for commercial and government applications, announced that the company has obtained a United States Government Services Administration (GSA) Schedule. The contract number GS-07F-0590T applies to Tampa Microwave's converter, carrier monitoring and satellite simulator products. This contract places Tampa Microwave on

an approved GSA schedule, enabling various government agencies to purchase products directly from the company.

FINANCIAL NEWS

■ **Ansoft Corp.** announced financial results for its third quarter of fiscal 2008 ended January 31, 2008. Revenue for the third quarter totaled $26.1 M, an increase of 15% compared to $22.7 M reported in the previous fiscal year's third quarter. Operating income for the third quarter was $10.0 M representing a 36% increase when compared to operating income of $7.4 M in the previous fiscal year's third quarter.

■ **RF Industries Ltd.** announced results for the fourth quarter and fiscal year ended October 31, 2007. For the quarter, sales were $4 M compared to $4.1 M in the same quarter last year. Net income was $490,000, or $0.13 per diluted share, compared to $473,000, or $0.13 per diluted share, in the same quarter last year.

NEW MARKET ENTRY

■ **Southeastern Sales RF** is a manufacturers' representative firm focused on active and passive RF, microwave, and optical components and sub-systems for markets served in the southeastern US. The company currently operates from two offices located Florida, with a new office to be opened shortly in Atlanta, GA. Contact Southeastern Sales RF at (772) 812-2700 or visit its web site at www.sesrf.com.

PERSONNEL

▲ *Duncan Cooper*

■ Surrey NanoSystems has appointed **Duncan Cooper** as its director of sales and marketing. With 25 years' experience in the semiconductor industry, he brings a wealth of know-how to the company as its new breed of tools for growing carbon nanotubes at low temperatures moves from R&D labs to commercial fabrication. Cooper has start-up experience gained in the industrial laser industry, along with experience in semiconductor fabrication tools and materials applications, gained from over a decade with Tokyo Electron and Hoya.

■ Phase Matrix has appointed **Alexander Chenakin** as director of its Frequency Synthesis Group. Chenakin is responsible for overseeing the development of a new generation of fast switching frequency synthesizers. An internationally recognized expert in the field of microwave frequency synthesis, he received his degree from Kiev Polytechnic Institute and has worked in a variety of technical and managerial positions around the world. He has led the development of advanced products for Celeritek, Nextek, Micro Lambda Wireless, General Electronic Devices and other companies.

world's smallest

2 WAY & 4 WAY SPLITTERS

5 to 2500 MHz from $1.69 ea. (qty. 1000) **IN STOCK**

Mini-Circuits tiny SBTC 2 way-0° and SCA 4 way-0° power splitters are the ***world's lowest priced*** and smallest size splitters operating within 5 to 2500 MHz band. But that's not all. Patented LTCC technology provides outstanding performance features including low insertion loss down to 0.3 dB typical, excellent 0.2 dB amplitude and 1 degree phase unbalance (typ), and ***superior temperature*** stability. Pads are solder plated, and connections are assembly welded for high temperature reflow reliability. As demand for smaller gets bigger, blow away the competition with Mini-Circuits space saving, ***money saving*** SBTC and SCA power splitters.

Mini-Circuits…we're redefining what VALUE is all about!

SBTC (0.15"x 0.15"x 0.15")

SCA (0.3"x 0.25"x 0.19")

Model	Frequency (MHz)	Z	Price $ea. (Qty. 25)
SBTC-2-10+	5-1000	50 Ω	2.49
SBTC-2-20+	200-2000	50 Ω	3.49
SBTC-2-25+	1000-2500	50 Ω	3.49
SBTC-2-10-75+	10-1000	75 Ω	3.49
SBTC-2-15-75+	500-1500	75 Ω	3.49
SBTC-2-10-5075+	50-1000	50/75 Ω	3.49
SBTC-2-10-7550+	5-1000	50/75 Ω	3.49
SCA-4-10+	5-1000	50 Ω	6.95
SCA-4-10-75+	10-1000	75 Ω	6.95
SCA-4-15-75+	10-1500	75 Ω	7.95
• SCA-4-20+	1000-2000	50 Ω	7.95

• LTCC construction

U.S. Patent No. 6,963,255

All models are RoHS compliant

Mini-Circuits®

ISO 9001 ISO 14001 CERTIFIED

ALL NEW minicircuits.com

P.O. Box 350166, Brooklyn, New York 11235-0003 (718) 934-4500 Fax (718) 332-4661 For detailed performance specs & shopping online see Mini-Circuits web site

YONI2™ Patent Pending ***The Design Engineers Search Engine*** *Provides ACTUAL Data Instantly From MINI-CIRCUITS At: **www.minicircuits.com***

IF/RF MICROWAVE COMPONENTS

354 Rev J

■ **Cristina Larrazabal** has joined RFMW as a field sales manager for the company's San Diego and Orange County territories. Larrazabal comes to the company from a long career in electronics distribution (as inside and field sales), having spent over four years with Newark Electronics and, most recently, more than eight years with Future Electronics.


▲ *Nigel Blakeway*

■ Omron Electronic Components LLC announced the appointment of **Nigel Blakeway** as its new chief operations officer (COO) and managing director. Blakeway previously served at Omron Component Business-European Union (OCB-EU) in Amsterdam as the COO. He moved to OCB-EU in 2003 to take over the independent components business. Previously, Blakeway worked for Matsushita (Panasonic Electronic Components) for 11 years. He was also at BC Components (originally Philips Passive Components) as part of the original divestment team and a director of the new operation.

■ MITEQ Inc. announced the appointment of **Howard Hausman** as president. Joining Hausman on the executive management team are David Krautheimer and Steven Spohrer. Together, the team brings many years of experience in management, sales, engineering and operations, and will take responsibility to manage MITEQ's ongoing operations.

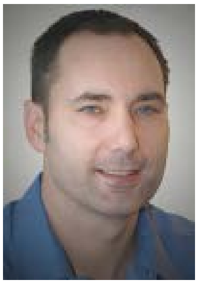
▲ *Chris Korson*

■ **Chris Korson** has joined LPKF Laser & Electronics to develop and manage the Plastic-Welding and Laser-Direct Structuring (LDS) product lines based in Detroit, MI. Korson formally worked for Lanxess Corp., a chemical company that was divested from Bayer Corp. in 2004. He has a bachelor's degree in mechanical engineering and 14 years of experience in the plastics field.

■ Provigent, a provider of system-on-a-chip solutions for the broadband wireless transmission market, announced that **Victor Koretsky** has joined the company as senior vice president, worldwide sales and business development. Prior to joining Provigent, Koretsky was corporate vice president of worldwide sales and marketing of the DSP Group, having joined the company at its inception. Koretsky has 25 years of experience in the telecommunication and semiconductor industries and holds a MSc degree in electronics from Moscow Technical University of Communication and Informatics and an MBA degree from Heriot-Watt University in Edinburgh. He also holds numerous patents in the field.

■ Aperto Networks, a builder of WiMAX base stations and subscriber units, announced the appointment of

Ruchir Godura as vice president, Global Customer Service and South Asia Sales. Over his career in India and North America, he has managed sales, customer service, and product management for a variety of communication technologies including WIMAX, CDMA, DSL, Metro Ethernet and IPTV. Most recently, Godura was CMO, Enterprise Services, at Bharti Airtel, India's largest GSM operator. Godura holds a BS degree in computer science and engineering from the Indian Institute of Technology, Delhi, and a MS degree in computer science from the University of Delaware.

■ Acceleware Corp., a developer of high-performance computing applications, announced the appointment of **Shawn Lorenz** as its vice president of sales. With over 25 years of experience in the high tech industry, Lorenz will be responsible for growing the organization's global sales initiatives for Acceleware's acceleration solutions. Prior to joining Acceleware, Lorenz held executive and director level positions with several successful companies such as EMC/Documentum, Gigaspaces and Verity.

■ Auriga Measurement Systems LLC announced the hiring of **Bruce L. Cohen** as president and CEO. Cohen joins Auriga with more than 35 years of industry experience. He was one of the founders of Chipcom Corp. and was instrumental in leading the company to an annual rate of more than $300 M per year in 10 years. After Chipcom, Cohen was CEO of Novasoft Systems and Top Layer Networks.

REP APPOINTMENTS

■ **Richardson Electronics Ltd.** has signed a global distribution agreement with **Crystek Corp.** of Fort Myers, FL, to distribute its High Performance Frequency Line. Crystek's products provide high performance frequency solutions needed in advanced applications, including cellular base stations, broadband communication infrastructure, military defense systems and industrial instrumentation equipment.

■ **Sprague-Goodman Electronics Inc.**, Westbury, NY, has appointed two new sales representatives to market its line of trimmer capacitors, transformers, fixed and variable inductors and tuning tools throughout the Pacific Northwest and Canada. **Cain-Sweet Co.**, headquartered in Bellevue, WA, will represent the Sprague-Goodman product line in the Pacific Northwest and the Province of British Columbia. **Dynamic Concepts**, located in Ottawa, will cover the Provinces of Ontario, Quebec, Alberta, Manitoba, New Brunswick, Newfoundland, Nova Scotia, Saskatchewan and Prince Edward Island.

■ **Digi-Key Corp.** and **Artaflex** have entered into a global agreement for the distribution of Artaflex's WirelessUSB™ modules. Utilizing Cypress' WirelessUSB radio system-on-a-chip devices, Artaflex's modules are intended for industrial and home automation applications.

CONNECTORIZED MI

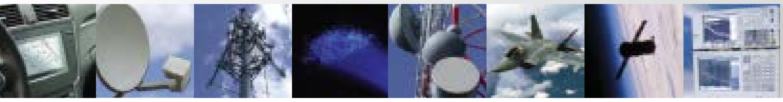

TEST & MEASUREMENT ♦ MILITARY

AMPLIFIERS - Low Noise, Drivers, PAs & >10 Watt PA Modules

	Frequency (GHz)	Function	Gain (dB)	OIP3 (dBm)	NF (dB)	P1dB (dBm)	Bias Supply	Package	Part Number
NEW!	1.8 - 4.2	Low Noise	26	26	0.7	15.5	+8V @ 112mA	C-10 Module	**HMC-C045**
NEW!	5 - 9	Low Noise	24	25	1.4	15	+12V @ 105mA	C-10 Module	**HMC-C048**
	29 - 36	Low Noise	20	22	2.9	11	+3V @ 80mA	C-10 Module	**HMC-C027**
	2 - 20	Wideband LNA	15	25	2.5	14	+12V @ 65mA	C-1 Module	**HMC-C001**
	2 - 20	Wideband LNA	14	26	2	18	+12V @ 60mA	C-2 Module	**HMC-C002**
	2 - 20	Wideband LNA	14	27	2	16	+8V @ 75mA	C-2B Module	**HMC-C022**
	7 - 17	Wideband LNA	22	25	2	14	+8V @ 93mA	C-1 Module	**HMC-C016**
	17 - 27	Wideband LNA	18	25	3	14	+8V @ 96mA	C-1B Module	**HMC-C017**
	0.01 - 15	Wideband Driver	16	33	3	23	+12V @ 195mA	C-3 Module	**HMC-C004**
	0.01 - 15	Wideband Driver	15	30	3	23	+12V @ 225mA	C-3B Module	**HMC-C024**
	2 - 35	Wideband Driver	12	29	3	18	+11V @ 92mA	C-10 Module	**HMC-C038**
	0.05 - 15	Wideband PA, 1/2 Watt	12	36	4	28	+11V @ 360mA	C-10B Module	**HMC-C036**
	0.05 - 15	Wideband PA, 1/2 Watt	12	36	4	28	+11V @ 360mA	C-12 Module	**HMC-C037**
	2 - 20	Wideband PA	15	34	4	26	+12V @ 310mA	C-2 Module	**HMC-C003**
	2 - 20	Wideband PA	15	34	4	26	+12V @ 310mA	C-2B Module	**HMC-C023**
	2 - 20	Wideband PA	31	33	3	26	+12V @ 400mA	C-3B Module	**HMC-C026**
	17 - 24	Wideband PA	22	33	3.5	24	+8V @ 250mA	C-10 Module	**HMC-C020**
	21 - 31	Wideband PA	15	32	5	24	+8V @ 215mA	C-10 Module	**HMC-C021**
	0.4 - 1.0	10 Watt PA	40	54	12	40	+12V @ 6.5A	C-7 Module	**HMC-C012**
	0.8 - 2.0	10 Watt PA	43	56	12	40	+12V @ 6.5A	C-7 Module	**HMC-C013**
	1.8 - 2.2	15 Watt PA	42	53	6	42	+14V @ 6.5A	C-7 Module	**HMC-C008**

ATTENUATORS

Frequency (GHz)	Function	Loss (dB)	Atten. Range (dB)	IIP3 (dBm)	Control Input (Vdc)	Package	Part Number
DC - 13	6-Bit Digital, Serial Control	3.6	0.5 to 31.5	32	Serial TTL/CMOS	C-6 Module	**HMC-C018**
DC - 13	6-Bit Digital	3.2	0.5 to 31.5	38	0 / +5V	C-6 Module	**HMC-C025**

FREQUENCY DIVIDERS (PRESCALERS) & PHASE / FREQUENCY DETECTORS

Input Freq. (GHz)	Function	Input Power (dBm)	Output Power (dBm)	100kHz SSB Phase Noise (dBc/Hz)	Bias Supply	Package	Part Number
DC - 18	Divide-by-2	-15 to +10	-4	-150	+5V @ 75mA	C-1 Module	**HMC-C005**
DC - 18	Divide-by-4	-15 to +10	-4	-150	+5V @ 93mA	C-1 Module	**HMC-C006**
0.5 - 8	Divide-by-5	-15 to +10	-1	-155	+5V @ 80 mA	C-1 Module	**HMC-C039**
DC - 18	Divide-by-8	-15 to +10	-4	-150	+5V @ 98mA	C-1 Module	**HMC-C007**
0.5 - 17	Divide-by-10	-15 to +10	-1	-155	+5V @ 152mA	C-1 Module	**HMC-C040**

FREQUENCY MULTIPLIERS - Active

Input Freq. (GHz)	Function	Output Freq. (GHz)	Input Power (dBm)	Output Power (dBm)	100kHz SSB Phase Noise (dBc/Hz)	Package	Part Number
3 - 5	Active x2	6 - 10	3	17	-140	C-10 Module	**HMC-C031**
9.0 - 14.5	Active x2	18 - 29	3	16	-132	C-10 Module	**HMC-C032**
12.0 - 16.5	Active x2	24 - 33	3	17	-132	C-10 Module	**HMC-C033**
16 - 23	Active x2	32 - 46	3	13	-130	C-10 Module	**HMC-C034**

Hittite MICROWAVE CORPORATION

RoHS EARTH FRIENDLY

ISO/TS 16949 TÜV SÜD ISO 9001

DETERMINING RADIATED PERFORMANCE OF MOBILE WIMAX DEVICES

The past year has seen a flurry of activity related to bringing the next generation of broadband wireless technology, commonly referred to as Mobile WiMAX, to the market. Based on the IEEE 802.16e standard for local and metropolitan area networks, released in 2005, Mobile WiMAX promises wireless data connections of 10 to 15 megabits per second in a typical cellular radius, far exceeding the capabilities of today's 2.5-3G wireless networks. The WiMAX Forum™ is an industry organization that was formed to promote the development of devices meeting the 802.16 standards and ensure that all components of the wireless network operate together correctly. Only devices passing a range of certification tests for conformance, interoperability and performance will receive the "WiMAX Forum Certified" designation. With hundreds of companies involved in all aspects of development for products, services and infrastructure, including industry giants like Sprint and Intel, there is considerable emphasis on ensuring that WiMAX technology provides an exceptional user experience from day one. Meeting this goal requires not only that WiMAX devices follow the 802.16e standard and work seamlessly with each other, but also that they provide a minimum level of performance across the entire network.

While basic "can you hear me now" type testing of a device on a wireless network may provide some level of confidence in its performance, it's not a very scientific approach to determining the radiated RF performance of a wireless device. In recent years, segments of the wireless industry have adopted laboratory test techniques for determining the over-the-air transmit and receive characteristics of wireless devices in simulated usage cases. In the United States, wireless carriers have come to rely on this performance data for evaluation of mobile phones prior to allowing them on their networks. In an industry where a 2 dB loss in radiated performance can result in the need for 25 percent more base stations (based on 40 dB per decade path loss as described in

MICHAEL D. FOEGELLE
ETS-Lindgren, L.P.
Austin, TX

Lee and Hata Models), the potential cost savings of performing this type of laboratory testing is significant. ETS-Lindgren recognized that the WiMAX industry would require a similar level of confidence in their products, and has spent the past year and a half developing the capability for performing these tests on 802.16e devices, as well as providing the principal contributions to the WiMAX Forum Radiated Performance Tests (RPT) for Subscriber and Mobile Stations.[1] In August of 2007 the company was the first to demonstrate fully automated total radiated power (TRP) testing of a WiMAX device, followed shortly thereafter by fully automated testing of total isotropic sensitivity (TIS). On January 10, 2008, ETS-Lindgren announced the installation of the first WiMAX RPT lab at AT4 wireless in Herndon, VA.[2]

INTRODUCTION TO RADIATED PERFORMANCE TESTING

The basic concepts of radiated performance testing (RPT) are relatively simple. The goal is to determine the "edge-of-link" performance of the device to determine the limits under which a wireless connection is likely to be maintained. Imagine carrying on a voice conversation with someone as you get further and further apart. Eventually you would be yelling at them while straining to hear what they were yelling back. The conversation would break down when one member of the conversation could not hear the other well enough to understand what was said. The link could break down either because the speaker could not yell loud enough or because the listener was hard of hearing. Added to that, any noise around the listener, including their own attempts to talk back to the speaker, would reduce the chances of their hearing what was said.

The same basic idea applies to a wireless link. Once a mobile device is unable to communicate with a base station, whether because of insufficient transmitter or receiver performance, the link breaks down. In this case, two standard metrics are typically used to represent the performance of a wireless device. The total radiated power (TRP) is the "talk" metric, and represents the average transmit performance of the device in any random direction. Conversely, the total isotropic sensitivity (TIS) is the "listen" metric and represents the average receiver sensitivity from any given direction. Similar to hearing or speech, the actual performance in any given direction varies, and the methodologies used to determine these quantities are capable of evaluating that directional behavior in addition to determining the overall average performance. Instead of measuring the combined behavior of the transmitter and receiver out in the field, each quantity can be evaluated separately in a laboratory environment.

While the specifics of TRP and TIS measurement methods are covered in detail elsewhere,[3–5] the methods used today evolved from passive antenna pattern measurement techniques, where the directional performance (gain) of an antenna is evaluated from all directions around the antenna. To do so requires an isolated free-space environment, typically produced by an RF absorber-lined shielded room known as a fully anechoic chamber. This ensures that only energy radiated by the device or transmitted directly to the device is measured. Within the chamber, the device to be tested is moved relative to a measurement antenna, either by moving the device, the measurement antenna, or both, in two orthogonal axes in order to cover the surface of a sphere around the device (think of latitude and longitude lines on the surface of the earth). A dual-polarized measurement antenna is typically used to determine the resultant field vector magnitude at each point on the spherical surface no matter what its orientation. To determine TRP, the device is made to broadcast at full power and the radiated power is measured in each direction. For

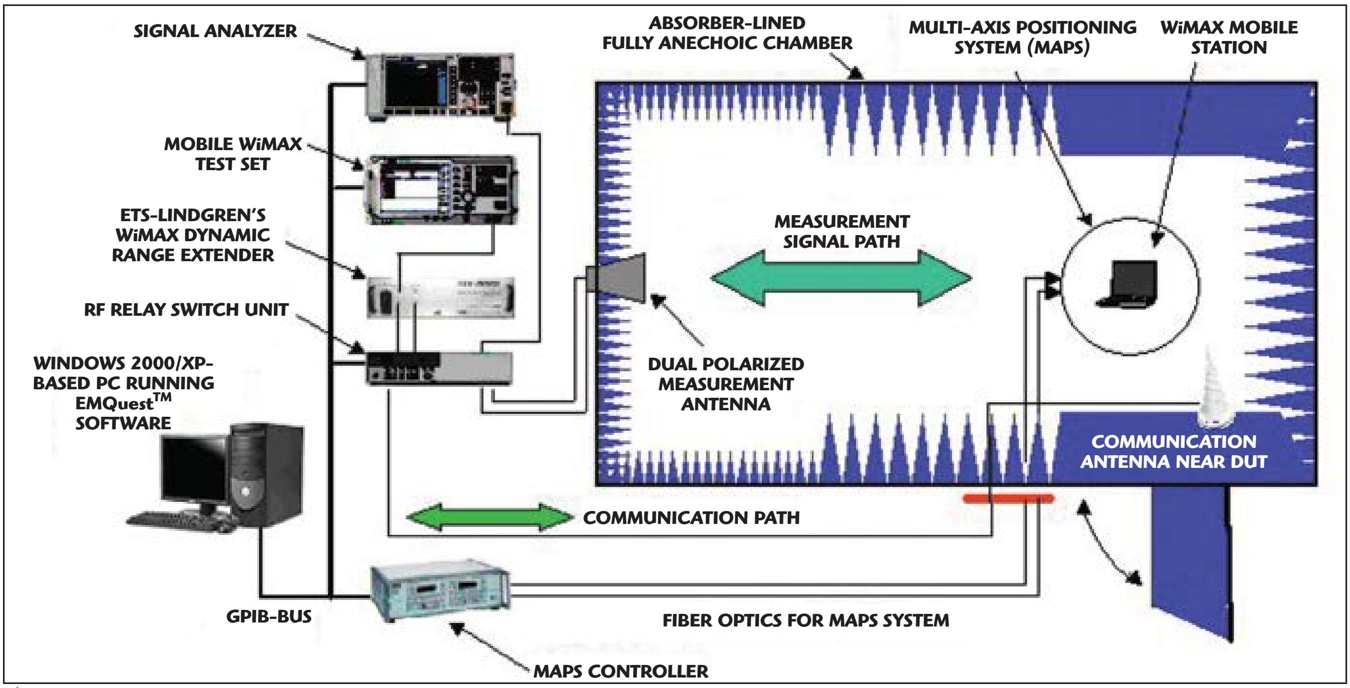

▲ *Fig. 1 Typical WiMAX RPT test system diagram.*

TIS, the signal level transmitted to the device is reduced until a specified number of errors are introduced into the data stream. The resultant power level is recorded for each direction around the device.

With active wireless devices, the goal of TRP and TIS testing is to evaluate the radiated performance of the radio through the integrated antenna(s) including the impact of objects typically found in the vicinity of the radio during use. This includes the platform in which the radio is installed (such as a cell phone or notebook PC) and possibly the operator (head, hands, etc.) or tabletop in proximity to the device. All of these can affect the transmit or receive radiation pattern of the device and thus the resulting radiated performance. In addition, electronic noise sources such as CPU clocks, displays, etc. can couple through the antenna causing desensitization of the receiver that cannot be determined through conducted tests.[6]

TESTING WiMAX MOBILE STATIONS

Developing the capability for radiated performance testing of any emerging technology is no mean feat. Ideally the devices to be tested would be in a configuration identical to that which the end user would obtain for use on a network. Given that WiMAX technology is still in development it's not possible to go down to the local electronics store to purchase a device to test. Obtaining prototype devices requires considerable cooperation between major developers in the industry. Even then, devices are rarely available in a configuration suitable for RPT. Most R&D testing, including that for protocol and radio conformance testing within the WiMAX Forum, is done in a conducted environment. Signals are routed directly to and from the radio without ever going through an antenna. In addition, mechanisms typically exist for getting information out of the WiMAX radio, usually through a digital cable connection.

In determining radiated performance, any cables attached to the device can significantly affect the radiation pattern of the device. Thus, it's critical that all of the required performance information be obtainable over the wireless interface. Currently this is complicated further due to the lack of a standardized wireless test interface in the 802.16e protocol.

Once a suitable WiMAX mobile device is available, the test development effort is far from over. In order to operate the device as it would on a real network, a base station emulator (BSE) is required to provide the other end of the link and produce the expected network behavior, as well as to perform various test functions. Of course for a new technology it takes time for this type of test equipment to become available to the market. Although several test equipment vendors are developing BSE solutions, as of this writing the Agilent E6651A Mobile WiMAX Test Set is the only BSE that has been successfully used to perform RPT tests. The early availability of this unit and Agilent's willingness to support the RPT development effort has been invaluable in the progress made to date.

Commercially available base station emulators are typically designed for conducted testing and thus are not expected to generate or respond to the range of signal levels usually seen on a real wireless network. A typical radio conformance test is intended to verify that the subscriber or mobile station device under test (DUT) meets a very specific set of requirements. The associated cable losses and expected signal levels are thus well known, such that the BSE does not have to adapt to a wide range of signals. However, once an antenna is attached to the radio, this is no longer the case. The signal level in any random direction can vary over a wide dynamic range, depending on whether the measurement antenna is directed towards a peak or a null in the radiation pattern. In addition, the path losses for over-the-air radiated propagation are considerably larger than that of the typical RF cable used in conducted tests. In order to overcome these limitations, external signal conditioning circuitry is typically required to extend the dynamic range of the BSE transmitter and receiver in order to perform radiated testing. This usually consists of a number of amplifiers, attenuators and high-speed switches. The TDD nature of the WiMAX signal adds a level of complexity to the signal conditioning, since the signal has to be separated into its uplink and downlink components

and amplified separately, then recombined into a bi-directional signal, all the while isolating the input of the opposite amplifier from the high power output of a given link direction. Doing so requires a control signal from the BSE to determine the direction of the radiated signal.

Often, a separate broadband power measurement device, such as a spectrum analyzer or IQ analyzer, is required to measure uplink power from the DUT. Since these devices can have considerable dynamic range, this is usually simpler than trying to measure using an integrated communications tester that combines the BSE with other measurement functions. The signal conditioning required to maintain a connection to the BSE may often interfere with the accuracy of an integrated measurement, and a broadband power measurement is typically faster and more forgiving of low signal levels than is a VSA where the signal must first be detected and demodulated in order to determine the power of a packet.

Of course all of these signals must be routed between the anechoic chamber and the test system, requiring an RF switch matrix in order to automate the system. A positioning system and controller as well as a controlling PC running test automation software is also required. ***Figure 1*** shows a system diagram for a typical WiMAX RPT test system.

Even given all of the pieces listed here, progress is often hampered by interoperability issues between the DUT and the BSE. The WiMAX requirements have been changing rapidly and developers and manufacturers are in a race to keep up with a moving target. Thus, it can be difficult to find compatible revisions to be able to test.

MEASURING TRP OF A WiMAX MOBILE STATION

To determine TRP, the wireless mobile station must be connected to the BSE and made to transmit uplink packets at full power to simulate usage at the edge of the link. This is not always as easy as it sounds since power control requirements are still in a state of flux and implementations vary. Some devices have manual power control overrides, but that always introduces the risk of a test mode that does not mirror real world behavior.

The 802.16e standard does provide an uplink padding mechanism that allows the BSE to tell the device to completely fill the uplink data channel with random data. However, in many device implementations, prolonged periods of uplink padding will result in a loss of connection. Presumably the device is unable to perform other network functions while sending this "useless" data and eventually gives up the connection.

Once the DUT is made to generate suitable uplink traffic, TRP is determined by making broadband power measurements of the uplink data bursts at each orientation and polarization around the DUT. This is typically done using an IQ analyzer in time do-

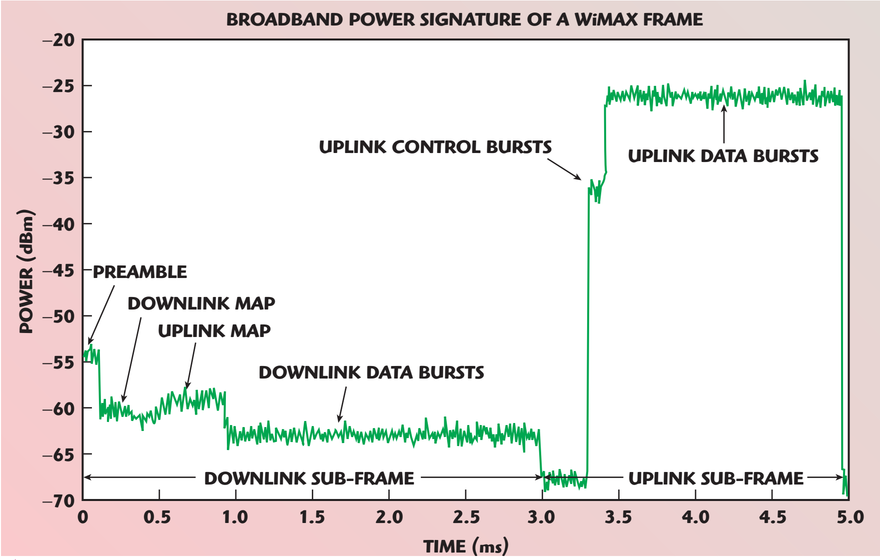

▲ *Fig. 2 Anatomy of a WiMAX TDD signal.*

main mode or a spectrum analyzer with a wide resolution bandwidth. ***Figure 2*** illustrates a typical WiMAX frame measured using an RMS detector. It's important to be able to detect valid uplink bursts and only measure the average RMS power of the uplink data burst, as shown in ***Figure 3***.

Figure 4 illustrates some of the first ever fully automated WiMAX TRP data measured on a PCMCIA card device installed in the middle of the right side of a notebook PC. The pattern clearly shows the shadowing effect caused by the display and base of the notebook, as well as the ripple caused by the constructive and destructive interference between the main lobe of the antenna and its image reflected from the display. In this configuration, the device generated a TRP of 26.3 dBm, while in another smaller laptop with the PCMCIA slot on the opposite side, the TRP was 24.1 dBm, illustrating just how much impact the platform can have on radiated performance. For research purposes, this data was sampled every 5°, which is considerably more than is necessary to obtain a valid TRP result. A theta dependent phi optimization was used to reduce the number of points measured near theta = 0° and 180° where the surface points are closer together. The test time at this sample density was on the order of 40 to 45 minutes per frequency, where an equivalent TRP result could be obtained in about 10 minutes with a coarser sampling grid.

MEASURING TIS OF A WiMAX MOBILE STATION

Measuring TIS involves repeated searches for sensitivity by lowering the transmit power of the BSE until a target packet error rate (PER) is reached. This simulates the case where the user is at the limits of the connection. Since the shape of the pattern varies as a function of orientation and frequency, the power level required to cause the target PER will vary and thus a search algorithm must be used to find the sensitivity level at each data point. Because the sensitivity measurement is referenced to the output power of the BSE, it requires that the output power of the BSE be calibrated for traceable measurements, and have enough dynamic range to cover the best sensitivity levels while still being able to maintain the connection through the deepest pattern nulls. Given the amount of time involved, it's impractical to perform the long PER measurements typically used to verify that a radio exceeds the sensitivity levels specified in 802.16. A bit error rate (BER) measurement is also not possible since there is no PHY layer loopback mode defined for WiMAX radios. In order to minimize the time required to search for sensitivity, statistical techniques are used to quickly determine a pass-fail criteria against a large target PER (10%), and a maximum packet count of 1000 frames is sufficient to have reasonable confidence in the results. The larger relative PER helps to narrow the range of power where the target value might be found, due to the steepness of the PER vs. power curve; since the sensitivity search results are integrated across the surface of a sphere to determine TIS, the effective number of packets evaluated for determining overall sensitivity is considerably larger than that for one search.

When performing a sensitivity measurement, it's important that the uplink signal is not degraded in order to ensure that the PER is solely due to the signal level on the downlink. Thus, just adding an attenuator between the BSE and the DUT is not a suitable way to measure sensitivity. Instead,

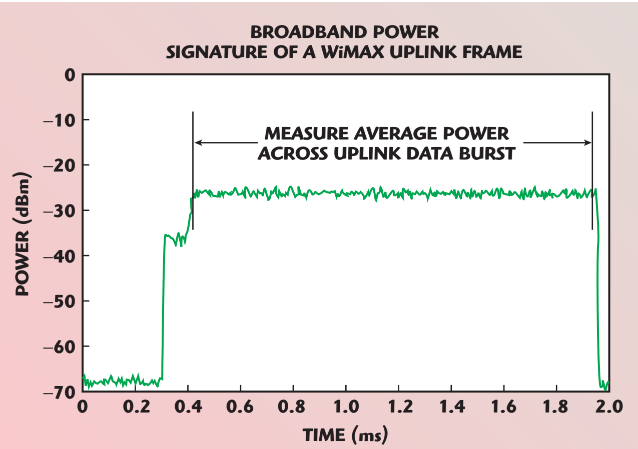

▲ *Fig. 3 WiMAX uplink sub-frame showing data burst measurement.*

separate uplink and downlink paths are typically used to ensure that the uplink has a lower path loss (see Figure 1).

Currently, the only way to perform a PER measurement of a WiMAX DUT as described is to use features of the TCP/IP protocol stack. The common method is to use an ICMP Ping/Echo request and count the number of echoes received. An alternate method involves sending UDP packets to an unused socket on the DUT and counting the ICMP "Destination Unreachable" responses. The disadvantage of these methods is that they require a full implementation of the protocol stack. This usually happens later in the design lifecycle of a product, once all drivers, etc. are complete. However, since a large part of what the TIS test evaluates is the impact of the platform on the receiver performance, it is desirable to be able to determine TIS early in the hardware development stage in order to resolve any RF issues that may require hardware modifications long before the device is near completion. This need should be addressed as devices are developed that are compliant with the "Wave 2" WiMAX certification requirements. These devices will be required to support Hybrid Automatic Repeat Requests (HARQ), which provide an error detection and acknowledgment (ACK/NACK) scheme within the 802.16 architecture that can be used for determining PER. By setting the retry count to zero, the DUT will indicate whether or not it received a valid packet, but the protocol will not try to recover the packet in following frames. Since this mechanism exists as part of the radio protocol itself, an embedded radio that is capable of making a wireless connection can potentially be installed in a platform (for example, a notebook PC) and tested without having to be able to access the device from the operating system.

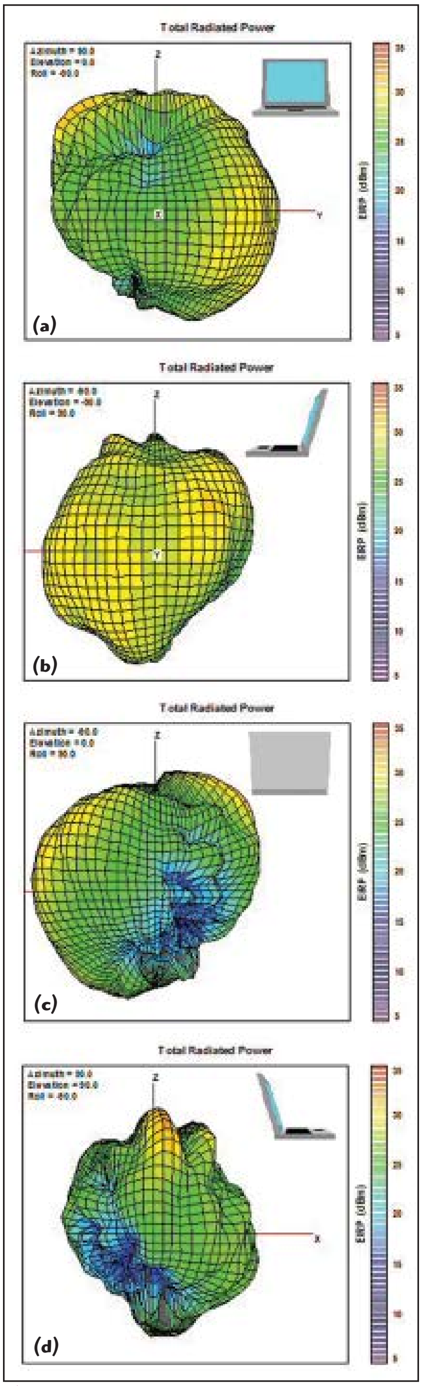

▲ *Fig. 4 Sample TRP data for a WiMAX PCMCIA card in the right side of a notebook PC.*

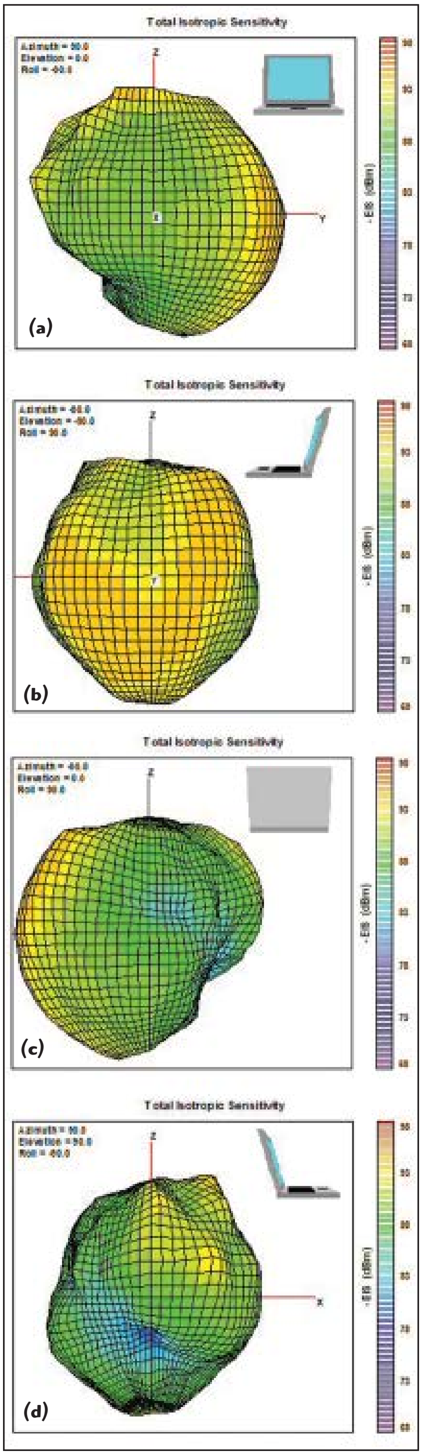

▲ *Fig. 5 Sample TIS data for a WiMAX PCMCIA card in the right side of a notebook PC.*

Figure 5 illustrates the first ever fully automated WiMAX TIS data measured on a PCMCIA card device installed in the middle of the right side of a notebook PC. Due to the required test time, the data was sampled at a 15° angular resolution using the same theta dependent phi optimization as for the TRP test. Difficulties maintaining connections make estimating a typical test time difficult, but under ideal circumstances, a test time of five to seven hours could be expected for this sampling resolution. Sampling at 30° would likely still provide a suitable TIS result for this device, reducing typical expected test time to less than two hours. In this configuration, the TIS of the device was determined to be –90.7 dBm.

INTERMEDIATE CHANNEL SENSITIVITY

One other piece of the RPT puzzle is what happens in between the frequencies where TRP and TIS have been determined. Due to the time required to perform these tests, it is impractical to repeat them at every supported channel of the device. In gen-

eral, measuring full radiation patterns at the low, middle and highest frequency in each band is sufficient to determine if there are any variations in pattern that might affect the behavior of the device. However, in the case of receiver sensitivity, where a narrow-band interference source from the platform could have a devastating effect on only a narrow range of channels, a method is needed to measure sensitivity performance across the entire band. While it's not necessary to test every 5 to 10 MHz wide channel at a 250 kHz spacing, at a minimum, one must be able to test a continuum of channels across the band to ensure that every possible interference frequency has been tested. This is where the intermediate channel sensitivity (ICS) comes in. Rather than performing TIS at every frequency, a much shorter normalization process is used. The assumption is that the pattern remains relatively constant, so that by re-measuring the sensitivity at one position on the TIS pattern for each desired frequency, the relative difference in sensitivity can be used to determine the corresponding TIS for each frequency. The resulting values have a slightly larger uncertainty than a full TIS scan, due to the reduced number of PER measurements used. As long as the DUT configuration is not altered between the reference and intermediate channel measurements, however, the result is sufficient for its intended purpose.

This last requirement tends to be difficult with the current state of devices. Most are configured to only connect to a single frequency without additional user intervention or to scan a very small range of frequencies. The number of intermediate frequencies to be tested across a band is larger than most frequency list tables implemented to support carriers with a given amount of bandwidth, and having the device scan every possible channel in the band is not a very efficient solution either. Since channel handoff functionality in WiMAX is currently still in the development stages, there is no way for the BSE to tell the DUT to switch to another channel. Instead the BSE can only change its signal to a target frequency and wait for the device to scan the band, find the signal, and register on the new channel. With as many as 1600 frequencies across a band, scanning all channels would be a slow process. Thus, to make this test practical, device firmware will need to be able to allow scanning a defined list of frequencies (up to about 90 for the worst case channel bandwidth/band combination) in order to allow the ICS measurement to be performed without user interaction with the DUT.

WHAT ABOUT MIMO?

This question seems to come up every time there's a discussion of radiated performance testing. WiMAX devices today are designed with a one transmit, two receive antenna configuration. In current implementations the two receive antennas typically provide some form of receive diversity, but by the time these devices are deployed, the intention is to offer downlink Multiple Input, Multiple Output (MIMO)

[Continued on page 186]

RESIDUAL PHASE NOISE MEASUREMENTS OF THE INPUT SECTION IN A RECEIVER

If not designed properly, the input section of an analog down-converter can introduce phase noise that can prevail over other noise sources in the system. Residual phase noise measurements on a simplified input section of a classical receiver that is composed of various commercially available mixers and driven by an LO amplifier are presented in this article.

A classical design approach for receivers operating at microwave frequencies is to down-convert the detected signal to some intermediate frequency before digitizing the signal. The final design of a receiver is chosen depending on performances, which can be described by various parameters. The most important ones are the broadband noise power, the close-in noise power, nonlinearity, a spurious free dynamic range, temperature stability, isolation between channels (for multiple channels systems), power consumption and price. The main parameter this article will be investigating is the close-in phase noise of the receiver's input section. The measurements of residual phase noise, up to 100 kHz away from the 1.3 GHz carrier, are of most interest. ***Figure 1*** shows a simplified prototype of the receiver's input section that has been constructed for applications in high-energy physics for the control of electromagnetic fields in superconducting RF cavities.[1] For this particular application, the demands for phase stability are approximately 0.01° of the integrated RMS phase noise. The main noise contributors are identified first.

Fig. 1 Block diagram of the receiver's analog front-end.

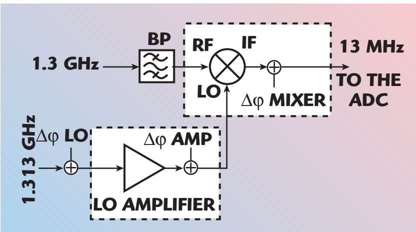

MIXER AND AMPLIFIER NOISE

The following is a short overview of microwave mixer and amplifier noise. The reader should refer to the literature listed at the end of the article for more detailed reading. According to Maas,[2] there are three types of noise generated in a mixer: Shot noise, thermal noise and flicker noise. Shot noise is caused by carriers passing through the junction of a PN diode. Thermal noise is caused by the series resistance in the mixer.[3,4] Flicker noise is related to surface-state density of the material and is not an issue at higher frequencies.[5] There are various parameters that define mixer noise performance and can be set by the designer. Among the most important are the LO power and the VSWR of the mixer ports.

UROS MAVRIC AND BRIAN CHASE
Fermi National Accelerator Laboratory
Batavia, IL

The LO power has no effect on thermal noise, since the series impedance does not change with power. On the other hand, in most mixers, shot noise changes with LO power and is correlated over the whole band. This means that there will be a certain increase in the noise floor due to the mixing of these coherent components. This increase in noise floor can be avoided if proper filtering is used. The noise figure of a mixer decreases with an increase in LO to a certain point.[2]

The noise figure of a mixer also depends on matching.[2,6,7] Using the wave representation of noise (as carried out by Penfield),[8] it can be shown that the noise figure is a function of the reflection coefficient. An obvious approach to solve this problem is to have the mixer ports properly matched. Mixer matching can be achieved by using amplifiers, circulators or passive matching.[6,9]

The output signal-to-noise ratio of a mixer also depends on the sensitivity of the mixer. The sensitivity, or the mixer slope, defines the output DC voltage in volts at the IF port per one radian of change in phase between the RF and LO ports. It is shown in the literature[6] how the mixer sensitivity changes with LO power and matching at the IF port. In general, a capacitive load on the IF improves mixer sensitivity. However, this also causes a decrease in IF bandwidth.

The other source of noise in the input section of the receiver is the microwave amplifier. It was decided to use the amplifier on the LO port since mixers usually demand relatively high LO power for linear and low noise operation. A detailed study of close-in noise added by a microwave amplifier has been presented.[10] Besides broadband noise, amplifiers exhibit close-in flicker noise, which is usually not given in the manufacturer's datasheet. This close-in phase noise generated by the amplifier is up-converted to the LO carrier that is being amplified, which is then transmitted to the IF port through the mixing process. The level of flicker noise close to the carrier that is generated by the amplifier depends on the input power to the amplifier. A more linear amplifier will decrease flicker noise.[10]

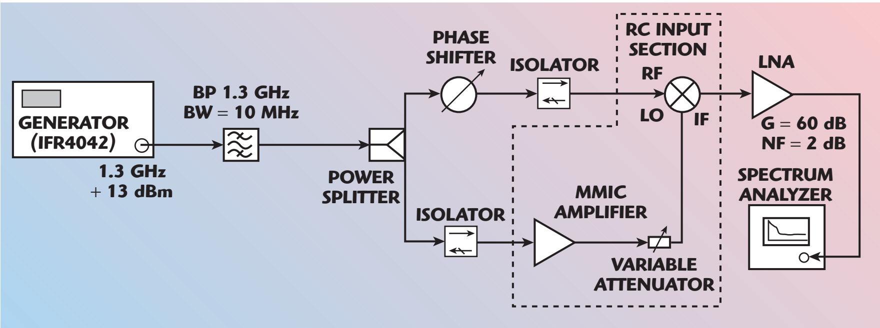

Fig. 2 Residual phase noise measurement test setup.

MEASURING METHOD

The method that was used in this article to measure the residual phase noise has been described in various textbooks and studied in various articles.[4,6] ***Figure 2*** shows a block diagram of the measurement setup.

The low noise RF signal is first split into two branches. One of the branches is delayed by 90° and the two signals are mixed with a mixer. The low noise amplifier on the IF port of the mixer increases the dynamic range of the measuring method. The output is measured with an oscilloscope or a spectrum analyzer. In formal representation, the mixing process is described by

$$A \sin\left(\omega_c t + \Delta\phi_{gen}\right) \bullet \cos\left(\omega_c t + \Delta\phi_{gen} + \Delta\phi_{amp+mixer}\right) \approx \frac{A}{2} \sin\left(\Delta\phi_{amp+mixer}\right) \propto \Delta\phi_{amp+mixer} \quad (1)$$

where


WHEN THERE IS NO MARGIN FOR ERROR...
OUR AIM IS TRUE.
ClearComm Technologies; proven reliability, performance and delivery. Our filter products have been fielded in the toughest environments - communications systems where down time is not an option. Our design capability allows us to address your complex filtering requirements, meeting performance and delivery needs.
Filters, Duplexers, Diplexers and RF assemblies covering the frequency range of 1 MHz to 18 GHz
Filter Responses – Lowpass, Highpass, Bandpass and Bandstop
Cavity and Discrete Element designs
Experienced in High RF Power Requirements
ClearComm technologies, LLC
28410 Crown Road, Fruitland, MD 21875, 410-860-0500, www.clearcommtech.com

ω_c = frequency of the carrier
$\Delta\phi_{gen}$ = phase noise added by the signal generator
A = product of both amplitudes
$\Delta\phi_{amp+mixer}$ = residual phase noise added by the input section of the receiver, that is, by the amplifier and mixer

The term representing the second harmonic is canceled out, since the phase noise is observed at base band. Small angles approximation is also assumed to obtain the expression on the RHS of Equation 1. The amplitude noise that could be included in Equation 1 as an additional amplitude modulation term is neglected since the mixer is driven close to saturation. In order to correctly translate the phase deviation into an equivalent amplitude deviation, the sensitivity (slope) of the mixer has to be measured. One of the possible ways to measure the slope is by applying slightly different frequencies (by approximately 100 kHz) on the RF and LO ports of the mixer. With an oscilloscope, one can measure a change in voltage over a time (phase) interval. The observed time interval has to be small (for instance 1/100) compared to the period of the signal for accurate slope measurements. As shown by Walls,[6] the mixer sensitivity is a function of frequency. For accurate measurements, it is therefore necessary to repeat the slope measurement for each offset frequency.

When measuring phase noise with the setup shown, it is important to reduce the amplitude noise as much as possible. Filtering and driving a balanced mixer in saturation will help to reduce the amplitude noise power. It is also important to have a good match on all the ports of the mixer, which can be achieved with isolators. At the same time this guarantees better isolation between splitter ports. Last but not least, the cables of the measurement setup should be kept as short as possible.

As a measurement method check, the close-in phase noise of the signal source was measured at 1.3 GHz. The measured values over a 10 MHz bandwidth are given in ***Figure 3***. The generator noise in dBc/Hz is compared to the manufacturer's values and to the specified phase noise values of the dielectric resonator oscillator (DRO).[14] The DRO was used to measure the generator noise using the phase noise analyzer from Wenzel Associates Inc.[15] The measurements show that, due to the measuring method, the noise of the generator is subtracted out. Consequently, a lower noise floor than the one shown in the figure is measured.

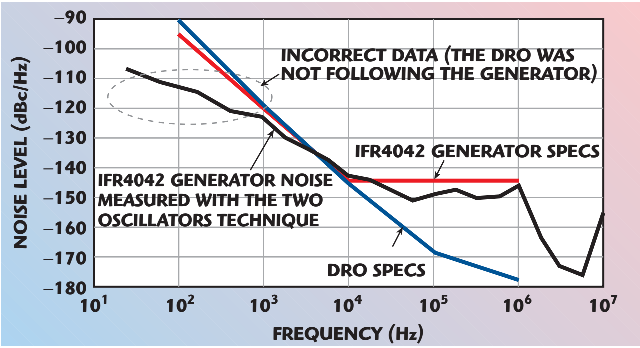

▲ *Fig. 3 Measured generator noise.*

MEASUREMENT RESULTS

Using the measuring technique described in the previous section, measurements using 7, 13, 10 and 17 dBm level mixers were carried out. The MMIC amplifier (HMC481 from Hittite)[11] in the LO

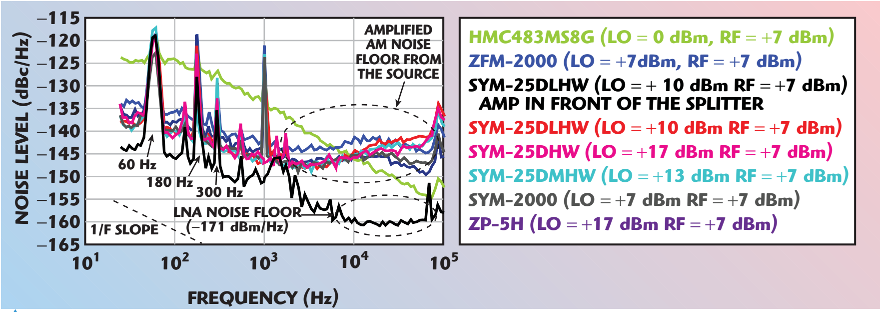

▲ *Fig. 4 Measured residual phase noise in the receiver front-end for various commercially available mixers.*

branch was the same in all cases (except for the measurement with the active mixer). By varying the attenuation at the output of the amplifier, various power levels were achieved that were needed for each particular mixer. ***Figure 4*** shows the relative noise floor of phase noise measurement results in dBc/Hz. In addition to passive mixers manufactured by Mini Circuits,[12] one active mixer from Hittite[13] was also measured. As mentioned at the beginning of this article, the measured close-in phase noise is supposed to be generated in both the LO amplifier and the mixer. In order to check which of the two is adding more noise, the amplifier was moved in front of the splitter. In this way, the phase perturbation of the amplifier is canceled out by the measuring method. The results of this test are shown in the figure. It is obvious that the majority of the noise is introduced by the amplifier. Measurements of various mixers, in the same configuration, show that different passive mixers with the same LO amplifier port exhibit the same flicker noise performance. This is more proof that the measured noise is dominated by the LO amplifier contribution. The green curve shows the noise floor of the active mixer.[13] Although the test setup is kept the same (except for the LO amplifier), the active mixer exhibits higher phase noise over the band from 100 Hz to 10 kHz.

The RMS jitter is an often-used measure of the close-in phase noise. It is equal to the integral of twice the values measured (the measured values are SSB) over the bandwidth of interest. ***Table 1*** summarizes the integrated RMS phase/time perturbation for some of the measured configurations. The integrated bandwidth is from 100 Hz to 100 kHz.

NONLINEARITY MEASUREMENTS OF MIXERS

In the present applications, the mixer is the input device to the receiver. According to the measurement results, the best choice for the input mixer would be a level 7 mixer since it needs the lowest LO power. However, other issues like linearity have to be considered. As mentioned previously, the LO power defines the linearity of the mixer. As a matter of fact, it is expected for a low level mixer to have poor linearity performance.

TABLE I

TIME AND AMPLITUDE JITTER EQUIVALENTS OF THE MEASURED RESIDUAL NOISES

Mixer	t_{jrms} (fs)	ϕ_{jrms} (°)
HMCA83MS8G (active)	2.4	1.1e-3
SYM25DLHW (L10)	1.6	7.8e-4
ZFM-2000 (L7)	1.7	8.1e-4
SYM25DHW (L17)	1.5	7.2e-4
SYM25DLHW amp in front of the splitter	0.3	1.6e-4

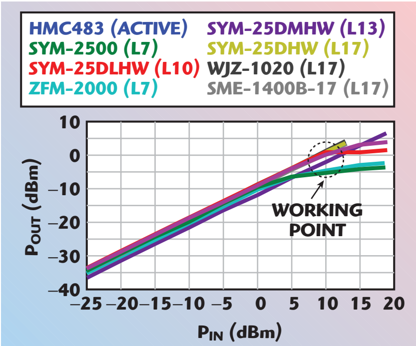

▲ *Fig. 5 Carrier output as a function of input power at the RF port for various mixers.*

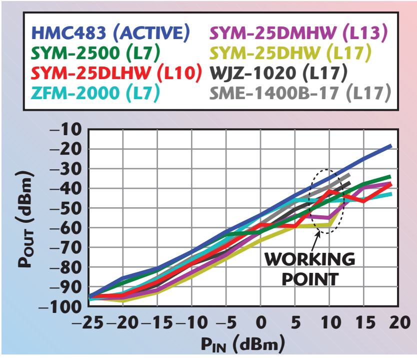

▲ *Fig. 6 Second harmonic power at the IF port as a function of input power at the RF port for various mixers.*

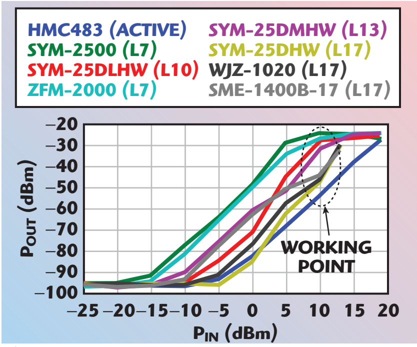

▲ *Fig. 7 Third harmonic power at the IF port as a function of input power at the RF port for various mixers.*

Measurements show that in practice there are exceptions to this rule. ***Figures 5, 6*** and ***7*** show linearity measurements for various commercially available mixers. It is interesting to note, for instance, that the level 13 mixer starts compressing at lower input power than the level 10 mixer. Measurements of the second and third harmonics give a more detailed insight into the linearity issues of various mixers. For example, measurements show that the second harmonic of the level 10 mixer can be compared at certain operating points to the linearity of a level 17 mixer. On the other hand, the third harmonic of the level 10 mixer is much higher than the third harmonic generated by a level 7 mixer at specific input power values. It is worth noting that the curves presented depend on LO power. It is therefore necessary for the designer to carry out extensive measurements before choosing a mixer and setting the operating point.

CONCLUSION

The residual phase noise introduced by a generic receiver's front-end was measured. Different commercially available mixers were used for the down-conversion. The measurements show that the major contributor to the close-in phase noise of the simplified input stage is the LO amplifier. From the close-in phase noise point of view, it is sometimes better to use a passive mixer with an external LO amplifier rather than an active mixer with an integrated LO amplifier. In the circumstances presented in this article, the mixer type has no effect on the relative noise floor measurements. As a consequence, the most appropriate mixer for a specific system should be chosen according to other parameters. In this article, linearity was investigated. As expected, measurements show that, as an average, level 17 mixers along with the active mixer exhibit the best linearity performance. However, at some working points a level 13 or even a level 10 mixer can produce lower second or third harmonics than a level 17 mixer. Depending on the design, the linearity and close-in phase noise characteristics of the receiver's front-end can be optimized by choosing the most appropriate mixer and amplifier. As an example, the requirements for a phase perturbation of 0.01° RMS and an RF port input power of +9 dBm were set. For this particular application, a mixer similar to HMC483MS8G cannot be used. According to the measurements shown, the SYM-25DLHM would be a good choice. ■

ACKNOWLEDGMENTS

The authors would like to thank Frank Ludwig and Stefan Simrock of Deutsches Elektronen Synchrotron (DESY) and Archita Hati of the National Institute of Standards and Technology for their valuable and helpful comments.

References

1. U. Mavric and B. Chase, "Analog Receiver and Transmitter Design for the ILC Main LINAC LLRF Control System," *2007 IEEE Eurocon*, Warsaw, Poland.
2. S.A. Maas, *Microwave Mixers*, Second Edition, Artech House Inc., Norwood, MA, 1993.
3. M.W. Muterspaugh, et al., "Single Balanced Mixer Output Filter," US Patent 5,034,994, July 1991.
4. F.L. Walls, et al., "Extending the Range and Accuracy of Phase Noise Measurements," *Proceedings of the 42nd Annual Symposium on Frequency Control*, 1998, pp. 432–441.
5. B.C. Henderson, "Mixers in Microwave Systems: Part 1," *Watkins-Johnson Co. Tech-Notes*, Vol. 17, No. 1, January 1990.
6. F.L. Walls, et al., "Accurate Measurements of Spectral Density of Phase Noise in Devices," *Proceedings of the 31st Annual Symposium on Frequency Control*, 1977, pp. 335–343.
7. P. Will, "Reactive Loads: The Big Mixer Menace," *Microwave*, April 1971, pp. 38–42.
8. P. Penfield, "Wave Representation of Amplifier Noise," *IRE Transactions on Circuit Theory*, Vol. 9, No. 1, March 1962, pp. 84–86.
9. "Doubly-balanced Mixer Termination," US Patent 4,601,063, July 1986.
10. A. Hati, et al., "Merits of PM Noise Measurements Over Noise Figure: A Study at Microwave Frequencies," *IEEE Transactions on Ultrasonics, Ferroelectrics and Frequency Control*, Vol. 53, No. 10, October 2006, pp. 1889–1894.
11. http://www.hittite.com/product_info/product_specs/amplifiers/hmc481mp86.pdf.
12. http://www.minicircuits.com/.
13. http://www.hittite.com/product_info/product_specs/mixers/hmc483ms8g.pdf.
14. http://www.psi.au.com.
15. http://www.wenzel.com.

Uros Mavric *received his BS degree in electrical engineering from the University of Ljubljana, Slovenia, and has been involved in particle accelerator physics ever since. He worked as a junior researcher at Instrumentation Technologies, Slovenia, for three years. In 2005, he won a scholarship at the Fermi National Accelerator Laboratory, where he is presently working on his PhD thesis. He has been involved in the design of the analog receiver and transmitter for the International Linear Collider main LINAC LLRF control system.*

Brian Chase *received his BS degree from the Illinois Institute of Technology in 1992. He is the group leader for RF control systems in the Accelerator Division at Fermi National Accelerator Laboratory. He is currently involved in the global design effort of the International Linear Collider. His research interests include digital processing schemes for precision closed loop RF control.*

A MICROSTRIP-FED MONOPOLE ANTENNA FOR WLAN USB APPLICATIONS

A compact design for a dual-band microstrip-fed antenna for WLAN USB is presented. The antenna structure consists of a bent copper sheet and a 50 Ω microstrip line. By adjusting the shape and dimensions of the copper sheet, the dual-band characteristics of the proposed antenna can be obtained. The measured bandwidth of the proposed USB antenna covers the WLAN bands (2.45/5.2/5.8 GHz) with a return loss greater than 10 dB. Furthermore, the effect of the metal below the USB antenna is also investigated. Details of the antenna design and experimental results of the constructed prototypes are presented and discussed.

Wireless communication systems have been developed to offer higher data transmission, such as the currently popular bands of Wireless Local Area Networks (WLAN), IEEE 802.11b (2.4 to 2.48 GHz) and 802.11a (5.15 to 5.35 and 5.725 to 5.825 GHz). The planar antenna has a simple structure, lower profile and easy manufacture. Therefore, many compact single or dual-band planar antenna designs for the WLAN bands have been proposed.[1–4] A compact, CPW feed, monopole antenna using a spiral strip and an inverted L strip, operating at both 2.4 and 5 GHz, has been reported.[1] Another compact dual-band antenna, with double L-slits, has also been proposed.[2] A CPW-fed circular slot antenna, with a pair of symmetrically positioned T-shaped slits embedded in the backpatch, has been described.[3] A 2.4/5 GHz dual-band operation was achieved. A broadband or a dual-band operation at 2.4/5 GHz was achieved with another compact dual-/multi-band antenna[4] by adjusting the location of the microstrip feed and designing a notched shape. However, these designs, with a large overall size, are unsuitable for WLAN bands with USB applications. Recently, a 2.4 GHz meander-line printed antenna[5] on a USB WLAN card was presented. But the single band operation is not suitable to WLAN in the 5 GHz band applications.

In this article, a dual-band design of a microstrip-fed monopole antenna is proposed for WLAN USB applications. By properly adjusting the shape of the copper sheet and feed structure, the dual-band design of the proposed antenna, operating at frequencies covering the 2.4/5 GHz WLAN bands, is achieved. This proposed antenna is suitable for a universal serial bus dongle installation on a laptop. The proximity effect of the metal on the antenna performance is investigated and compared with the printed antenna.

WEN-SHAN CHEN AND
KUANG-YUAN KU
Southern Taiwan University
Tainan, Taiwan, ROC

ANTENNA DESIGN

Figure 1 shows the geometry of the dual-band antenna for WLAN USB applications. The proposed antenna is fabricated on an FR4 substrate with a thickness h = 1.6 mm and a relative permittivity ε_p = 4.4 with dimensions of 16 × 50 mm. The material of the proposed antenna is a 0.1 mm copper sheet, which is connected to a 50 Ω microstrip line. By using a bent copper sheet, the antenna size can be made compact. The total height of the proposed antenna is (h + 8 mm) from the ground plane. The dimensions of the proposed antenna are W_1 = 8 mm, W_2 = 18 mm, W_3 = 6 mm and W_4 = 13 mm. In addition, four different feed structures on the copper sheet connected to the 50 Ω microsrip line have been investigated, with a 1 mm separation from the ground plane of the FR4 substrate. The first resonant frequency is determined by the dimensions of the bent copper sheet and the higher resonant mode is excited by varying the feed structure of the copper sheet near the 50 Ω feed line.

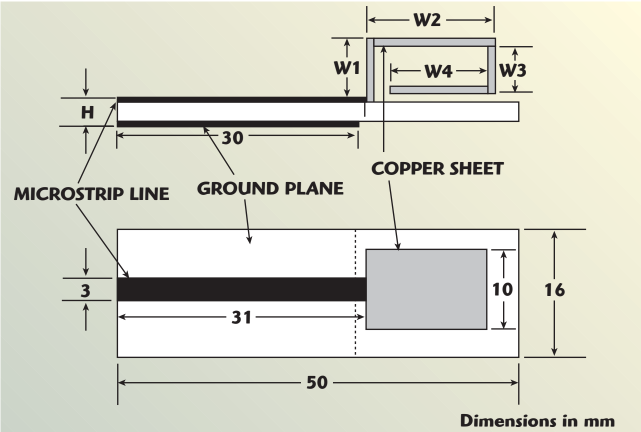

Fig. 1 Geometry of the dual-band antenna for WLAN USB.

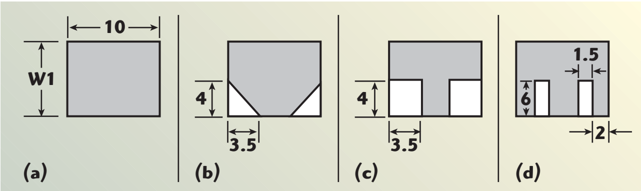

Fig. 2 Geometries of the different feed shapes.

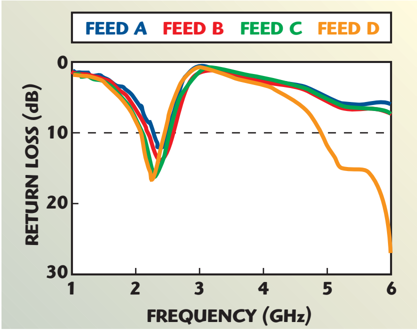

Fig. 3 Measured return losses for different feed structures.

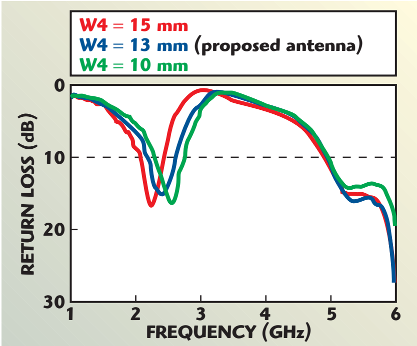

Fig. 4 Measured return losses for different values of W4.

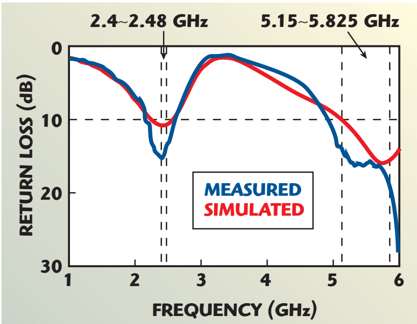

Fig. 5 Measured and simulated return losses of the proposed dual-band antenna.

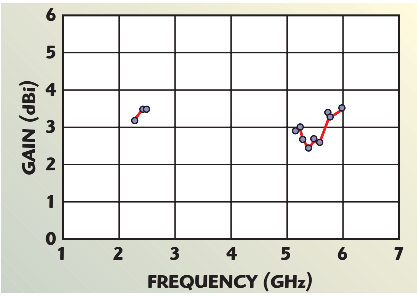

Fig. 6 Measured gain of the dual-band antenna.

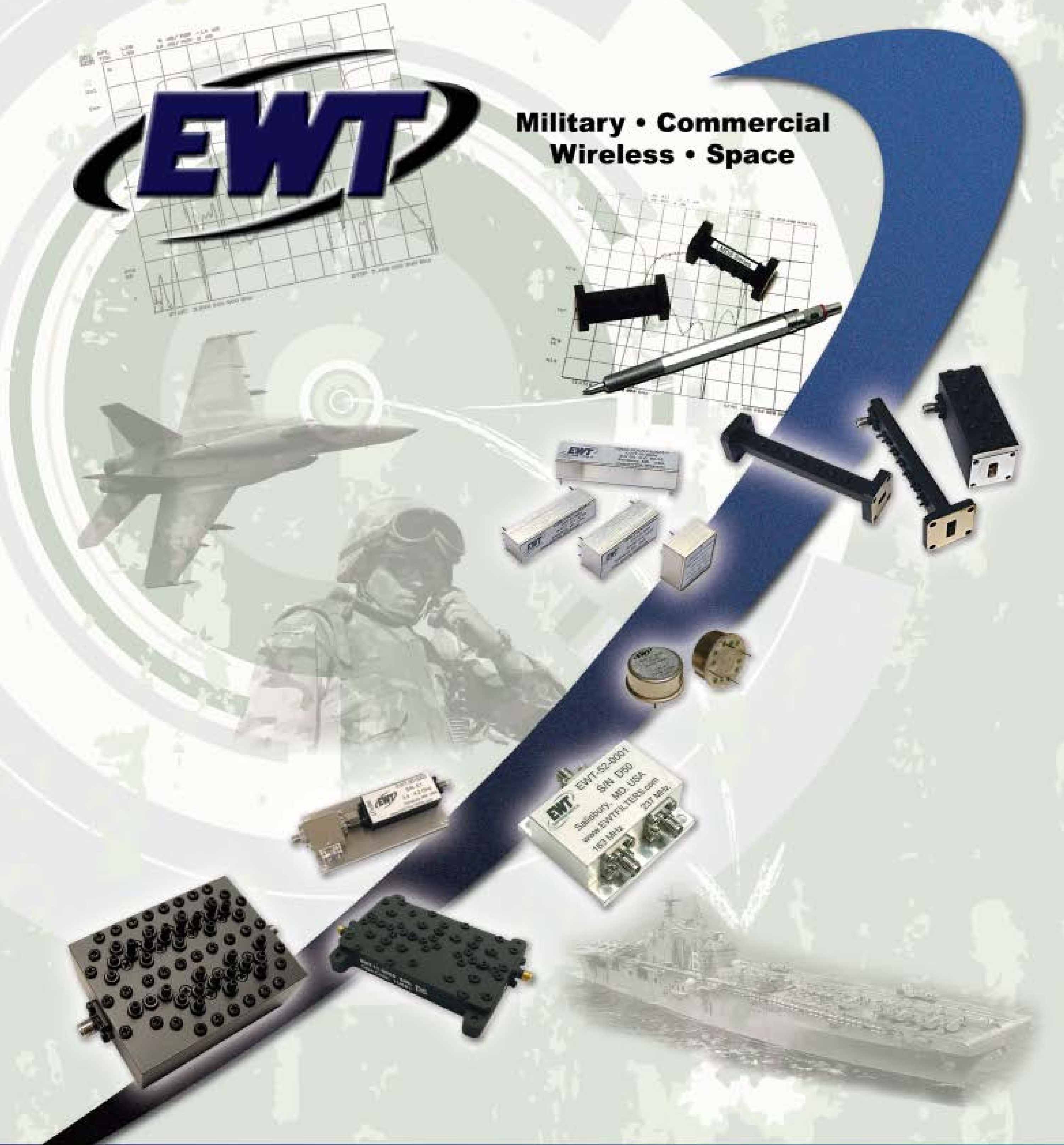
EWT
Military • Commercial
Wireless • Space
EWT-52-0001
S/N D50
Salisbury, MD USA
www.EWTFILTERS.com
163 MHz
237 MHz

PARAMETRIC STUDY AND DISCUSSION

Design with Different Shape of the Feeds

Figure 2 shows the various feed geometries of the proposed antenna. Four feed structures have been tried: rectangular (A), trapezoid (B), two notches (C) and two slits (D).

The measured return losses for the different feeds are shown in ***Figure 3***, where W_1 = 8 mm, W_2 = 18 mm, W_3 = 6 mm and W_4 = 15 mm. It can be seen that the higher resonant mode is excited by the feed structure D. The feed structure D was adopted for all the antennas discussed in this article.

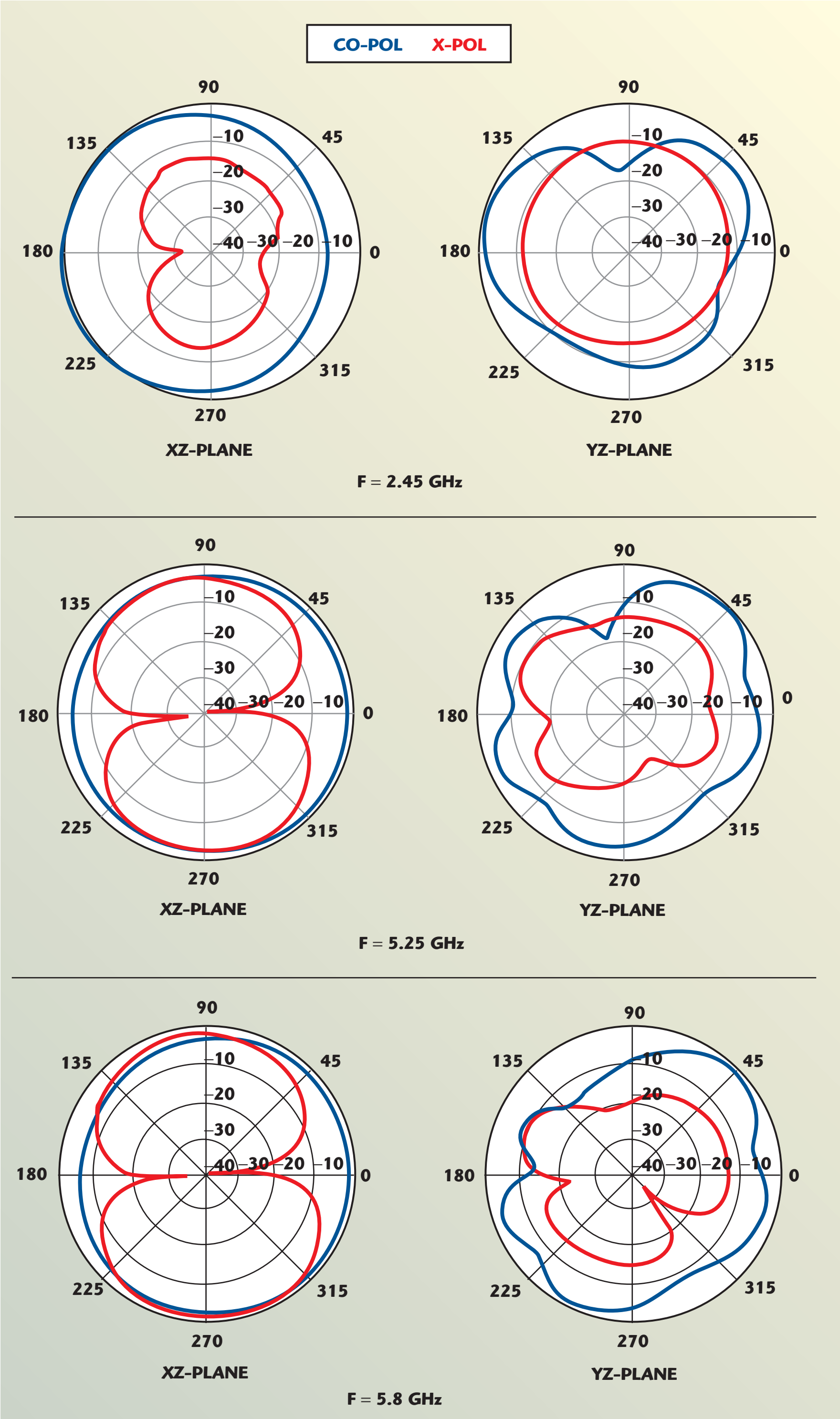

▲ *Fig. 7 Measured xz-plane and yz-plane radiation patterns of the dual-band antenna.*

Different Values of Copper Sheet Length W_4

The measured return losses for different values of length W_4 of the copper sheet are shown in ***Figure 4***. It is observed that the length W_4 is the important parameter to determine the lower frequency (2.4 GHz band). As W_4 decreases, the lower band moves to a higher frequency. On the other hand, the upper fre-

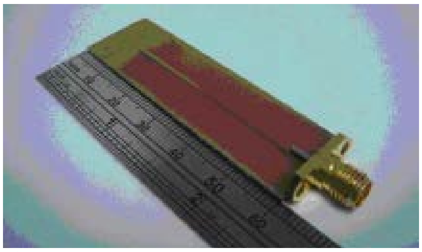

▲ *Fig. 8 The printed antenna.*

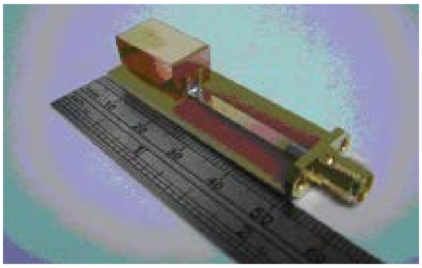

▲ *Fig. 9 The proposed dual-band antenna.*

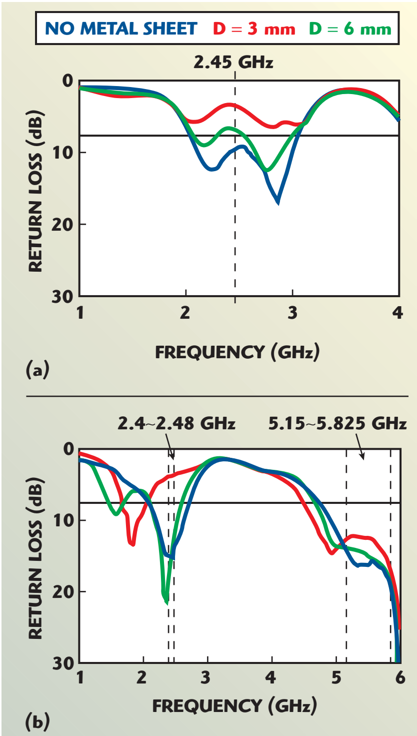

▲ *Fig. 10 Measured return losses showing the effect of a metal sheet on antenna performance for the (a) printed antenna and (b) proposed dual-band antenna.*

quency (5 GHz band) is insensitive to changes in W_4.

Optimized Design

Figure 5 shows the measured and simulated return losses of the proposed dual-band antenna with the following dimensions: W_1 = 8 mm, W_2 = 18 mm, W_3 = 6 mm and W_4 = 13 mm. The simulated results were obtained by using the High Frequency Structure Simulator (HFSS). Reasonable agreement between the measured and simulated results is observed. The obtained impedance bandwidths are 18.9 percent (2.15 to 2.6 GHz) at the lower band and over 19.6 percent (4.93 to 6 GHz) at the upper band, covering WLAN (2.4 to 2.4835 GHz, 5.15 to 5.35 GHz and 5.725 to 5.850 GHz) operating bands. The proposed antenna possesses the advantage of low profile, small size, simple structure and easy manufacture. It is suitable for use in portable devices of wireless applications.

The far field radiation patterns for the proposed antenna were measured in an anechoic chamber. ***Figure 6*** shows the measured peak gain for the dual-band antenna. The 2.4 GHz band (2.3 to 2.5 GHz) has a peak gain of approximately 3.4 dBi; the gain variation is less than 0.3 dBi. For the 5 GHz band (5.15 to 5.8 GHz), the peak antenna gain is approximately 3.3 dBi and the gain variation is less than 0.92 dBi; the gain variation in the proposed antenna is stable. The measured radiation patterns of the proposed antenna at some typical frequencies are also investigated. ***Figure 7*** plots the measured radiation patterns of the dual-band antenna at 2.45, 5.2 and 5.8 GHz.

The Effect of Metal on the Antenna Performance

For practical applications, the effects on the impedance bandwidth of adding a copper sheet below the proposed antenna have been investigated. In addition, a printed meander line monopole antenna was fabricated, following the design process described by C.C. Lin, et al.[5] A photograph of the printed antenna for WLAN USB is shown in ***Figure 8***. A photograph of the constructed prototype dual-band antenna is shown in ***Figure 9***. ***Figure 10*** shows the measured return loss when adding a metal sheet below the antennas. The parameter d is the distance between the ground of the antennas and a large copper sheet (size 200 × 200 mm). As seen, the printed antenna is significantly affected by adding a copper sheet below the ground plane of the antenna, while for the proposed antenna, adding a copper sheet below the ground plane causes a small frequency shift of the 2.45 GHz band. The effect of adding a large copper sheet slightly affects the bandwidth performance of the proposed antenna in the 5 GHz band. This is probably because the resonance mode at 5 GHz of the proposed antenna is mainly contributed by the vertical part of the antenna configuration.

CONCLUSION

In this article, a dual-band, small size and simple configuration USB antenna for WLAN applications was proposed. The dual-band characteristic for the 2.4/5 GHz bands can be achieved by using two slits on the feed structure of the copper sheet. Finally, the proximity effect of a metal on the antenna performance was investigated. The proposed antenna has good radiation characteristics, better than a planar printed antenna, because of its solid radiator. ■

References

1. T.H. Kim and D.C. Park, "CPW-fed Compact Monopole Antenna for Dual-band WLAN Applications," *Electronic Letters*, Vol. 41, 2005, pp. 291–293.
2. T.H. Kim and D.C. Park, "Compact Dual-band Antenna with Double L-slits for WLAN Operations," *IEEE Antennas and Wireless Propagation Letters*, Vol. 4, 2005, pp. 249–252.
3. J.Y. Sze, C.I.G. Hsu and J.J. Jiao, "CPW-fed Circular Slot Antenna with Slit Back-patch for 2.4/5 GHz Dual-band Operation," *Electronics Letters*, Vol. 42, 2006, pp. 563–564.
4. N. Behdad and K. Sarabandi, "A Compact Dual-/Multi-band Wireless LAN Antenna," *2005 IEEE Antennas and Propagation Society International Symposium Digest*, pp. 527–530.
5. C.C. Lin, S.W. Kuo and H.R. Chuang, "A 2.4 GHz Printed Meander-line Antenna for USB WLAN with Notebook-PC Housing," *IEEE Microwave and Wireless Components Letters*, Vol. 15, No. 9, August 2005, pp. 546–548.

EFFECT OF RESISTIVITY VARIATIONS ON THE PERFORMANCE OF LOSSY MICRO-MACHINED RESONATORS

This article examines the effect of wafer resistivity on micro-machined resonator performance. Two similar topologies, on two wafers of different (low and high) resistivities, have been compared at X-band. The high resistivity wafer shows a 10 dB improvement in insertion loss, compared to the CMOS grade silicon wafer. A bond strength measurement has been carried out. Furthermore, the effect of filling the cavity with polyimide on the electrical characteristics has also been compared with other topologies.

Microstrip resonators have very important applications in microwave or millimeter-wave systems. They are important components of microstrip filters, microstrip oscillators and microstrip antennas, and enable miniaturization of microwave equipment with improved performance. The performance of a microstrip resonator relies on the electromagnetic field distribution, the resonant frequency and the quality factor, Q. Microwave high-Q resonators are traditionally made of metallic rectangular or cylindrical waveguides, which are heavy, costly to manufacture and difficult to integrate with monolithic circuits.

Microwave and millimeter-wave planar integrated circuits having low loss and high-Q are gaining popularity and demand. Compared to standard topologies, they offer cost-reduction, planarity and improved performance, and can be fabricated easily on silicon substrates due to micro-machining capabilities. They are also amenable for integration into a compact, stable package meeting environmental requirements.

Resonators, using bulk micro-machining on high resistivity silicon substrates with interface layers of oxide and nitride, have been described by Papaloymerou, et al.[1] But the effect of a low resistivity wafer on the performance was not discussed. It was stated by some authors that the effect of substrate resistivity becomes negligible when using interface layers of oxide and nitride. This article demonstrates the considerable effect of the substrate resistivity on the performance of the

KAMALJEET SINGH AND
K. NAGACHENCHAIAH
Semiconductor Laboratory (SCL)
S.A.S Nagar, Chandigarh, India

micro-machined resonators, in spite of using passivation layers. Two similar microstrip lines resonators, with one fabricated on a high resistivity silicon (HRS) substrate (ρ > 7 kΩ-cm) and the other on a low resistivity CMOS grade silicon (LRS) substrate ($\rho \approx$ 3 to 5 Ω-cm), have been compared. For accurate measurement of the quality factor, the structures were made lossy by using a weak coupling, using displacement of the slots rather than narrowing down the slot dimensions.[2] The use of polyimide has found great potential due to its compatibility with the MMIC and CMOS integration processes, leading towards an RFIC/SoC concept. This article details the configuration, fabrication steps and a comparison of the measured results of all the fabricated topologies.

RESONATOR ANALYSIS

A planar micro-machined resonator is shown in ***Figure 1***. Two stacked wafers, the bottom one including a micro-machined cavity, are eutectically bonded. The top wafer couples the electromagnetic energy into the cavity through the two slots and acts as a feed. By using the equivalence principle, the slots can be replaced by perfect electric conductors with equivalent magnetic currents flowing above their surface. Thus, the cavity and the microstrip lines are separated by the ground plane of the microstrip lines. The lumped equivalent model of the resonator is also shown in ***Figure 2***.

The slots are modeled by ideal transformers and the cavity behavior by an RLC parallel circuit. The altering of the slot positions is equivalent to changing the transformer turns ratio, which in turn changes the response bandwidth. The magnetic coupling is ensured by two microstrip lines through the two slots located in the ground plane of the top wafer. These two apertures provide magnetic coupling to the cavity. The coupling coefficient between the microstrip lines and the cavity can also be controlled by the size and location of the slots. By decreasing the slot distance, the bandwidth can be reduced.[3] The design of the micro-machined cavity resonators is based on the theory of rectangular cavities. The resonators are operated in the fundamental TE101 mode. The resonant frequency of the cavity is evaluated using the following equations:

$$f_{res} = \frac{c}{2\sqrt{\varepsilon_r}}\sqrt{\left(\frac{m}{l}\right)^2+\left(\frac{n}{h}\right)^2+\left(\frac{o}{w}\right)^2} \quad (1)$$

$$\delta = \frac{1}{\sqrt{\pi f \nu \sigma}} \quad (2)$$

$$\varepsilon_{eff} = \frac{\varepsilon_r+1}{2}+\frac{\varepsilon_r-1}{2}\left[1+\frac{12h}{W}\right]^{-\frac{1}{2}} \quad (3)$$

$$\lambda = \frac{c}{f_{res}\sqrt{\varepsilon_{eff}}} \quad (4)$$

where l, w, h are the cavity length, width and height, and m, n, o are the Eigenvalues 1,0,1 for the fundamental mode. The microstrip width and height is denoted as W and h.

FABRICATION

The X-band resonator is fabricated using standard micro-machining techniques.[4] Two silicon wafers, 675 μm thick, are stacked together with the bottom wafer micro-machined to realize the cavity using a KOH etch. Two variants are fabricated, one having a high resistivity top wafer and a low resistivity wafer at the bottom (HRS). The second has low resistivity wafers at both top and bottom (LRS). The microstrip lines, made of Cr/Au, were fabricated using E-beam metallization and patterned by a lift-off lithography technique. The bottom of the feed (top wafer), which contains the coupling slots, was aligned and metallized (Cr/Au) by a lift-off process and acts as a ground plane. Oxide (0.5 μm) and nitride (0.25 μm) layers were deposited on the low resistivity wafers using a LPCVD process.

To make the cavity, the low resistivity silicon bottom wafer is etched with KOH to a depth of 0.45 mm by controlling the etch rate. The bottom wafer is then metallized with 1 μm gold. The top and bottom wafers are stacked together using eutectic bonding. The wafers are misaligned during bonding so that after dicing the wafer a small opening is created, which acts as a ground and facilitates testing in the microstrip mode itself. The length and width of the cavity are selected to be 15.5 and 15.38 mm, respectively, to get a resonant frequen-

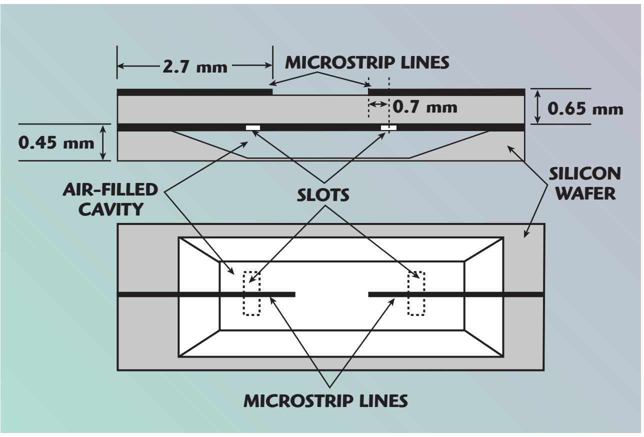

▲ *Fig. 1 A micro-machined resonator with machined cavity.*

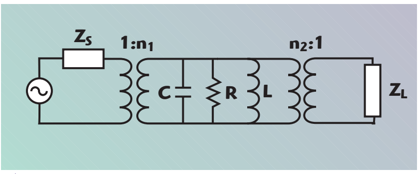

▲ *Fig. 2 Equivalent circuit of the micro-machined resonator.*

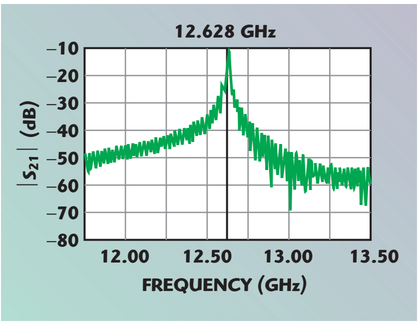

▲ *Fig. 3 Simulated response for the high resistivity substrate (HRS) resonator.*

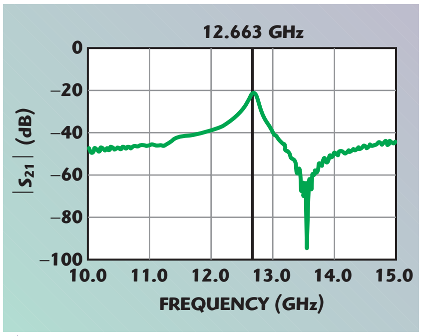

▲ *Fig. 4 Simulated response for the low resistivity substrate (LRS) resonator.*

RF MOSFETs

Richardson Electronics & SEMELAB

50V RF MOSFETs

Semelab provides one of the broadest lines of Silicon RF Power MOSFETs for all of your HF, VHF & UHF applications.

SEMELAB's 50V RF MOSFETs offer:

- High gain

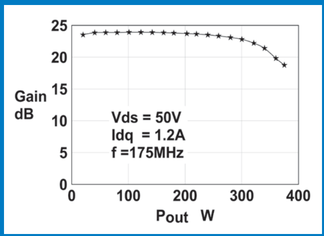

- Usable to 500MHz

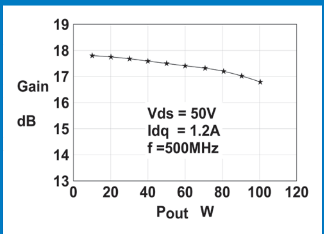

Ideal for:

- Broadcast Transmitters
- Jammers
- Switch-mode Amplifiers

Technical Excellence in RF Performance

SEME LAB

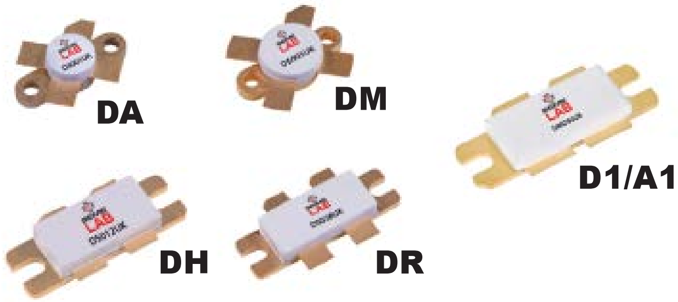

Device	Minimum Output Power (W)	Minimum Efficiency (%)	Minimum Gain (dB)	Test Frequency (MHz)	Package Style
D5001UK	20	50	16	175	DA
D5005UK	80	50	16	175	DM
D5012UK	100	50	10	500	DH
D5028UK	300	60	13	175	DR
D5029UK	350	60	13	175	DR
DMD5012	100	65	15	500	D1/A1
DMD5028	300	60	20	175	D1/A1
DMD5029	350	60	20	175	D1/A1

RoHS Compliant *Richardson offers RoHS compliant SEMELAB products.*

Contact your Richardson sales engineer to identify the best SEMELAB solution for your next amplifier design.

Connect to the latest SEMELAB products and information at www.rell.com/Semelab

Your Global Source for RF, Microwave and Power Conversion Products

Richardson Electronics

Visit www.rell.com/locations.asp for a complete listing of our 70 worldwide locations.
Call 1-800-737-6937 (USA/Canada) • rfwireless.rell.com • rwc@rell.com

cy of approximately 12.5 GHz. The slots are placed nearer to the open-ended feed line rather than a $\lambda/4$ distance away to introduce a weak coupling and consequently increasing the losses. This results in an insertion loss of approximately 10 dB, thereby facilitating the accurate measurement of the quality factor. The slot width and length are kept approximately 0.63 and 2.9 mm, respectively.

The cavity is then filled with polyimide after the normal fabrication steps. The polyimide is cured for one hour at 120°C and sealed with a conductive epoxy. The total assembly is further cured for one hour.

RESULTS AND DISCUSSIONS

A simulation study was carried out on the two resonators using the 3D simulator from CST[5] based on the finite element method (FEM). The simulated results of the two kinds of resonators are shown in ***Figures 3*** and ***4***, respectively. It can be seen that the simulated resonance is approximately 12.5 GHz, but with a difference of 10 dB in the insertion loss. The measured results are shown in ***Figures 5*** and ***6***, respectively. The results show an insertion loss of approximately 12 dB for HRS and 21.5 dB for LRS at approximately 11.5 GHz. The measured difference of 9.5 dB in insertion loss is in close agreement with the simulated 10 dB difference. The increase in insertion loss of approximately 2.0 dB is attributed to the conductor loss and other parasitics introduced in the testing. The conductor loss can be overcome by increasing the metallization thickness.

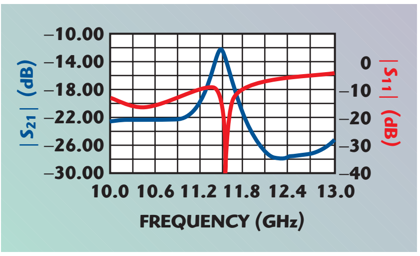

▲ *Fig. 5 Measured response for the high resistivity substrate (HRS) resonator.*

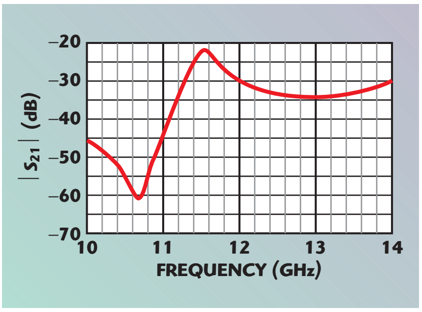

▲ *Fig. 6 Measured response for the low resistivity substrate (LRS) resonator.*

The measured results show a resonance frequency lower by 1.5 GHz from the simulated value. This can be explained as follows: the structures are tested in the microstrip mode by introducing a ribbon bond. A 20-mil ribbon with a 2 mm length introduces an inductance of approximately 0.32 nH, resulting in a lower frequency. The simulations carried out to validate this drift used the jig shown in ***Figure 7***.

The singly loaded Q of the structures can be calculated as[8]

$$Q_L = \frac{2f_0}{f_u - f_l} = 220,$$

$$S_{21}(dB) = 20\log_{10}\frac{(Q_l)}{Q_e} \qquad (5)$$

$$Q_e = 826, \; \frac{1}{Q_l} =$$

$$\frac{1}{Q_u} + \frac{1}{Q_e}; \; Q_u = 300 \qquad (6)$$

The value achieved shows a much higher Q than the microstrip structure. The eutectic bond strength is measured using a bond pull/die shear tester (DAGE-22 A) on a number of structures and a minimum bond strength of 5 g is observed.

The polyimide-filled cavity changes the effective permittivity, resulting in a value close to 1.625. This results in a resonant frequency theoretically close to 9.05 GHz, which is also validated by practical measurements. The frequency scaling has been done without compromising the

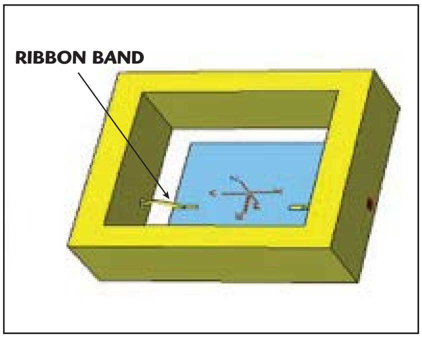

▲ *Fig. 7 Resonator structure with ribbon bond.*

TABLE I

COMPARISON OF MEASURED RESULTS FOR DIFFERENT TOPOLOGIES

Type	HRS	LRS	Polyimide-filled Cavity of LRS
Resonant frequency (GHz)	11.48	11.48	9.05
Bandwidth (MHz)	~ 100	~ 150	~ 160
Insertion loss (dB)	11	~ 20	21

TABLE II

COMPARISON OF VARIOUS TOPOLOGIES

Type	Unloaded Q
Microstrip	~ 60
High resistive wafer (HRS)	300 (meas.)
Low resistive wafer (LRS)	170 (meas.)
Polyimide-filled LRS	124 (meas.)

size of the structure. ***Tables 1*** and ***2*** compare the results of all the topologies previously discussed.

CONCLUSION

The effect of substrate resistivity and polyimide filling on the RF performance of micro-machined resonators has been detailed in this article. The resonators realized using low and high resistivity substrates showed a difference of 10 dB in insertion loss as expected. Also, the different structures give identical resonant frequencies in spite of passivation layers of oxide and nitride in case of the LRS structure. The polyimide-filled cavity lowers the resonant frequency by 2.5 GHz. This shows that frequency scaling can be done without increasing the size of the structure. This property can be useful for designing low frequency circuits without increasing the size. Also, due to polyimide compatibility with the MMIC/CMOS processes, the structure finds a wide range of applications. The structures also show repeatable performances. The quality factor achieved in these structures is much higher than that achievable with a microstrip configuration. The measured Q is less than the simulated one due to extra parasitics involved while testing. Considering all these aspects, including the size reduction and the measured bond strength, these structures are suitable candidates for the development of narrow band filters in the planar environment. ■

References

1. J. Papaloymerou, J.C. Cheng, J. East and L.P.B. Katehi, "A Micro-machined High-Q X-band Resonator," *IEEE Microwave and Guided Wave Letters*, Vol. 7, No. 6, June 1997, pp. 168–170.
2. Hill, J. Papaloymerou and Zilokowski, "High-Q Micro-machined Resonant Cavities in a K-band Configuration," *IEEE Proceedings on Microwave Antenna and Propagation*, October 2001, pp. 307–312.
3. L. Harle, J. Papaloymerou, J. East and L.P.B. Katehi, "The Effects of Slot Positioning on the Bandwidth of a Micro-machined Resonator," *European Microwave Conference Digest*, 1998.
4. M. Stickel, G.V. Eleftheriades and P. Kremer, "High-Q Bulk Micro-machined Silicon Cavity Resonator at Ka-band," *Electronics Letters*, Vol. 37, No. 7, March 2001, pp. 433–435.
5. CST Microwave Studio, 2006 B.
6. G. Duchamp, L. Casadebaig, S. Gauffre and J. Pistre, "A New Tool for Slot-microstrip Transition Simulation," *IEEE Microwave and Guided Wave Letters*, Vol. 7, No. 9, September 1997, pp. 276–278.
7. C. Schollhorn, M. Morschbach and E. Kasper, "Attenuation Mechanism of Aluminum Millimetric-wave Coplanar Waveguides on Silicon," *IEEE Transactions on Electron Devices*, Vol. 50, No. 3, March 2003, pp. 740–746.
8. R. Rhea, "EM Enables Classic Filter Technique," *Microwave Journal*, Vol. 50, No. 2, February 2007, pp. 138–146.

Kamaljeet Singh *received his MS degree from Rajastan University and his M. Tech (microwaves) degree from Delhi University in 1999. He joined the ISRO satellite center, Bangalore, in 1999, where he worked in the receiver division. Since August 2006, he has been working in the RF MEMS area of the Semiconductor Laboratory, Chandigarh, India.*

K. Nagachenchaiah *received his BE degree in electronics and communication engineering and his M. Tech degree in computation and control engineering from Andhra University and IIT Kharagpur, respectively. He joined the Space Applications Center, Ahmerabad, in 1974, and was involved in the design and development of various optical infrared remote sensors for aircraft and space platforms, ground-based instruments and sensor test facilities. He is currently the director of the Semiconductor Laboratory, Chandigarh, India.*

A HIGH LINEARITY AND EFFICIENCY UHF RF POWER AMPLIFIER WITH CARTESIAN FEEDBACK FOR DIGITAL MODULATION

A high linearity and high efficiency UHF, wide bandwidth RF power amplifier is presented. An adaptive bias technique is used to achieve linearity while preserving good efficiency. The bandwidth analysis and the wide bandwidth matching networks of the power amplifier are discussed. Measurements performed on the open loop power amplifier showed an output power of 34 dBm at the 1 dB power compression point, an adjacent channel power ratio (ACPR) of –37 to –38 dBc and a power-aided efficiency (PAE) of 35 to 37 percent in the frequency range of 800 to 900 MHz. For the closed loop amplifier, with a Cartesian feedback IC, an ACPR of –65 to –67 dBc has been demonstrated on a prototype board.

Achieving high linearity while preserving high efficiency in a power amplifier is a real design challenge. A few approaches have been reported to achieve good linearity and high efficiency in a power amplifier. These techniques use envelope tracking of the input voltage and adaptive bias methods. Hanington, et al.[1] achieved an ACPR greater than 26 dB with a dynamic power supply voltage for CDMA. Anderson, et al.[2] have demonstrated an efficiency increase from 20 to 32 percent for CDMA IS-95 using the envelope tracking method. With an adaptive bias technique, Noh, et al.[3] showed an ACPR improvement of 4 dB with a deep pinch-off bias.

In this article, an adaptive bias technique is proposed to meet the high linearity requirements of the high degree digital modulation standard. The adaptive bias technique is investigated to improve both linearity and efficiency of the power amplifier. The optimal device loading impedances and the design of the matching networks are studied for wide bandwidth applications. A prototype power amplifier is demonstrated with an output power of 34 dBm at the 1 dB compression point, an ACPR of –37 to –38 dBc and an efficiency of 35 to 37 percent in the 800 to 900 MHz frequency

M.F. AIN, J.S. MANDEEP AND S.I.S HASSAN
University Sains Malaysia
Penang, Malaysia
K. NARENDRA
Motorola Technology
Penang, Malaysia

range. The power amplifier prototype was extended with a Cartesian feedback IC and an overall ACPR performance from –65 to –67 dBc was measured.

PRINCIPLE OF OPERATION

Adaptive Bias Technique

The adaptive bias technique allows the change of the quiescent current of a device with respect to the input power level, meaning that a low quiescent current at low output power level and an increasing quiescent current at high output power can be achieved. This technique simultaneously provides both high linearity and efficiency characteristics over a broad range of power levels.[2] For multistage amplifiers, similar techniques can be employed for each stage of the amplifier. This can give high gain, high output power and high efficiency at the same time. Each stage of the amplifier operates in deep class AB at fairly low quiescent current. As soon as the input power is applied to the amplifier, the bias point is shifted to produce optimum power performance. ***Figure 1*** shows a single-stage power amplifier utilizing an adaptive bias technique.

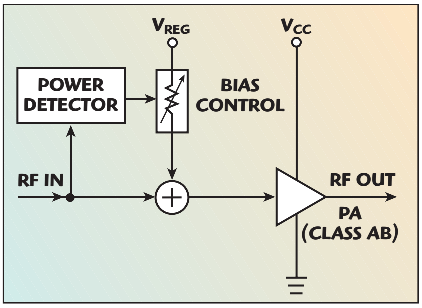

▲ *Fig. 1 Basic block diagram of an adaptive bias technique incorporating a closed loop system.*

Bandwidth Analysis

The inherent bandwidth $(BW)^i$ is the bandwidth obtained under conjugate matching conditions, where the matching loads terminate the two-port device. A conjugate match means that $\Gamma_S = \Gamma_{IN}^*$ or $Y_S = Y^*$ and Y_{IN}, where Γ_S and Γ_{IN} are the reflection coefficients of the matching network and the device, respectively. Y_S and Y_{IN} are the corresponding admittances. The inherent bandwidth is given by

$$(BW)^i = \frac{f_0}{Q}(Hz) \qquad (1)$$

where f_0 is the frequency where the conjugate match values were obtained and Q is the quality factor of the parallel network defined by

$$Q = \omega_0 RC = \frac{R}{\omega_0 L} \qquad (2)$$

By substituting Equation 2 into Equation 1, one can express the inherent bandwidth as

$$(BW)^i = \frac{2f_0 G}{|B|} \qquad (3)$$

where

$R \;\; = 1/2G$
$|B| = \omega_0 C = 1/\omega_0 L$

From Equation 1, to achieve a wide bandwidth, the Q of the network has to be low enough. Similarly from Equation 3, it should be noted that the conductance G must be high enough, while keeping the susceptance B at a low level in order to maximize the bandwidth.

Cartesian Feedback

A Cartesian feedback generates high output power signals with good ACPR. This is accomplished by coupling off a part of the demodulated signal to pre-distort the input baseband I and Q signals, via a comparator circuit.[4] The block diagram of the Cartesian feedback architecture is shown in ***Figure 2***.

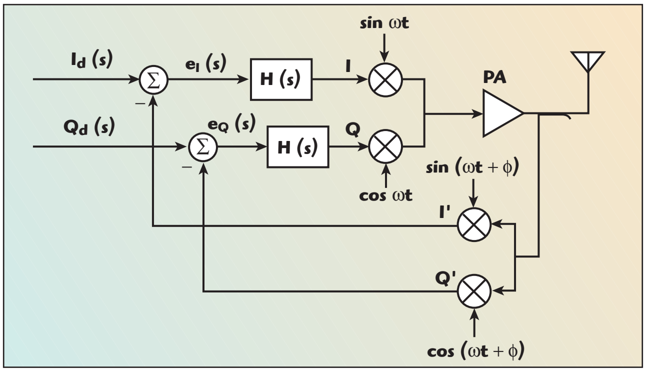

▲ *Fig. 2 Typical Cartesian feedback system.*

The modulated signals are considered as a sum

$$A(t)\sin(\omega_0 t + \Phi(t)) = I(t)\sin\omega_0 t + Q(t)\cos\omega_0 t \qquad (4)$$

$$I(t) = A(t)\cos\Phi(t) \qquad (5)$$

$$Q(t) = A(t)\sin\Phi(t) \qquad (6)$$

The demodulated signals of Cartesian feedback can be expressed as

$$I' = (I\sin\omega t + Q\cos\omega t)\sin(\omega t + \Phi) \qquad (7)$$

$$Q' = (I\sin\omega t + Q\cos\omega t)\cos(\omega t + \Phi) \qquad (8)$$

where ω is the carrier frequency.

DESIGN EXAMPLE USING A GaAs HBT POWER AMPLIFIER

The goal for the power amplifier is to achieve an ACPR of 35 dBc at an operating power of 30 dBm in the frequency range of 800 to 900 MHz. The device used in the three-stage power amplifier is the RF2173[5] transistor from RF Micro Devices, which has been found suitable for the present task. It offers an operating gain of 32 dB and is manufactured in an advanced gallium arsenide heterojunction bipolar transistor (GaAs HBT) process technology. In order to keep the junction temperature within a margin below the specifications, an obligatory power-added efficiency (PAE) higher than 30 percent was calculated for an operating power of 30 dBm.

The device utilizes an adaptive bias scheme. A low gate voltage is applied to the device, which provides a deep class AB bias, keeping the quiescent current at a low level. A broadband matching network with a loaded Q of 5 is chosen to transform the optimum load impedance Z_{OL} to the 50 Ω load termination. The load impedance is obtained from a

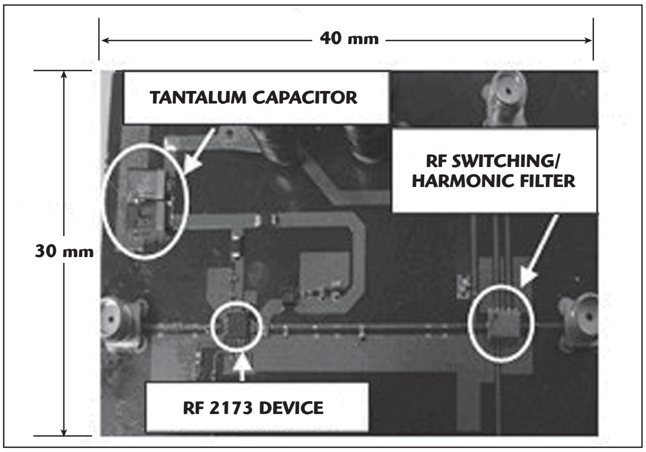

▲ *Fig. 3 RF power amplifier test board.*

simulation template and correlated with the measurement data. A three-stage, low-pass matching network is used to transform the optimum load impedance to 50 Ω. The first matching component is a tapered microstrip line, which significantly increases the efficiency for a wide frequency band.

A second harmonic trap is introduced in the final stage feeding line. The bonding wires together with the external capacitor form a series resonator that should be tuned to the second harmonic frequency in order to increase the efficiency and reduce spurious output. The grounding of each stage is essential and must be directly connected to the ground plane by vias under the device. A short path is required to obtain optimum performance as well as to provide good thermal dissipation.

MEASUREMENT RESULTS

A test board using FR-4 material was fabricated. The printed circuit board (PCB) has a dielectric of 4.5 and a thickness of 14 mils. The test board is shown in ***Figure 3***. The test board size is 40 × 30 mm. Experimental studies show that a 200 μF tantalum capacitor (POSCAPS model from Sanyo) is required at the supply line to improve the transient ACPR due to switching and wide band noise. When changing the power level from noise power to steady-state power, the transient ACPR due to switching depends upon the switching time. Typically, in digital modulation, the input RF (I and Q baseband signals) will provide the control of the switching time. Nevertheless, the common practice to identify the problem is by observing the peak-to-peak ripple of supply voltage. The high-speed Agilent 1 GHz oscilloscope (4GSa/s) 54832B DSO is used to mea-

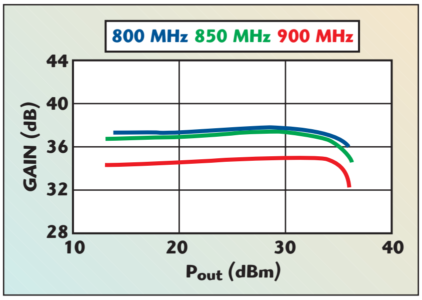

▲ *Fig. 4 Measured gain at the 1 dB compression point.*

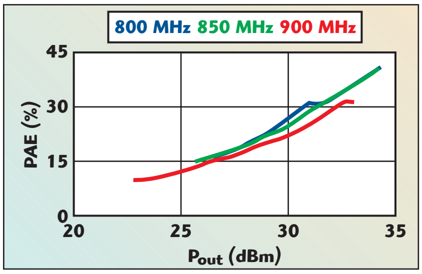

▲ *Fig. 5 Measured power-added efficiency.*

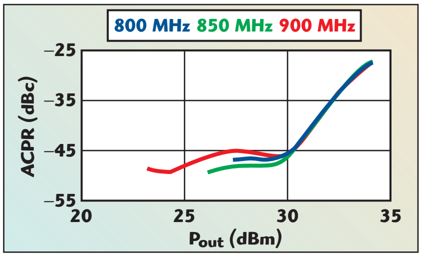

▲ *Fig. 6 Measured ACPR vs. power output.*

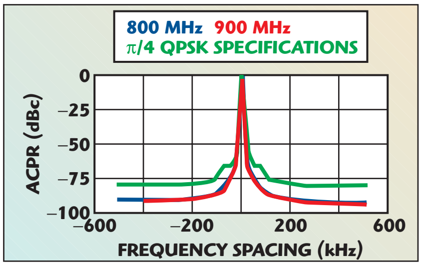

▲ *Fig. 7 Measured ACPR spectrum.*

sure the ripple voltage. In the prototype board, the peak-to-peak ripple of supply voltage is approximately 180 mV. High Q capacitors (from AVX) are used for matching networks.

For the 1 dB compression point and efficiency characterizations, a gate bias with a duty cycle of 25 percent and a pulse width of 600 µs is applied. The ACPR parameter is measured with an IFR 2310 Digital Modulation Analyzer. A π/4QPSK modulation is used to measure the ACPR parameter. A current probe with a Tektronix scope was used to measure the DC current. The measured power at saturation, 1 dB compression point, gain at the rated power, PAE and ACPR are shown in ***Figures 4*** to ***6***, respectively.

To measure the closed loop ACPR performance, a Cartesian feedback IC is used. The amplifier test board is used with a Cartesian feedback IC provided by Motorola. An additional ACPR value of 30 dBc is obtained at ±25 kHz with the closed loop performance. Measurement results of the closed loop ACPR across the bandwidth (800 to 900 MHz) are shown in ***Figure 7***. The ACPR results are plotted for frequency spacings of ±25 to ±512 kHz. The ACPR performance are within the π/4QPSK modulation specifications.

With the improvement in ACPR, the power amplifier is classified as a more linear device and is applicable to most of the wireless communications. Consequently, a power amplifier with good efficiency as well as good linearity has been designed with the aid of a Cartesian feedback.

CONCLUSION

This article explains how to achieve a high degree of linearity to fulfill digital modulation (π/4QPSK) standard requirements. A high linearity and high efficiency UHF RF power amplifier, with a wide bandwidth, is presented using an adaptive bias technique. The bandwidth analysis and wide bandwidth matching networks of the power amplifier are discussed. An output power of 34 dBm at the 1 dB power compression point, an ACPR of –37 to –38 dBc and a PAE of 35 to 37 percent for the frequency range of 800 to 900 MHz are measured on an open loop power amplifier. A power amplifier linearization concept, based on a Cartesian feedback, is presented. The concept has been applied for the digital modulation (π/4QPSK) standard in the 800 to 900 MHz frequency range. For the closed loop amplifier with a Cartesian feedback IC, an ACPR of –65 to –67 dBc has been demonstrated on a prototype board. The power amplifier with Cartesian feedback fulfills the digital modulation (π/4QPSK) specifications. ■

References

1. G. Hanington, P.F. Chen, P.M. Asbeck and L.E. Larson, "High Efficiency Power Amplifier Using Dynamic Power Supply Voltage for CDMA Applications," *IEEE Transactions on Microwave Theory and Techniques*, Vol. 47, No. 8, August 1999, pp. 1471–1476.
2. D.R. Anderson and W.H. Cantrell, "High Efficiency High Level Modulator for Use in Dynamic Envelope Tracking CDMA RF Power Amplifiers," *2001 IEEE MTT-S International Microwave Symposium Digest*, Vol. 3, pp. 1509–1512.
3. Y.S. Noh and C.S. Park, "An Intelligent Power Amplifier MMIC Using a New Adaptive Bias Control Circuit for W-CDMA Applications," *IEEE Journal of Solid State Circuits*, Vol. 39, No. 6, June 2004, pp. 967–970.
4. B. Razavi, *RF Microelectronics*, Prentice-Hall Inc., Upper Saddle River, NJ, 1979.
5. RF2173 RF Micro Devices datasheet; Rev A6 030514.


Network or spectrum analyzer – you choose the mode
The R&S®ZVL – the instrument with two faces
Many users need both a network analyzer and a spectrum analyzer. But budgets are often tight and space is limited. And sometimes a portable solution may be required. Rohde & Schwarz has the answer: the new R&S®ZVL. Not only is it the most compact and lightweight network analyzer in its class, it also is a full-fledged spectrum analyzer.
The R&S®ZVL features exceptional characteristics in each operating mode:
Bidirectional two-port network analyzer with spectrum analyzer functionality
Two models from 9 kHz to 3 GHz or 6 GHz
Only 7 kg in weight and extremely compact
Battery operation or DC power
DUAL MODE
7 kg only
www.rohde-schwarz.com/ad/zvl
ROHDE & SCHWARZ

A HIGHLY INTEGRATED HBT DOWN-CONVERTER MMIC EMPLOYING OPTIMALLY DESIGNED SPIRAL INDUCTOR FILTERS

In this article, a highly integrated down-converter monolithic microwave integrated circuit (MMIC), employing heterojunction bipolar transistors (HBT), is described for application to a one-chip transceiver solution for a Ku-band commercial wireless communication system. The down-converter MMIC includes a mixer, a filter, an amplifier and input/output matching circuits. Spiral inductor structures, employing SiN film, were used to suppress the LO and its second harmonic leakage signals. They were designed so that their self-resonance frequency was accurately tuned to the LO and its second harmonic frequencies, and were integrated in the down-converter MMIC.

Ku-band down-converter MMICs and receiver chips have been reported in the literature.[1–3] However, for one-chip transceiver applications in Ku-band, the following problems should be solved:

- Ku-band commercial down-converter MMICs have been fabricated using GaAs MESFETs and HEMTs[1–3] because they can be easily integrated on one chip with a Ku-band low noise amplifier (LNA) employing GaAs MESFET or HEMT. Owing to the high power characteristics of heterojunction bipolar transistors (HBT), power amplifiers (PA) have been fabricated using GaAs HBT in Ku- and higher frequency bands.[4] However, this has been an obstacle in the realization of a one-chip transceiver solution (including PA, LNA, mixer and IF amplifier). The HBT has recently been employed for applications to an LNA, and a fairly good noise performance of 3.7 dB in the X-/Ku-bands was observed.[5,6] This result indicates that, at Ku- or higher frequency bands, a down-converter MMIC, employing HBTs, is a promising candidate to realize a one-chip transceiver (including PA, LNA, mixer and IF amplifier).
- As is well known, in Ku- or higher frequency bands, an IF filter such as a surface

YOUNG YUN, IN-HO KANG AND JI-WON JUNG
Korea Maritime University
Busan, Korea

acoustic wave (SAW) filter[7] has been employed to suppress the LO leakage signal at the IF output. However, this IF filter occupies a very large area in the transceiver of a wireless communication system, which makes it impossible to integrate on a MMIC.[6] Therefore, the large size of this IF filter has been an obstacle to the realization of a one-chip transceiver and has been the main cause for the comparatively high cost of transceivers in wireless communication systems.

In this article, a highly integrated down-converter MMIC, including filters, a mixer and an IF amplifier is described, which uses InGaP/GaAs HBTs[5,6] for application to Ku-band one-chip transceivers. To suppress the leakage signals of the LO and its second harmonic, a spiral inductor filter, which can be integrated on MMICs due to its small size, was realized using the self-resonance characteristics of the spiral inductor. Consequently, bulky external IF filters (outside of the MMIC) were not required for the operation of the down-converter MMIC.

INTEGRATION OF A SPIRAL INDUCTOR FILTER ON A MMIC

The down-converter MMIC was designed for applications to the Direct Broadcast Satellite (DBS) system. The RF and IF frequencies are 12 and 1 GHz, respectively, with an LO frequency of 11 GHz. ***Figure 1*** shows the circuit of the proposed down-converter MMIC. A spiral inductor, employing SiN film, was used in the filters, and the LO and its second harmonic leakage signals were suppressed to a great extent by the sharp LC resonance originating from the parasitic capacitance of the SiN film.

Figure 2 shows the top and side view of the spiral inductor structure. ***Figure 3*** shows the equivalent circuit of the spiral inductor where the LC parallel resonance with the series resistance[8] leads to the self-resonance characteristic of the spiral inductor. The spiral line is directly connected to port 1; the extended line is connected to port 2 through a contact. In order to induce a parasitic capacitance, SiN film was placed between the spiral and extended lines, resulting in a parasitic capacitance C_c occurring between the spiral and the extended lines. This parasitic capacitance plays a very important role for the self-resonance characteristic of a spiral inductor.

As shown in the equivalent circuit, C_c, L_m and R_p for the parallel resonance circuit, and the admittance Y_s of the parallel resonance circuit can be expressed as

$$Y_s = \frac{1}{R_p + j\omega L_m} + j\omega C_c = \frac{R_p}{R_p^2 + \omega^2 L_m^2} + j\left(\omega C_c - \frac{\omega L_m}{R_p^2 + \omega^2 L_m^2}\right) \quad (1)$$

In Equation 1, R_p is much smaller than ωL_m ($R_p << \omega L_m$), in the vicinity of the resonance frequency, because the metal loss R_p can be reduced by increasing the thickness of the spiral line. Therefore, Equation 1 can be expressed as

$$Y_s \approx \frac{R_p}{\omega^2 L_m^2} + j\left(\omega C_c - \frac{1}{\omega L_m}\right) = \frac{1}{R_{p1}} + j\left(\omega C_c - \frac{1}{\omega L_m}\right) \quad (2)$$

Therefore, from Equation 2, a resonance occurs at the following frequency

$$\omega_0 = \frac{1}{\sqrt{L_m C_c}} \quad (3)$$

Equation 3 indicates that the self-resonance frequency of the spiral inductor can be controlled by L_m and C_c. The self-resonance frequency can be tuned exactly to the LO frequency by adjusting the parasitic capacitance, which makes the proposed spiral inductor structure very practical for application to LO leakage suppression. In other words, for a suppression of the LO leakage signal, the self-reso-

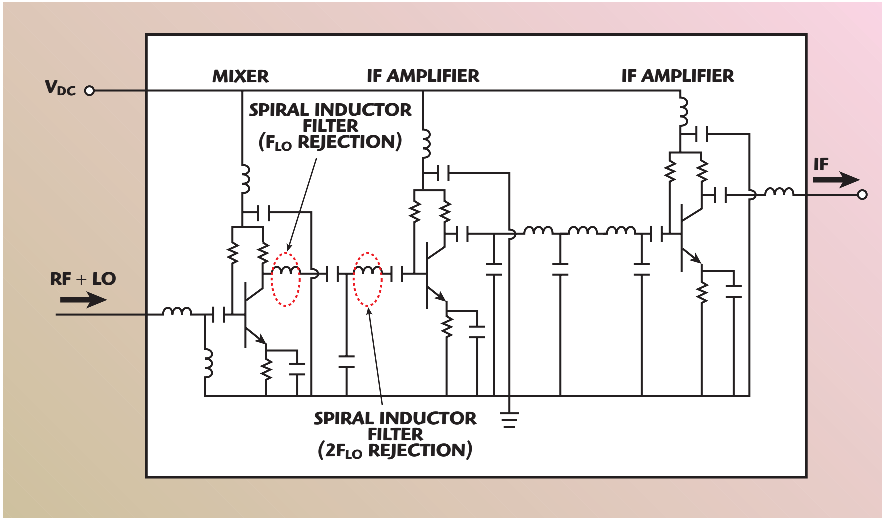

▲ *Fig. 1 Schematic of the MMIC down-converter circuit.*

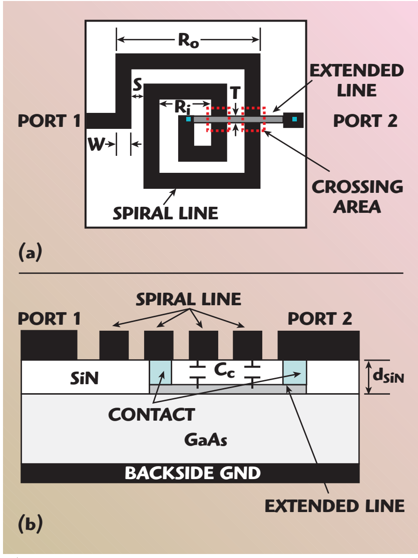

▲ *Fig. 2 Spiral inductor structure; (a) top view and (b) side view.*

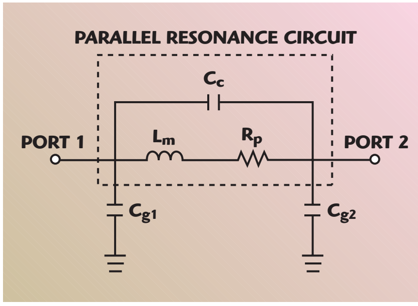

▲ *Fig. 3 Equivalent circuit of the spiral inductor using a SiN film.*

nance frequency can be tuned to the LO frequency by a two-step design procedure. By adjusting L_m, the spiral inductor was designed so that the self-resonance frequency was tuned to a frequency near the LO frequency. Then, by adjusting the C_c, it was tuned exactly to the LO frequency. The inductance L_m can easily be adjusted by the number of turns of the spiral inductor. A simple equation for the inductance value L_m can be given by[8]

$$L_m = 0.1555aN^{\frac{5}{3}} \ln\left[8\left(a/c\right)\right] \quad (4)$$

where

a = quarter of the sum of the inner and outer diameters
c = quarter of the difference between the inner and outer diameters
N = number of turns

$$C_c = N_c \frac{\varepsilon_{SiN} \times W \times T}{d_{SiN}} \quad (5)$$

where ε_{SiN} and d_{SiN} are the permittivity and thickness of the SiN film, respectively, and N_c, W and T are the number of crossings between the spiral and extended lines, the width of the spiral line and the width of the extended line, respectively. Using Equations 3 to 5, the structure of the spiral inductor was optimally designed by determining the number of turns N and the width of the extended line T so that the self-resonance frequency was tuned to the LO frequency of 11 GHz. ***Figure 4*** shows the dependence of the self-resonance frequency on the number of turns N and the width of the extended line T for a SiN thickness of 100 nm. The calculated results were obtained from Equations 3 to 5. As shown in Equation 4, L_m is proportional to $N^{5/3}$. The self-resonance frequency of Equation 3 changes substantially according to a change of N ($f_0 \propto N^{-5/6}$), which makes the tuning range of the self-resonance frequency very wide. However, fine tuning cannot be performed by only adjusting N. In this work, fine tuning of the self-resonance frequency was achieved by adjusting the capacitance C_c. The width of the extended line T was adjusted in order to make the self-resonance frequency accurately tuned to the LO frequency (11 GHz). From Equations 3 and 5, it can be seen that the self-resonance frequency changes by a very small quantity of approximately 0.2 GHz for a 1 µm change in T, which enables fine tuning. The rate of change is 0.23 GHz/µm. The self-resonance frequency can be tuned from 11.7 to 9.4 GHz, for a range of T from 5 to 15 µm. As mentioned previously, the spiral inductor was designed by a two-step procedure to suppress the LO leakage signal. First, the number of turns N was set to six turns so that the self-resonance frequency is tuned to 10.25 GHz, which is nearest to the LO frequency of 11 GHz. Finally, the self-resonance frequency was accurately tuned to 11 GHz by selecting the appropriate value T = 8 µm. Using the above-mentioned procedure, a spiral inductor was designed to suppress the second harmonic leakage signal of the LO at 22 GHz. Accordingly, N and T were set to three turns and 7.5 µm, respectively. ***Figure 5*** shows the measured insertion loss of the spiral inductors optimally designed for a rejection of the LO (11 GHz, N = 6 turns and T= 8 µm) and its second harmonic signal (22 GHz, N = 3 turns and T = 7.5 µm). As shown in this figure, the self-resonance frequency was tuned exactly to LO and its second harmonic frequency, and the spiral inductors show band-rejection characteristics in the vicinity of LO (11 GHz) and its second harmonic frequency (22 GHz). On the other hand, they show bandpass characteristics in the vicinity of the IF frequency of 1 GHz. The LO frequency rejection characteristic of the spiral inductor with N = 6 turns and T = 8 µm leads to a suppression of RF leakage signal at the IF output because the RF frequency (12 GHz) is very close to the LO frequency (11 GHz). Although the RF leakage signal at the IF output does

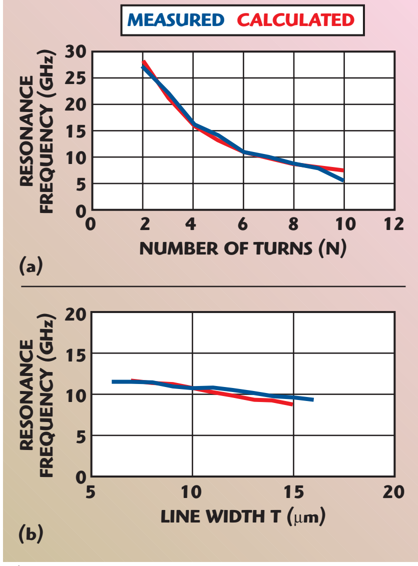

▲ *Fig. 4 Dependence of the self-resonance frequency of the spiral inductor (a) from the number of turns and (b) from the extended line width.*

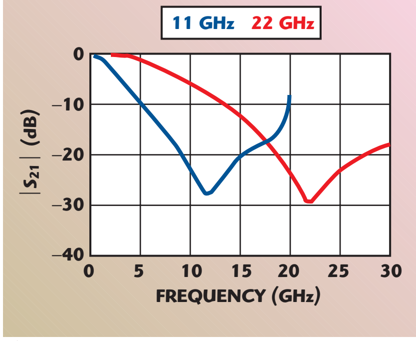

▲ *Fig. 5 Insertion loss of the spiral inductors designed for rejection of the LO and its second harmonic.*

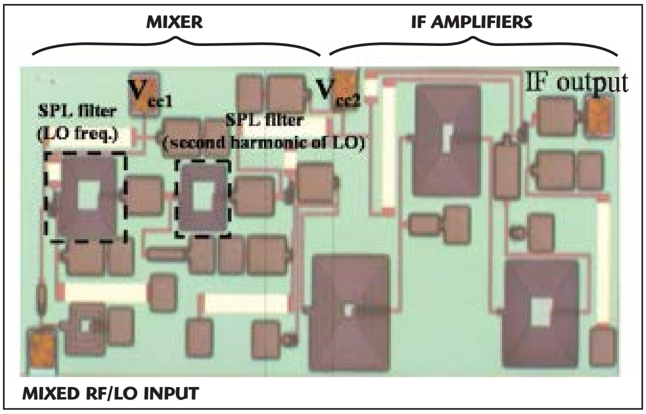

▲ *Fig. 6 The down-converter MMIC.*

not have a fatal effect on the performance of wireless communication systems, the suppression of the RF leakage is encouraged for stable operation of the system. For the same reason, the spiral inductor designed for a rejection of the second harmonic signal of LO (22 GHz) also highly suppresses the second harmonic signal of the RF (24 GHz).

Figure 6 is a photograph of the down-converter MMIC. The sizes of the spiral inductors for suppression of the LO and its second harmonic signals are 0.2 × 0.2 and 0.16 × 0.16 mm, respectively. Therefore, the two spiral inductors occupy a size of 0.0656 mm^2 on the MMIC. The total area is only 1.9 percent of that of a conventional IF filter with a size of 2.3 × 1.5 mm^2[7], which enabled the integration of the spiral inductors on a MMIC.

PERFORMANCE OF THE HIGHLY INTEGRATED DOWN-CONVERTER MMIC EMPLOYING HBTs

Figure 7 shows the measured conversion gain. As shown, the down-converter MMIC gives only a conversion gain of 12 dB in the saturated region because it only includes the mixer and IF amplifier. Only a two-stage

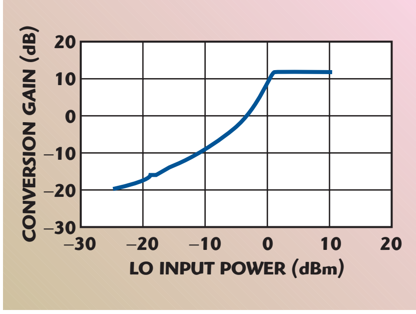

▲ *Fig. 7 Measured conversion gain of the down-converter MMIC.*

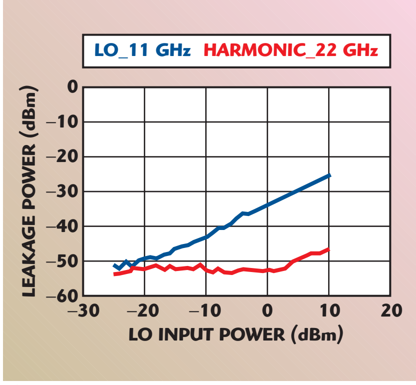

▲ *Fig. 8 Measured LO and its second harmonic leakage powers at the IF output.*

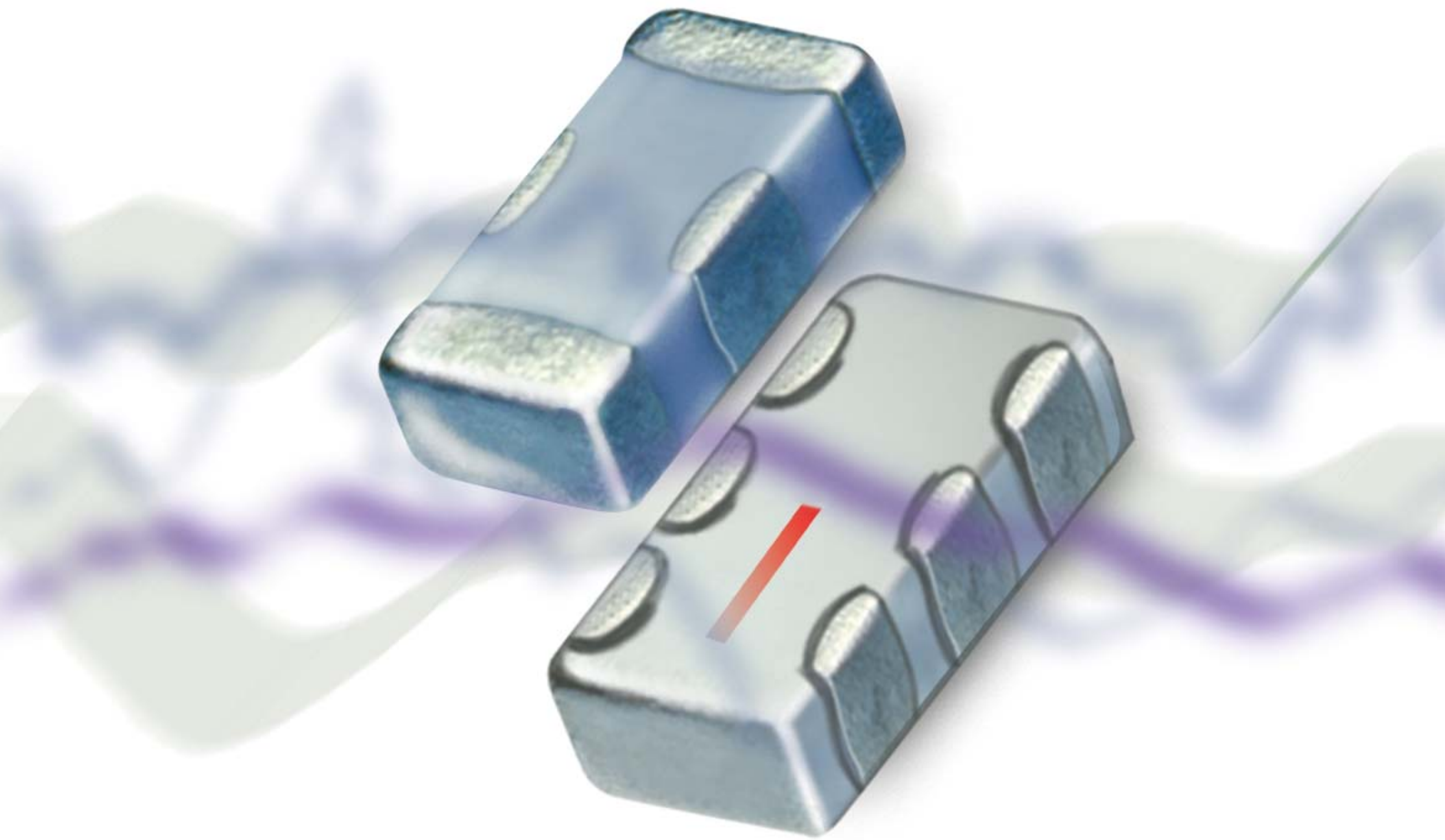

IF amplifier was used because the objective of this work was not to obtain a high conversion gain. ***Figure 8*** shows the LO and its second harmonic leakage powers at the IF output at their corresponding frequencies. As shown, the leakage powers for the LO and its second harmonic signals were suppressed to a great extent by using the optimally designed spiral inductors. At a LO power of –1 dBm, the LO and its second harmonic leakage powers are –35 and –53 dBm, respectively. Considering that a LO leakage power of less than –25 dBm is required for the normal operation of commercial DBS systems including an external IF filter,[1–3] the above results indicate that the down-converter MMIC, including spiral inductors, is sufficient and an external filter is not required for the normal operation of a commercial DBS system.

CONCLUSION

A highly integrated down-converter MMIC employing HBTs has been developed for application to a Ku-band one-chip transceiver solution. The down-converter MMIC includes a mixer, filter, amplifier and input/output matching circuits. To suppress the leakage signals of the LO and its second harmonic, spiral inductor structures employing a SiN film with a parasitic capacitance C_c were used. Considering that the spiral inductor has conventionally been used as a matching element in a much lower frequency range than the self-resonance frequency, the concept of filter application in this work is very challenging. The total size of spiral inductors for a suppression of LO and its second harmonic frequency was 1.9 percent of a conventional IF filter, which enabled the integration of a spiral inductor in a down-converter MMIC. Owing to the LC resonance characteristics of the spiral inductor structure employing SiN film, the down-converter MMIC showed a highly suppressed LO leakage power of –35 dBm and a second harmonic leakage power of –53 dBm, without an external filter, which made external filters unnecessary for normal operation of the DBS system. In addition, the LC resonance characteristics of the spiral inductors also led to a high suppression of RF and its second harmonic leakage signals. The design approach of the spiral inductor filter introduced in this article is also applicable to silicon devices as well as millimeter-wave III-V devices. ■

ACKNOWLEDGMENT

This work was supported by the Korea Research Foundation Grant (R05-2004-000-12754-0) and the second stage of Brain Korea 21. This work was also supported by the IT R&D Project funded by the Korean Ministry of Information and Communications.

References

1. E. Camargo and W. Kennan, "An E-mode GaAs FET Operating as a Single Balanced Gate Mixer," *1996 IEEE MTT-S International Microwave Symposium Digest*, pp. 951–954.
2. K. Hubbard, K. MacGowan, C. Kau, D. Smith and S. Maas, "A Family of Low

Cost, High Performance HEMT MMICs for Commercial DBS Applications," *1995 IEEE MTT-S International Microwave Symposium Digest*, pp. 1649–1652.
3. Y. Yun, T. Fukuda, T. Kunihisa, T. Tanaka and O. Ishikawa, "A Low Noise and Low Power Dissipation Down-converter MMIC for DBS Applications," *Technical Journal of the IEICE*, Vol. ED2001-198, January 2002, pp. 7–12.
4. M. Salib, A. Gupta, F. Ali and D. Dawson, "A 1.8 W, 6 to 18 GHz HBT MMIC Power Amplifier with 10 dB Gain and 37% Peak Power-added Efficiency," *IEEE Microwave and Guided Wave Letters*, Vol. 3, September 1993, pp. 325–326.
5. K.S. Park, et al., "A Ku-band High Linearity LNA Using the InGaP/GaAs HBT MMIC Process," *Proceedings of the Asia-Pacific Microwave Conference*, Seoul, South Korea, November 2003, pp. 377–380.
6. S. Kurachi, J. Chen, Y. Shimamatsu, H. Liu and T. Yoshimasu, "A Wideband Amplifier MMIC with InGaP/GaAs HBT Technology," *Proceedings of the International Symposium on Microwave and Optical Technology*, Fukuoka, Japan, August 2005, pp. 764–766.
7. K. Onishi, et al., "An Application of a Flip-chip Bonding Technique to GHz Band SAW Filters for Mobile Communication," *IEICE Transactions on Electronics*, Vol. E76-C, No. 6, June 1993, pp. 993–999.
8. B.C. Wadell, *Transmission Line Design Handbook*, Ch. 6, Artech House Inc., Norwood, MA, 1991.

Young Yun *received his BS degree in electronic engineering from Yonsei University, Seoul, South Korea, in 1993, his MS degree in electrical and electronic engineering from the Pohang University of Science and Technology, Pohang, South Korea, in 1995, and his PhD degree in electrical engineering from Osaka University, Osaka, Japan, in 1999. From 1999 to 2003, he worked as an engineer at Matsushita Electric Industrial Co. Ltd., Osaka, Japan, where he was engaged in the research and development of MMICs for wireless communications. In 2003, he joined the department of radio sciences and engineering at Korea Maritime University, Busan, Korea. He is now an assistant professor whose research interests include design and measurement for RF/microwave and millimeter-wave ICs, and design and fabrication for HEMT and HBT circuits.*

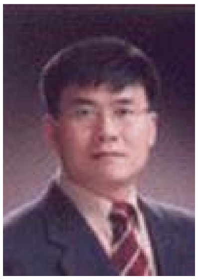

In-Ho Kang *received his PhD degree from Sogang University, Seoul, South Korea, in 1995. He is now a professor in the division of radio and information communication engineering at Korea Maritime University, Busan, South Korea. His research interests include LTCC and MMIC filters for the RF single chip of 5.5 GHz WLAN, WiMAX and UWB applications, including MMIC filters for power amplifier harmonics suppression.*

Ji-Won Jung *received his BS, MS and PhD degrees in electronics engineering from Sungkyunkwan University, Seoul, South Korea, in 1989, 1991 and 1995, respectively. From 1990 to 1992, he was with the LG Research Center. From 1995 to 1996, he was with Korea Telecom (KT). From 2001 to 2002, he was an invited researcher at the Communication Research Center, Canada. Since 1996, he has been in the department of radio science and engineering at Korea Maritime University, Busan, South Korea. His research interests include channel coding, digital modem, FPGA design technology and digital broadcasting systems.*

A DISTRIBUTED TRANS-IMPEDANCE AMPLIFIER USING INGAP/INGAAS ENHANCEMENT-MODE PHEMT TECHNOLOGY

A broadband trans-impedance amplifier using a 0.5 μm InGaP/InGaAs E-mode PHEMT process is reported for optical electronic communication applications. The distributed amplifier was achieved with a trans-impedance gain of 50 dB-Ω and a bandwidth of 15.2 GHz in the 2.2 to 17.4 GHz range. It also attained a noise figure range from 3.34 to 5.03 dB in the bandwidth of 1 to 10 GHz. The trans-impedance amplifier utilizes the distributed technique with gain cells to enhance the gain and bandwidth performances. This trans-impedance amplifier technique provides an ultra-broad bandwidth for optoelectronic transmission communication applications.

An optoelectronic device performs the transition between optical and electrical components. The trans-impedance amplifier is the most suitable preamplifier configuration in optoelectronic receivers. A block diagram of the circuit module is shown in ***Figure 1***. The trans-impedance amplifier is the first stage electrical amplifier in the receiver chain and thus enhances the input sensitivity of the receiver in the communication system. Meanwhile, the performance parameters of impedance conversion, gain, bandwidth and noise figure are very important for the trans-impedance amplifier. This optoelectronic transition is necessary to transform the optical impedance into the impedance of the microwave circuit. The input impedance of an optical device varies significantly in microwave circuits. Generally, the optoelectronic signals are relatively low at the input of the first stage of a receiver module, and it is necessary to increase their

Fig. 1 Block diagram of the optical receiver.

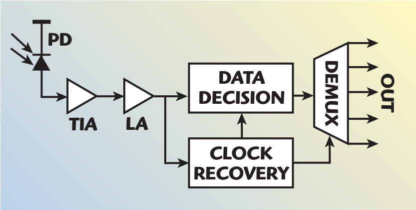

CHIA-SONG WU AND HSING-CHUNG LIU
Vanung University
Chung-Li, Taiwan, ROC
HSIEN-CHIN CHIU AND WEI-HSIEN LEE
Chang Gung University
Lin Kou, Taiwan, ROC

amplitude in the optoelectronic system. Therefore, a trans-impedance amplifier was developed. It provides gain as well as impedance transformation and converts the photocurrent into a voltage. The low noise figure and high bandwidth performance meet most of the amplifier's specifications.

The performance of a conventional lumped element design in the trans-impedance circuit is limited by the feedback capacitance of the FET device. Hence, it is difficult to achieve a greater than 10 GHz bandwidth amplifier with a flat gain. One way to overcome this issue is to utilize a distributed amplifier, which can achieve a broad bandwidth in the gain stage of the trans-impedance amplifier. The gain-bandwidth product of the distributed amplifiers substantially exceeds the transistor unit-current gain frequency (f_T) because of the input and output capacitances of the active devices. The distributed structure uses inductors to compensate for the parasitic capacitances of the devices and enhances the broad bandwidth in the trans-impedance amplifier.

This article describes the design and implementation of the microwave monolithic integrated circuit (MMIC) of the distributed trans-impedance amplifier. It uses 0.5 μm InGaP/InGaAs enhancement-mode PHEMT technology, which is appropriate for the use of a gate recess etching stop material and exhibits favorable RF characteristics.

DESIGN OF THE DISTRIBUTED AMPLIFIER CIRCUIT

In a conventional amplifier, the gain-bandwidth product is limited by paralleling the FET's parasitic capacitance. The trans-conductance (gm) of the FET is compensated by the increase in the input and output capacitances. The distributed amplifier overcomes this difficulty by adding inductors in the circuit. The input and output capacitances of the FET can be compensated by the inductors in the distributed structures. That is, these inductors provide the circuit matching as well as compensate for the parasitic capacitances of the devices.

This article describes a flat trans-impedance gain and broad bandwidth distributed amplifier. In the beginning, the S-parameters, noise and trans-impedance gain of the trans-impedance amplifier were simulated by ADS (Agilent's Advanced Design System). Considering the circuit performance and chip size, a three-stage distributed amplifier was chosen as the trans-impedance amplifier configuration. ***Figure 2*** depicts the distributed amplifier configuration. It consists of three stages to achieve a high gain and a broad bandwidth with the input and output inductors coupled by the PHEMTs. The inductors Ll to L4 are the drain inductors, and L5 to L8 are the gate inductors. The gate and drain inductors are periodically loaded by the PHEMT gate-source capacitance and drain-source capacitance, respectively, and are terminated in the characteristic impedance at the end. As the RF signal is transmitted by the gate inductors, each transistor is excited by the traveling voltage wave and transfers the signal to the drain inductors through its transconductance.

The signal phase velocities on the gate and drain inductors are identical and when these signals arrive at the drain inductor output they are added in the forward direction. The out-of-phase waves, traveling in the reverse drain direction, will not be cancelled and will be absorbed by the drain-inductor's termination. Meanwhile, the resistors R1 and R2 provide matching to the 50 Ω characteristic impedance. The capacitors C1 and C2 act as a DC block. In addition, a bias tee is used at the input port for the RFin/Vg connection and at the output port for RFout/Vg. Finally, the matching inductances and capacitances were determined and the trans-impedance amplifier was obtained, with a trans-impedance gain of 50 dB-Ω and a bandwidth of 15.2 GHz in the 2.2 to 17.4 GHz frequency range.

DEVICE STRUCTURE AND TRANS-IMPEDANCE AMPLIFIER CIRCUIT FABRICATION

For PHEMT fabrication consideration, the InGaP/InGaAs E-mode PHEMT offers an excellent selective etching for the gate recess between the InGaP and GaAs, which increases the device manufacturability. In addition, the InGaP does not form DX-centers and causes less deep level defects, which results in the potential to substantially improve the reliability of the PHEMTs. ***Figure 3*** shows the epitaxial structure of the $In_{0.5}Ga_{0.5}P$/$In_{0.24}Ga_{0.76}As$ E-mode PHEMTs.

The structure includes two Si planar δ-doped layers on either side of the InGaAs undoped channel layer with an AlGaAs spacer layer for high transconductance consideration. An undoped 100 Å InGaP Schottky layer was grown on intrinsic GaAs to form

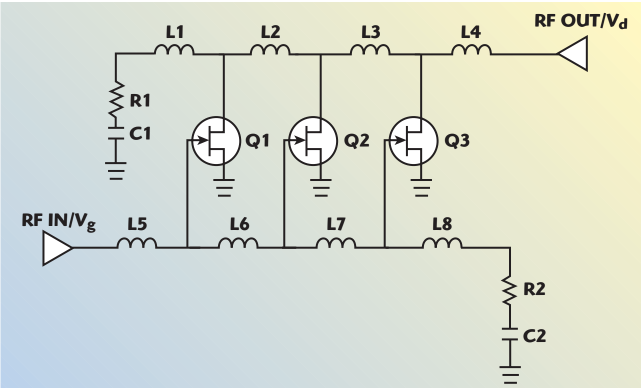

▲ *Fig. 2 Schematic of the distributed amplifier circuit.*

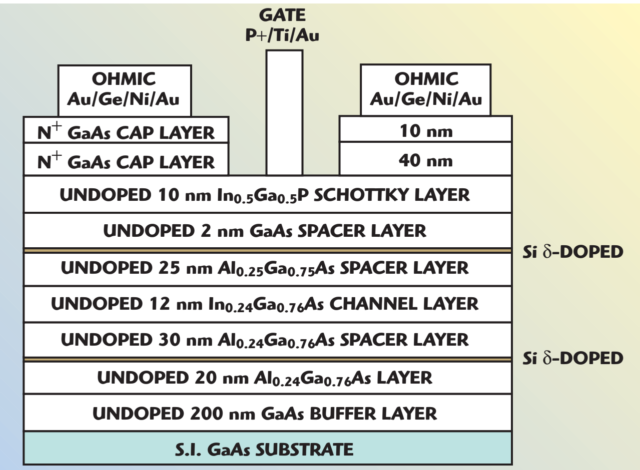

▲ *Fig. 3 Epitaxial structure of the InGaP/InGaAs E-mode PHEMT.*

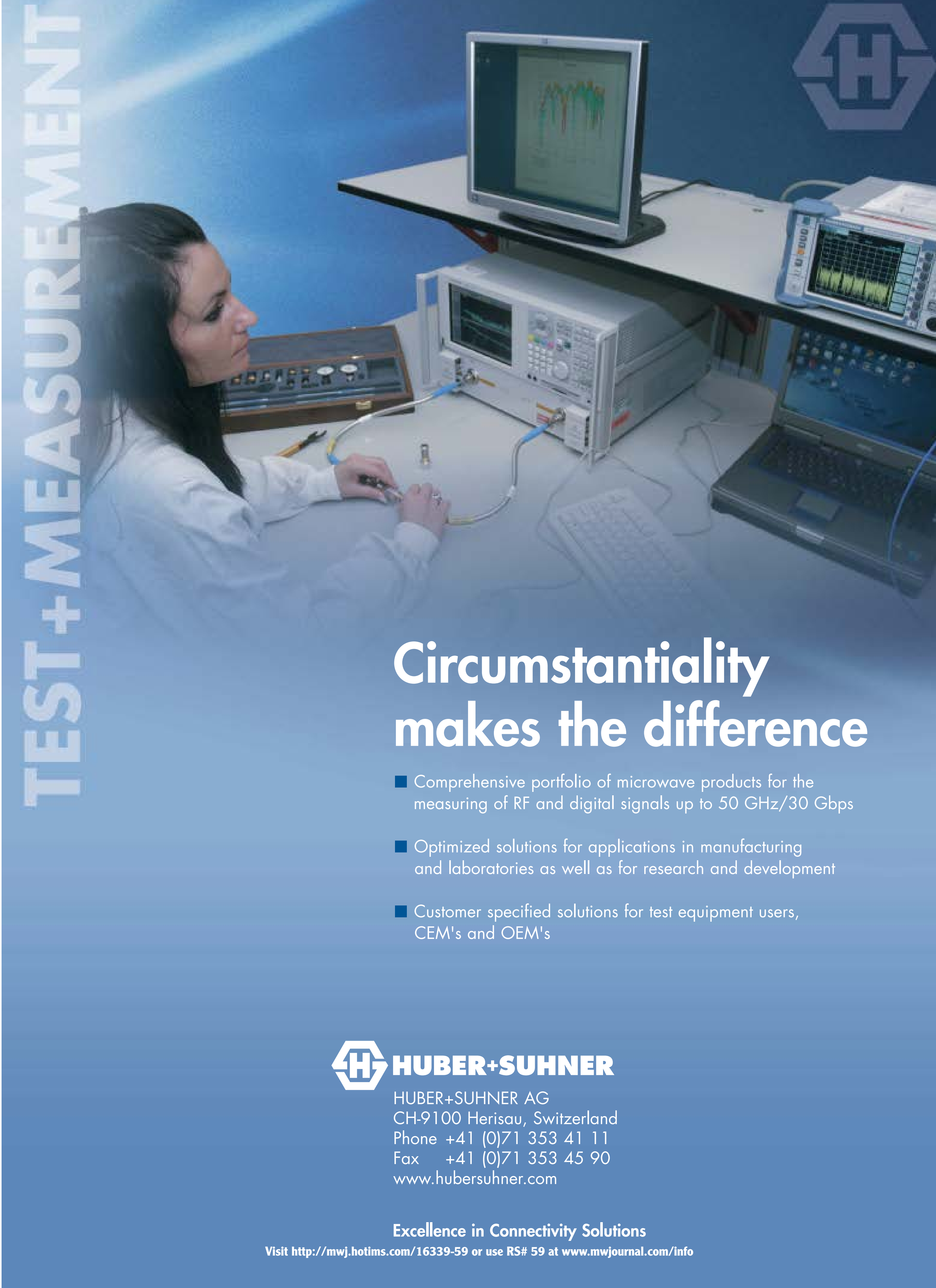
TEST+MEASUREMENT
Circumstantiality makes the difference
Comprehensive portfolio of microwave products for the measuring of RF and digital signals up to 50 GHz/30 Gbps
Optimized solutions for applications in manufacturing and laboratories as well as for research and development
Customer specified solutions for test equipment users, CEM's and OEM's
HUBER+SUHNER
HUBER+SUHNER AG
CH-9100 Herisau, Switzerland
Phone +41 (0)71 353 41 11
Fax +41 (0)71 353 45 90
www.hubersuhner.com
Excellence in Connectivity Solutions
Visit http://mwj.hotims.com/16339-59 or use RS# 59 at www.mwjournal.com/info

SUPER ULTRA WIDEBAND

AMPLIFIERS

+24 dBm output... 0.7 to 21GHz from $845 ea.

Simply calling the ZVA-183X and ZVA-213X "wideband" amplifiers doesn't begin to describe them. The super ultra wideband ZVA-183X amplifier operates from 0.7 to 18.0 GHz while the ZVA-213X amplifier covers even more "spectral ground," with a range of 0.8 to 21.0 GHz. Both super ultra wideband amplifiers deliver +24 dBm typical output power at 1 dB compression by merit of 26 dB typical small-signal gain with ±1 dB typical gain flatness. Both provide wide dynamic range along with the bandwidth, with typical noise figure of 3 dB and typical IP3 of +33 dBm. These versatile amplifiers are ideal for broadband commercial and military applications, from radar systems to test equipment. The ZVA-183X and ZVA-213X amplifiers are unconditionally stable. In fact, they are so rugged, they can even withstand load mismatches as severe as an open or short circuit at full 1dB compression output power.

Mini-Circuits...we're redefining what VALUE is all about!

TYPICAL SPECIFICATIONS

MODEL	FREQ. (GHz)	GAIN (dB)	POUT (dBm) @ 1 dB Comp.	NOISE FIG. (dB)	PRICE (1-9)
ZVA-183X+	0.7-18	26	+24	3.0	845.00
ZVA-213X+	0.8-21	26	+24	3.0	945.00

Note: Alternative heat-sink must be provided to limit maximum base plate temperature.

MODEL	FREQ. (GHz)	GAIN (dB)	POUT (dBm) @ 1 dB Comp.	NOISE FIG. (dB)	PRICE (1-9)
ZVA-183+	0.7-18	26	+24	3.0	895.00
ZVA-213+	0.8-21	26	+24	3.0	995.00

All models IN STOCK!

RoHS compliant

Mini-Circuits®

ISO 9001 ISO 14001 CERTIFIED

ALL NEW minicircuits.com

P.O. Box 350166, Brooklyn, New York 11235-0003 (718) 934-4500 Fax (718) 332-4661 For detailed performance specs & shopping online see Mini-Circuits web site

YONI2™ Patent Pending

The Design Engineers Search Engine *Provides ACTUAL Data Instantly From MINI-CIRCUITS At:* ***www.minicircuits.com***

IF/RF MICROWAVE COMPONENTS

440 Rev A

Visit http://mwj.hotims.com/16339-92 or use RS# 92 at www.mwjournal.com/info

a Schottky layer. Finally, two n^+GaAs cap layers were grown to improve the ohmic contact resistivities. The designed structure demonstrated a sheet charge density of 2.2×10^{12} cm^{-2} together with a Hall mobility of 6120 cm^2/V-sec at 300°K, after removing the n^+ GaAs cap layer. For device fabrication, ohmic contacts of Au/Ge/Ni/Au metals were deposited by e-beam evaporation and patterned by a conventional lift-off process.

An ion-implant isolation technology was applied for mesa isolation to avoid sidewall gate leakage current. After the high selectivity succinic acid gate recess process,[1] 0.5 µm long Pt/Ti/Au-gates (40 Å/500 Å/4000 Å) were deposited by a lift-off process. Typical DC drain-to-source current (I_{ds}) versus drain-to-source voltage (V_{ds}) characteristics of the fabricated InGaP/InGaAs E-mode PHEMT are shown in ***Figure 4***. As can be seen, the device can be operated with a gate voltage up to 1.4 V, which corresponds to a I_{ds} of 230 mA/mm when the drain voltage is 3 V, owing to the high Schottky barrier (0.86 eV.) of the metal-InGaP contact and the large ΔE_c (0.4 eV.) between the InGaP and InGaAs.[2] The drain-to-source leakage current at V_{ds} = 2 V and V_{gs} = 0 V is less than 0.2 µA/mm. A low drain-to-source steady-state leakage current is beneficial for suppressing the device power consumption and signal loss, particularly at low bias conditions.

The V_{gs} dependence of trans-conductance (g_m) and I_{ds} at V_{ds} = 2 V are also shown. The threshold voltage (V_{th}) is 0.34 V (defined as I_{ds} = 1mA/mm) and the maximum I_{ds} and g_m are 235 mA/mm and 390 mS/mm, respectively. The final circuit is achieved when the matching inductors and capacitor device are fabricated. The distributed amplifier was realized using a 0.5 µm InGaP/InGaAs E-mode PHEMT technology. A die microphotograph of the distributed amplifier, with a chip size of 0.62 mm^2, is shown in ***Figure 5***.

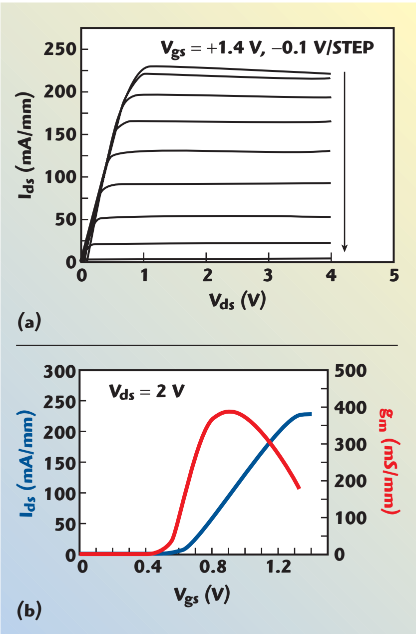

▲ *Fig. 4 InGaP/InGaAs E-mode PHEMT characteristics; (a) I_{ds}-V_{ds} and (b) I_{ds}/gm-V_{ds}.*

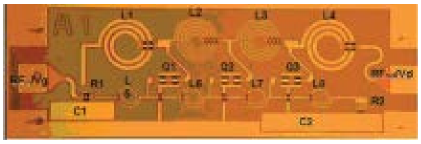

▲ *Fig. 5 Microphotograph of the distributor amplifier chip.*

MEASURED RESULTS

The distributed amplifier performance was measured by on-wafer probing while biased at V_{gs} = 0.7 V and V_{ds} = 2.3 V, respectively. From the device I_{ds} versus V_{ds} characteristics, it is found that the drain current I_{ds} is 14.46 mA when the drain voltage is 2.3 V and the total power consumption is 33.25 mW.

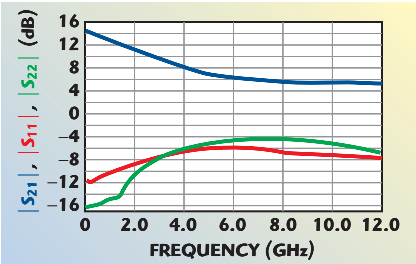

▲ *Fig. 6 Measured gain and input and output return losses of the distributed amplifier.*

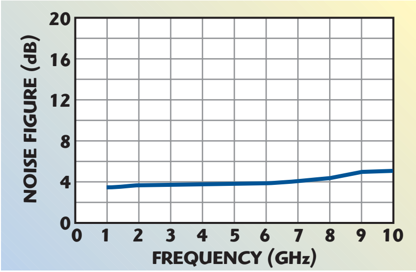

▲ *Fig. 7 Measured noise figure of the distributed amplifier.*

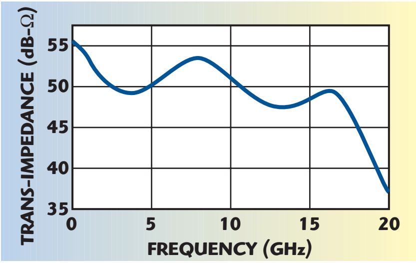

▲ *Fig. 8 Calculated trans-impedance of the distributed amplifier.*

The S-parameters of the amplifier, including the gain, and input and output return loss, are shown ***Figure 6***. The input return loss (S_{11}) and output return loss (S_{22}) remain less than –4 dB from DC to 12 GHz. ***Figure 7*** shows the noise figure, which is lower than 5.03 dB in the frequency range from 1 to 10 GHz.

The trans-impedance gain curve, calculated from the S-parameters, is illustrated in ***Figure 8***. The trans-impedance gain curve reveals that it is not flat. In other words, the distributed amplifier is not completely matched to 50 Ω at all frequencies, because the real part of the impedance of the gate and drain inductors remains nearly constant, whereas the imaginary part varies with frequency.

The distributed amplifier achieves a trans-impedance gain of 50 dB-Ω and a bandwidth of 15.2 GHz at the –3 dB frequency (f_{3dB}) from 2.2 to 17.4 GHz. ***Table 1*** lists the characteristics of recently reported trans-impedance amplifiers compared with this work. It shows that the present trans-impedance distributed amplifier has a relatively low noise figure and power consumption. Consequently, this high performance distributed amplifier, which offers a noise figure in the range from 3.34 to 5.03 dB, a DC power consumption of 33.25 mW and broadband characteristics between 2.2 GHz to 17.4 GHz, is very suitable for high speed opto-electronic transmission system applications.

CONCLUSION

In this article, a distributed amplifier using InGaP/InGaAs PHEMTs has been demonstrated that can increase bandwidth and reduce noise figure. The distributed amplifier was fabricated using the WIN III-V foundry 0.5 µm InGaP/InGaAs PHEMT technology. The distributed amplifier circuit consumed 33.25 mW when biased at V_{gs} = 0.7 V and V_{ds} = 2.3 V, achieved a mean trans-impedance gain of 50 dB-Ω and a bandwidth of 15.2 GHz at the –3 dB fre-

View Microwave Frequency & Stability - in Real Time

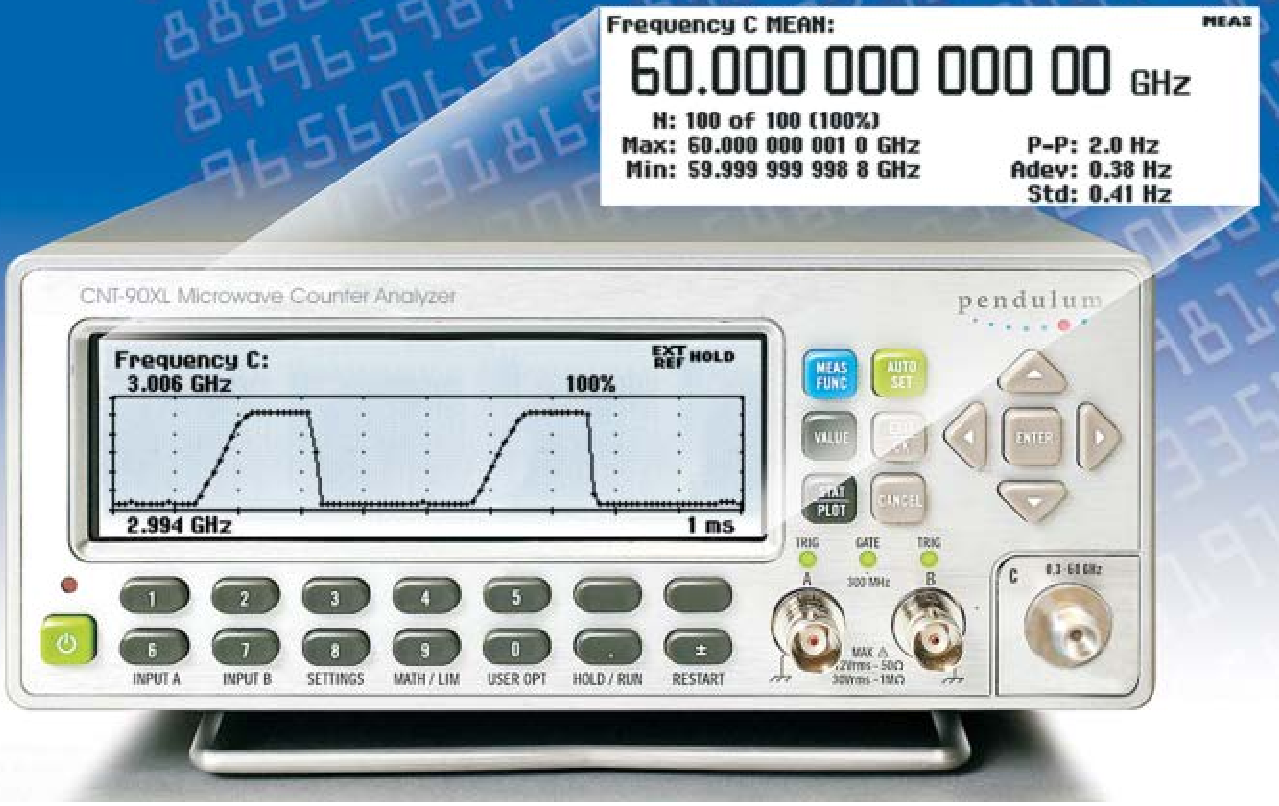

CNT-90XL Microwave Counter/Analyzer

Ultimate Frequency Range, Resolution & Analysis

Ultra High Range, Speed and Resolution

- 250k meas./sec. of frequency or power
- 27, 40, 46 or 60 GHz frequency range
- mHz resolution on GHz signals

Fast Analysis

- Modulation domain analysis to 60 GHz
- View FM or AM on graphical display
- Frequency or power stability, settling or drift

Versatility

- Frequency or power, CW or burst to 60 GHz
- All timer/counter functions to 300 MHz

Pendulum Instruments

- Experts in Time & Frequency Calibration, Measurement and Analysis

Phone: +1 510-428-9488 (US/Canada), +46 8 598 510 57 (World-wide). info@pendulum.se

www.pendulum-instruments.com

pendulum

Incorporating XL Microwave

TABLE I

COMPARISON OF PUBLISHED TRANS-IMPEDANCE AMPLIFIERS' PERFORMANCE

Fabrication Technology	BW (GHz)	TZ Gain (dB-Ω)	N.F. (dB)	Chip Size (mm^2)	Total Pdc (mW)	Amplifier Topology	Ref.
0.18 μm CMOS	9	62	–	0.52	108	differential	3
0.18 μm CMOS	9.2	54	–	0.49	138	differential	4
0.25 μm SiGe HBT	7	63	–	–	60	differential	5
0.25 μm Si BiCMOS	9	20	–	–	140	differential	6
0.18 μm CMOS	15	8.6	< 6	2	200	distributed	7
0.5 μm InGaP/ InGaAs pHEMT	15.2 (2.2–17.4)	50	< 5.02	0.62	33.25	distributed	this work

quency (f_{3dB}) from 2.2 to 17.4 GHz. The noise figure is less than 5.03 dB in the frequency range from 1 to 10 GHz. In conclusion, the distributed amplifier has good RF characteristics and is very suitable for high-speed optoelectronic transmission applications. ■

ACKNOWLEDGMENTS

The authors are grateful to WIN Semiconductors Corp. for circuit fabrication. Additional thanks are extended to the National Nano Device Laboratories, Hsin-Chu, Taiwan, for noise measurements.

References

1. H.C. Chiu, C.S. Cheng and Y.J. Shih, "High Uniformity Enhancement- and Depletion-mode InGaP/InGaAs PHEMTs Using Selective Succinic Acid Gate Recess Process," *Semiconductor Science and Technology*, Vol. 21, 2006, pp. 55–59.
2. T.J. Miller, G.B. Backes and M.I. Nathan, "Schottky Barrier Height Modification on n- and p-type GaInP with Thin Interfacial Si," *Journal of Applied Physics*, Vol. 76, 1994, pp. 7931–7934.
3. M. Kossel, C. Menolli, T. Mod, M. Schmalz and T. Toifl, "Wideband CMOS Trans-impedance Amplifier," *IEEE Electronics Letters*, Vol. 39, No. 7, April 2003, pp. 587–588.
4. A.K. Peterson, K. Kiziloglu, T. Yoon, F. William and M.R. Sandor, "Front-end CMOS Chip for 10 Gb/s Communication," *2002 IEEE RFIC Symposium Digest*, pp. 93–96.
5. B.M.R. Samadi, I.A. Karsilayan and J. Silva-Martinez, "Design of Trans-impedance and Limiting Amplifier for 10Gb/s Optical Communication Systems," *Proceedings of the 45th IEEE Midwest Symposium on Circuits and Systems*, Vol. 3, August 4–7, 2002, pp. 164–167.
6. H.H. Kim, S. Chandrasekhar, C.A. Burrus, Jr. and J. Bauman, "A Si BiCMOS Trans-impedance Amplifier for 10-Gb/s SONET Receiver," *IEEE Journal of Solid-State Circuits*, Vol. 36, No. 5, May 2001, pp. 769–776.
7. R.C. Liu and H. Wang; "DC-to-15 and DC-to-30 GHz CMOS Distributed Trans-impedance Amplifiers," *2004 Radio Frequency Integrated Circuits (RFIC) Symposium Digest*, 2004, pp. 535–538.

Chia-Song Wu *received his MSEE degree from Tsing Hua University, Hsinchu, and his PhD degree from National Central University, Chungli, Taiwan, in 1985 and 1998, respectively. In 1986, he joined the Chung Shan Institute of Science and Technology (CSIST), where he focused on infrared detector technology. In August 2003, he joined the department of electrical engineering at Vanung University, where he is currently involved in research on microwave and millimeter-wave integrated circuits. His research interests include OEIC and MMIC, such as laser diode, sub-micron technology, microwave, millimeter devices and MMICs.*

Hsing-Chung Liu *received his PhD degree in electrical engineering from Kent State University, OH, in July 1985. In 1985, he joined the Chung Shan Institute of Science and Technology (CSIST), where he focused on infrared detector technology. In March 2002, he became the dean of the R&D Office at Vanung University, where he is currently involved in research on microwave and millimeter-wave integrated circuits. His research interests include OEIC and MMIC.*

Hsien-Chin Chiu *received his BS and PhD degrees in electrical engineering from National Central University, Chungli, Taiwan, in 1998 and 2003, respectively. In 2003, he joined WIN Semiconductors Corp., Tao Yuan, Taiwan, where he was engaged in the research and development of 6-inch GaAs PHEMTs and related integrated circuits. In June 2004, he joined the department of electrical engineering at Chang Gung University focusing on microwave and millimeter-wave integrated circuits, fiber communication circuits and nano-technology. His research interests include deep submicron electron-beam lithography technology, solid-state physics, compound semiconductor, microwave and millimeter devices, and integrated circuits.*

Wei-Hsien Lee *received his BS degree in aeronautical engineering from National Formosa University, Yunlin, Taiwan, in 2003, and his MS degree in electronics engineering from Chang Gung University, Lin Kou, Taiwan, in 2006. His research interests include all areas of optical communications and millimeter-wave circuit design.*

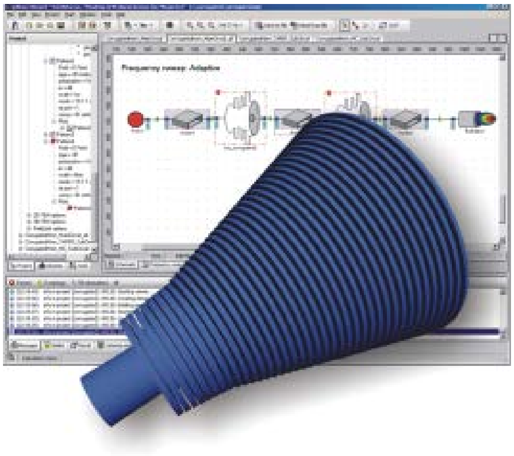

HORN ANTENNA SYNTHESIS CAD TOOL

Hybrid mode horn radiators with high aperture efficiency and low cross-polarization levels are commonly used in wideband or multi-beam antennas in modern telecommunications. Such applications usually require the accurate prediction and optimization of the antenna performance parameters for both fundamental and higher order mode operation. Although various analysis tools for the calculation of horn antennas are available, the synthesis and optimization of broadband, low cross-polarization and high directivity horns is still a challenge. To ease and accelerate the antenna design for engineers, Mician has developed a new horn antenna synthesis tool for multi-mode and tracking horns that supports many profile types, such as general corrugated, smooth wall or Potter horns.

The new synthesis tool utilizes body of revolution (BOR) elements, which are well suited to a specific design of circular and coaxial waveguide horns. This tool can either be used as standalone software or be plugged into the company's µWave Wizard, where the existing Component Object Model (COM) capability of the software is utilized and extended to use the newly implemented features. The main window of the synthesis tool is used for basic definitions and the horn profile type, and for each different horn type a specific input window is provided to set up the geometry.

Individual windows are provided for the following horn types:

- Conical horns, dual-mode horns (Potter horns)
- Modified Potter horns
- Profiled smooth wall horns
- Corrugated horns with corrugation perpendicular to the horn axis
- Ring loaded corrugated horns

MICIAN GMBH
Bremen, Germany

EXECUTIVE INTERVIEW SERIES

MWJ SPEAKS WITH PETER KRAUSS, MANAGING DIRECTOR, MICIAN. VISIT WWW.MWJOURNAL.COM TO READ THIS IN-DEPTH INTERVIEW.

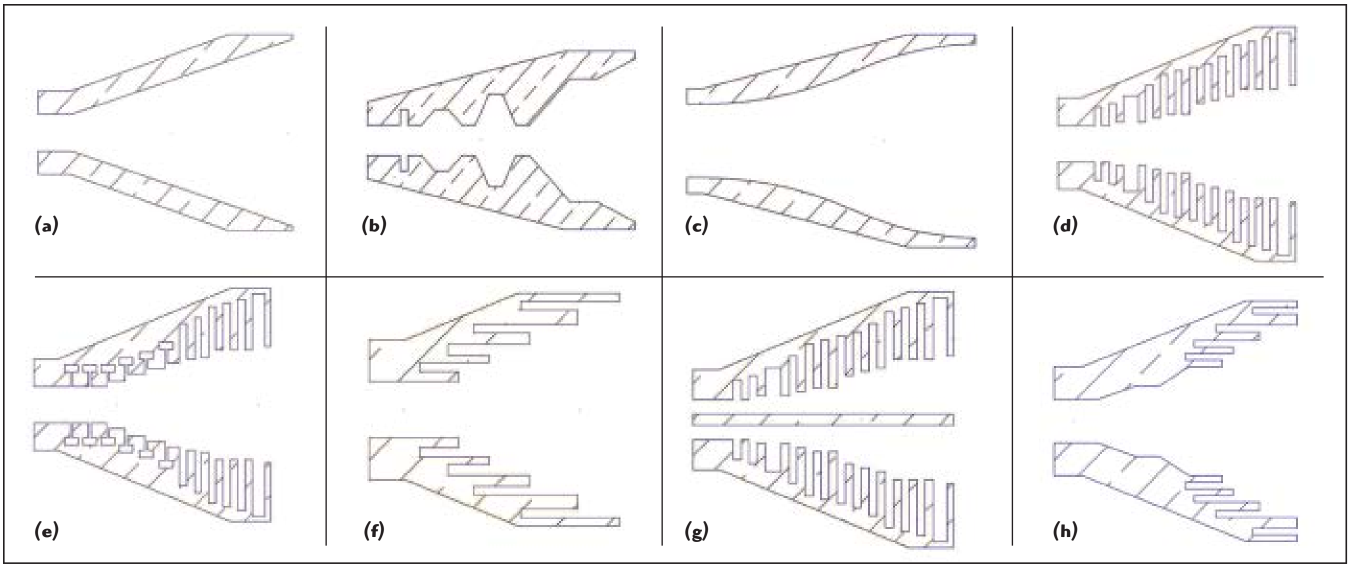

▲ *Fig. 1 Types of horn antennas: (a) conical circular waveguide; (b) modified Potter; (c) profiled smooth wall; (d) conventional corrugated; (e) ring-loaded corrugated; (f) axially corrugated; (g) coaxial waveguide corrugated and (h) hybrid geometry (smooth wall/axial corrugations).*

- Corrugated horns with axial corrugations
- Coaxial waveguide corrugated horns
- Hybrid geometry horns with axial and vertical corrugations

Figure 1 gives examples of these eight different types of horn antenna.

BOR LIBRARY ELEMENTS

A set of new elements has been developed for the radiation library of the µWave Wizard, which exploit the body of revolution symmetry of circular waveguide horn antennas. These elements coincide with the specifications for the various horn profiles. For example, there are elements for the (modified) Potter, the corrugated and the ring loaded horn profiles. This makes the setup of the entire horn geometry much easier than previously, when the entire geometry had to be broken down into single circular waveguide and coaxial waveguide steps. The latter process is now carried out automatically inside the element.

Although the new set of BOR elements is calculated with the Mode-Matching (MM) method, the elements accelerate the computation for simultaneous analysis of fundamental and higher order mode excitations by subdividing the set of modes into decoupled axial orders.

Additionally, these elements have been equipped with new types of output and calculation capabilities. Unlike other elements, where the electromagnetic fields are calculated only at one given position (for example, iris cross-section) and a single excitation (amplitude/phase), the field calculation inside the BOR elements comprises the entire structure and calculates the maximum over all incident phases. These calculated maximum fields can either be plotted along the horn profile or against the frequency by using the µWave graph tool provided by µWave Wizard.

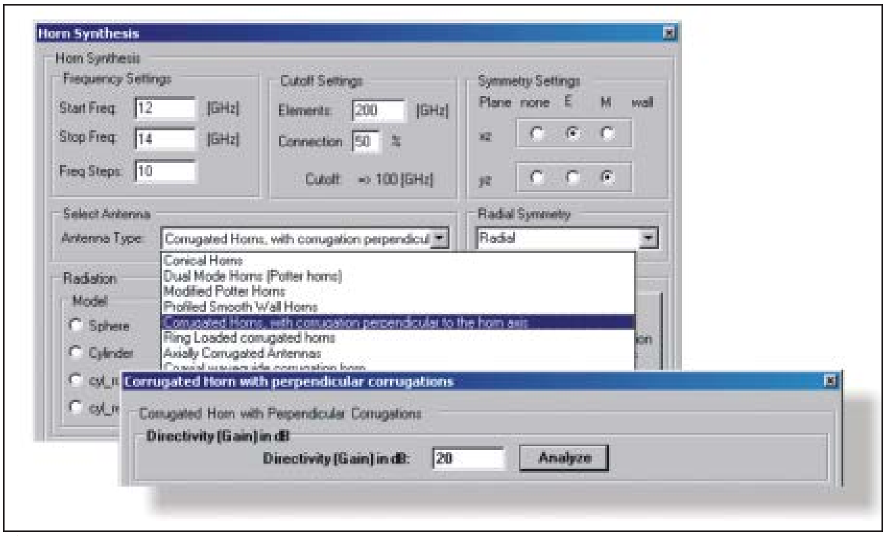

▲ *Fig. 2 A selection of required horn antenna types and specification of the gain.*

PERFORMANCE PARAMETERS

The software is capable of calculating the following horn electrical performance parameters:

- Input return loss for the fundamental mode excitation and for the higher order modes (TMmn and TEmn) mode excitation
- Co-polar and cross-polar radiation patterns for the fundamental mode and for the higher order modes at any given distance from the radiator aperture
- Spherical Wave Expansion (SWE) parameters are optionally written to a data file either in µWave Wizard specific or in TICRA Grasp compatible format
- Phase center location, aperture efficiency, and 3 and 10 dB beamwidth are derived from the co-polar radiation patterns
- Electromagnetic fields and aperture field distribution along the horn
- Maximum field strengths versus frequency
- Ohmic losses

At Filtronic Compound Semiconductors we are driven by a common goal –

helping you design systems that meet your customers' current and future requirements.

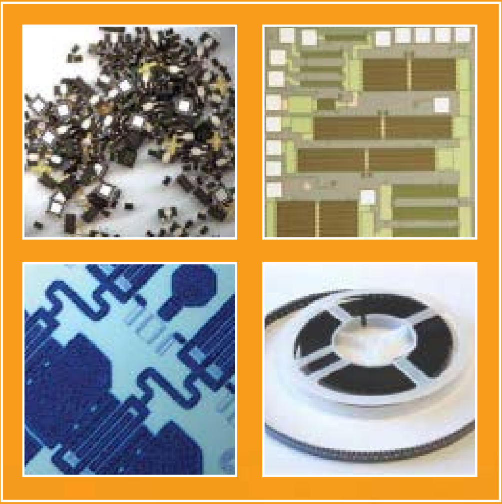

As the mobile handset market and emerging wireless systems continue to evolve, the requirement for high-performance infrastructure equipment continues. At Filtronic we are prepared to meet these needs with our newest High Linearity High Gain Packaged MMIC Amplifiers, the **FMA3025SOT89E** and **FMA3067SOT89E**. These newest MMIC Amplifiers are ideally suited for Wireless Infrastructure and PCS/Cellular markets where low cost and peak performance are required. Both amplifiers are ROHS compliant.

FMA3025SOT89E

Freq (GHz)	Gain (dB)	S11 (dB)	S22 (dB)	NF (dB)	OIP3 (dBm	P1dB (dBm)	Vcc +6V	Typical Applications
0.3-4	12 to 15	-17	-15	2.1	42	24.0	Id 160mA	• Driver Amplifiers for GSM, CDMA, W-CDMA • CATV/DBS Amplifiers • WiFi/WiMAX/WiBro • Point-to-point Radio Systems • High Linearity Gain Block • This product can be used in TX as well as RX

FMA3067SOT89E

Freq (GHz)	Gain (dB)	S11 (dB)	S22 (dB)	NF (dB)	OIP3 (dBm	P1dB (dBm)	Vcc +6V	Typical Applications
0.8-0.9 1.8-2.1	18.5 16.5	-23.5 -21	-25.5 -21	3.0 3.2	40 38	25.0 23.0	Id 170mA	• High Linearity and High Gain Block • GSM, CDMA, W-CDMA Cellular Infrastructure • This product can be used in TX as well as RX

Filtronic is a world leader in the design and manufacture of RF, microwave and millimeter wave components and subsystems. Filtronic offers a broad range of products used in electronic warfare, cellular backhaul, broadband communication infrastructure and point-to-point radio and are available in die form or packaged in industry standard outlines.

Richardson Electronics

These and other Filtronic Products are available through our Authorized Distributor, Richardson Electronics. USA/Canada Toll Free Sales: 1-800-737-6937 / www.rfpowernet.com

Filtronic

Filtronic Compound Semiconductors, Ltd.
Heighington Lane Business Park, Newton Aycliffe, Co. Durham, DL5 6JW, United Kingdom
Main Phone: +44 (0)1325 301111 • Main Fax: +44 (0)1325 306177 • Email: sales@filcs.com
US Sales Phone 1: 530.550.2957: Phone 2: 408.850.5740 / Fax: 831.621.8074 / www.filtronic.com

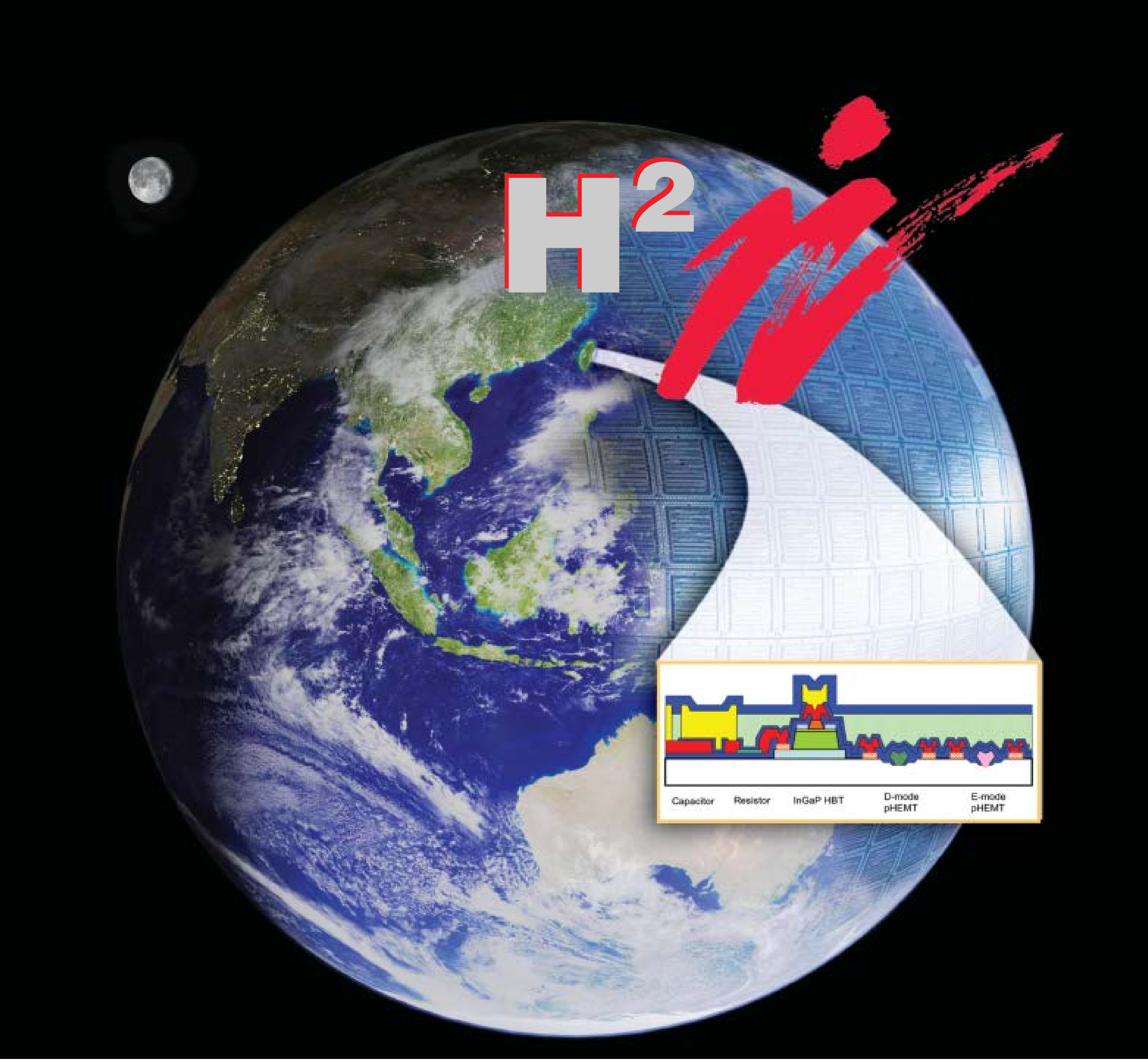
H2
Capacitor
Resistor
InGaP HBT
D-mode pHEMT
E-mode pHEMT

SYNTHESIS

A typical design window for the synthesis of a horn antenna is shown in ***Figure 2***. Initially, the user inserts general design parameters like frequency ranges and polarizations. Depending on the user's demand and specifications (for example, cross-polar level, bandwidth) the type of horn is chosen. For most applications either a perpendicular corrugated horn profile or a Potter horn profile is sufficient to cover the specifications. Since closed form expressions exist for these horn types (and for the conical horn), the initial geometry is set up from a few additional design parameters (for example, maximum co-polar gain or beamwidth). In Figure 2 a gain of 20 dBi is specified for the corrugated horn antennas.

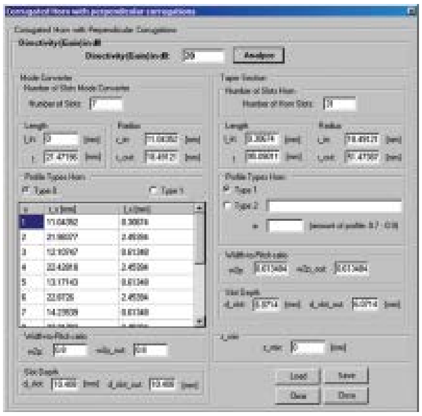

▲ *Fig. 3 Geometries of the synthesized horn antenna.*

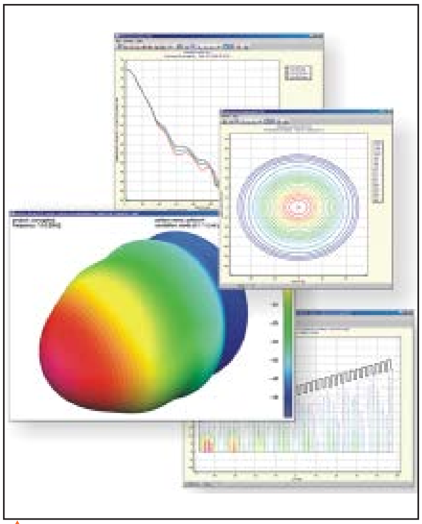

▲ *Fig. 4 Results for a corrugated horn synthesized from closed form expressions.*

The initial definition of the frequency settings, horn profile type and the specification are input values of the closed form expression for a corrugated horn.[1,2] The closed form results lead to initial values for all required geometries to generate a schematic of the corrugated horn. The values (see ***Figure 3***) are assigned automatically to the project variables for the µWave Wizard schematics. Furthermore, all properties of the new BOR elements and the radiation module are specified by the direct link to the project variables.

The user can visualize the corrugated horn and begin an analysis of the horn antenna to calculate the input return loss response and the antenna patterns. The antenna pattern can be displayed as a 2D plot, a 2D-isoline plot and a 3D output plot. The typical computation time for one frequency step is about three seconds on a low end PC (Pentium Centrino). Besides the 3D output of the radiation pattern, a new feature enables the visualization of the field distribu-

tion along the longitudinal axis of the horn antenna. ***Figure 4*** shows the results for a corrugated horn synthesized from closed form expressions.

The more experienced user also has the ability to overwrite the initial geometries given from the synthesis. These values are assigned as initial values to the µWave Wizard schematics of the corrugated horn and modification of the schematic variables provides users with maximum flexibility.

OPTIMIZATION

The setup for optimization consists of two main parts: the defining of the optimization variables (degrees of freedom), including minimum and maximum values (constraints), and the defining of the goal functions (including the election of weight factors for various performance specifications). The geometry parameters from the synthesis are automatically set as optimization variables with an initial permissible variable range (usually ±10 percent).

At this stage the user controls these optimization variables and either fixes the values (for restrictive guidelines, for example, fixed input radius), redefines the constraints (for example, minimum gap widths) or sets up equations for a number of variables to limit the number of degrees of freedom for faster optimization. ***Figure 5*** shows the specification of the goal function for an optimization.

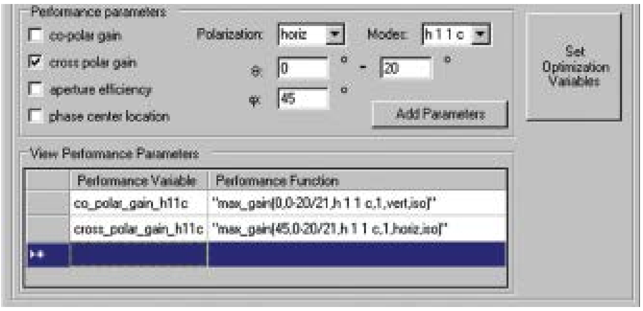

Fig. 5 Specification of the goal function for an optimization.

The next step is the definition of the goal function and the selection of an optimizer, the maximum number of iterations and the maximum computation time during an optimization task. The goal function consists of various specifications over certain frequency ranges, to which individual

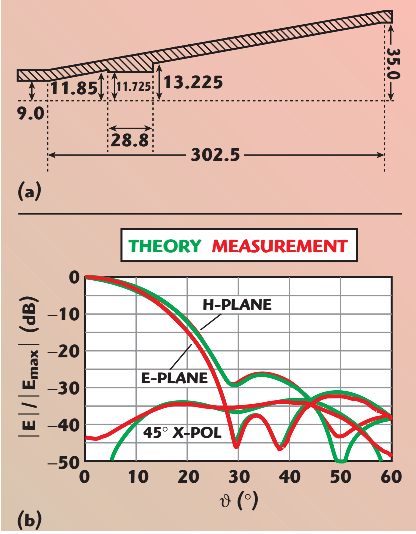

Fig. 6 Theoretical and measured performance of an optimized Potter horn.

weight factors are added. For basic specifications like telecom mode return loss, maximum co-polar and cross-polar gain, phase center variation, aperture efficiency and 3 or 10 dB beamwidth, there are easy to use pre-defined output variables. The inclusion of these variables into the goal function can be switched on or off in the synthesis tool. More advanced specifications can be defined by using these output variables in user-defined equations.

After the optimization setup is complete, the user starts the optimization. The user can monitor the process as the goal function is minimized, including partial errors for each optimization specification and the behavior of the variables in the desired range. The best result is stored automatically. Therefore, the user can interrupt the optimization at any stage, can change some settings (goal function weight factors or variable ranges) and then continue the optimization without losing the previous optimal result. If required, the user can also check the power handling performance during the optimization process by inserting a field calculation analysis. The field calculation inside the structure usually takes much longer than ordinary analysis, so it is not enabled by default.

If the results of the optimization are either within a given error limit, within the user-controlled maximum number of iterations or if the maximum computation time is reached, a final overall analysis is performed. For this the user normally adopts a slightly modified setup (for example, more frequencies, higher accuracy settings, more comprehensive output) compared to the analyses performed during optimization.

VALIDATION

The radiation feature based on the spherical wave expansion is verified against measured radiation patterns.[3,4] Apart from simple geometries (for example, radiating circular waveguide) this has been done for an optimized Potter horn, as shown in ***Figure 6***. The measured co-polar and cross-polar patterns are also depicted in the figure. It should be noted that the results coincide with the original data (curve labeled 'Theory').

CONCLUSION

The new horn antenna synthesis tool provides many horn profiles for different kinds of horn antennas. The initial geometry given by a closed form expression is assigned directly to the element properties of the new BOR radiation elements. Built-in optimizers can be used to efficiently improve the initial performance to meet most stringent horn performance requirements. The new software is fully compatible with the general µWave Wizard software, which when combined optimizes the radiated antenna performance, including the feed chain RF response (even with manufacturing errors). This novel CAD tool provides exceptional design capabilities by yielding very accurate performance predictions. The output data in the form of SWE can then be used as input for general reflector antenna analysis.

ACKNOWLEDGMENT

This work has been funded by ESA/ESTEC under contract number 19986/06/NL/JA and was performed with the collaboration of MacDonald, Dettwiler and Associates Corp. (MDA). The company also wishes to thank Jarek Uher and Sylvain Richard from MDA and Pablo Sarasa from ESA/ESTEC for their help and guidance.

References

1. C. Granet, G.L. James, R. Bolton and G. Moorey, "A Smooth-walled Spline-profile Horn as an Alternative to the Corrugated Horn for Wideband Millimeter-wave Optimization," *IEEE Transactions on Antennas and Propagation*, Vol. 52, No. 3, March 2004, pp. 848–834.
2. C. Granet and G.L. James, "Design of Corrugated Horns: A Primer," *IEEE Antennas and Propagation Magazine*, Vol. 47, No. 2, April 2005, pp. 76–84.
3. C. Reiter, "Dielektrisch Ausgekleidete Rundhornstrahler," PhD Thesis, University of Braunschweig, VDI, Series 21, No. 165, 1994.
4. J.M. Reiter, "Analytische Felddarstellung auf Nichtseparablen Oberflächen," PhD Thesis, University of Bremen, VDI, Series 21, No. 180, 1995.

Mician GmbH,
Bremen, Germany,
+49 (421) 168 993 51,
www.mician.com.

RS No. 303


PUT YOUR TEST PLANS
IN MOTION
with the MS2690A
Precision:
* 241-Point Amplitude Calibration
* Unique IF Phase Calibration
Versatility:
* Wide Analysis Bandwidth
31.25 MHz Standard/125 MHZ Option!
* Analyzes Uplink and Downlink of WiMAX & LTE
* Tests DigRFv3 RFICs & W-CDMA BTS with a single box
Speed:
* Up to 1000 Measurements per Second
* Stable Readings without Averaging
MS2690A
Spectrum Analyzer, Broadband
Vector Signal Analyzer, and Digitizer
Standard in the Basic Chassis.
Add the Optional Vector Signal Generator
to Create a One-Box TX/RX Tester.
Save Space, Save Time, Save Money!
Get your free WiMAX poster at:
www.toolsfortesting.com/MS2690
For more information, call 1-800-ANRITSU
or email us at us-sales@anritsu.com
Anritsu
Test and Measurement Solutions
Sales Offices: USA and Canada 1-800-ANRITSU, Europe 44 (0) 1582-433433, Japan 81 (46) 223-1111, Asia-Pacific (852) 2301-4980,
South America 55 (21) 2527-6922, www.us.anritsu.com ©2008 Anritsu Company
Visit http://mwj.hotims.com/16339-14 or use RS# 14 at www.mwjournal.com/info

NEW INSIGHTS INTO VARYING RF PHENOMENA WITH LIVE RF

The rapid expansion of digital RF applications has driven the measurement needs of many applications including mobile communications and spectrum management beyond the capabilities of swept spectrum and vector signal analysis. To address these new requirements, Tektronix has developed Digital Phospor Technology (DPX™) with live RF that first became available in the RSA6100A performance series introduced in 2006. This technology is now being offered in the mid-range RSA3000B Series of real-time spectrum analyzers, enabling detailed RF signal discovery capability for a broad range of digital RF applications including RFID, radio communications and spectrum management. DPX transforms volumes of real-time data, and produces a live RF spectrum display that reveals previously unseen RF signals and signal anomalies.

DPX waveform image processor technology in the new RSA3300B Series and RSA3408B models displays the live spectrum by processing > 48,000 spectrum updates per second, similar to the previously announced RSA6114A model. This is over 500 times more information than is shown by spectrum analyzers without DPX, minimizing the analysis gaps inherent in swept spectrum and vector signal analyzers. To achieve > 48,000 spectrum measurements per second, DPX makes use of dedicated, real-time hardware to process the incoming signal.

DPX can be used to find illegal jammers captured off-the-air. ***Figure 1*** displays an example on an intentional jammer of GSM sig-

TEKTRONIX INC.
Beaverton, OR

nals captured by a spectrum management agency using Tektronix Real-time Spectrum Analyzer (RTSA) using DPX.

In addition to live RF, the waveform image processor also provides an intensity-graded persistence display that holds anomalies until the eye can see them to show the history of occurrence for dynamic signals and immediate feedback on signal variations over time. This provides engineers the ability to rapidly see on screen both transients and signals that ordinarily could not be seen, either because they are masked by other signals or could only be deduced after time-consuming offline analysis. DPX waveform imaging will enhance productivity by quickly capturing elusive anomalies and transient events, improving accuracy and insight, and accelerating design debug.

DIGITAL RF CHANGES RF WORLD

The explosion of digital RF has created a highly complex spectral environment. In a crowded RF spectrum, signals must use time varying techniques to avoid interference and ensure seamless operation. To improve performance and spectral efficiency, digital RF devices employ signals that change from one instant to the next, including some that hop frequencies, while others use signals that quickly pulse on and off. With numerous devices transmitting simultaneously within a limited radio frequency spectrum, frequent collision and interference problems occur. This makes it important to ensure these devices do not transmit RF energy at unwanted times or unwanted frequencies and are able to function correctly in the presence of interference.

Common to all of the new digital RF technologies is the dimension of time. Enabled by the power of computing in the time-domain world, powerful DSP applied to the RF (frequency-domain) world has necessitated the analysis of spectrum over time. Digital RF technologies can exhibit frequency-domain and modulation changes that occur over time—sometimes milliseconds, sometimes microseconds, or even faster. The limited architecture of traditional RF tools is not able to fully characterize frequency events over time, and time can no longer be ignored. Digital RF creates new requirements for tools whose capabilities mirror the time-varying nature of today's signals. RF engineers need real-time instruments that can discover how their device operates over time, trigger on intermittent events that occur in frequency, capture them seamlessly and analyze accumulated data representing the passage of time.

The RSA3000B allows engineers to discover the unexpected problems with DPX live RF that are commonplace in digital RF, and selectivity trigger and capture these signals into memory. Once captured into memory, this enables complete time-correlated, multi-domain analysis without the need to recapture the signal.

DPX MAKES THE DIFFERENCE

Using a parallel processing architecture, DPX technology produces greater than 500x improvement in the spectrum processing rate. Conventional swept spectrum analyzers typically do not exceed 50 spectrum measurements per second. The RSA3000B Series with DPX technology delivers over 48,000 spectrum measurements per second, with a 100 percent probability of detecting RF spectrum events with minimum signal duration as fast as 31 microseconds (RSA3408B).

By continuously converting time domain signals into the frequency domain, as shown in ***Figure 1***, DPX technology provides a means of displaying both frequent and infrequent events, distilling real-time computing discrete Fourier transform (DFT) at frame rates far above what is perceivable by the human eye and converting them into an intuitive, full motion display.

The RSA3000B Series is able to display live RF signals that have never been visible before, except by using the high performance Tektronix RSA6100A Series. With variable color-graded persistence that holds anomalies until they can be seen, these analyzers help reveal elusive glitches and other transient events, as demonstrated in ***Figure 2***. With each update, the power level values at each frequency across the capture bandwidth are recorded, and the incidence of power over time at each frequency is shown by varying colors on the display. This gives the DPX display a translucent quality that reveals spectral information below the peak amplitude of the time-varying spectral envelope (see Figure 1).

As shown in ***Figure 3***, the figure on the left is a typical display of a signal that can be seen with the fastest swept-spectrum analyzer technology. The Tektronix DPX display on the

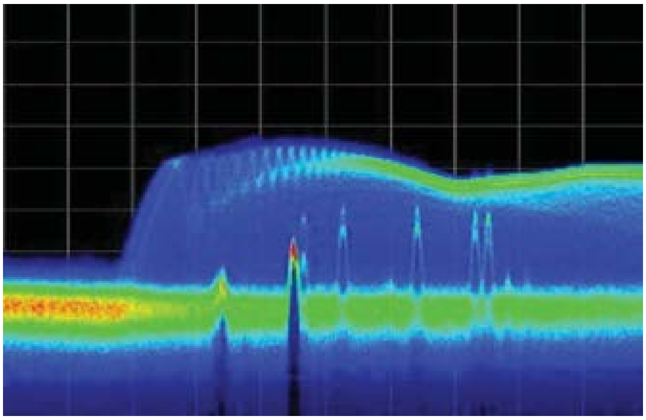

Fig. 1 Example of GSM signals captured using a Tektronix Red-time Spectrum Analyzer using DPX technology.

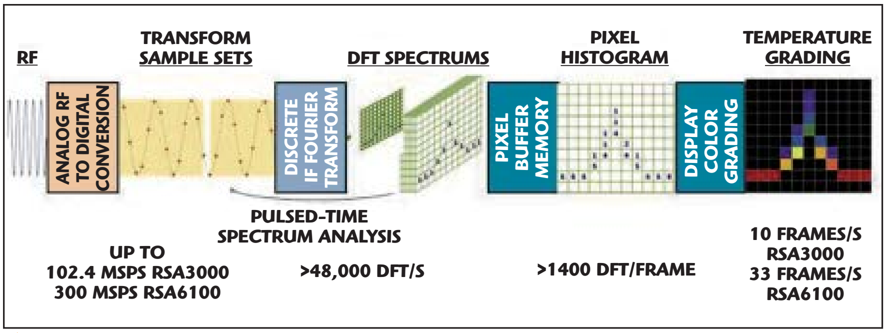

Fig. 2 The DPX transform engine.


GREAT SERVICE ISN'T EXPENSIVE...
...IT'S PRICELESS.
EXCELLENT SERVICE
EXCELLENT DELIVERY
EXCELLENT QUALITY
RELCOMM TECHNOLOGIES, INC.
RMS-6S3AB-1
28Vdc D/C
RF COAXIAL RELAYS
SMA, N AND PCB LAUNCH
STANDARD AND CUSTOM DESIGNS
RELCOMM TECHNOLOGIES, INC.
• Mission Critical Communications:
- Security, Safety and Intelligence
- Commercial Telecom Infrastructure
- Military Defense Fixed, Mobile & Shipboard
• Instrumentation:
-Test and Measurement
RF Relay Store.com is the answer to your urgent small quantity needs.
RF Coaxial Relays available from Stock at www.rfrelaystore.com
sales@relcommtech.com • www.relcommtech.com • 410-749-4488
EXCELLENCE BY DESIGN

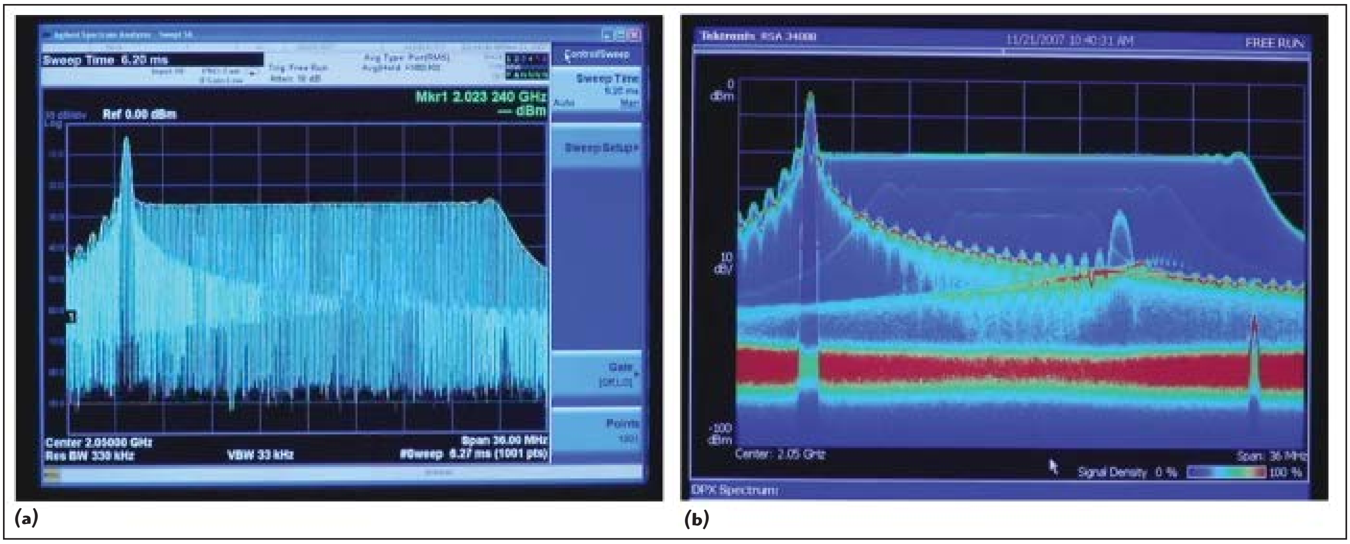

▲ *Fig. 3 Typical signal display (a) seen with the fastest swept-spectrum analyzer technology and (b) the Tektronix DPX display showing complex signals and pulses that change frequency and level over time.*

right shows complex signals and pulses that change frequency and level over time, and can be immediately identified with DPX persistence.

CAPTURE ELUSIVE RF EVENTS IN REAL TIME

To improve capacity and performance, modern RF signals often employ sophisticated combinations of RF techniques such as bursting, frequency hopping and adaptive modulation. The intricacy and prevalence of these time varying RF signals create challenges for designers to capture and analyze. This leads to a need to detect and characterize RF signals and events over a wide range of strengths, durations and environments. Traditional spectrum analyzers and vector signal analyzers are limited to power level or external event triggering. However, since many time varying transients do not increase the signal amplitude when they happen, and signals do not always tell you where they are going, these triggers do not always satisfy the need to isolate spectrum events efficiently for analysis.

This need is addressed by the Frequency Mask Trigger (FMT) in the RSA3000B Series that allows the user to trigger a measurement based on the occurrence of a unique pattern of events in the frequency domain. The high dynamic range of the FMT also allows triggering on weak transient signals while ignoring strong known signals. Operating across either the 15 or 36 MHz real-time bandwidth, the FMT reliably captures elusive RF signals or frequency abnormalities.

The FMT is useful for finding short duration or time varying signals while troubleshooting RF circuits. It can detect sporadic signals, the presence of intermodulation products and transient spectrum containment violations. The FMT is also appropriate for surveillance and radio communications applications, with the ability to capture a spectrally interesting event, such as a weak signal pulse under complex spectral conditions.

MID-RANGE FITS MANY APPLICATIONS

The RSA3300B Series and RSA3408B, with DPX Spectrum, provide 100 percent probability of intercept for transients as brief as 31 microseconds on the RSA3408B and 41 microseconds on the RSA3300B Series models. This is combined with the ability to trigger on transient signals in both the time and frequency domains for troubleshooting and debugging of a wide variety of digital RF designs and for use in many different application areas.

The RSA3300B Series is available with either DC to 3 GHz or DC to 8 GHz frequency coverage. With a 15 MHz capture bandwidth and 70 dB spurious free dynamic range (SFDR), the RSA3300Bs are well-suited for use in the design and debugging of 3G mobile systems, near-field systems (such as RFID and Bluetooth), and narrow to medium bandwidth communications systems.

The RSA3408B with DC to 8 GHz frequency coverage, a 36 MHz capture bandwidth and 73 dB SFDR is tailored for higher bandwidth and dynamic range applications including 3G mobile components and system debugging, WLAN (IEEE 802.11 a/b/g/n), MIMO and WiMAX system design, demanding spectrum management applications and general purpose digital RF debug.

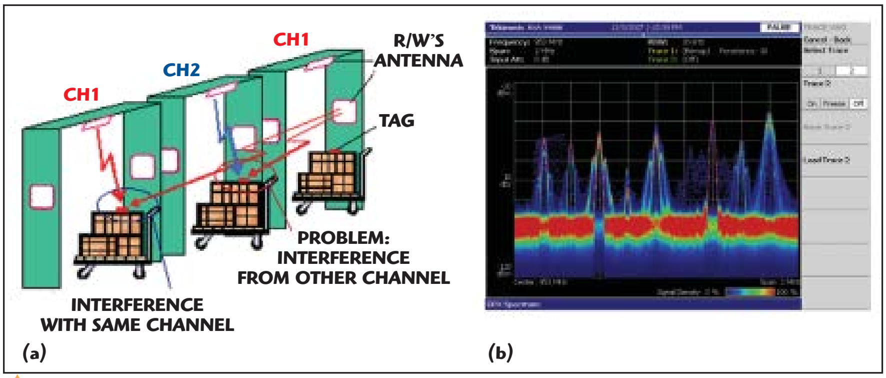

▲ *Fig. 4 Live RF unveils the complex environment of RFID interoperability.*


Custom.
Commercial.
Microminiature.

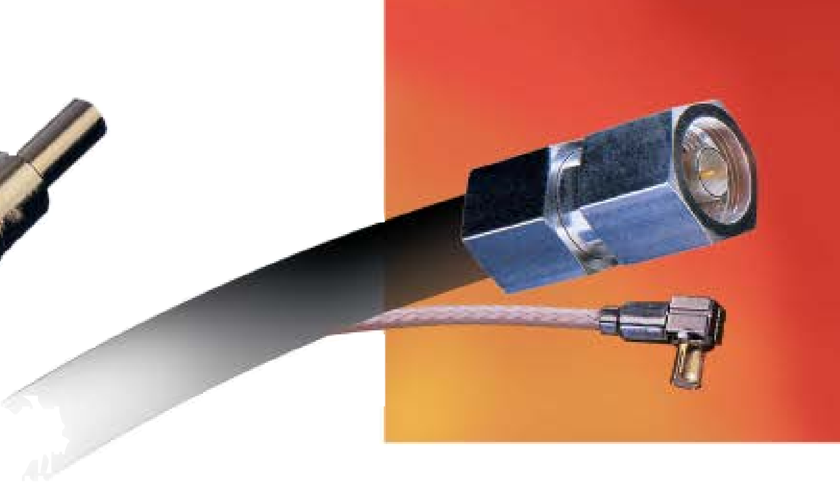

COMPREHENSIVE RFID/NFC STANDARDS SUPPORT

Adding to an already extensive support of RFID industry standards, Tektronix now supports ISO 18000-7 and ISO 15693 RFID standards. With this support, the RSA3000B Series provides integrated analysis for the most comprehensive set of RFID/NFC standards in the industry: ISO 18000-4 (Mode 1); ISO 18000-6 (Type A, B, C); ISO 1444-3-2 (Type A/B); ePC Global Gen 1 and Gen 2; and ISO 18092 (424k). These are performed using simplified standards-based measurements for timing, frequency, modulation, decoding and bit-rate measurements for the RFID standards.

Active and passive RFID are part of a much larger hierarchy to tag and track everything in the supply chain. Though adequate infrastructure has not yet been deployed, retailers would like to see a supply chain developed so every piece of merchandise could be managed from the manufacturing origin through the point of sale.

Testing is required for standards compliance, design verification and troubleshooting during chip design, tag integration with the antenna and system integration. More complete testing is required for full compliance and interoperability testing at independent testing labs. Testing is also needed to ensure interoperability between tag and interrogator manufacturers throughout the RFID value chain.

For RFID measurements, the RSA3000B goes beyond the conventional compliance tester. It functions as a field interoperability tester for real-time interference troubleshooting. The DPX live RF capability sees and measures interrogator-tag transactions live to debug problems such as tag confusion caused by adjacent interrogators, high power tag interference with low power tags and listen-before-talk bugs, as shown in ***Figure 4***.

CONCLUSION

Tektronix real-time spectrum analyzers are designed specifically to solve problems created by digital RF technologies. The addition of DPX technology with live RF from the high performance RSA6100A Series combined with a broad range of application-specific measurements make the mid-range RSA3300B Series and RSA3408B well-suited for tough RF discovery and debug problems, and for use as an everyday spectrum analysis and system characterization tool.

Tektronix Inc.,
Beaverton, OR (800) 833-9200,
www.tektronix.com.

RS No. 301

LOW-COST PC-CONTROLLED SIGNAL GENERATORS

Signal generators have traditionally been amongst the most expensive pieces of test equipment found in RF and microwave test laboratories. Due to their high cost they are often in short supply and must be shared among multiple employees, between various test set-ups and sometimes even among multiple laboratories. This lack of equipment can result in delayed schedules, decreased productivity and, in the worst cases, can create unhealthy competition for resources among coworkers.

With this in mind, Vaunix Technology Corp. has introduced an innovative line of Lab Brick® signal generators. Covering 50 MHz to 6 GHz in four models, these devices deliver a true phase-locked RF signal with full output power control just like expensive, full sized RF signal generators, but at a fraction of the price. They are powered and controlled by a PC or laptop via any USB port. The Lab Brick graphical user interface (GUI) features intuitive controls with a large, uncluttered display making these devices simple to use. Lab Brick signal generators are a fast, easy and cost-effective solution to most signal generation needs.

PERFORMANCE

Table 1 summarizes each model's key performance specifications. The LSG-251 operates from 50 to 250 MHz, the LSG-152 operates from 250 to 1500 MHz, the LSG-402 operates from 1000 to 4000 MHz and the LSG-602 operates from 1500 to 6000 MHz. The output frequency resolution is 100 kHz with better than ±2 PPM initial accuracy. Each Lab Brick signal generator model is capable of producing +10 dBm of output power over its entire frequency range. The output power is adjustable in 0.5 dB steps over 55 dB of dynamic range.

SMALL SIZE

Lab Brick signal generators are enclosed in a rugged aluminum housing. Each unit measures just 4.90" × 3.14" × 1.59" and weighs less than one pound, making them ideal for bench top or rack mount use. Each housing features two external 0.25" diameter counter-bored through holes that can be used for mounting purposes. Device orientation does not affect performance.

COMPLIANCE

Lab Brick signal generators have been tested and comply with international EMC emissions and immunity requirements for Class A ISM devices. This insures that they will not interfere with nor will they be affected by other pieces of test equipment in close proximity. A copy of the compliance certificate can be viewed at the link provided at the end of this article.

VAUNIX TECHNOLOGY CORP.
Haverhill, MA

TABLE I

LAB BRICK SIGNAL GENERATOR KEY PERFORMANCE SPECIFICATIONS[1]

Model Number	LSG-251	LSG-152	LSG-402	LSG-602
Electrical				
Frequency range (MHz)	50 to 250	250 to 1500	1000 to 4000	1500 to 6000
Frequency resolution (kHz)	100	100	100	100
Frequency accuracy[2] (ppm)	±2	±2	±2	±2
Guaranteed output power (dBm)	+10	+10	+10	+10
Output power range (dB)	55 min.	55 min.	55 min.	50 min.
Output power resolution (dB)	0.5	0.5	0.5	0.5
Output power accuracy (dB)	+1.5/–0.5	+1.5/–0.5	+1.5/–0.5	+1.5/–0.5
SSB phase noise @10 kHz offset (dBc/Hz)	–105 typical	–95 typical	–85 typical	–75 typical
SSB phase noise @100 kHz offset (dBc/Hz)	–125 typical	–115 typical	–105 typical	–95 typical
Harmonic level (dBc)	–10 max.	–10 max.	–10 max.	–10 max.
Non-harmonic spurious level (dBc)	–70 max. –80 typ.	–70 max. –80 typ.	–70 max. –80 typ.	–70 max. –80 max.
Output VSWR	1.5 max.	1.5 max.	1.5 max.	1.5 max.
DC power	via USB	via USB	via USB	via USB
Operating modes	continuous frequency frequency stepping, single sweep frequency stepping with continuous sweep			
GUI compatibility[3]	Windows™ 2000/XP/Vista			
Mechanical				
Length (inches (mm))	4.90 (124)			
Width (inches (mm))	3.14 (80)			
Height (inches (mm))	1.59 (40)			
Weight (lbs (kg))	< 1.0 (0.45)			
RF connector	SMA			
USB cable[4]	USB 2.0 A to Mini B			

Notes: 1. These specifications are subject to change without notice.
2. This figure does not include aging effects.
3. The GUI software is included with purchase of each Lab Brick signal generator.
4. A 6' USB cable is included with the purchase of each Lab Brick signal generator.

GRAPHICAL USER INTERFACE

Figure 1 shows the Lab Brick signal generator's graphical user interface. The GUI allows the operator to control the device by either keyboard or mouse. The user can enter parameter settings simply by typing directly into a specific parameter window. The GUI also features convenient up-/down-arrow keys for frequency and power control that allows the user to scroll through a range of settings using a mouse. The arrow step sizes can be adjusted by selecting from the standard increment soft-buttons or by selecting a user-defined value.

▲ *Fig. 1 Lab Brick's graphical user interface.*

To further simplify operation every instance of an open GUI will display both the serial number and model number of the device to which it is coupled. Once the GUI has coupled with a specific Lab Brick signal generator, the GUI adapts to that device by tailoring the range of settings of the various operating parameters to those that are specific to that model number.

Device operating settings can be saved directly into the Lab Brick signal generator's internal memory allowing the user to define the configuration of the device at power-up. The GUI also includes a comprehensive help function with guides to further resources for technical assistance.

OPERATION

Lab Brick signal generators are easy to use. Each unit is shipped with a 6' USB cable and a thumb drive containing the GUI software and a soft copy of the user manual. Once the Lab Brick signal generator is plugged into a host computer or hub, the green LED on the side of the product will light up indicating that the device has been recognized by the host. When opened, or if the GUI is already running, it will automatically recognize the device and display both its model number and serial number. This instance of the GUI is now coupled to this Lab Brick signal generator. As additional Lab Brick signal generators are plugged into the USB and as additional instances of the GUI are opened, this coupling feature will automatically engage, allowing several Lab Brick signal generators to operate from a common host without confusion.

In continuous wave (CW) mode Lab Brick signal generators deliver a fixed frequency, sinusoidal signal. ***Figure 2*** shows a measured phase noise plot of an LSG-152 model taken with the output frequency set to 1 GHz. ***Figure 3*** further demonstrates spectral purity by showing the output spectrum over a 100 MHz span. Typically, its non-harmonic spurious content is below –80 dBc. The output power is adjustable from +10 to –45 dBm with 0.5 dB resolution. The output signal can also be completely turned off via the RF ON/OFF control buttons on the GUI.

In addition to the CW operating mode, each model has the ability to simulate a frequency sweep func-

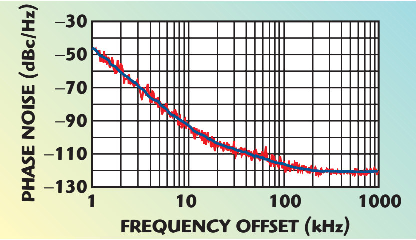

▲ *Fig. 2 Phase noise of the model LSG-152 at 1 GHz.*

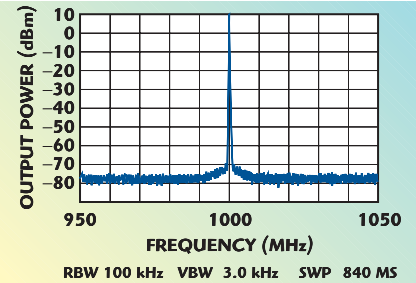

▲ *Fig. 3 Output spectrum of the model LSG-152.*

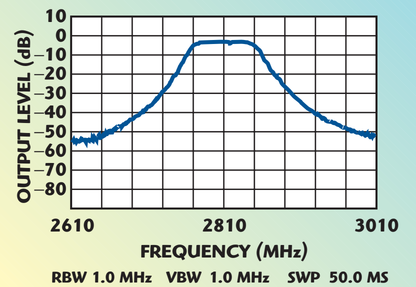

▲ *Fig. 4 Bandpass filter characteristics generated using a Lab Brick signal generator.*

tion by stepping through a user-defined frequency band. In this mode the user also defines the frequency step size and the frequency dwell time. When used in conjunction with the "max/hold" function on a spectrum analyzer, this feature can be used to generate amplitude versus frequency response plots to characterize networks or devices. ***Figure 4*** shows the amplitude characteristic of a ceramic bandpass filter having a center frequency of 2.81 GHz, a 3 dB bandwidth of 86.7 MHz and an insertion loss of 3.17 dB at the center frequency.

COMPATIBILITY

Lab Brick signal generators can be used with any PC or laptop having a USB 2.0 port. They can also be run from a powered USB 2.0 hub. Multiple Lab Brick signal generators can be run from a single host computer. Compatible operating systems include Windows 2000, Windows XP and Vista. A detailed programming guide is available upon request for those users who wish to integrate Lab Brick signal generators into existing ATE systems.

CONCLUSION

Due to their low cost and small size, Lab Brick signal generators eliminate the need for sharing and moving bulky pieces of equipment among laboratory coworkers. These rugged devices are also well suited for use on the manufacturing floor and in ATE systems. Their low price makes it an easy decision to integrate them into dedicated ATE and breadboard systems. They are even small enough to be brought on the road to support on-site service calls and product demonstrations. Additional information may be obtained by contacting the company via the company's web site at www.labbrick.com.

Vaunix Technology Corp., Haverhill, MA (978) 662-7839, www.labbrick.com.

RS No. 300


NEVER
COMPROMISE
YOUR
CONNECTION

A LOW-COST DIGITAL SYNTHESIZER

The conversion from analog to digital technologies, in such fields as wireless communications, music and video, has historically emerged first in the high end of their respective markets. Initial appearances of digital technology are usually seen in those applications requiring leading-edge performance. The same pattern has been emerging, albeit slowly, with respect to broadband microwave synthesizers based on direct digital synthesis (DDS) technology.

DDS-based synthesizers have traditionally led the industry in frequency agility, but they have also led in high recurring costs. These high costs stem from the typically complex nature of DDS-based synthesizers and have resulted in such synthesizers being utilized primarily in military applications where performance considerations have taken precedence over cost.

Fig. 1 The WaveCor Synthesized Local Oscillator top level block diagram.

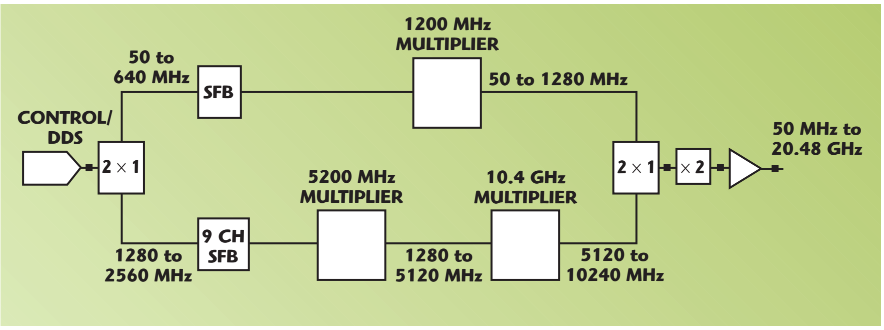

This cost disadvantage has, in effect, left the market for lower cost synthesizer solutions to those manufacturers utilizing analog technologies. Vendors offering YIG-based products have enjoyed a long history of dominating the market for low-cost microwave synthesizers.

The WaveCor™ Synthesized Local Oscillator (SLO) is the next step in the evolution of digital synthesizers and is designed to dramatically reduce this cost disadvantage, while still offering customers a higher performance solution. This synthesizer provides 50 MHz to 20.48 GHz of usable bandwidth in a very compact package. As with ITT's other DDS-based synthesizers, the WaveCor SLO

ITT MICROWAVE SYSTEMS
Lowell, MA


a new
7/16
has hatched
A new composite 7/16
- 100% intermateable with standard 7/16
- 60% lighter
- Better Intermodulation withstanding
- No corrosion
- Reduction of your total cost of ownership
colors
RADIALL
The next conneXion
Visit http://mwj.hotims.com/16339-111 or use RS# 111 at www.mwjournal.com/info

provides low phase noise and spurious performance combined with fast tuning.

Where the WaveCor SLO differentiates itself from other digital solutions, though, is in the value proposition it provides. The price of this synthesizer is very much cost competitive with commercially available YIG-based synthesizers.

The price and performance of the WaveCor SLO is now feasible due to the signal purity of ITT's patent-pending low-spurious direct digital synthesis technology, which provides 2.5 GHz of useable bandwidth directly from the DDS output. This wide bandwidth has spurious free dynamic range of greater than –70 dBc and is combined with the usual DDS benefits of low phase noise, precise frequency control and maximum switching time of 10 µs.

In the past, applying prior generations of DDS technology was limited by high spurious content and narrow output bandwidths, which necessitated "cleanup" circuitry using such techniques as mix/divide to provide usable output. The WaveCor SLO eliminates the need for this complicated and expensive circuitry. With the DDS output of the WaveCor SLO combining wide bandwidth and signal purity, a radical simplification of the synthesizer's architecture is finally possible. In fact, the high performance of the WaveCor SLO can be realized with simple multiplier blocks. The top-level block diagram is shown in ***Figure 1***.

The 2.5 GHz bandwidth output of the DDS is split, filtered, and then sent to a series of multiplier modules for conversion and filtering. A final multiplier module is used to double the chosen path to the desired output frequency and an output amplification stage is used for power leveling.

The result is the WaveCor SLO, a 50 MHz to 20.48 GHz synthesizer, with a resolution of 1 kHz, 10 GHz phase noise of –126 dBc/Hz at a 10 kHz offset, typical spurious levels of –64 dBc and powered through a single +28 VDC supply. The WaveCor SLO measures 6" × 6" × 2.75" and is controllable through a standard BCD interface utilizing TTL signaling.

The WaveCor SLO is a significant step forward in synthesizer design. All aspects of its design are intended to maximize value for the user. With the significant simplification in architecture achieved, it is now economically feasible to select a high performance digital synthesizer in many more applications. More information may be obtained from the company's web site.

ITT Microwave Systems,
Lowell, MA (978) 441-0200,
www.ittmicrowave.com.

RS No. 300

The International Microwave Symposium is the headline conference of the IEEE Microwave Theory and Techniques Society (MTT-S). This will be the largest technical Conference to be held in Atlanta in the next two years and will feature a large trade show as well as a wide variety of technical papers and workshops. The IEEE MTT-S International Microwave Symposium 2008 (IMS2008) will be held in Atlanta, GA, Sunday, June 15 through Friday, June 20, 2008, as the premiere event of Microwave Week 2008.

Microwave Week 2008: The IMS 2008 technical sessions will run from Tuesday through Thursday of Microwave Week. Workshops will be held on Sunday, Monday and Friday. In addition to IMS2008, a microwave exhibition, a historical exhibit and the RFIC Symposium (www.rfic2008.org) will also be held in Atlanta during Microwave Week 2008.

Fabless in Hyderabad

AMTL develops standard products based on robust and reliable designs fabricated at GaAs foundries around the world. AMTL products are tested and packaged as per customer requirement at the state-of-the-art facility available with the parent company. AMTL also designs high performance MMICs for customer specific applications. AMTL designs for military, space and telecom applications.

Astra Microelectronic Technologies Ltd.
6-3-639/640, 303, 3rd Floor,
Golden Edifice Building,
Khairatabad, Hyderabad, India

www.astramtl.com

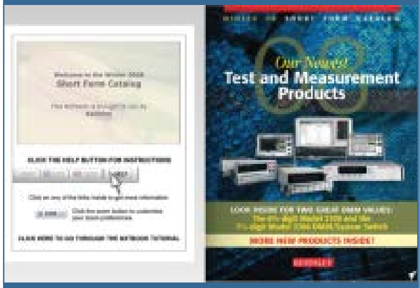

Online Catalog

Keithley Instruments Inc. announces the release of its 2008 Test and Measurement Product Guide. This handy product guide offers details and specifications on Keithley's general-purpose and sensitive sourcing and measurement products, DC switching, RF switching and measurement, data acquisition solutions, semiconductor test systems and optoelectronics test hardware. Tutorials simplify choosing solutions for specific applications.

Keithley Instruments Inc.
28775 Aurora Road,
Cleveland, OH 44139

www.keithley.com

Engineering Activities

This web site is dedicated to activities of the company's Engineering Division, which designs and manufactures a comprehensive range of waveguide and coaxial microwave components, assemblies and subsystems. As well as presenting an overview of the division's capabilities, the web site provides easy access to .pdf datasheets on a wide variety of standard products for applications in the DC to 40 GHz frequency range. These include horn antennas, rotary joints, attenuators and many more.

Link Microtek Ltd. UK,
Intec 4.1, Wade Road,
Basingstoke, RG24 8NE, UK

www.linkmicrotekeng.com

Life Without Wires

Life Without Wires is a blog by Eric Broockman, CEO of Alereon Inc. Follow along with Broockman at the birth of a new era in consumer electronics, personal computer and cell phone applications and technology. Broockman has more than 23 years of leadership experience in the fabless semiconductor and communication IC industries, with specific experience in managing product development, customer and strategic marketing, branding, marketing communications and public relations.

Alereon Inc.
7600 North Capital of Texas Highway,
Building C, Suite 200, Austin, TX 78731

www.alereon.com

New at Narda East

Narda Microwave-East has completely redesigned its web site at www.nardamicrowave.com/east. The site is much easier to use and provides greater resources than its predecessor. The new site makes finding information about the company's products, as well as design and application information and customer support far easier and faster than ever before. All products and product families are more fully described, with detailed specifications and drawings that are easily accessible.

Narda Microwave – East,
435 Moreland Road,
Hauppauge, NY 11788

www.nardamicrowave.com

Simplicity on the Menu

Navigation of the AtlanTec web site is easy. The new product menu remains on the screen permanently, which means that users can quickly move around the site and always know exactly where they are. The site showcases the company's complete product range, which comprises passive, active and control components and both standard and custom equipment for the RF and microwave industry. Quotes and brochures for any of these products can be requested at the press of a button.

AtlanTec,
40A Springwood Drive,
Braintree, Essex, UK

www.atlantecrf.com

Interconnect on the Web

Tensolite Co. is a designer and manufacturer of high-performance wire and cable and interconnect systems. The company's products are targeted at applications in the aerospace, test and measurement, defense electronics and specialty applications. Please go to the newly redesigned web site for more information.

Tensolite Co.,
100 Tensolite Drive,
St. Augustine, FL 32092

www.tensolite.com

Cables on Demand

CablesonDemand.com provides genuine top-quality Amphenol cable assemblies and accessories in stock and ready to ship same day. Backed by Amphenol Corp., CablesonDemand.com has the expertise and quality that can only come from designing and manufacturing cables for over 75 years. The site also has real-time online and phone support to handle cabling questions.

Amphenol,
20 Valley Street,
Endicott, NY 13760

www.cablesondemand.com

AR Virtual Library

The AR Information Resource Center is a convenient virtual library featuring the company's complete educational and informative offerings including software and software updates, application notes, newsworthy articles and exciting product demonstrations, including two new presentations. The first one is about AR's line of field monitoring equipment, while the second presentation highlights the company's 8 to 20 GHz solid state amplifier series and also includes a tour of AR's microelectronics facility.

AR RF/Microwave Instrumentation,
160 School House Road,
Souderton, PA 18964

www.ar-worldwide.com

IMAPS Technical Publications

IMAPS online library, iKnow Microelectronics, provides a centralized, searchable database of the technical papers and slides from IMAPS events and publications offered by the Society. iKnow Microelectronics currently contains more than 2,700 articles and publications from symposia, conferences, workshops, web meetings and other publications from 2003 through 2008. IMAPS will continue to incrementally load additional historical publications from 2002 and earlier throughout 2008.

IMAPS,
611 2nd Street, NE,
Washington, DC 20002

www.imaps.org

Capacitor Technical Papers

Evans Capacitor manufactures high energy density capacitors for demanding defense and aerospace applications. Typical applications replace standard military capacitors, or augment batteries and power supplies where size, weight, reliability and quality are important factors of component selection. Evans has met US Department of Energy and US military quality and performance specifications for the design and manufacture of capacitors.

Evans Capacitor Co.,
72 Boyd Avenue,
East Providence, RI 02914

www.evanscap.com

Comprehensive Product Info

This web site has recently added new product lines including high-speed digital logic, passives and variable gain amplifiers. The site details full specifications for over 630 products, application notes, quality assurance and product support tools, including Product Cross Reference, Parametric Search, PLL Phase Noise and Mixer Spur Chart Calculators, and expanded e-commerce. The company's new three-volume 2008 Designer's Guide, product selection guide, newsletter and CD can also be requested from the site.

Hittite Microwave Corp.,
20 Alpha Road, Chelmsford, MA 01824

www.hittite.com

Foegelle *[From page 92]*

for increased bandwidth and throughput over the current Single Input, Single Output (SISO) implementation. So how is MIMO tested in the above configuration?

The short answer is, it isn't. Remember that the initial purpose of these tests is to determine edge of link performance as a fundamental indication of radio performance. MIMO does not work at the edge of the link, since it requires a considerable signal-to-noise ratio (SNR) to be able to resolve the multiple data streams. Thus, when asking "What about MIMO?," the more important question is, "What do you want to know about MIMO?" Is it maximum possible throughput, or average throughput under a range of conditions? Or is the question, "What is the impact of the antennas and platform on ideal MIMO performance?" Or maybe just, "How well do the diversity antennas respond to a faded channel?" Each of these questions would have a different answer and require a considerably different test system implementation in order to measure them. However, until the wireless industry as a whole decides what radiated performance testing of MIMO means, and can then judge the value of such testing, the question will, for the time being, remain unanswered.

This does bring us to one of the last hurdles in RPT testing, which is fundamental to RPTs roots in passive antenna testing. The one underlying assumption when performing TRP or TIS measurements is that the radiation pattern does not change as it is being measured. However, with two receive antennas and a diversity algorithm applied to the two receivers, the device can react to the signal that it receives and change the relationship between the two antennas, thereby altering the radiation pattern and apparent performance of the device. While this "diversity gain" is actually a useful quantity to determine, it is not really the point of the TIS test. Moreover, the test itself makes the assumption that the device does not change, especially between the measurements of the two orthogonal polarizations of the measurement antenna. The assumption is that these two measurements are the components of one static field vector, but if the device can change its behavior between the measurements, that assumption is no longer valid. The reported result can actually be better than what is possible in real life. Worse yet, device orientation within the test system can alter the result, proving that this interaction between the test system and the device could completely invalidate the results of the test if it was allowed to occur.[7,8]

In order to avoid this possibility, it is necessary to test the receive performance of each antenna separately, or to disable any diversity algorithms such that the relationship between antennas remains fixed throughout the TIS test. This is not a function typically provided by WiMAX devices and will have to be added in order to ensure the integrity of RPT tests. Unfortunately, it's not as simple as just disconnecting each antenna to test one at a time, since most devices use one of the antennas for uplink. Disconnecting the uplink antenna in order to test the second downlink antenna would remove the uplink from the system, preventing the connection to the BSE.

CONCLUSION

Wireless consumers are about to see a revolution in their mobile wireless experience in the form of WiMAX Forum Certified devices operating on a WiMAX network. By developing technology based on a non-proprietary international standard, and creating a certification program to cover conformance, interoperability and performance, the WiMAX Forum is poised to help companies deliver an international broadband wireless access network unlike any seen to date. The technical expertise that has gone into improving existing cellular technologies over the past decade is now being applied to emerging WiMAX devices to ensure that they meet demanding performance requirements at launch.

At the time of this writing, the WiMAX Forum™ Radiated Performance Tests (RPT) for Subscriber and Mobile Stations is in the final stages of balloting so that manufacturers may be prepared for RPT certification testing that will be required later this summer. In addition, because RPT provides final stage "user experience" test metrics, the Forum has also chosen to use RPT testing to help reduce overall test requirements. Manufacturers incorporating pre-certified "compliant portion" radio modules in their platforms can avoid repetition of many of the conformance and interoperability tests by just performing RPT to verify that the integrity and performance of the device is maintained. Through this approach, not only will overall test time be reduced, but also device manufacturers will be able to better understand the radiated performance of their products and learn to improve them throughout the product lifecycle. ■

References

1. *WiMAX Forum™ Radiated Performance Tests (RPT) for Subscriber and Mobile Stations*, V0.1.0 Draft, WiMAX Forum, Beaverton, OR, December 2007.
2. "Agilent Technologies, ETS-Lindgren Test Equipment Selected by AT4 wireless for Use in First Test Facility for WiMAX™ Radiated Performance Test," www.forbes. com, January 10, 2008.
3. M.D. Foegelle, "Spherical Pattern Measurement Techniques for Low Directivity Antennas," *24th Proceedings of the Antenna Measurement Techniques Association (AMTA 2002)*, Cleveland, OH, pp. 175–180.
4. M.D. Foegelle, "Antenna Pattern Measurement: Concepts and Techniques," Compliance Engineering, *2002 Annual Reference Guide*, Vol. XIX, No. 3, pp. 22–33.
5. M.D. Foegelle, "Antenna Pattern Measurement: Theory and Equations," Compliance Engineering, *2002 Annual Reference Guide*, Vol. XIX, No. 3, pp. 34–43.
6. M.D. Foegelle, "Analysis of Interaction Factors for Active Wireless Devices," *29th Proceedings of the Antenna Measurement Techniques Association (AMTA 2007)*, St. Louis, MO, A07-0014.
7. M.D. Foegelle, "Over-the-Air Performance Testing of Wireless Devices with Multiple Antennas," *RF Design*, February 2006, pp. 44–52.
8. M.D. Foegelle, "OTA Performance Testing of Wireless Devices with Multiple Antennas," *28th Proceedings of the Antenna Measurement Techniques Association (AMTA 2006)*, Austin, TX, A06-0524.

Michael D. Foegelle *is director of technology development at ETS-Lindgren, Cedar Park, TX, and is the editor and principal contributor for the WiMAX Forum™ Radiated Performance Tests (RPT) for Subscriber and Mobile Stations test plan. He received his PhD degree in physics from the University of Texas at Austin, where he performed theoretical and experimental research in both condensed matter physics and electromagnetic compatibility (EMC). In 1994 he began working for EMCO in Austin, TX (now ETS-Lindgren). There he has been integral to the development of products, software and test methods for wireless, RF and EMC testing. He has been involved in numerous national and international standards committees on EMC and wireless, including the ANSI ASC C63 working groups, the CTIA Certification Program Working Group on over-the-air performance testing of wireless devices, the IEEE 802.11 Task Group T for wireless performance prediction of 802.11 devices, the Wi-Fi Alliance Wi-Fi Mobile Convergence Group, the CTIA/Wi-Fi Alliance Converged Wireless Group and the WiMAX Forum's Radiate Performance Test working group. He is co-chair of the CTIA's Converged Devices ad-hoc group and has served as vice-chair of the Wi-Fi Alliance's Wi-Fi/Mobile Convergence group. He has authored or co-authored numerous papers in the areas of electromagnetics, EMC, wireless performance testing and condensed matter physics, and is dedicated to advancing the state-of-the-art in radiated RF testing of emerging wireless technologies.*

ATC's Family of Broadband Capacitor Products

Your Best Broadband Option for Reliability and Widest Frequency Coverage

RoHS Compliant

Attributes

- SMT Broadband Devices
- Ultra-Low Insertion Loss
- Flat Frequency Response
- One Piece Construction
- Orientation Insensitive*
- Tape and Reel, Surface Mountable
- Rugged Ceramic Construction
- RoHS Compliant
- Unit-to-Unit Performance Repeatability

** Except 500 Series*

Applications

- Optoelectronics
- High Speed Data Communications
- SONET – OC192, OC768
- Broadband Microwave / Millimeter-Wave
- Broadband Test Equipment
- Broadband DC Block / Bypass, 40+ GHz

ATC Series	Operating Frequency	Insertion Loss	Capacitance	Voltage Rating (WVDC)	Termination Options
545 L	16 KHz to 40+ GHz	< 0.5dB	100 nF	16 V	Tin, Solder, Gold
530 L	16 KHz to 18 GHz	1dB max.	100 nF	16 V	Tin
520 L	160 KHz to 16 GHz	1dB max.	10 nF	16 V	Tin
500 S	1 GHz to 40 GHz	1dB max.	0.1 pF to 10 pF	0.1 to 4.7 pF: 100 V 5.1 to 10 pF: 50 V	Platinum / Gold

A M E R I C A N   T E C H N I C A L   C E R A M I C S

ATC North America
631-622-4700
sales@atceramics.com

ATC Europe
+46 8 6800410
sales@atceramics-europe.com

ATC Asia
+86-755-8366-4318
sales@atceramics-asia.com

THE ENGINEERS' CHOICE™

w w w . a t c e r a m i c s . c o m

Visit http://mwj.hotims.com/16339-11 or use RS# 11 at www.mwjournal.com/info

LTE Test Mobile

Aeroflex has introduced the TM500 LTE test mobile designed to address the challenges of 3GPP LTE (3G Tong Term Evolution) network infrastructure development test and rollout. The TM500 LTE's extensive Layer 1, Layer 2 and higher layer test features provide complete visibility into even the lowest layers of the radio modem by generating the detailed diagnostic data needed for engineers to verify the required functionality and optimize network operation and performance. The TM500 LTE incorporates test, logging and measurement features at all layers of the protocol. Graphical displays and charts give a visualization of the signal quality and the system status enabling engineers to quickly characterize and isolate problems. It is also possible to override signalling, or even force data corruption, to enable simulation of abnormal conditions in order to test the system response and robustness or expose difficult problems.

Aeroflex Inc.,
Plainview, NY (516) 694-6700,
www.aeroflex.com.

RS No. 216

Surface-mount Test and Measurement

StratEdge has released its SMX Series surface-mount DC to 18 GHz packages for test and measurement, VSAT, point-to-point, point-to-multipoint and WiMAX applications. These power packages have low insertion loss, good return loss and excellent thermal properties. The SMX Series ceramic packages were designed to provide good electrical transition performance for die in the DC to 18 GHz range, although they have been used and performed well in applications beyond 18 GHz. The packages are made to provide wideband electrical performance and incorporate copper composite bases for enhanced thermal dissipation. These are true surface-mount packages that allow automated assembly and soldering for high volume production of devices without sacrificing electrical and thermal performance. They are sealed with cup-shaped liquid crystal polymer lids with B-stage epoxy preforms that are provided with the packages.

StratEdge,
San Diego, CA (858) 569-5000,
www.stratedge.com.

RS No. 217

Current Monitor

Drawing a typical quiescent current less than half that of alternative devices, the ZXCT1041 bidirectional high-side current monitor from Zetex simplifies two-way current measurement in battery and power supply management as well as motor control applications. With a typical Iq specified at just 35 µA, the ZXCT1041 monitors the voltage developed across an external sense resistor and converts it into a single proportional unipolar output voltage. The direction of current flow is indicated by a flag pin, which removes the complication of output offset adjustment inherent in other monitors and simplifies microcontroller interfacing. Provided in the 3.1 mm × 3.0 mm footprint SOT23-5 package and integrating a gain setting resistor achieving an internal gain of 10, the ZXCT1041 presents a highly cost-effective and space efficient solution.

Zetex Inc.,
Hauppauge, NY (631) 360-2222,
www.zetex.com.

RS No. 218

Interferometer Test Optics

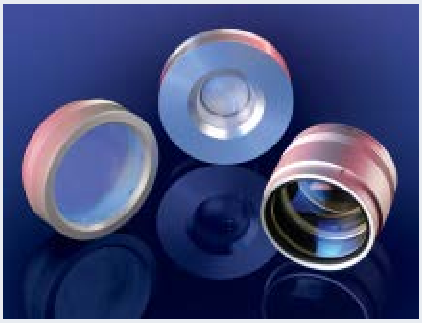

The Melles Griot Optics Group has released additional Fizeau interferometer test optics to complement its Absolute™ Fizeau l/40 transmission sphere product line. The addition of Absolute™ Fizeau l/50 concave and convex reference spheres will allow the user to record and store reference wavefronts for subtraction from interferometric test data, substantially improving their interferometer system's absolute accuracy. Absolute™ Fizeau l/50 transmission flats have been added to the product line to cost effectively increase the absolute accuracy of Zygo® style Fizeau surface and wavefront-testing interferometers to l/50 without the need to store, manipulate, or subtract reference wavefronts during the testing process. New Absolute™ Fizeau l/50 reference flats have also been introduced to support applications requiring reference wavefront subtraction.

Melles Griot Optics Group,
Rochester, NY (585) 244-7220,
www.mellesgriot.com.

RS No. 219

Model Parameter Extraction Software

Agilent Technologies Inc. is shipping its model parameter extraction tool for the advanced PSP complementary metal oxide semiconductor (CMOS) device model. For use with Agilent's Integrated Circuit Characterization and Analysis Program (IC-CAP) software platform, the PSP Model Extraction Package takes advantage of the IC-CAP flexible architecture to accommodate the PSP model, which provides better accuracy than existing BSIM models for designs with very small geometries and helps designers efficiently and accurately model CMOS devices. With Agilent's new PSP Model Extraction Package and IC-CAP, designers can generate complete models based on the most recent version of the Compact Modeling Council's standardized PSP model. The PSP package includes an easy-to-use interface for measurement collection, recommended extraction flows and model implementation. The package has been verified with 65 nm data from prominent CMOS foundries.

Agilent Technologies Inc.,
Santa Clara, CA (800) 829-4444,
www.agilent.com.

RS No. 220

Microwave Design and Analysis Suite

Applied Computational Sciences (ACS) has released a new version of its LINC2 Pro RF and microwave design, synthesis and simulation software suite. Version 2.71 adds user defined equations to the LINC2 simulation control toolset. Equations can include any number and combination of variables and math operations. Equations can be assigned to circuit component parameters so that tuning or optimizing any equation variable will update the component value through the relation defined in the associated equation. The latest edition of LINC2 also offers enhanced schematic capture, including an all new snap-to-grid feature for easy placement and alignment of components on the schematic page. Circuits can be entered manually or created automatically by a number of circuit synthesis modules.

Applied Computational Sciences,
Escondido, CA (760) 612-6988,
www.appliedmicrowave.com.

RS No. 221

Femtocell Reference Design

Manufacturers of WiMAX femtocell access point equipment can now leverage a reference design from Freescale Semiconductor and Sequans Communications that shrinks form factors, lowers costs and streamlines the development of high performance femtocell base station products. The joint solution is delivered on a 165 mm × 135 mm printed circuit board and enables rapid creation of WiMAX femtocell access point products capable of supporting more than 50 simultaneous users. The joint solution's high performance results from the integration of Freescale's PowerQUICC® II Pro MPC8313E processor and Sequans' SQN2130 single-chip Mobile WiMAX 802.16e PHY + MAC ASIC.

Sequans Communications,
Paris, France +33-1-70-72-16-00,
www.sequans.com.

RS No. 222

COMPONENTS

Self-shielding RF Circuits

RF Micro Devices Inc. (RFMD) has introduced a new self-shielding technology for RF circuits. RFMD's self-shielding technology is designed to eliminate the need for custom external shields by integrating RF shielding into the RFIC or module. This reduces the volume required for RF sections by approximately 30 to 50 percent and provides customers with RF components that are not sensitive to board placement. RFMD's self shielding technology is applicable to any RFMD product and will be available first in RFMD's POLARIS 3 TOTAL RADIO solution.

RF Micro Devices Inc.,
Greensboro, NC (336) 664-1233,
www.rfmd.com.

RS No. 223

Antenna Tuning Switch

Peregrine Semiconductor Corp. released the UltraCMOS™ PE42641 SP4T antenna tuning switch delivering IMD performance of –110 dBm, making it ideal for converged designs requiring high linearity and low distortion. The UltraCMOS™ silicon-on-sapphire-based PE42641 incorporates Peregrine's HaRP™ technology enhancements to deliver exceptional harmonic results, linearity and overall RF performance: high linearity of +68 dBm IP3 or –110 dBm IMD; harmonics better than –80 dBc, low insertion loss of 0.5 dB (typical); high isolation of 35 dB at critical paths; and complete monolithic integration. Additionally, the new switch offers Class 2 ESD (2 kV HBM) on all pins, and Class 3 (4 kV HBM) at the antenna.

Peregrine Semiconductor Corp.,
San Diego, CA (858) 731-9400,
www.peregrine-semi.com.

RS No. 224

WiMAX Cavity Duplexer

Networks International Corp. (NIC) introduced a new 3.5 GHz cavity duplexer designed for use in WiMAX applications. The duplexer features mutual isolation of greater than 70 dB and a passband insertion loss of 1.5 dB max. The duplexer operates within specification between –40° to +90°C and is available in a profile of 4.0 × 3.0 × 1.1 in. Custom designs are available.

Networks International Corp.,
Overland Park, KS (913) 685-3400,
www.nickc.com.

RS No. 226

Aerospace-grade Fiber-optic Cable

Tensolite introduced its LITEflight™ EP (enhanced performance) family of aerospace-grade fiber-optic cables. The new LITEflight™ EP series provides all the performance and benefits of its predecessor necessary to function in the harsh environments of aerospace and military applications but with lower loss, tighter bend radius, improved thermal stability and better handling during termination and installation. LITEflight™ EP is available in multiple sizes, configurations and temperature ratings to 260°C in order to meet numerous application requirements.

Tensolite Co.,
St. Augustine, FL (800) 458-9960,
www.tensolite.com.

RS No. 227

12-bit ADC

Linear Technology Corp. introduced the LTC2309, a 12-bit analog-to-digital converter (ADC) that communicates via an I2C-compatible two-wire interface with 14 ksps throughput rate. This flexible ADC features an eight-channel integrated multiplexer to measure eight single-ended input channels, four differential channels, or combinations of both. The input channels are software selectable for unipolar or bipolar ranges. Operating from a single 5 V supply, the LTC2309 draws just 1.5 mW at a 1 ksps throughput rate and only 35 µW in shutdown mode. Packaged in a tiny 4 × 4 mm QFN-24 with internal reference, the LTC2309 is a great fit for portable instrumentation and space-constrained designs using I2C. The LTC2309 achieves excellent DC specifications when measuring unipolar or bipolar input signals, including ±1LSB INL and DNL, ±6LSB (max) zero-scale error and ±6LSB (max) full-scale error. The LTC2309 also excels when digitizing AC input signals, measuring 73 dB SINAD and –88 dB THD at 1 kHz.

Linear Technology Corp.,
Milpitas, CA (408) 432-1900,
www.linear.com.

RS No. 228

Simplex Fiber Switch

Electro Standards Laboratories (ESL) has introduced its new QuickSwitchÒ Model 4294 four-way all-optic simplex fiber switch with threaded FC connectors, 100/140 graded index fiber, UPC. This QuickSwitch features optical scalability. The M4294 is bit-rate and data transparent and service/protocol transparent. This switch has switch position memory. When power is lost, the switch automatically changes to its default position and will continue to pass data. QuickSwitchÒ 4294 remotely controllable FC simplex A/B/C/D switch is designed with fiber optic mirror technology. The Model 4294 allows a fiber optic device connected to the unit's FC simplex COMMON connector to access any of the four fiber optic networks connected to the A, B, C, or D ports. Switch position can be changed via front-panel pushbuttons, or from an RS232 Serial Remote Port located on the rear panel.

Electro Standards Laboratories,
Cranston, RI (401) 943-1164,
www.electrostandards.com.

RS No. 229

ESD/EMI Modules

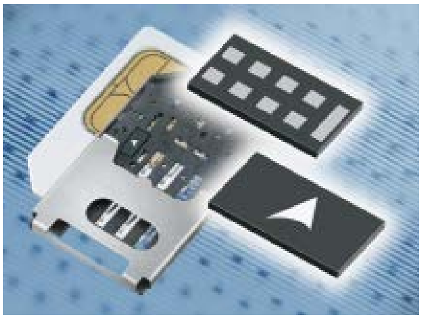

EPCOS has developed the CeraDiode(r) CDA6 array series for the ESD protection of two USB 2.0 ports. In addition to protecting the two or four data lines, it also shields the supply voltage against overvoltages. The ESD protection satisfies Level 4 of IEC 61000-4-2. Unlike conventional TVS diodes, the protection is effective against both positive and negative voltages. The 1012 package as well as the configuration of the pads enable the array to replace the more expensive SOT23-6L diode solutions with no redesign of the circuit board. The CeraDiode solution also offers a better thermal response than the semiconductor-based designs. The array is suited for operating voltages up to 5.6 VDC. In addition to an extremely low response time of less than 0.5 ns, it features a low parasitic capacitance of only 5 pF (typical), so that no significant signal distortion or attenuation occurs even at high data rates.

EPCOS Inc.,
Iselin, NJ (732) 906-4386,
www.epcos.com.

RS No. 230

Coaxial Relay

RelComm Technologies Inc. has introduced a new high power 1P2T failsafe coaxial relay with side-launched connectors. This robust device incorporates type N connectors and is enhanced throughout with low loss, high temperature dielectrics. The side-launch connector configuration adds versatility for system layout, particularly when cabling into through-panel applications. Performance is rated to 3 GHz VSWR 1.20:1 maximum, insertion loss 0.20 dB maximum and isolation better than –60 dB. Power handling is rated 1 kW at 1 GHz and 650 W at 3 GHz. This device includes auxiliary position indicators.

RelComm Technologies Inc.,
Salisbury, MD (410) 749-4488,
www.relcommtech.com.

RS No. 225

WiFi/WLAN Internal Antenna

Ethertronics introduced its third-generation quad-band WiFi/WLAN internal antenna solu-

tion. Designed to operate on 2.4, 4.9, 5.2 and 5.8 GHz spectrum bands (also known as 802.11a/b/g/n+), this robust antenna is ideal for integration into a variety of devices including mobile phones, notebook computers, industrial handhelds and access points. Ethertronics' WiFi/WLAN quad-band antenna is based on the company's patented Isolated Magnetic Dipole (IMD) technology, allowing for quicker time to market, minimizing antenna size without degrading performance, optimizing antenna patterns and operating characteristics without being effected by surrounding component placement and supporting high volume manufacturing processes by being surface mountable and fully compliant with the European RoHS directive 2002/95/EC.

Ethertronics Inc.,
San Diego, CA (858) 550-3820,
www.ethertronics.com.

RS No. 231

AMPLIFIERS

High-power Amplifiers

Amplical Corp. has announced the availability of a new family of broadband maximally flat high power amplifiers designed with MMIC technology, resulting in an economical and reliable solution. The model AMP800G2.5-23-35 is an 800 MHz to 2.5 GHz amplifier that features 23 dB gain with gain flatness better than ±1.25 dB. The amplifier outputs at least 2 W of power. Current draw is 650 mA from +24 V. Connectors are SMA (f) and delivery is typically from stock. Other models are available that feature additional gain, different input voltages and frequency ranges.

Amplical Corp.,
Verona, NJ (201) 919-2088,
www.amplical.com.

RS No. 235

50 W 700 to 800 MHz SSPA

Stealth Microwave introduced the SM07080-47, a GaAsFET amplifier designed for next-generation 700 MHz applications. The unit operates from 700 to 800 MHz with a P1dB of +47 dBm (min.). Small-signal gain is 55 dB with a flatness of ±0.5 dB across the band. Standard features include thermal protection with auto reset and over/reverse voltage protection. Optional features include TTL on/off, RF sampling and high speed switching up to 1 µs. In module form, the unit measures 7.5 × 3.97 × 0.79 in.

Stealth Microwave Inc.
Trenton, NJ (609) 538-8586,
www.stealthmicrowave.com.

RS No. 232

Solid-state Power Amplifier Drivers

MITEQ introduced a new line of linear SSPA drivers. Three models cover all of the common satellite communication bands: AMFLD-05700850-60-16P for C-/X-band, AMFLD-12501850-60-18P for Ku-/DBS-band and AMFLD-27003100-60-12P for Ka-band. All three models have a common outline of 3.7 × 2.5 × 0.73 in., SMA connectors for RF I/O and a multi-pin connector for supply, controls and detector output. The linear drivers have a typical gain of 25 dB flat to within 1 dB, P1dB of 16 dBm and output IP3 of 26 dBm. Power monitor DC output and gain are well compensated, allowing for a compliant temperature range of –25° to +80°C. Also incorporated is 30 dB of linear gain control. Drivers have a noise figure of less than 6 dB and operate from a single 15 V supply and draw 400 mA (typical).

MITEQ,
Hauppauge, NY (631) 439-9220,
www.miteq.com.

RS No. 233

Low-noise Amplifier

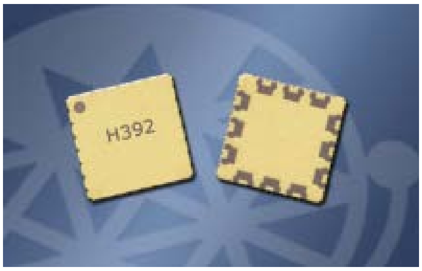

Hittite Microwave Corp. released a hermetically packaged SMT GaAs MMIC low-noise amplifier for use in microwave radio, military and space applications from 3.5 to 7 GHz. The HMC392LH5 is a hermetic SMT LNA that provides 15 dB of gain, while contributing only 2.5 dB of noise figure over the frequency range of 3.5 to 7 GHz. The amplifier provides excellent output IP3 performance of +24 dBm as well as an output P1dB of +14 dBm. In addition to the flexibility of selecting six possible bias options that allow the user to choose the desired bias point and output power, the amplifier's I/Os are internally matched to 50 ohms and DC blocked for robust wideband performance. The HMC392LH5 MMIC LNA is housed in a hermetic RoHS-compliant, 5 × 5

mm leadless SMT package, and consumes typically 43 mA of current from a single +5 V supply.
Hittite Microwave Corp.,
Chelmsford, MA (978) 250-3343, www.hittite.com.
RS No. 234

MMIC Amplifiers

M/A-COM, a business unit of Tyco Electronics, introduced two new HBT MMIC amplifiers. The MAAM-007865-0P1R00 and the MAAM-007866-0P1R00 exhibit exceptional broadband frequency performance using only a single application circuit to cover frequency bands from 50 MHz to 2000 MHz, and 50 MHz to 3300 MHz, respectively. The MAAM-007865-0P1R00 is designed to have 20 dB gain with ±1.2 dB flatness across the frequency band. The P1dB level is 18 dBm and output IP3 is 29 dBm. The MAAM-007866 is a two-stage device designed to have 27 dB gain with ±1.2 dB flatness across the frequency band. The P1dB level is 22.5 dBm and ouput IP3 is 34 dBm. The design of the MAAM-007865-0P1R00 and MAAM-007866-0P1R00 incorporates an on-chip active bias network, reducing the number of off-board components thus easing application implementation. Both amplifiers require a single bias supply of +5 V, with a +5 V reference pin for power-down and power control capability. Each model is available in a 3 mm 12 lead PQFN package and assemblies are RoHS-compliant.
Tyco Electronics, M/A-COM Products,
Lowell, MA (800) 366-2266, www. tycoelectronics.com.
RS No. 236

SOURCES

Voltage-controlled Oscillator

Z-Communications Inc. has released its new lead-free, RoHS-compliant voltage-controlled oscillator in S-band (2280 to 2450 MHz) for fixed

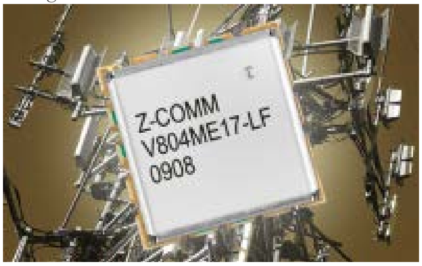

wireless applications. The V804ME17-LF offers an ultra-low phase noise performance of –95 dBc/Hz at 10 kHz offset (typical). It provides an average tuning sensitivity of 98 MHz/V and excellent typical harmonic suppression of –20 dBc over the extended operating temperature range of –40° to 85°C. It covers the entire bandwidth between 0.5 to 4.5 V, at DC supply voltage of 5 V drawing 20 mA (typical). The V804ME17-LF comes in ZCOMM's industry-standard MINI package measuring 0.50 in. × 0.50 in. × 0.13 in.
Z-Communications Inc.,
San Diego, CA (858) 621-2700, www.zcomm.com.
RS No. 237

Temperature-compensated Crystal Oscillator

Vectron International has released its smallest temperature-compensated crystal oscillator (TCXO) to date. The new VTM3 TCXO offers simi-

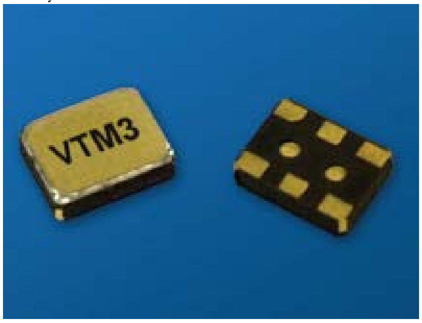

lar phase noise performance to Vectron's proven VTC4 and VTC1 TCXOs in a 50 percent smaller package (3.2 mm × 2.5 mm), enabling customers in the communications, industrial, test and military markets to benefit from the flexibility of a smaller, lower power oscillator without compromising the tight stability and superb phase noise performance they have come to expect from Vectron TCXOs. The VTM3 offers a phase noise floor of

–155 dBc/Hz) while providing enhanced frequency stabilization in an expanded temperature range (enabling the stabilization of frequencies between 8 to 45 MHz in a temperature range of –30° to 80°C at better than 0.5 ppm).
Vectron International,
Hudson, NH (603) 598-0070, www.vectron.com.

RS No. 238

Single OCXO

MtronPTI introduced its XO5120 Series OCXO, an industry standard 1 × 1.4 in. single OCXO. The XO5120 Series offers excellent phase noise capabilities at –155 dBc performance at 10 kHz offset at 10 MHz nominal frequency. This series also provides ±2 ppb stability performance over commercial temperatures and ±3 ppb over industrial temperatures. Applications include microwave radios, base stations and test and measurement equipment. With its stability performance, it can replace double OCXOs in some applications.
MtronPTI,
Yankton, SD (605) 665-9321, www.mtronpti.com.

RS No. 239

Temperature-compensated Voltage-controlled Crystal Oscillator

Bliley Technologies Inc. has introduced its TV79B temperature-compensated voltage-controlled crystal oscillator (TCVCXO). Fully RoHS-compliant, Bliley's low-profile DIP TCVCXO enables cost reductions for many communication and other applications, including cellular base stations and telephony, test and other electronic equipment. Product specifications for Bliley's TV79B TCVCXO include: ±0.28 ppm frequency stability over temperature; ±4.6 ppm frequency stability over all conditions (20 years of aging); standard footprint DIP package with an industry leading 0.3 in. height or several other package heights; 0.625 to 52 MHz operating frequency range; optional voltage-controlled frequency tuning; up to –40° to +85°C operating temperature range; CMOS, sine, clipped sine or TTL output options and 3.3, 5.0, 12.0 or 15.0 V supply options.
Bliley Technologies Inc.,
Erie, PA (814) 838-3571, www.bliley.com.

RS No. 240

SUBSYSTEMS

FCC Category B Antenna

Radio Waves Inc. has announced a new low profile high performance 2' antenna for FCC Catergory B applications in the 11 GHz microwave band. The new HPLP2-11 offers 34 dBi of gain in a low profile package that is the smallest FCC Category B antenna available on the market. The new HPLP2-11 has a shroud that is only 4 in. deep and has a diameter of 24.5 in. The new HPLP2-11 is FCC Category B compliant and use Radio Waves' exclusive hybrid-cassegrain feed system for optimal efficiency. The new HPLP2-11 can be developed with a mounting system to directly integrate to an OEM manufacturer's radio or outdoor unit.

Radio Waves Inc.,
N. Billerica, MA (978) 459-8800, www.radiowavesinc.com.

RS No. 241

We're Driven!
The same things that drive you, drive us. We're passionate about finding new ways to help our customers be more productive. To make testing faster, easier, and more accurate. To make equipment more reliable and more cost-effective. To be ready for the future, today.
Building Blocks! That's The Idea Behind Our Subampability™ Concept!
We're building amplifiers that can grow as your needs change. When you need a more powerful amp, you simply add the power instead of tossing out the old amplifier. Smart!
Adaptable, Constantly Changing.
The TGAR system, for automotive transient immunity testing, is so flexible it can handle most existing specs … and most new ones as they emerge.
Survival Of The Fittest.
AR amps stand up to the toughest conditions with infinite VSWR tolerance. You get every watt of power, every time.
Powerhouse!
When it comes to power and reliability, those who know come to AR. For amplifiers like the 10000A250A, with 10,000 watts of power, 6:1 VSWR tolerance, and a frequency range of 100 kHz - 250 MHz.
Our Conducted Immunity Test Systems Stand Alone!
The CI self-contained RF Conducted Immunity Test Systems have no equals. For ease of use, accuracy, flexibility, reliability, or any features that really matter. Testing to CE, MIL and Auto Standards.
Safe Bet!
AR's highly-advanced Starprobe® laser probes have 3 levels of safety to protect your equipment and the reliability of your data. AR battery and laser probes cover 5 kHz to 60 GHz.
Radiant Arrows.
Our unique "bent element" Radiant Arrows are about 60% smaller than standard log periodic antennas. They produce high fields even in the toughest applications.
We've Seen The Future. And We're In It.
No one knows exactly what's next in EMC and Wireless testing. But AR will always be several steps ahead, with the amps and accessories that meet the changing needs.
Your Test Is Only As Good As The Sum Of Its Parts.
It doesn't make sense to compromise the quality of AR amplifiers with inferior parts. AR offers accessories that are power and frequency matched to our amps.
Get Ready For The Next Wave In EMI Receivers.
The CER2018 Receiver is a complete EMI test solution with continuous coverage from 20 Hz to 18 GHz and expendability to 110 GHz. To ensure accuracy, it self-calibrates on demand at every frequency scan.
AR Modular RF Is A Leading Supplier Of Booster Amplifiers For Tactical Military Radios.
Our battle-tested booster amplifiers cover the broadest frequencies and wave forms and are compatible with virtually every transceiver. We're also supplying some of the most high efficiency modules for jamming applications.
A Wide Range of Modules and Amplifier Systems.
AR Modular RF not only offers modules and rack mounted amplifiers from 10 kHz to 6 GHz (with power that goes from watts to kilowatts), we also provide customer-specific designs and modifications of our products to meet the most demanding requirements.
WOW!
AR Systems like the AS40000 Radiated Immunity Test System can perform entire tests with just the press of a few buttons … and with unmatched accuracy and reliability.
One Company, Infinite Solutions
ar®
rf/microwave instrumentation • modular rf • receiver systems • ar europe
USA 215-723-8181. For an applications engineer, call 800-933-8181.
Visit http://mwj.hotims.com/16339-17 or use RS# 17 at www.mwjournal.com/info
In Europe, call ar emv United Kingdom 441-908-282766 • ar emv France 33 -1-47-91-75-30 • emv Germany 89-614-1710 • emv Netherlands 31-172-423-000
Copyright© 2008 AR. The orange stripe on AR products is Reg. U.S. Pat. & TM. Off.

S-band Radar Amplifier

Aethercomm Model Number SSPA 3.1-3.5-1500-RM is a high power, pulsed RF amplifier that operates from 3.1 to 3.5 GHz in a rack-mounted configuration. It will also operate down to 3.0 GHz if requested. The amplifier is packaged in a 3u high, 19 in. rack mounted enclosure with multiple fans that form the internal thermal management system. It has a typical peak output power of 2000 W at a 5 percent duty cycle with a 64 µs pulse width. The SSPA 3.1-3.5-1500-RM offers a typical saturated gain of 55 dB with a typical power flatness of ±1.0dB. Input and output VSWR is 1.5:1 maximum and it operates from 220 VAC with a universal input transformer that will operate at 208 VAC also. There is a forward power RF sample port along with an output forward voltage pulse available. The output is fully protected from an infinite VSWR at the RF output port. The input RF connector is SMA Female. The output RF connector is a type N female. The amplifier has a rise time of 100 ns typical and a 20 ns fall time. Output spurious emissions are < –65 dBc.

Aethercomm Inc.,
San Marcos, CA (760) 598-4340, www.aethercomm.com.

RS No. 242

Narrowband RF Module

Radiocrafts AS has expanded its product line with a high power narrowband RF module for the European market. The RC1280HP, offering up to 500 mW output power for increased range, is based on the RC1280 RF transceiver module for FSK operation with embedded protocol. When used with quarter-wave antennas, a line-of-sight range of 5 to 6 km can be achieved. The new RC1280HP module uses the same protocol and channels as the RC1280. Interoperation between RC1280 and RC1280HP is therefore possible in a network with both long- and shorter range modules. The module is pre-certified and CE marked for operation under the European radio regulations for license-free use in the 868 MHz band, operating in three channels in the sub-band at 869.400 to 869.650 MHz. The new module measure only 19.5 × 60.5 × 6.0 mm, and comes in a DIL-style package with 2.00 mm pin pitch made for low profile board-to-board connection.

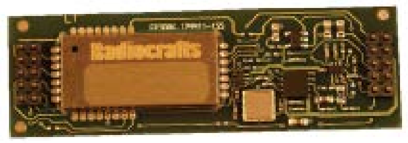

Radiocrafts AS,
Oslo, Norway (+47) 4000 5195, www.radiocrafts.com.

RS No. 243

ZigBee Tranceiver

AeroComm Inc. enhanced its ZB2430 transceiver line to feature output power, receive sensitivity and line-of-sight range up to three miles. Based on the Texas Instruments 802.15.4 System-on-Chip and Z-Stack™ technology, ZB2430 targets secure, low power, mesh network applications. It communicates in the 2.4 GHz ISM band, making it ideal for OEMs preferring to standardize on one global platform for their end product

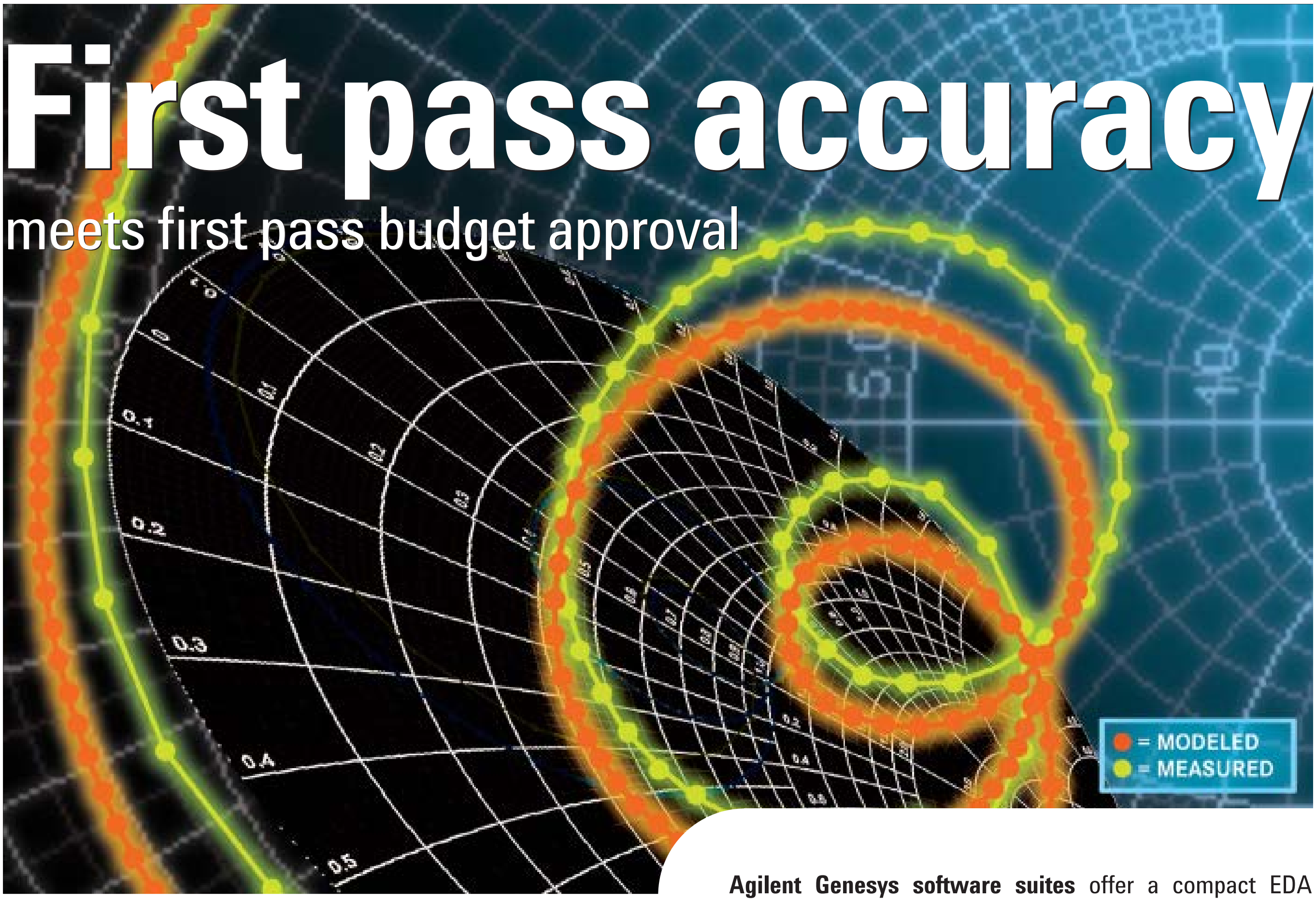

Agilent Genesys software suites offer a compact EDA environment for your specific RF and microwave physical design – at about half the price of our competitors. Each suite is customized to feature only the applications you need. And with Momentum GX, our newly integrated accurate planar EM simulator, you can test designs before they're even built.

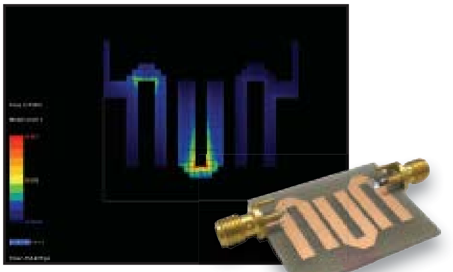

Momentum GX EM simulation of a DUT, just part of the new capabilities of Genesys

Four Agilent Genesys suites under $10k

- *Core* *$3,995**
- *Nonlinear Pro* *$9,995**
- *Comms Pro* *$9,995**
- *Designer Pro* *$9,995**

See for yourself. Download a 30-day free trial at **www.agilent.com/find/eesof-genesys-firstpass** or call an Agilent representative to find out which Genesys suite is best for you. With fully functional, microwave design environments starting at just $3,995, first pass success is suddenly within reach.

u.s. 1-800-829-4444
canada 1-877-894-4414

Download a free 30-day trial at

www.agilent.com/find/eesof-genesys-firstpass

Agilent Technologies

Visit http://mwj.hotims.com/16339-9 or use RS# 9 at www.mwjournal.com/info

needs. Modules are offered as either coordinators and routers or end-devices. Network scan, auto-configuration, dynamic routing, discovery and security enable the mesh network, delivering reliable redundancy, secure multi-communication nodes and long range performance. Embedded flash memory of 128 KB provides room for larger, more complex application profiles.

AeroComm Inc., Lenexa, KS (913) 492-2320, www.aerocomm.com.

RS No. 244

Bonder Upgrade Software

Palomar Technologies has released bonder performance upgrade packages for its CBT6000 and Model 8000 automatic wire bonders and the Model 3500 component placement work cell. The upgrade packages include the latest operating software, improved vision systems for pattern recognition and new features like Bond Data Miner (BDM). BDM, included in Palomar's current bonder models, is a software package that monitors machine and process trends to provide increased yields and predictive maintenance. Bond Data Miner can track and archive traceability data for each part, die, wire and bond; automatically adapt its process parameters to address lot to lot and/or part variations; capture and analyze process and machine trends to optimize yield; and report its own uptime and statistics to any computer in the world.

Palomar Technologies Inc., Carlsbad, CA (760) 931-3600, www.bonders.com.

RS No. 245

MICROWAVES ON MY MIND
ATLANTA
IMS 2008
INTERNATIONAL MICROWAVE SYMPOSIUM
June 15–20, 2008

The International Microwave Symposium is the headline conference of the IEEE Microwave Theory and Techniques Society (MTT-S). This will be the largest technical Conference to be held in Atlanta in the next two years and will feature a large trade show as well as a wide variety of technical papers and workshops. The IEEE MTT-S International Microwave Symposium 2008 (IMS2008) will be held in Atlanta, GA, Sunday, June 15 through Friday, June 20, 2008, as the premiere event of Microwave Week 2008.

Microwave Week 2008: The IMS 2008 technical sessions will run from Tuesday through Thursday of Microwave Week. Workshops will be held on Sunday, Monday and Friday. In addition to IMS2008, a microwave exhibition, a historical exhibit and the RFIC Symposium (www.rfic2008.org) will also be held in Atlanta during Microwave Week 2008.

NEW LITERATURE

RF TEST PROBES

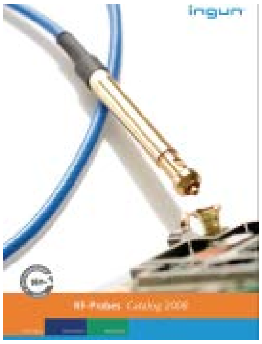

The new RF Test Probe catalog from Ingun Prüfmittelbau GmbH Germany is a unique and timesaving reference manual and therefore a global innovation on the radio-frequency market. The plug/jack register guides you to the recommended RF test probe for your application. With just one step, you can find the matching solution. The catalog shows the special variants and the application versatility of INGUN RF Test Probes for 2, 4 and 6 GHz applications.

Ingun Pruefmittelbau GmbH,
Konstanz, Germany +49 7531 8105-62,
www.ingun.com.

RS No. 200

FREQUENCY CONTROLS

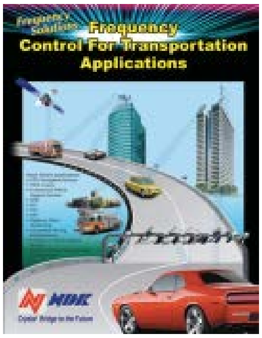

Nihon Dempa Kogyo Co. Ltd. (NDK) has developed a new four-page color brochure highlighting its frequency control products for these applications. The brochure reviews in-vehicle and telematic applications. NDK's transportation components have proven to deliver excellent performance in the harshest of applications. Products covered in the brochure include crystals, TCXOs and XOs.

Nihon Dempa Kogyo Co. Ltd.,
Tokyo, Japan +81-3-5453-6771,
www.ndk.com.

RS No. 201

SATCOM FILTERS & COMPONENTS

Microwave Filter Co. introduces the latest addition to its industry-specific publications. The new "SatCom Filters & Components Catalog" provides a comprehensive listing of C, Ku, X, K and Ka-band filters and components offered by the company. Over the past 40 years, MFC has designed and manufactured a wide variety of filters for commercial and military applications.

Microwave Filter Co.,
East Syracuse, NY (315) 438-4700,
www.microwavefilter.com.

RS No. 202

EMI/RFI COMPONENTS

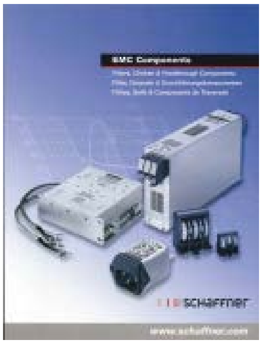

Schaffner EMC has a catalog featuring its complete line of filters, chokes and feedthrough components. The 240-page catalog extensively details Schaffner's wide range of RFI suppression chokes, and filters, such as PCB filters, IEC inlet filters, single-phase filters, feedthrough capacitators and filters, three-phase filters, as well as the company's power control products. Each section contains general information as well as photos, diagrams, selection tables, specifications, insertion loss charts, mechanical data and electrical schematics for individual products.

Schaffner EMC Inc.,
Edison, NJ (732) 225-9533,
www.schaffnerusa.com.

RS No. 203

BOOK OF KNOWLEDGE

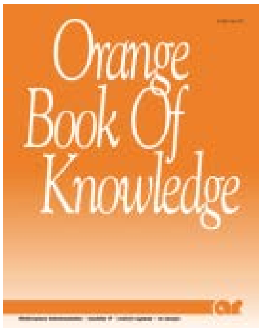

The AR Orange Book of Knowledge contains articles and application notes on a wide range of topics and applications, from the importance of mismatch capability to testing beyond specs, and everything in between. The book represents the cumulative knowledge of all AR companies, making it perhaps the most comprehensive resource in the industry.

AR RF/Microwave Instrumentation,
Souderton, PA (215) 723-8181,
www.ar-worldwide.com.

RS No. 204

OVERSTOCKED COMPONENTS

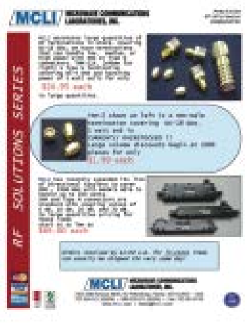

MCLI has compiled a quick-reference brochure, highlighting all of its currently overstocked items. These are items that are available for immediate delivery and due to their over-stocked status, pricing has been greatly discounted. Orders received before 11:00 AM EST can usually be shipped the very same day.

Microwave Communications Laboratories Inc.,
St. Petersburg, FL (727) 344-6254,
www.mcli.com.

RS No. 205

High Power Caseless 90° Couplers

Stock To 30 Day Delivery

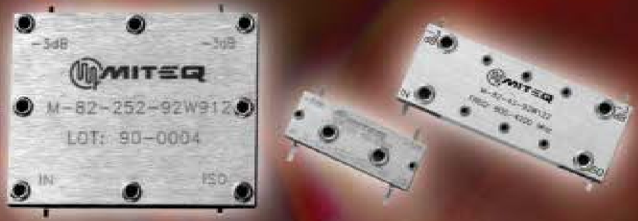

FREQUENCY (MHz)	MODEL NUMBER	AVERAGE POWER (CW Watts)	AMPLITUDE BALANCE (±dB, Max.)	PHASE BALANCE (±Deg., Max.)	ISOLATION (dB Min./Typ.)	INSERTION LOSS (dB, Max.)	VSWR (Max.)
50 – 110	M-51-111-96W802	600	0.3	2.0	20/23	0.30	1.2:1
100 – 500	M-12-52-92W502	200	0.85	2.5	14/18	0.85	1.35:1
100 – 500	M-12-52-98WF502	800	0.8	2.0	18/20	0.30	1.2:1
120 – 230*	M-121-231-92W012	300	0.5	2.0	20/27	0.30	1.2:1
150 – 250	M-151-251-94W012	400	0.3	2.0	20/25	0.30	1.2:1
200 – 400*	M-22-42-92W102	250	0.5	2.0	20/25	0.30	1.2:1
200 – 400	M-22-42-95WB302	500	0.4	2.0	19/23	0.25	1.2:1
200 – 1000*	M-22-13-92WD502	250	0.75	3.0	20/23	0.50	1.3:1
250 – 500	M-251-52-92W102	250	0.5	2.0	20/25	0.30	1.2:1
300 – 500	M-32-52-92W102	250	0.4	2.0	20/23	0.25	1.2:1
300 – 950	M-32-951-92W102	250	0.6	2.0	20/23	0.25	1.25:1
400 – 550	M-42-551-92W102	250	0.2	2.0	20/25	0.20	1.2:1
400 – 700	M-42-72-92W012	250	0.5	2.0	20/25	0.30	1.2:1
400 – 1000*	M-42-13-92W102	250	0.6	2.0	18/20	0.25	1.2:1
400 – 1000	M-42-13-95WB302	500	0.6	2.0	20/23	0.20	1.2:1
400 – 1000	M-42-13-91KW402	1000	0.6	2.0	20/25	0.20	1.2:1
440 – 880	M-441-881-92W102	250	0.5	2.0	20/25	0.20	1.2:1
700 – 1400*	M-72-142-92W102	250	0.5	2.0	18/25	0.30	1.25:1
800 – 1600	M-82-162-92W102	250	0.5	2.0	20/23	0.25	1.2:1
800 – 1600	M-82-162-95WB302	500	0.5	2.0	20/25	0.20	1.25:1
800 – 1600	M-82-162-91KWB912	1000	0.5	2.0	20/25	0.20	1.3:1
800 – 2500*	M-82-252-92W122	200	0.6	4.0	18/20	0.40	1.25:1
800 – 4200	M-82-43-92W122	200	0.5	4.0	16/20	0.20	1.2:1
960 – 1220	M-961-1221-92W102	200	0.3	2.0	18/25	0.30	1.25:1
960 – 1220	M-961-1221-95WB302	500	0.4	2.0	20/23	0.20	1.2:1
1000 – 2000	M-13-23-92W102	200	0.5	3.0	18/24	0.30	1.25:1
1000 – 2000	M-13-23-95WB302	500	0.5	3.0	18/22	0.20	1.2:1
1200 – 1400	M-122-142-92W102	250	0.4	3.0	20/23	0.25	1.2:1
1200 – 1400	M-122-142-95WB302	500	0.4	2.0	20/25	0.20	1.2:1
1300 – 3000	M-132-33-92W102	200	0.6	3.0	18/23	0.25	1.2:1
1400 – 2400	M-142-242-92W102	200	0.5	3.0	16/20	0.25	1.2:1
1400 – 2800	M-142-282-92W102	200	0.5	3.0	16/20	0.25	1.2:1
1500 – 3000	M-152-33-92W102	200	0.6	3.0	18/22	0.25	1.25:1
1700 – 2500	M-172-252-92W102	200	0.4	3.0	20/23	0.25	1.2:1

* Multiple packages are available on these models, please contact MITEQ.180 degree and coaxial versions are available upon request

For additional information or technical support, please contact our Sales Department at (631) 439-9220 or e-mail components@miteq.com

3 YEAR WARRANTY

MITEQ

100 Davids Drive, Hauppauge, NY 11788
(631) 436-7400 FAX: (631) 436-7430
www.miteq.com

Fundamentals of Vector Network Analysis

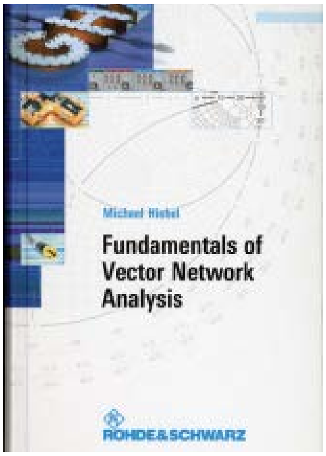

Michael Hiebel
Rohde & Schwarz • 419 pages; €68
ISBN: 978-3-939837-06-0

This book is ideal for beginners in the field of network analysis and supplements the highly specific information provided in operating manuals, application notes and academic papers. It can also serve as a reference book for experts. With this purpose in mind, important terminology has been highlighted in bold print and information has been listed in tabular form where possible. Chapter 1 describes a network analyzer, the most complex and versatile piece of test equipment in the field of RF engineering. Chapter 2 is devoted to the design of a heterodyne N-port network analyzer. Measurement accuracy and calibration is the subject of Chapter 3. Chapter 4 covers some typical measurements that fall under the category of linear measurements. Chapter 5 discusses the fundamental concepts behind time-domain analysis and shows its relation to frequency-domain analysis, with examples of time-domain measurements described in Chapter 6. Nonlinearity means that ratios such as the S-parameter or the reflection coefficient depend on the applied stimulus level. Nonlinear measurements are explained in Chapter 7. Mixers are components that are used primarily to handle frequency conversion. Chapter 8 discusses the basic principle of a mixer along with the relevant signals and their parameters as well as mixer measurements. Antenna and radar cross-section measurements are the subject of Chapter 9. The author suggests reading Chapter 1 as an introduction. If information on how to perform a specific measurement task is required, Chapters 4, 6, 7 and 8 should be read. If how the instruments are designed and function is sought, Chapter 2 should be read. Chapter 3 should be read to select the right calibration method for the task considered or optimize the accuracy of the test setup.

To order this book, contact:
Rohde & Schwarz
GmbH & Co. KG
Mühldorfstrasse 15
81671 München, Germany

Adaptive Antennas and Phased Arrays for Radar and Communications

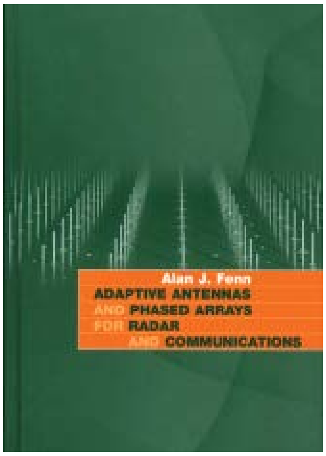

Alan J. Fenn
Artech House • 416 pages; $139, £77
ISBN: 978-1-59693-273-9

Adaptive antennas and phased arrays, with rapidly scanned beams or multiple beams, are commonly suggested for radar and communication systems in ground-based, airborne and spaceborne applications that must function in the presence of jamming and other sources of interference. The book starts with a discussion of the fundamentals of adaptive antennas pertaining to radar and communication systems, with an emphasis on consumption of adaptive array degrees of freedom from the jammer's viewpoint. Displaced phase center antenna array mutual coupling effects in the problem of adaptive suppression of radar clutter is discussed in Chapter 2. Next, in Chapters 3 through 5, a theoretical foundation for a focused near-field technique that can be used to quantify the far-field adaptive nulling performance of a large aperture adaptive phased-array system is described. Experimental testing of the focused near-field adaptive nulling technique for phased arrays is described in Chapter 6. An experimental high-resolution multiple-beam adaptive-nulling antenna system is described in Chapter 7. Chapter 8 provides an introduction to phased-array theory. In Chapter 9, finite and infinite array analyses and measurements for periodic phased arrays of monopole elements are presented. Chapter 10 describes the focused near-field polarization characteristics of monopole phased arrays. Chapter 11 describes a test bed phased array that implements the displaced phase center antenna technique. The planar near-field scanning method for measuring low-sidelobe radiation patterns of phased arrays is described in Chapter 12. Experimental arrays of horizontally polarized loop-fed slotted cylinder antennas (Chapter 13), dual-polarized dipole arrays (Chapter 14) and ultra-wideband dipole arrays (Chapter 15) are described. In Chapter 16, rectangular waveguide arrays are analyzed.

To order this book, contact:
Artech House
685 Canton St.
Norwood, MA 02062
(781) 769-9750 ext. 4030; or
46 Gillingham St.
London SW1V 1HH, UK
+44 (0) 207-8750

Career Corner

Impact of Technology Trends on the Microwave Engineer Job Market

Globalization and the emergence of commercial applications relying on electromagnetic science and technologies are increasing the demand for related microwave engineering skills. The mention of "Silicon Valley becoming a wireless industry hot spot" among the "top 10 wireless trends for 2008" published on CNNMoney.com supports this statement. More supporting evidence can be concluded from the growing number of standards and associations (e.g. CTIA, WiFi, Wimax, Bluetooth, etc.), each developing its regulatory base, technology and test disciplines.

Today's RF engineers can choose between exciting career paths in any of the "traditional" and "new" industries. Among the examples are the automotive industry, which long ago shifted gears into the electromagnetic age, wireless communications introducing new applications and standards, and RF tagging technologies revolutionizing storage and trade of goods. These are only a few examples. The typical antenna engineer before the mid-1990s would most likely develop a long and stable career with one of the defense/aerospace contractors, government agencies or somewhere along that food chain. Commercialization of wireless technologies across global markets and availability of inexpensive test and measurement setups and CAD tools open up endless opportunities. Even low-budgeted startups can offer technically challenging positions. Today's antenna/microwave graduates can choose between industries and disciplines that are substantially different in the technology challenges, work environment and business culture.

RF engineers have always been considered a somewhat unique group among electrical engineers. Experience-based intuition and creativity are essential tools for the RF engineer to derive quality solutions. The term "Black Magic" frequently used in this context really conveys this idea. A successful career move will have the engineer placed in a position where he or she is most creative and passionate about the job. With the diversified demand for RF engineers, a perfect match is not too much to ask for.

Career Planning thus gains new meaning. Considering technological horizons, work environment and future opportunities for personal growth in different markets yield career decisions better tailored to one's personality and expectations. Information supporting career decisions and recruiting efforts will become even more profession and technology specific and is therefore of growing relevance to the agenda of RF and microwave engineering media. *Microwave Journal* and ElectroMagneticCareers.com have recognized the depth of the emerging need for industry-specific career resources, and are proud to be pioneers leading the industry media with a vision to raise awareness and discussions addressing the unique interests of RF engineers.

Isaac Mendelson
ElectroMagneticCareers.com
Isaac@ElectroMagneticCareers.com

ADVERTISING INDEX

RS No.	Advertiser	Page No.	Phone	Fax	Web Address
1	Acceleware	99			http://mwj.hotims.com/16339-1
2	Advanced Switch Technology	200	613-384-3939	613-384-5026	http://mwj.hotims.com/16339-2
3	Aeroflex	9	516-694-6700	516-694-2562	http://mwj.hotims.com/16339-3
4	Aeroflex/Inmet, Inc.	192	734-426-5553	734-426-5557	http://mwj.hotims.com/16339-4
5	Aeroflex/Weinschel, Inc.	169	800-638-2048	301-846-9116	http://mwj.hotims.com/16339-5
6,7,8,9	Agilent Technologies, Inc.	19,89,139,199	800-829-4444	415-857-5518	http://mwj.hotims.com/16339-6
10	American Microwave Corporation	124	301-662-4700	301-662-4938	http://mwj.hotims.com/16339-10
11	American Technical Ceramics	187	631-622-4700	631-622-4748	http://mwj.hotims.com/16339-11
12	AML Communications Inc.	53	805-388-1345	805-484-2191	http://mwj.hotims.com/16339-12
13	AMTA 2008	166	425-868-2558		http://mwj.hotims.com/16339-13
14	Anritsu Company	159	800-ANRITSU	972-671-1877	http://mwj.hotims.com/16339-14
15	Ansoft Corporation	37	412-261-3200	412-471-9427	http://mwj.hotims.com/16339-15
16,17	AR Worldwide	83,197	215-723-8181		http://mwj.hotims.com/16339-16
18	Artech House	172	800-225-9977	781-769-6334	http://mwj.hotims.com/16339-18
19	Astrolab, Inc.	119	732-560-3800	732-560-9570	http://mwj.hotims.com/16339-19
20	Atlantic Microwave Ltd.	116	44-1376-550220	44-1376-552145	http://mwj.hotims.com/16339-20
21	AWR	13	310-726-3000		http://mwj.hotims.com/16339-21
22	B&Z Technologies	39	631-444-8827	631-444-8825	http://mwj.hotims.com/16339-22
23	Bird Technologies Group	48	866-695-4569		http://mwj.hotims.com/16339-23
24	Boonton Electronics (a Wireless Telecom Group Company)	COV 2	973-386-9696	973-386-9191	http://mwj.hotims.com/16339-24
25	Bowei Integrated Circuits Co., LTD.	172	+86-311-87091891	+86-311-87091282	http://mwj.hotims.com/16339-25
26	CAP Wireless Inc.	141	805-499-1818		http://mwj.hotims.com/16339-26
27	Cernex, Inc.	98	408-541-9226	408-541-9229	http://mwj.hotims.com/16339-27
28	Channel Microwave Corporation	22	805-482-7280	805-987-8794	http://mwj.hotims.com/16339-28
29	Ciao Wireless, Inc.	56	805-389-3224	805-389-3629	http://mwj.hotims.com/16339-29
30	ClearComm Technologies, LLC	97,208	410-860-0500	410-860-9005	http://mwj.hotims.com/16339-30
31	Cobham Defense Electronic Systems	24–25	978-557-2400	978-557-2800	http://mwj.hotims.com/16339-31
32	Coilcraft	17	800-322-2645	847-639-1469	http://mwj.hotims.com/16339-32
33	Commercial Microwave Technology, Inc.	67	916-631-4363	530-642-9798	http://mwj.hotims.com/16339-33
34	Compac	110	631-585-3400	631-585-3534	http://mwj.hotims.com/16339-34
35	CPI Beverly Microwave Division	45	978-922-6000	978-922-2736	http://mwj.hotims.com/16339-35
36	CST of America, Inc.	31	508-665-4400	781-576-5702	http://mwj.hotims.com/16339-36
37	CTIA Wireless 2008	202	202-736-3664	202-785-0721	http://mwj.hotims.com/16339-37
38	Daico Industries, Inc.	109	310-507-3242	310-507-5701	http://mwj.hotims.com/16339-38
39	dBm, LLC	44	973-709-0020	973-709-1346	http://mwj.hotims.com/16339-39
40	Dow-Key Microwave Corporation	6	805-650-0260	805-650-1734	http://mwj.hotims.com/16339-40
41	Eastern Wireless TeleComm, Inc.	107	410-749-3800	410-749-4852	http://mwj.hotims.com/16339-41
42	Electro Magnetic Careers	208			http://mwj.hotims.com/16339-42
43	EM Research, Inc.	76	775-345-2411	775-345-1030	http://mwj.hotims.com/16339-43
44	EMC Technology Inc.	21	772-286-9300	772-283-5286	http://mwj.hotims.com/16339-44
45	Empower RF Systems, Inc.	85	310-412-8100	310-412-9232	http://mwj.hotims.com/16339-45
46	Endwave	29	408-522-3180	408-522-3181	http://mwj.hotims.com/16339-46
47	EPX Microwave	102			http://mwj.hotims.com/16339-47
48	ET Industries	195	973-394-1719	973-394-1710	http://mwj.hotims.com/16339-48
49	ETS-Lindgren	81	512-531-6400		http://mwj.hotims.com/16339-49
50	EuMW 2008	183	+ 44 20 7596 8742	+ 44 20 7596 8749	http://mwj.hotims.com/16339-50
51	Filtronic Compound Semiconductors, Ltd.	153	408-850-5740	831-621-8074	http://mwj.hotims.com/16339-51
44	Florida RF Labs Inc.	21	800-544-5594		http://mwj.hotims.com/16339-44
52	Focus Microwaves Inc.	87	514-684-4554	514-684-8581	http://mwj.hotims.com/16339-52
53	Herley-CTI	58	973-884-2580	973-887-6245	http://mwj.hotims.com/16339-53
54	Herotek, Inc.	118	408-941-8399	408-941-8388	http://mwj.hotims.com/16339-54
55,56,57,58	Hittite Microwave Corporation	71,75,77,78–79	978-250-3343	978-250-3373	http://mwj.hotims.com/16339-55
59	Huber + Suhner AG	143	+41 (0)71 353 41 11	+41 (0)71 353 45 90	http://mwj.hotims.com/16339-59
	IEEE Comcas 2008	176			www.comcas.org
	IEEE MTT-S International Microwave Symposium	207	781-769-9750	781-769-5037	www.ims2008.org

RS No.	Advertiser	Page No.	Phone	Fax	Web Address
60	Integra Technologies, Inc.	92	310-606-0855	310-606-0865	http://mwj.hotims.com/16339-60
61	Interplex NAS, Inc.	47	201-367-1300	201-768-8788	http://mwj.hotims.com/16339-61
62	ITT Microwave Systems	62	978-441-0200		http://mwj.hotims.com/16339-62
63	ITU-Shows	203	+41 22 730 6161	+41 22 730 6444	http://mwj.hotims.com/16339-63
64	JFW Industries, Inc.	167	317-887-1340	317-881-6790	http://mwj.hotims.com/16339-64
65	K&L Microwave, Inc.	7	410-749-2424	443-260-2268	http://mwj.hotims.com/16339-65
66	Keithley	41	888-588-9238		http://mwj.hotims.com/16339-66
67	KR Electronics, Inc.	200	732-636-1900	732-636-1982	http://mwj.hotims.com/16339-67
68	Krytar	50	877-734-5999	408-734-3017	http://mwj.hotims.com/16339-68
69	Lorch Microwave	59	800-780-2169	410-860-1949	http://mwj.hotims.com/16339-69
70	LPKF Laser & Electronics	52	800-345-LPKF	503-682-7151	http://mwj.hotims.com/16339-70
71	MECA Electronics, Inc.	191	973-625-0661	973-625-9277	http://mwj.hotims.com/16339-71
72	MegaPhase	193	877-MegaPhase		http://mwj.hotims.com/16339-72
73	MiCIAN GmbH	42	+49(421)16899351	+49(421)16899352	http://mwj.hotims.com/16339-73
74	Micro Lambda Wireless, Inc.	121	510-770-9221		http://mwj.hotims.com/16339-74
75	Micronetics	10	603-883-2900	603-882-8987	http://mwj.hotims.com/16339-75
76	Microsemi	40	408-986-8031		http://mwj.hotims.com/16339-76
77	Microwave Filter Company, Inc.	158	800-448-1666	315-463-1467	http://mwj.hotims.com/16339-77
	Microwave Journal	194,196,198, 200,204,209,213	800-225-9977	781-769-5037	www.mwjournal.com
78	Milmega Limited	177	+44 (0) 1983 618004	+44 (0) 1983 811521	http://mwj.hotims.com/16339-78
79	Mimix Broadband, Inc.	33	281-988-4600	281-988-4615	http://mwj.hotims.com/16339-79
80,81,82, 83,84,85, 86,87,88, 89,90,91, 92,93,94	Mini-Circuits	4–5,20,35, 63,64,73, 91,101,113, 123,135,144, 145,189,211	718-934-4500	718-332-4661	http://mwj.hotims.com/16339-80
95,96,97	MITEQ Inc.	3,54–55,205	631-436-7400	631-436-7430	http://mwj.hotims.com/16339-95
98	Modco, Inc.	200	775-331-2442	775-331-6266	http://mwj.hotims.com/16339-98
99	Molex RF/Microwave Connector Division	165	317-834-5600	317-834-5611	http://mwj.hotims.com/16339-99
100	Narda Microwave-East, an L3 Communications Co.	117	631-231-1700	631-231-1711	http://mwj.hotims.com/16339-100
101	NoiseWave Corp.	8	973-386-1119	973-386-1131	http://mwj.hotims.com/16339-101
	Northrop Grumman	208	817-496-0408		www.northropgrumman.com
102	OML Inc.	151	408-779-2698	408-778-0491	http://mwj.hotims.com/16339-102
103	Pendulum Instruments	147	+46 8 598 510 57		http://mwj.hotims.com/16339-103
104	Picosecond Pulse Labs Inc.	126	303-209-8100	303-447-2236	http://mwj.hotims.com/16339-104
105,106,107	Planar Monolithic Industries, Inc.	51,66,134	301-631-1579	301-662-2029	http://mwj.hotims.com/16339-105
108	Programmed Test Sources, Inc.	COV 3	978-486-3400	978-486-4495	http://mwj.hotims.com/16339-108
109	Pulsar Microwave Corporation	136	800-752-3043	973-779-2727	http://mwj.hotims.com/16339-109
110,111	Radiall	43,175	33-1-49-353535	33-1-48-546363	http://mwj.hotims.com/16339-110
112	Reactel, Incorporated	60	301-519-3660	301-519-2447	http://mwj.hotims.com/16339-112
113	RelComm Technologies, Inc.	163	410-749-4488	410-860-2327	http://mwj.hotims.com/16339-113
114	Remcom	171	814-861-1299	814-353-1420	http://mwj.hotims.com/16339-114
115	REMEC Defense & Space	38	858-560-1301		http://mwj.hotims.com/16339-115
116	RF Micro Devices	105	336-678-5570	336-931-7454	http://mwj.hotims.com/16339-116
117	RF TEC Mfg., Inc.	200	770-487-2187	770-486-9499	http://mwj.hotims.com/16339-117
118	RFcore Co., Ltd.	100	82 31 708 7574	82 31 708 7596	http://mwj.hotims.com/16339-118
119,120,121	RFHIC	84,86,88	82-31-250-5011	82-31-250-5088	http://mwj.hotims.com/16339-119
122	Richardson Electronics, Ltd.	115	800-737-6937	630-208-2550	http://mwj.hotims.com/16339-122
123	RLC Electronics, Inc.	27	914-241-1334	914-241-1753	http://mwj.hotims.com/16339-123
124	Rogers Corporation	103	480-961-1382	480-961-4533	http://mwj.hotims.com/16339-124
125,126,127, 128,129	Rohde & Schwarz GmbH	125,127,129, 131,133	+49-1805-124242	+49-89-412913777	http://mwj.hotims.com/16339-125
130	Rohm & Haas	149	540-552-4610		http://mwj.hotims.com/16339-130
131	Rosenberger	72	+49-8684-18-0	+49-8684-18-499	http://mwj.hotims.com/16339-131
132	Sector Microwave Industries, Inc.	200	631-242-2300	631-242-8158	http://mwj.hotims.com/16339-132
133	Sigma Systems Corporation	111	619-258-3700	619-258-3712	http://mwj.hotims.com/16339-133

ADVERTISING INDEX

RS No.	Advertiser	Page No.	Phone	Fax	Web Address
134	Skyworks Solutions, Inc.	93	781-376-3000		http://mwj.hotims.com/16339-134
135	Sonnet Software, Inc.	23	315-453-3096	315-451-1694	http://mwj.hotims.com/16339-135
136	Spacek Labs Inc.	138	805-564-4404	805-966-3249	http://mwj.hotims.com/16339-136
137	Spectrum Elektrotechnik GmbH	137	+49-89-3548-040	+49-89-3548-0490	http://mwj.hotims.com/16339-137
138,139	Synergy Microwave Corporation	69,201	973-881-8800	973-881-8361	http://mwj.hotims.com/16339-138
140	Talley Communications	49	800-949-7079		http://mwj.hotims.com/16339-140
141	Tecdia, Inc.	74	408-748-0100	408-748-0111	http://mwj.hotims.com/16339-141
142	Teledyne Relays	95	888-551-0448		http://mwj.hotims.com/16339-142
143	Telogy LLC	161	800-835-6494		http://mwj.hotims.com/16339-143
144	Tensolite	15	800-458-9960	904-829-3447	http://mwj.hotims.com/16339-144
146	Thunderline-Z	155,157	603-329-4050		http://mwj.hotims.com/16339-146
147	T-Tech, Inc.	148	800-379-1530	770-455-0970	http://mwj.hotims.com/16339-147
148	Universal Microwave Components Corporation	132	703-642-6332	703-642-2568	http://mwj.hotims.com/16339-148
149	Vectron International	11	1-88-VECTRON1	888-FAX-VECTRON	http://mwj.hotims.com/16339-149
150	Volex Group plc	173	828-485-4500		http://mwj.hotims.com/16339-150
151	Waveline Inc.	96	973-226-9100	973-226-1565	http://mwj.hotims.com/16339-151
152	WCA International	156	202-452-7823	202-452-0041	http://mwj.hotims.com/16339-152
153	Weinschel Associates	106	877-948-8342	301-963-8640	http://mwj.hotims.com/16339-153
154	Werlatone, Inc.	COV 4	845-279-6187	845-279-7404	http://mwj.hotims.com/16339-154
155	Win Semiconductors Corp.	154	310-530-8485	310-530-8499	http://mwj.hotims.com/16339-155
156	Zeland Software, Inc.	185	510-623-7162	510-623-7135	http://mwj.hotims.com/16339-156

***Visit* Microwave Journal *on the Web at* www.mwjournal.com**

Visit mwjournal.com/info and enter RS# to request information from our advertisers

SALES REPRESENTATIVES

microwave journal

CARL SHEFFRES, PUBLISHER **ED JOHNSON, ASSOCIATE PUBLISHER** **KEN HERNANDEZ, TRAFFIC ADMINISTRATOR**

Eastern and Central Time Zones
Chuck Boyd
Northeast Reg. Sales Mgr.
(New England, Upstate NY, Eastern Canada)
685 Canton Street
Norwood, MA 02062
Tel: (781) 769-9750
FAX: (781) 769-5037
cboyd@mwjournal.com

Michael Hallman
Eastern Reg. Sales Mgr.
(Mid-Atlantic, Southeast, Midwest)
4 Valley View Court
Middletown, MD 21769
Tel: (301) 371-8830
FAX: (301) 371-8832
mhallman@mwjournal.com

Eastern and Central Time Zones
Ed Johnson
Associate Publisher
PO Box 5962
Ocala, FL 34478-5962
Tel: (352) 620-2442
FAX: (352) 620-2443
ejohnson@mwjournal.com

Pacific and Mountain Time Zones
Wynn Cook
Western Reg. Sales Mgr.
PO Box 23200
San Jose, CA 95153
Tel: (408) 224-9060
FAX: (408) 224-6106
wcook@mwjournal.com

International Sales
Richard Vaughan
International Sales Manager
46 Gillingham Street
London SW1V 1HH, England
Tel: +44 207 596 8742
FAX: +44 207 596 8749
rvaughan@horizonhouse.co.uk

Germany, Austria, and Switzerland (German-speaking)
Juergen Wissling
Wissling Marketing Services
Riedstrasse 5
72813 St. Johann-Wuertingen
Germany
Tel: +49 7122 828140
FAX: +49 7122 828145
jwissling@horizonhouse.com

Israel
Oreet Ben Yaacov
Oreet International Media
15 Kineret Street
51201 Bene-Berak, Israel
Tel: +972 3 570 6527
FAX: +972 3 570 6526
obenyaacov@horizonhouse.com

Korea
Young-Seoh Chinn
JES Media International
2nd Floor, ANA Bldg.
257-1, Myungil-Dong
Kangdong-Gu
Seoul, 134-070 Korea
Tel: +82 2 481-3411
FAX: +82 2 481-3414
yschinn@horizonhouse.com

Japan
Katsuhiro Ishii
Ace Media Service Inc.
12-6, 4-Chome,
Nishiiko, Adachi-Ku
Tokyo 121-0824, Japan
Tel: +81 3 5691 3335
FAX: +81 3 5691 3336
amskatsu@dream.com

If you have to ask how much it costs.....

you <u>can</u> afford it

for synthesizers from PTS, you don't even have to ask,

all our technical information, (web, catalog, data sheets) shows the price of our units. PTS produces fast switching, low noise synthesizers with the best performance/price ratio on the market. Our total installed base, first in the ATE industry, confirms this fact.

Are there ... that hav... e? Abso... how much ... you know t... story...

anything from a 10 MHz slot to a 6.4 GHz band, covered with numerous models

If you should need information on our products, you're free to ask. We shall gladly answer your questions about specs and price.

PTS THE FASTER SOURCE NOW TO 6400 MHz

INDUSTRY'S LARGEST INSTALLED BASE

synthesized

LO sources

with:

- crystal control
- ultra-low phase noise
- µs-switching
- multi-octave coverage
- fine resolution
- 0.1 MHz - 6.4 GHz

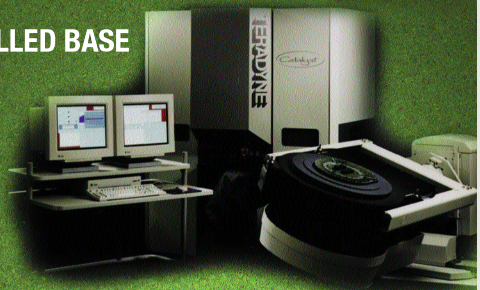

PTS
FREQUENCY SYNTHESIZERS
PROGRAMMED TEST SOURCES, INC.
9 Beaver Brook Road
Littleton, MA 01460

Tel: 978 486-3400
Fax: 978 486-4495
http://www.programmedtest.com
e-mail: sales@programmedtest.com

PROGRAMMED TEST SOURCES, INC.

CABLES & CONNECTORS 2008

MICROWAVE JOURNAL
50 years
1958 2008
as the Industry Standard

A Special Supplement to Microwave Journal

Cables & Connectors Supplement

Table of Contents

FEATURES

Staff

Publisher: Carl Sheffres
Associate Publisher: Edward Johnson
Editor: David Vye
Managing Editor: Keith W. Moore
Technical Editor: Frank M. Bashore
Associate Technical Editor: Dan Massé
Staff Editor: Jennifer DiMarco
Editorial Assistant: Barbara Walsh
Consulting Editor: Howard I. Ellowitz
Consulting Editor: Harlan Howe, Jr.
Consulting Editor: Peter Staecker
Consulting Editor: Dan Swanson
Web Editor: Samantha Bookman
Traffic Manager: Edward Kiessling
Traffic Administrator: Ken Hernandez
Director of Production & Distribution: Robert Bass
Multimedia Designer: Greg Lamb
Web Site Production Designer: Michael O'Brien
DTP Coordinator: Janet A. MacDonald

EUROPE

European Editor: Richard Mumford
Office Manager: Eugenie Hardy

CORPORATE STAFF

Chairman: William Bazzy
CEO: William M. Bazzy
President: Ivar Bazzy
Vice President: Jared Bazzy

Supplement to the March 2008 issue of Microwave Journal

Horizon House also publishes *Telecommunications®*

Posted under Canadian international publications mail agreement #0738654

Proven high performance in demanding applications

Continuing the Adams-Russell Tradition of Quality

M/A-COM cables...tough enough to endure the harshest environments
- 65g vibration; -65° to 200°C at 70,000 feet; and 100,000 flexures
- Extremely low loss, high-power flexible cables from .05" to 1.4" diameter
- Complete in-house manufacturing for cables, connectors, and assemblies

Download our free custom cable design program at www.macom.com/cables or contact your local M/A-COM sales office for assistance.

New M/A-COM Cables

New lightweight cables are up to 30% lighter than traditional designs

North America 800.366.2266 • Europe +44 (0)1908.574200 • Asia/Pacific +81.44.844.8296 • www.macom.com

Tyco Electronics

Our commitment. Your advantage.

Microwave Journal • Vol. 4 • No. 11 • November 1961

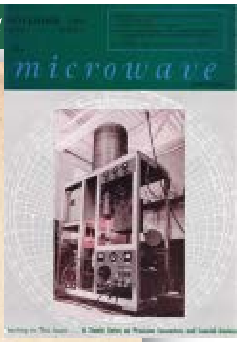

RF LEAKAGE CHARACTERISTICS OF POPULAR COAXIAL CABLES AND CONNECTORS, 500 MC TO 7.5 GC.

JOHN ZORZY
R. F. MUEHLBERGER
GENERAL RADIO COMPANY
West Concord • Massachusetts

Introduction

In the design and use of coaxial devices, a knowledge of the leakage characteristics of radio-frequency cables and connectors is important, both in measurements and in the design of operational and test equipment.

The evaluation and measurement of electromagnetic leakage through solid conductors, braids, screens, slits and other configurations employed to confine the electromagnetic fields in apparatus, has been the subject of a great deal of analysis and research. Some investigators have been concerned with the leakage phenomenon itself,[1,2,3,4,5] others with its measurement [6,7,8,9,10,11]. The experimental procedure employed is usually chosen in accordance with the particular manifestation of the electromagnetic leakage that is of interest. For example, for conducted leakage or coupling, a special direct metallic connection may be made between the leakage source and the detector; for induction or near-field leakage, probes or loops are placed in proximity with the leakage source; and, for radiated leakage, probes, loops, or the more distributed version of these, antennas, are placed at what is considered the far field of the leakage source. The three are commonly evaluated, *in toto*, by surrounding the leakage source with a closed coaxial system. The usual practice is to couple some of the basic leakage modes to the TEM mode of the coaxial system.

Usually the equipment designer is successful in confining stray electromagnetic fields within the equipment package except, of course, in open systems such as slotted lines. However, the connection of coaxial cables, flexible and solid, and coaxial components to the equipment introduces a source of leakage. In the case of immittance bridges, cable or connector leakage introduces a spurious signal path between the source and the detector, usually resulting in measurement errors. Leakage is a cause of error in precision slotted-line measurements through spurious coupling of the pick-up probe to the source; in attenuation measurements and filter-response measurements, by spurious coupling between the input and the output circuits. In complex electronic systems, as for example in a missile system, the spurious coupling between the interconnecting cables of the separate systems can result in malfunction in the operation of an element of the system.

It is the purpose of this paper to demonstrate the relative shielding effectiveness of popular flexible cables and connectors, and to describe the measurement technique. Test results are presented in terms of both relative leakage power and surface transfer impedance. The unique feature of this work is the frequency range of measurement. The majority of previous contributions were concerned with the frequency range below 500 Mc.

Measurement Technique

The measurement of the leakage from connectors and cables is performed by collecting the leakage energy in a coaxial system surrounding the leakage source. An outline of the instrumentation is shown in Figures 1 and 2 respectively, and a photograph in Figure 3. The device from which leakage is to be measured, connector or cable, is incorporated in a uniform transmission line which is terminated in a matched load. The matched termination simplifies both the measurement procedure and data reduction. This complete coaxial system is embodied within a cylinder which forms, externally, a second coaxial system. The second coaxial system is terminated at one end in an adjustable short-circuiting plunger and at the other in a

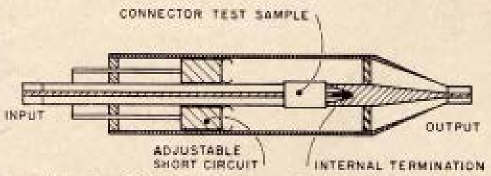

Figure 1 — Tri-Axial Connector Leakage Test Unit.

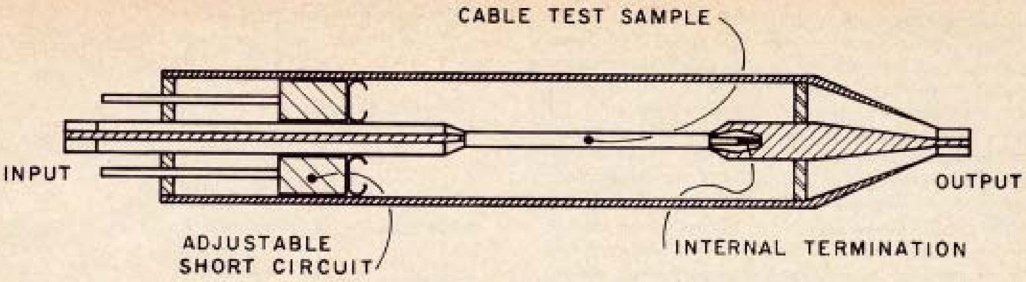

Figure 2 — Tri-Axial Cable Leakage Test Unit.

tapered transition to a standard connector. In connector measurements, the outer coaxial line is terminated in a matched detector. Except for the adjustable short-circuit feature, this tri-axial system has been employed by others.[5,7,8]

For direct leakage measurements the adjustable short circuit serves several purposes both in connector and cable measurements. In connector measurements, the short-circuit position is adjusted to assure that an adequately low impedance appears behind the equivalent leakage generator. A matched termination can be substituted, but the resulting 6-db loss cannot be tolerated in some cases. In addition, if the leakage source is directional, as it indeed is for cables and connectors with multiple leakage, it is possible for the leakage to be directed to this termination at some frequencies and not collected by the detector. For surface transfer-impedance measurements on cables or connectors with leakage from more than one point in the connector, however, a matched termination is desirable in order to simplify the transformation of the measured data to transfer impedance data. This latter consideration is discussed at greater length in the Appendix.

The equivalent leakage generator, in general, can have field components in the radial, axial, and circumferential* directions. Furthermore, these components are not necessarily circularly symmetric. Locally, TE, TM, and TEM modes can all exist, and in fact, for complete leakage measurements, the detector should couple to all. The excitation of the outer coaxial line, however, is believed to be principally TEM, since the currents in the internal line are predominantly axial and symmetric. In the particular test configuration employed here, only the TE_{11} mode can be propagated, and this only above 3.5 Gc. In the transition to the smaller coaxial line, the TE_{11} mode is filtered out, but some of it couples to the principal TEM mode, delivering this power to the detector. Special care is taken to assure that the test cable or connector system is mounted concentrically, to minimize TE_{11} mode generation.

Despite the possible limitations cited above, the tri-axial system is a simple and effective system for measuring the net leakage. It is indeed well suited for axial surface transfer-impedance measurements. It can serve as a standard method only, however, if the leakage characteristics or axial surface transfer impedance of axially symmetrical components are to be evaluated. Accurate measurement of each mode of leakage, each manifestation of leakage, and each component of surface impedance will, in general, require a specific test configuration for the particular measurement.

The characteristic impedance of the outer coaxial line of the tri-axial system, which is formed with the cable

* *The circumferential E-field component is not usually present in axially symmetric components. See References 1, 2.*

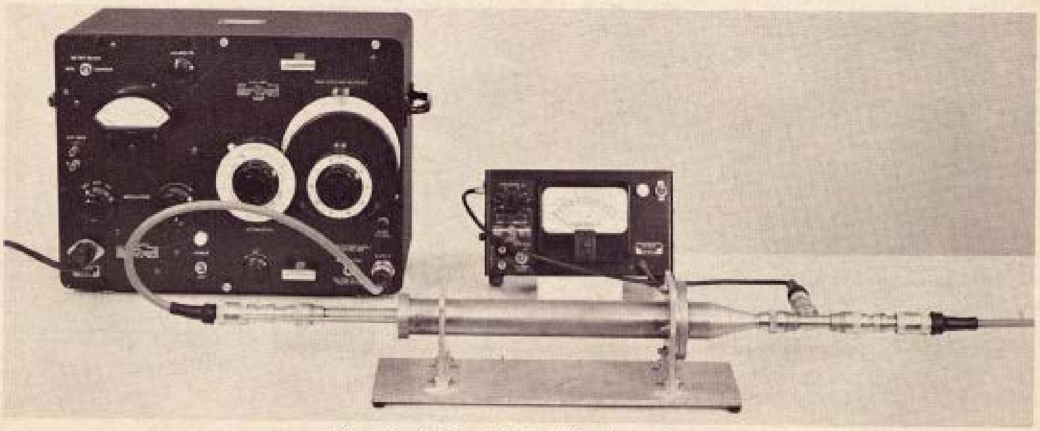

Figure 3 — Tri-Axial Unit and Equipment Setup.

braid as the inner conductor, should be matched to the detector. As a matter of convenience, but with some sacrifice in accuracy and ease of data reduction, one outer conductor size was employed for all cables. The characteristic impedance was therefore generally higher than 50 ohms. The steps in conductor size at the cable connectors also produce capacitance discontinuities. These can be measured or calculated[12]. The effects of the characteristic impedance discontinuity are described in the Appendix.

The leakage power ratio is defined here as the ratio of the power detected in a 50-ohm detector at the output of the tri-axial unit to the power flowing through the internal 50-ohm connector or cable system. It is basically the attenuation through the tri-axial system. This definition appears arbitrary in the sense that 50 ohms is an arbitrary load impedance. However, since the leakage source impedance is comparatively low, the voltage at the detector is essentially the open-circuit leakage voltage. The ratio of the input voltage to the leaky cable, to this output voltage is an absolute leakage quantity, as is the measured power ratio, which is identically equal to the square of this voltage ratio.

The surface transfer impedance is obtained from this ratio as follows:

The surface transfer impedance is,

$$Z_{21} = \frac{e_2}{i_1} \qquad (1)$$

where

i_1 = Current flowing in internal line.
e_2 = Equivalent leakage voltage in external line.

In the connector leakage case, considering the equivalent leakage generator to be e_2 with an extremely low source impedance, this voltage e_2 appears at detector terminals, and the adjustable short circuit assures this. For a 50-ohm transmission-line system, the input power is,

$$50\, i_1^2$$

The measured output power is,

$$\frac{e_2^2}{50}$$

The measured power ratio A^2 is therefore,

$$A^2 = \frac{\frac{e_2^2}{50}}{50\, i_1^2} = \frac{e_2^2}{(50)^2 i_1^2} \qquad (2)$$

Substituting and by definition,

$$Z_{21} = \frac{e_2}{i_1} = 50\, A \qquad (3)$$

In the cable leakage case, the calculation is not as straightforward, especially where the outer tri-axial line is not terminated in its characteristic impedance. The calculations required to reduce the measured results given in this paper to transfer impedance per unit length are not included for that reason. The tri-axial system was set up principally to assess the relative leakage.

For the measurement of surface transfer impedance of cables, the outer coaxial line of the tri-axial system should be terminated in its characteristic impedance at the source end and in a similarly matched detector at the output end. In this case the relation between the measured leakage power ratio, A^2, and the surface transfer impedance per unit length is, in a 50-ohm system,

$$Z_{21} = \frac{100\, A\, (\beta - \beta_o)}{1 - e^{-j(\beta-\beta_o)L}} \qquad (4)$$

where

L = length of leaky cable section.
β = propagation constant in the test cable.
β_o = propagation constant in external line of tri-axial system.

This expression is obtained from Equation (5) in the Appendix which describes the forward TEM wave launched by the cable.

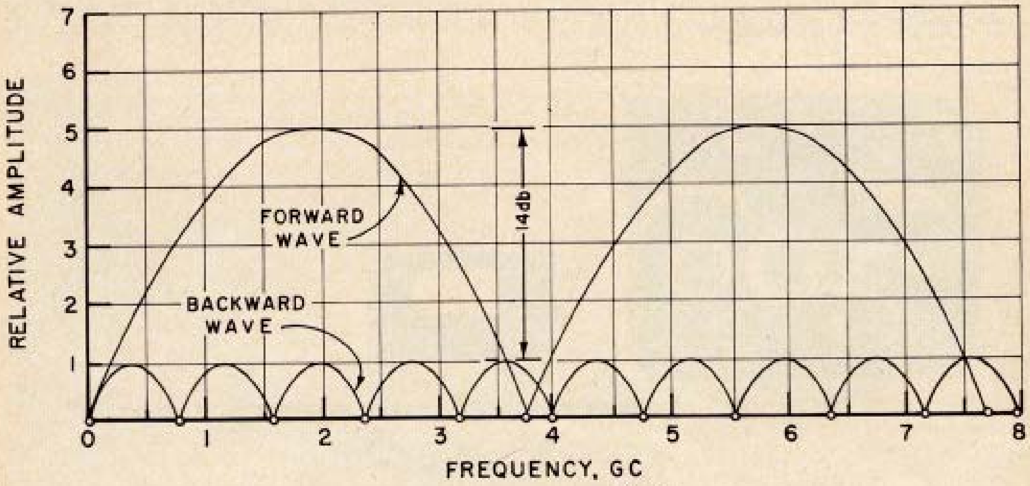

Figure 4 — Forward and Backward Wave, Matched Case, $\frac{\beta - \beta_0}{\beta_0} = 0.52$, 15-cm Long Cable.

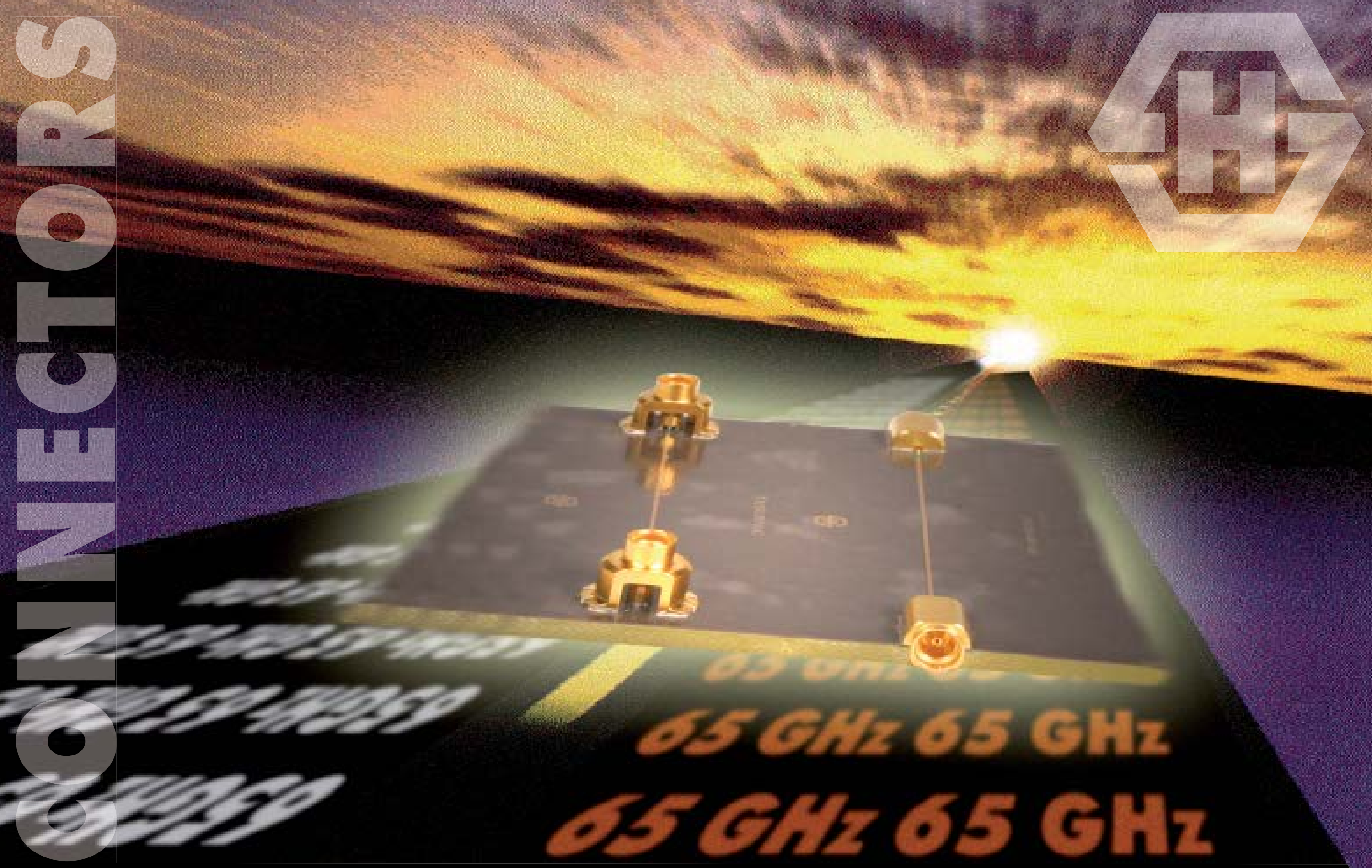
SNAP CONNECTORS
65 GHz 65 GHz
65 GHz 65 GHz

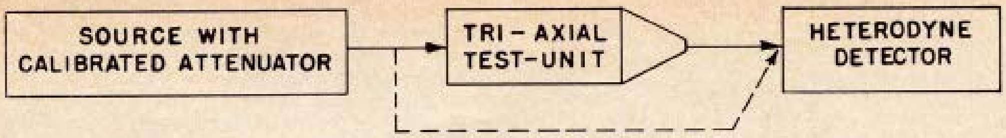

Figure 5 — Block Diagram of the Measuring System.

A null in this forward wave occurs when $(\beta-\beta_o)L=2n\pi$ and a maximum when $(\beta-\beta_o)L=(2n-1)\pi$. The variation of forward wave amplitude with frequency is shown in Figure 4. Also shown is the backward wave, which is the signal that would appear in a detector at the source end of the outer line. This is obtained from Equations (5) and (9) in the Appendix, employing a polyethylene-dielectric internal line and air-dielectric external line.

Measurement Procedure

In measuring the leakage power ratio, A^2, basically a substitution technique is employed. A matched detector system is installed at the output connector of the tri-axial unit, and the unit is driven as shown in Figure 5. In this setup, the short circuit is adjusted to produce a maximum indication at the detector. The detector is then connected directly to the source through a calibrated attenuator, and the attenuation required to yield the initial detector level is measured.

The sensitivity of this system is obviously limited by the sensitivity of the dectector and the power available. A sensitive superheterodyne system was employed, and for the low-leakage configurations about 30 milliwatts of power was required.

The principal sources of error are attenuator errors and mismatch at the receiver (mixer) input. For connector measurements, the error due to mismatch is directly proportional to VSWR since the equivalent leakage source impedance is small. The indicated leakage power can vary between the extremes, P x VSWR to P ÷ VSWR, where P is the power that would be delivered to a matched system. A VSWR of 2 will produce ±3-db error therefore.

In advance of installing the inner coaxial system into the outer cylinder of the tri-axial system, the inner system may be excited, and the immediate vicinity of the leakage point or associated connector and attachment points probed with a small loop or dipole to establish how critical are the mating of the connector and cable joints.

Test Results

Connector Leakage and Surface Transfer Impedance

The above procedure was employed to assess the leakage characteristics of three widely used connectors, the General Radio 874-B, the BNC (Bayonet Coupling), and the N (Threaded Coupling), and in addition, the new General Radio Locking Connector, the 874-BL which comprises the basic 874-B Connector with an outer, threaded coupling nut to shield and join the mating parts securely.

Leakage results are shown in Figure 6. These results were transformed to equivalent transfer impedance, Z_{21}, and this result is shown in Figures 7 and 8.

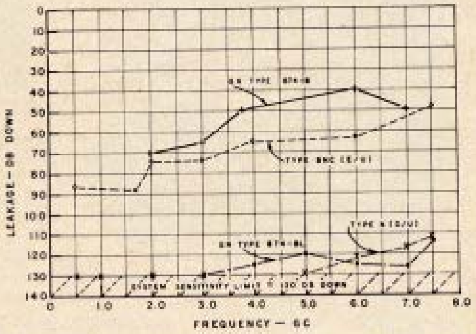

Figure 6 — Leakage Characteristics of the Type BNC, N, and General Radio Type 874-B, and Type 874-BL Connectors.

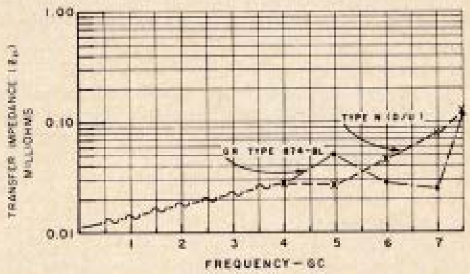

Figure 7 — Surface Transfer Impedance of the Type N and General Radio Type 874-BL Coaxial Connectors.

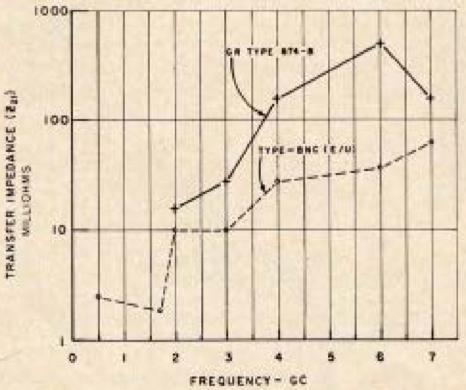

Figure 8 — Surface Transfer Impedance of the Type BNC and General Radio Type 874-B Coaxial Connectors.

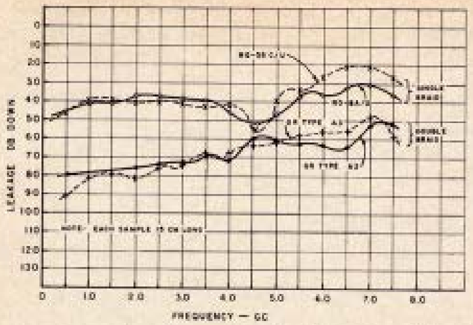

Figure 9 — Leakage Characteristics of RG-58, RG-8, and General Radio Types 874-A2 and 874-A3 Flexible Coaxial Cables.

The leakage characteristics of several popular flexible coaxial cables are shown in Figure 9. The RG-8 and RG-58 are single-braid cables. The General Radio A-2 and A-3 are double-braid cables of approximately the same size as RG-8 and RG-58 respectively. The corresponding surface impedance per unit length, calculated from the leakage measurements, is shown in Figures 10 and 11. Simple theory indicates that the transfer impedance is principally inductance. A linear surface impedance variation with frequency is, therefore, predicted. A linear frequency curve is shown in the graphs in this connection. For single-braid cables, the linear relation exists up to about 5 Gc, while for the double-braid cables the linear relation exists only up to about 2 Gc.

The single-braid leakage data indicate the periodicity expected in the forward wave launched by the leaky cable, and is explained, therefore, by an orderly arrangement of incremental leakage sources.

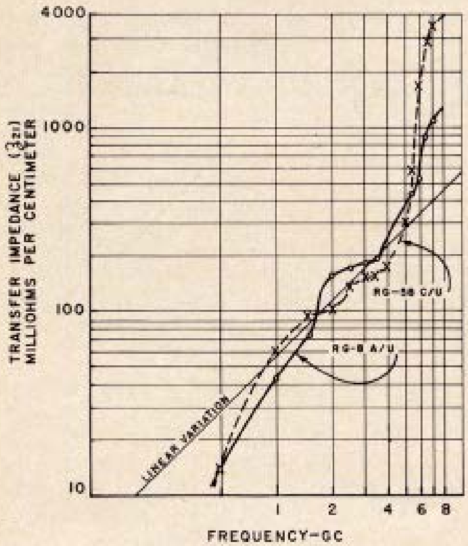

Figure 10 — Surface Transfer Impedance Per Unit Length of RG-58 and RG-8 Single-Braid Cables.

The double-braid data are devoid of the periodic variation. Perhaps the double-shield arrangement cannot be represented as a series of equal incremental generators as well as can the single-braid, because the contact between the outer and inner braids may not be as regular as the weave of the braid. Subsequent measurements will be performed to verify this result, and to separate the forward and backward waves launched by the cable. This will permit a more accurate measurement of transfer impedance.

APPENDIX

The Forward and Backward Waves Launched by Leaky Cables—Analysis

Loose coupling between adjacent transmission lines under matched conditions has been analyzed typically by Shelkunoff and Odarenko[13], and Jungfer[6]. An analysis is given here for the coupling of the leaky cable into the secondary, external coaxial line of the tri-axial system, under general conditions of match. The particular case in which the source end of the external, collecting line is terminated in a short-circuit, and the output end of the external line is terminated in a load not matched to this line, is also analyzed.

Voltage at Output End and Forward Wave

The wave propagating toward the output is given as the forward wave. It is the signal appearing at a detector

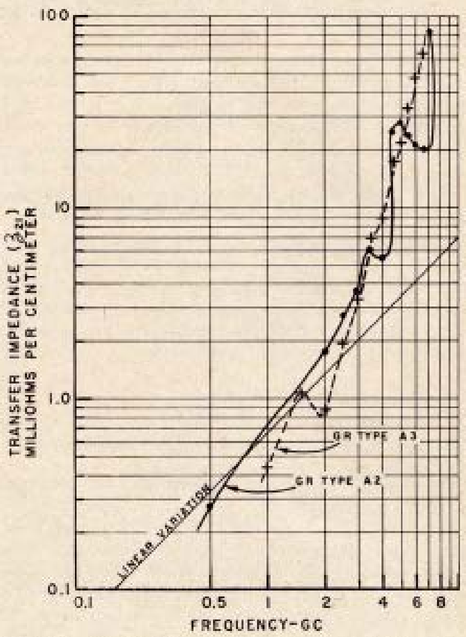

Figure 11 — Surface Transfer Impedance Per Unit Length of General Radio Types 874-A2 and 874-A3 Flexible Coaxial Double-Braid Cables.

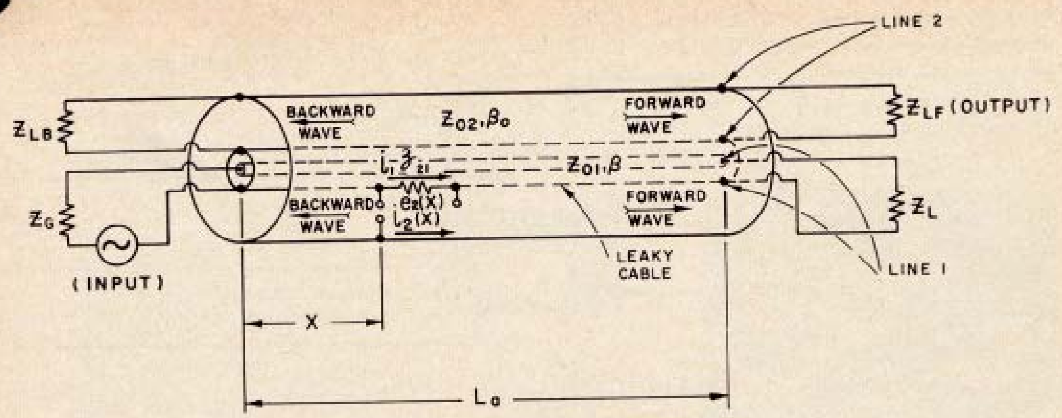

Figure 12 — Schematic, Tri-Axial Transmission System.

placed at the output end of the tri-axial unit under matched conditions. The total voltage at the output end is obtained as follows:

In Figure 12, current, i_1, flowing internally in the cable produces the voltage e_2 at the surface impedance, z_{21}. This voltage appears externally in series with the cable outer conductor and produces a current $i_2(x)$, in the outer line.

The wave to the right produced by $i_2(x)$ is obtained as follows:

The incremental voltage e_2 at x is

$$e_2(x) = i_1 z_{21} e^{-j\beta x}\, dx \qquad (1)$$

where: i_1 = current in internal line (assumed uniform).
z_{21} = surface transfer impedance per unit length.
β = propagation constant in cable.

The incremental current in the external line 2, at plane x is therefore,

$$i_s(x) = \frac{e_2(x)}{Z_2(x)}$$

$$= \frac{i_1 z_{21}}{Z_2(x)} e^{-j\beta x}\, dx \qquad (2)$$

where:

$Z_2(x)$ = the series combination of Z_{LF} transformed to plane x, and Z_{LB} transformed to plane x,
$= Z_B(x) + Z_F(x)$.

$$Z_B(x) = Z_{02} \frac{Z_{LB} + jZ_{02} \tan \beta_o x}{Z_{02} + j\, Z_{LB} \tan \beta_o x},$$

$$Z_F(x) = Z_{02} \frac{Z_{LF} + j\, Z_{02} \tan [\beta_o(L_a - x)]}{Z_{02} + j\, Z_{LF} \tan [\beta_o(L_a - x)]}.$$

L_a = length of leaky cable.
β_o = propagation constant in external line.

The incremental voltage across the external line at $x = L_a$, or across Z_{LF} is,

$$de_F = [e_2(x) - i_2(x) Z_B(x)] \cos [\beta_o(L_a - x)] - j[i_2(x)\, Z_{02}] \sin [\beta_o(L_a - x)]$$

$$= i_1 z_{21} \left[1 - \frac{Z_B(x)}{Z_2(x)}\right] \cos [\beta_o(L_a - x)]\, e^{-j\beta x}\, dx - j\, i_1 z_{21} \left[\frac{Z_{02}}{Z_2(x)}\right] \sin [\beta_o(L_a - x)]\, e^{-j\beta x}\, dx \qquad (3)$$

Integration of (3), which is the summation of the contributions from the series of incremental leakage generators, yields the total voltage across Z_{LF}, that is,

$$e_F(L_a) = i_1 z_{21} \int_0^{L_a} \left\{\left[1 - \frac{Z_B(x)}{Z_2(x)}\right] \cos [\beta_o(L_a - x)]\, e^{-j\beta x} - j\left[\frac{Z_{02}}{Z_2(x)}\right] \sin [\beta_o(L_a - x)]\, e^{-j\beta x}\right\} dx \qquad (4)$$

Note that when the external system is matched at both ends, (4) reduces to the forward wave:

$$e_F(L_a) = j \frac{i_1 z_{21}}{2(\beta - \beta_o)} e^{-j\beta_o L_a} \left[1 - e^{-j(\beta - \beta_o) L_a}\right] \qquad (5)$$

For the tri-axial connections described in the text, the output voltage was the sum of the complex voltages of the forward and backward waves obtained by integration of Equation (4).

For this setup, Z_{LB} was a short-circuited length of coaxial line of characteristic impedance Z_{02}. In this case,

$$Z_{LB} = j\, Z_{02} \tan (\beta_o L_b)$$

In addition, the load Z_{LF} was not matched to Z_{02}, therefore, Equation (4) applies, employing the above substitution for Z_{LB} in $Z_B(x)$, wherein $Z_2(x) = Z_B(x) + Z_F(x)$.

In the experimental procedure, L_b, the length of the short circuit is adjusted to produce a maximum in the total voltage across Z_{LF}, the detector impedance. The result of integration of (4) for this general case is complex.

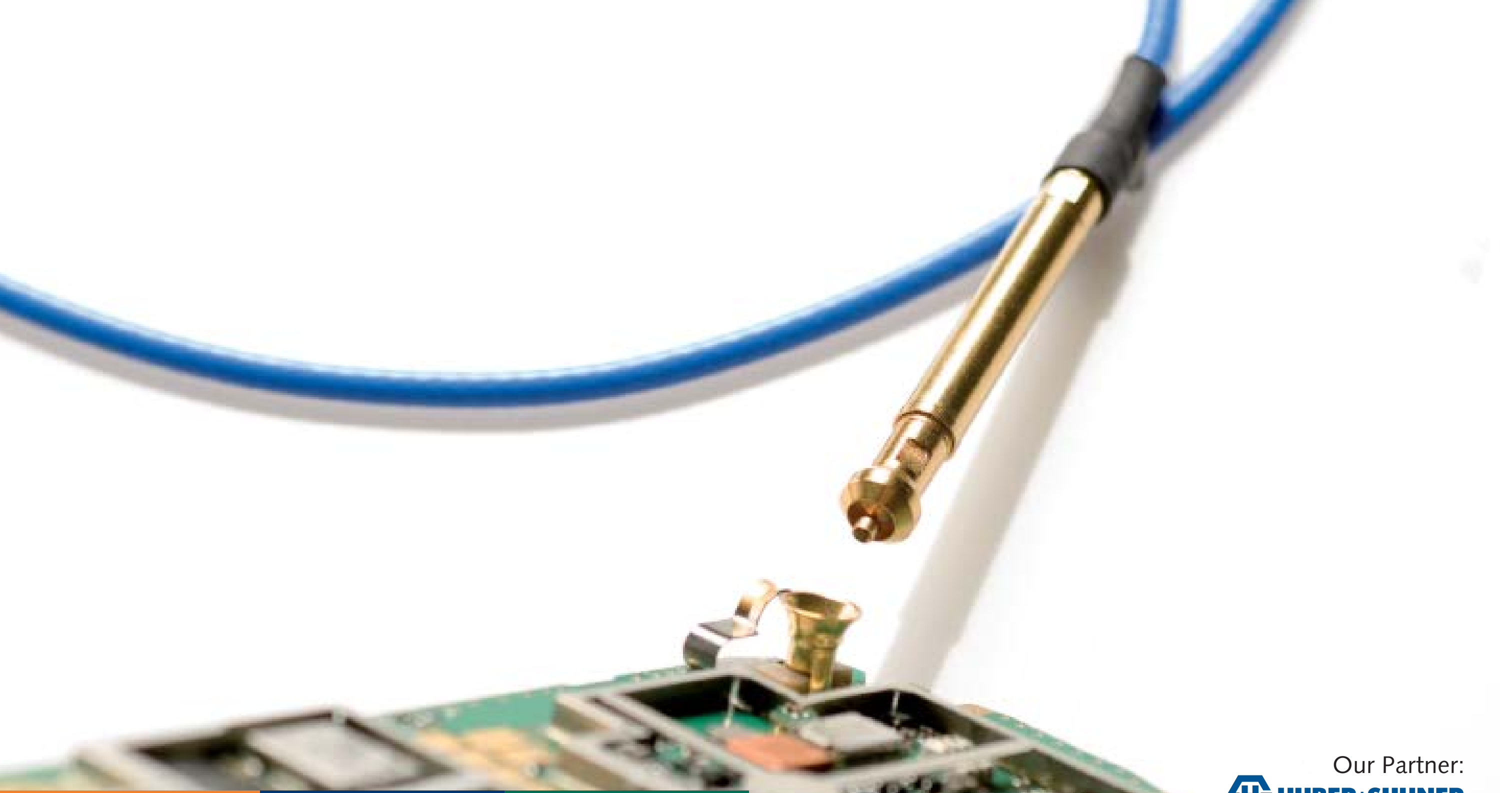

Test Probes | Test Fixtures | Test Systems

Our Partner:
HUBER+SUHNER

Top RF Technology up to 6 GHz

Discover the unique solution set from INGUN for high-precision measurements up to 6 GHz – no matter whether for Wireless-LAN, Bluetooth or PDA´s.

INGUN is a global leader in the field of testing equipment. In cooperation with the Swiss RF specialist HUBER+SUHNER, we have developed a standardised and reliable complete solution, which can be used worldwide.

Our Solution Sets:

– **HFS-810 or HFS-840** with MCX Plug connector **SE-810 V** for applications up to 4 GHz
– **HFS-860** with MCX Plug connector **SE-860 V** for applications up to **6 GHz**

In the new catalog you can find RF Test Probes for 2, 4 and 6 GHz applications. They are available with and without a screw-in option, in compact designs and as non-rotating or asymmetrical versions for contacting the common types of plugs and jacks such as: MMCX, MCX, SMB, SMC, 1.0/2.3, BMA, N, UFL, MM 8430 / MS-156, FAKRA I / FAKRA II, HSD, PCB-Layout.

IPC PRINTED CIRCUITS EXPO APEX and the DESIGNERS SUMMIT

APEX, April 1-3, 2008
You will find us on booth No. 234

ingun

ingun Prüfmittelbau GmbH
Max-Stromeyer-Straße 162
78467 Konstanz
Germany
Tel. +49 7531 8105-0
Fax +49 7531 8105-65
info@ingun.com
www.ingun.com

Visit http://mwj.hotims.com/16584-6 or use RS# 6 at www.mwjournal.com/info

Therefore, in order to illustrate the summation of the forward and backward wave, when a short circuit is used, consider the case where the external line is terminated in a matched detector at the output end, and $Z_{03}=Z_{02}$. The total voltage across Z_{LF}, simplifies to,

$$e_F=\frac{i_1 z_{21}}{2}\left[\frac{1-e^{-j(\beta-\beta_o)L_a}}{\beta-\beta_o}+\frac{1-e^{-j(\beta+\beta_o)L_a}}{\beta+\beta_o}e^{-j\beta_o L_a}\right] \qquad (6)$$

When the short circuit is adjusted for maximum output voltage this reduces to,

$$e_F(\max)=\frac{i_1 z_{21}}{2}\left[\left|\frac{1-e^{-j(\beta-\beta_o)L_a}}{\beta-\beta_o}\right|+\left|\frac{1-e^{-j(\beta+\beta_o)L_a}}{\beta+\beta_o}\right|\right] \qquad (7)$$

The first term is recognized as the forward wave for the matched case, Equation (5). The second term is recognized as the backward wave for the matched case, Equation (9) below.

Voltage at Input End and Backward Wave

The wave propagating toward the source or input is given as the backward wave. It is the signal appearing at a detector placed at the input end of the tri-axial unit under matched conditions. The total voltage at the input end is obtained in the same manner as for the forward wave, yielding the following result:

$$e_B(o)=i_1 z_{21}\int_0^{L_a}\left\{\left[1-\frac{Z_F(x)}{Z_2(x)}\right]\cos(\beta_o x)\,e^{-j\beta x}-j\left[\frac{Z_{02}}{Z_2(x)}\right]\sin(\beta_o x)\,e^{-j\beta x}\right\}dx \qquad (8)$$

This is the total voltage across Z_{LB}.

Note that when the external system is matched at both ends, (8) reduces to the backward wave:

$$e_B=j\frac{i_1 z_{21}}{2(\beta+\beta_o)}\left[1-e^{-j(\beta+\beta_o)L_a}\right] \qquad (9)$$

These equations describe the frequency behavior of the tri-axial unit leakage output voltage, and relate this to the surface transfer impedance. The measured result is the ratio of power at output to power input incident on internal cable, and is directly related to e_F/i_1. The transfer impedance, z_{21}, is calculated from this measured result, employing the value for L_a obtained by physical measurement and from known or measured values of the propagation constants β and β_o.

References

1. K. Ikrath, "Leakage of Electromagnetic Energy from Coaxial Cable Structures," Proc. of the Fourth Conf. on Radio Interference Reduction and Electronic Compatibility, pp. 311-357, Oct. 1-2, 1958.
2. D. P. Kanellakos and L. C. Peach, "The Performance of Shielding Materials," Proc. of the Fifth Conf. on Radio Interference Reduction and Electronic Compatibility, pp. 316-341, Oct. 6, 7, 8, 1959.
3. J. D. Meindl and E. R. Schatz, "The External Electromagnetic Fields of Shielded Transmission Lines," Proc. of the Sixth Conf. on Radio Interference Reduction and Electronic Compatibility, pp. 388-405, Oct. 4, 5, 6, 1960.
4. H. Kaden, Wirbelstrome und Schirmung In der Nachrichtentechnik. Springer-Verlag, Berlin, pp. 272-282, (1959).
5. L. Krugel, "Abschirmwirkung Von Aussenleitern Flexibler Koaxialkabel," Telefunken-Zeitung, Jg 29, pp. 256-266, Dec., 1956, heft 114.
6. H. Jungfer. "Die Messung des Kopplungswiderstandes Von Kabelabschirmungen bei hohen Frequenzen," NTZ, Jg 9, pp. 553-560, Aug. 1956, heft 8.
7. J. A. Allen, "A Proposed Standard for Testing the Shielding Effectiveness of Coaxial Cables and Shielding Materials," Proc. of the Sixth Conf. on Radio Interference Reduction and Electronic Compatibility, pp. 372-387, Oct. 4, 5, 6, 1960.
8. Handbook of Microwave Measurements, Vol. I, Polytechnic Inst. of Brooklyn, M. R. I., (1954), Section XI.
9. R. F. Robl and E. R. Schatz, "A Free-Space Method for Measuring Coaxial Cable Shielding Effectiveness," Proc. of the Fourth Conf. on Radio Interference Reduction and Electronic Compatibility, pp. 372-386, Oct. 1, 2, 1958.
10. A. R. Anderson, "Cylindrical Shielding and its Measurement at Radio Frequencies," Proc. IRE, 34, 5, pp. 312-322, May, 1946.
11. L. Krugel, "Mehrfachschirmung Flexibler Koaxial Kabel," Telefunken-Zeitung, Jg 30, pp. 207-214, September, 1957, heft 117.
12. T. Moreno, Microwave Transmission Design Data, 1st Ed., McGraw-Hill Book Co., Inc., New York, p. 96, (1948).
13. S. A. Shelkunoff and T. M. Odarenko, "Crosstalk Between Coaxial Transmission Lines," Bell Sys. Tech. J., Vol. XVI, No. 2, pp. 144-164, April, 1937.

a.) K. E. Gould, "Crosstalk in Coaxial Cables — Analysis Based on Short-Circuited and Open Tertiaries," Bell Sys. Tech. J., 19, 341, (1940).

b.) R. P. Booth and T. M. Odarenko, "Crosstalk Between Coaxial Conductors in Cable", Bell Sys. Tech. J., 19, 358, (1940).

c.) S. A. Shelkunoff, "Electromagnetic Waves," D. Van Nostrand Inc., Princeton, N.J., (1943). (See page 228, Surface Transfer Impedance).

d.) C. G. Montgomery, "Technique of Microwave Measurement," 1st Ed. (1947) McGraw-Hill Book Co., Inc., New York, (1947).

7/16 Connectors and Cable Assemblies


Popular Panel Receptacles Under $6.00


Specialized Reduced Flange Receptacles


Right Angle Receptacles for Medical and Base Station Applications


Male Receptacles Featuring Single Piece Construction


Rugged and Reliable Within Series Adapters


Between Series Adapters Engineered to Maintain Signal Integrity


Quality Dust Caps for Secure Protection From the Elements


Professionally Built and Competitively Priced Cable Assemblies

Performance

Frequency Range:	DC-7.5 GHz
Voltage Rating:	2700 V RMS (sea level)
Nominal Impedance:	50 ohms
DWV:	4000 V RMS @ 60 Hz (sea level)
Insulation Resistance:	10,000 megohms
Temperature Range:	-55°C to +155°C

Materials

Dielectrics:	PTFE Fluorocarbon, Type 1, GR1, CLA
Contacts (Female):	Phosphor bronze
Male Outer Contacts:	Phosphor bronze
Gaskets:	Silicone rubber, Class II, GR 50-60
Other Metal Parts:	Brass per ASTM-B-16

Plating

Center Contacts:	Silver or gold
Metal Parts:	Albaloy or silver

Delivery

Standard Models:	2 to 3 weeks (average)

Custom designs a specialty

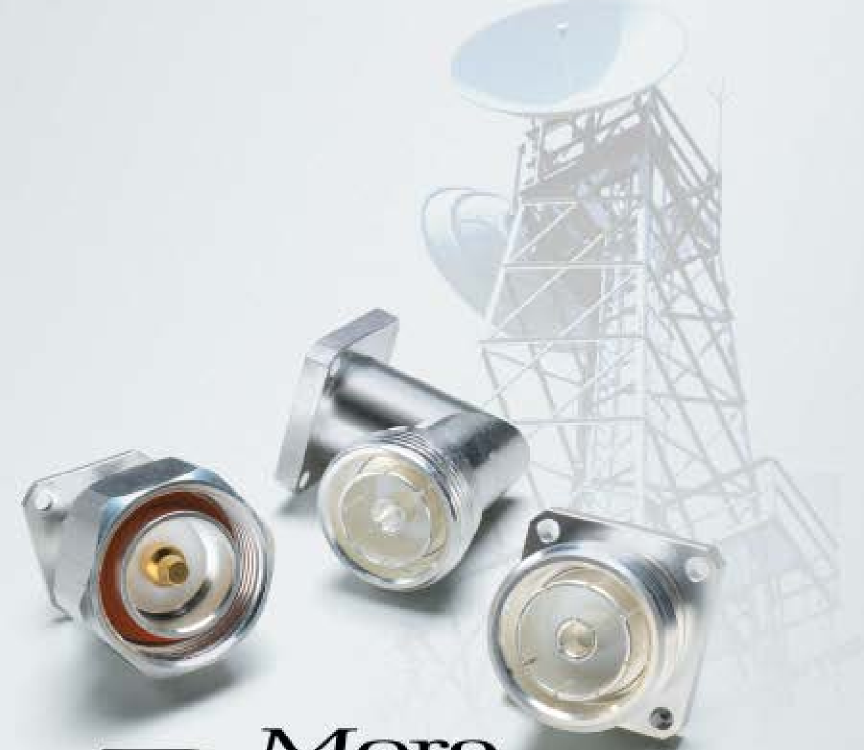

More Power to the Tower

Santron 7/16s are the answer when every dB counts

Innovative design and meticulous machining make Santron 7/16s the only choice for critical signal transmissions. Our 7/16s consistently deliver passive intermodulation performance below -168 dBc. And we use the highest quality materials to ensure our 7/16s perform for a lifetime on towers in even the harshest environments. Compare our 7/16 prices by requesting a quote from our Web site today.

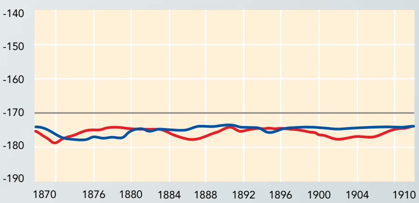

Engage with Santron

San-tron

ISO 9001

www.santron.com

978-356-1585

ROHS compliant

IMPROVING SHIELDING EFFECTIVENESS OF FLEXIBLE COAXIAL CABLES

Early flexible coaxial cables, circa World War II, typically consisted of a bare copper round wire inner conductor, solid or stranded, and a full density extruded polyethylene insulating dielectric making up the core. A copper round wire braid formed the outer conductor. The braid wires could be bare copper or tinned. Silver-plated copper was used for "higher" frequencies. The braiding process consisted of a group of round wires, usually five or six, laid side by side to create a ribbon-like conductor, which in turn was formed into a basket weave to surround the core. This process resulted in an approximately 90 percent coverage of the surface, which was, for the most part, adequate to serve as an outer conductor from an attenuation perspective. Sometimes a second braid was applied over the first braid to obtain better shielding. An extruded polyvinyl chloride jacket completed the cable, providing mechanical protection for the braided outer conductor.

RF transmission lines for government (military) use had achieved a degree of standardization, including a numbering system. RG-/U was the designator, with RG referring to "radio guide."[1] It should be noted here that flexible cables were used then only when necessary and then generally at lower frequencies. Rigid coaxial lines consisting of silver-plated brass or copper tubing and rods were the preferred construction used to carry microwave power, especially at higher frequencies.

In the November 1961 *Microwave Journal* article "RF Leakage Characteristics of Popular Coaxial Cables and Connectors, 500 MC to 7.5 GC" by John Zorzy and R.F. Muehlberger, the state-of-the-art for RF leakage of flexible cables is given as nominally –40 dBc for a single round wire braid, RG-8 and RG-58, and –60 dBc for double braid outer conductors over the frequency range of 500 MHz to 7.5 KMC (GHz). These values were obtained by means of a novel triaxial leakage test unit. Prior to this development, techniques, which were very subjective, consisted of so-called "sniff tests" using a small loop, monopole, or

HARMON BANNING
W.L. Gore & Associates
Elkton, MD

MegaPhase® GrooveTube® Technology

Use GrooveTube® for your ATE or VNA:

For **Consistent Measurements**. Every Time, All The Time.
The **Best Phase and Amplitude Stability**. Period.
Save Money Over OEM Test Cables.

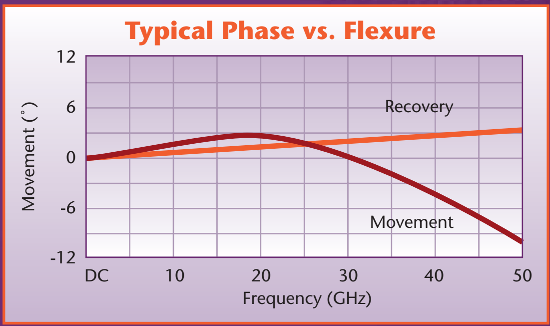

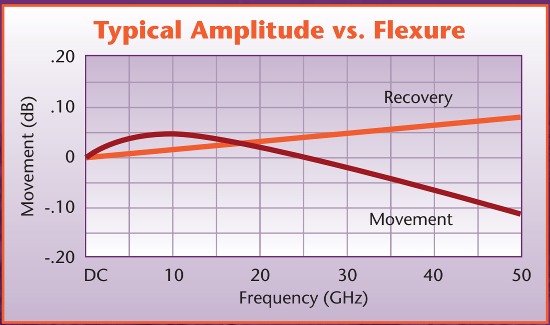

GrooveTube® Test Cable Products

Your Application ➧	VNA High Performance Test Cable	MegaRED™ Bench Test Cable	SightLine™ Field & Prod. Test Cable	Superflex Low Loss Test Cable
MegaPhase® Series	**VN Series**	**TM Series**	**SL Series**	**SF Series**
DC - 4 GHz	VN4	TM4	SL4	SF4
DC - 8 GHz	VN8	TM8	SL8	SF8
DC - 18 GHz	VN18	TM18	SL18	SF18
DC - 26 GHz	VN26	TM26	SL26	SF26
DC - 40 GHz	VN40	TM40	SL40	-
DC - 50 GHz	VN50	TM50	SL50	-
Max. Frequency	50 GHz			26.5 GHz
Inner Conductor	Solid			Stranded
Dielectric	Solid PTFE			PTFE Tape
Outer Conductor	Super-Flexible Copper GrooveTube® by MegaPhase®			
Finished Outer Diameter	0.625 in. 15.88 mm	0.285 in. 7.24 mm	0.500 in. 12.70 mm	0.285 in. 7.24 mm
Ruggedization	Metal Braid over Metal Armor	Metal Braid	Metal Braid over Metal Armor	Metal Braid
Outer Jacket	PET Braid	Polyolefin	Neoprene	Polyolefin
Bend Radius	1.5 in. 38.1 mm	0.5 in. 12.7 mm	1.5 in. 38.1 mm	0.5 in. 12.7 mm
Flexibility Rating – Highest = 5.0	4.0	4.5	4.0	5.0

Repeatable & Consistent Measurements: GrooveTube® is a super-flexible copper outer conductor that maintains its geometry – flexure after flexure. GrooveTube® doesn't cage, kink and fatigue like traditional braid/foil outer conductors. As a result calibrations won't degrade over time.

Superior Phase & Amplitude Stability to 67 GHz: GrooveTube® outer conductor is the industry's best phase & amplitude performance vs. flexure. When flexed, the inner conductor stays dead center.

Cost Savings vs. OEM Test Cables: Save your budget dollars – GrooveTube® test cables eature the lowest cost per measurement: fewer calibrations, longer life and less procurement. MegaPhase® rugged test cables feature precision connectors, ISO-level quality, and fast deliveries.

Broadband Probe Station Adapter

For data on the full line of MegaPhase® products:
MegaPhase.com
1-877-MegaPhase / 570-424-8400
GrooveTube@MegaPhase.com

MegaPhase®

Testing, Connecting, and Enabling Electronic Systems from DC-67 GHz.


MCL B 744
ADP-2-10
MCL A 745
ADPQ-140
MCL B 538
SCA-4-15
MCL
QBA-12
071838
MCL
SBA-2-20
071840
MCL
BP2C
MCL
BPNC

dipole to explore the perimeter of the device (cable in this case) for leakage.

The triaxial cavity, which by the authors' admission did not capture all the modes of leakage present, certainly advanced the technology. They argue most of the energy will probably end up flowing axially along the cable (as in the case of a long wire antenna, ed.) At this point in time, RF leakage was just becoming an issue, as systems were slowly growing in complexity and becoming more sensitive to unwanted RF energy. Interestingly, RG-8 and RG-58 are still available today for low frequency applications such as CATV and communications.

In the early '70s, W.L. Gore & Associates (Gore) was producing a product called Multi-Tet, which began as a ribbonized arrangement of parallel conductors. These conductors, which were individually insulated by wrapping them with full density polytetrafluoroethylene (PTFE) tape, were sandwiched accurately between two layers of PTFE strips. This provided controlled registration of the conductors, allowing the automated connectorization at the terminating ends. As time went on, customers wanted coaxial cables included in these arrangements. These coaxes were made reminiscent of the early cables, although extruded PTFE was becoming more popular because of its higher temperature rating. Gore, on the other hand, was using a PTFE tape wrapping process, as opposed to extrusion, which permitted better impedance control and uniformity. These products were used for low frequency applications—less than 100 MHz.

Gore began experimenting with a "foil" layer as the first shield layer, instead of the traditional braid. The foil was a metallized (aluminum) layer on a polyester tape, which was helically wrapped on the core. It was necessary to run a "drain" wire under the foil to maintain a continuous ground from turn-to-turn, and to allow for termination in the connector. An outer round wire braid held everything together and enhanced the shielding effectiveness. This was a good low frequency solution and was used popularly for intermediate frequency (IF) and digital applications. From a microwave perspective, however, it failed to provide good shielding, lacking the full surround of metal, and also gave rise to poor attenuation and impedance performance.

Fast forward to 1975. The state-of-the-art flexible microwave coaxial cables now consist of a center conductor wrapped with layers of PTFE tape and an outer shield where the individual braid wires have been replaced with ribbons of silver plated-copper foil. Sometimes the PTFE tape was perforated to lower the ε_r, which in turn reduced the attenuation due to a larger inner conductor for a given impedance.

The following equations explain how this comes about.

$$\alpha_t = \alpha_c + \alpha_d = \frac{\Re}{2Z_0} + \frac{GZ_0}{2} \qquad (1)$$

where

$$Z_o = \frac{1}{2\pi}\sqrt{\frac{\mu}{\varepsilon}}\ln\left(\frac{r_0}{r_2}\right) \qquad \Omega$$

$$\Re = \frac{\Re_s}{2\pi}\left(\frac{1}{r_0}+\frac{1}{r_2}\right) \qquad \Omega m^{-1} \qquad (2)$$

$$G = 2\pi\omega\varepsilon_0\varepsilon''\left[\ln\frac{r_0}{r_2}\right] \qquad Sm^{-1} \qquad (3)$$

where

r_0 = radius of the outer conductor, meters
r_j = radius of the inner conductor, meters
μ = $\mu_r\mu_0$, permeability, Henrys/meter
ε = $\varepsilon_r\varepsilon_0$, dielectric constant, Farads/meter
ε'' = loss factor of the dielectric
R_s = skin effect surface resistivity of the conductors, Ω
ω = frequency, radians/second
α_t = total attenuation of a TEM transmission line, Nepers/meter
α_c = attenuation due to conductor loss, Nepers/meter
α_d = attenuation due to dielectric loss, Nepers/meter
= 8.686 (α_c+α_d), dB/meter

Equation 1 shows the attenuation of a coaxial cable consisting of loss due to the finite conductivity of the metallic surfaces and the loss due to energy dissipated in the dielectric materials. It is assumed no significant RF leakage is present. For a given conductivity, from Equation 3 it is seen that RF resistance is inversely proportional to the radii of the conducting surfaces, so bigger is better. Equation 2 shows that for a given impedance, the ratio of these radii is inversely proportional to the square root of the dielectric constant. A lower dielectric constant produces a smaller ratio. For a given outer conductor radius, a larger inner radius will result and attenuation is reduced. A further reduction takes place as the dielectric material is replaced by air. A benefit of the reduced attenuation is that as more signal gets through the cable, less is converted to heat. This allows for higher power handling for a given size of cable.

RF leakage performance with this construction was still hampered by the inability to obtain 100 percent coverage, but the RF performance of the cable had improved such that it is acceptable to at least 12.4 GHz. Hence, a true flexible microwave cable now existed. Stability with flexure was greatly improved and the PTFE provided lower loss and better power handling characteristics. The flat wire "braid" was often wrapped with a metallized plastic tape to reduce RF leakage, but somewhat at the expense of flexibility

At Gore, engineers Roger Kauffman, who had been working with the Multi-Tet cable, and Don Slothour, who had been responsible for the coax cable, began exchanging ideas about ways to improve their products. Semi-rigid cable, with its solid copper tube outer conductor, was clearly the benchmark for shielding but was not very flexible. Hence, the name semi-rigid.

Their exchanges led to the idea of trying to wrap a true foil (silver-plated copper with no plastic tape) over the core. This would emulate the high shielding effectiveness of the semi-rigid cable, but retain the flexibility of the metallized tapes and braid combinations. Another engineer, Howard Arnold, had already developed specialized tape wrappers for placing layers of PTFE tapes on various wire and cable products. These machines gave good control over the on wire properties of the wrapped layers, at the same time offering a lot of flexibility over standard purchased machines. It was thus a relatively easy task to modify the machines to apply the solid foil over the core. This made the process of determining the geometry and tension of the foil considerably easier. A solution was found to satisfy both the "feel" of the cable and its electrical properties. As before, the use of a round wire braid over the foil layer insured the mechanical integrity of the foil layer and later proved to be the key for good connector attachment. But this was just the beginning.

Bob Gore, the son of the company's founders, had found a way to stretch PTFE in a controlled fashion (see ***Figure 1***) such that a uniform structure of "nodes and fibrils" was produced (shown in ***Figure 2***), giving rise to a new and exciting material—expanded PTFE or ePTFE. ePTFE was eventually used to make one of Gore's most popular consumer products: GORE-TEX® Fabric. The microporosity of the ePTFE dramatically altered many of the electrical and mechanical properties of its parent. Notably, for the microwave world, the dielectric constant, ε_r, went from 2.1 to between 1.7 and 1.3, depending on the processing. Loss tangent, tan Δ, was proportionally reduced, depending on the air/PTFE ratio. Fortunately, the excellent temperature and chemical resistant properties of the base PTFE were not degraded.

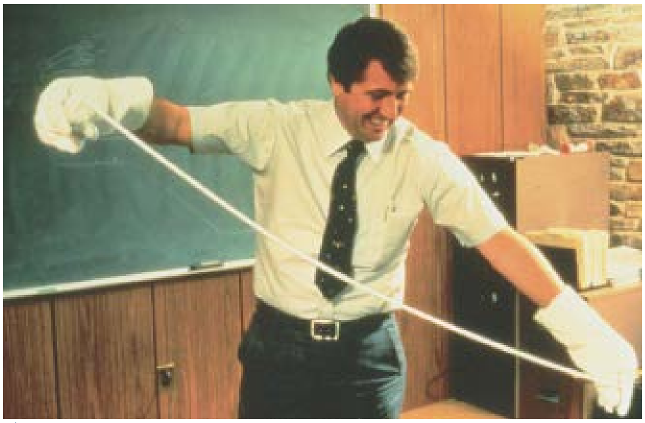

Fig. 1 Bob Gore stretching PTFE.

With this new invention, Gore Associates were looking for ways to utilize the new wonder material. Due to Bill and Vieve Gore's style of leading the enterprise, all ideas were fair game. Ideas from tennis racquet strings to bubblers for aquariums were considered. Bill saw to it that ideas were to be explored for their value on the spot, not just put on a list to be voted on sometime by "management." With this freedom Don and Roger decided to try ePTFE as the core insulator for cable.

Constructing a cable with an ePTFE core and a foil/braid outer conductor was easy; characterizing the resulting product, however, was

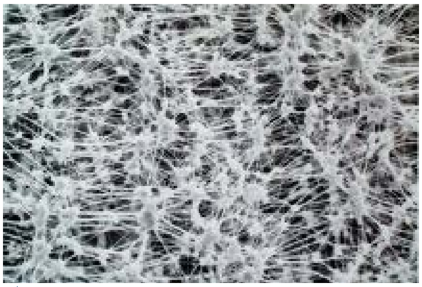

Fig. 2 The "nodes and fibrils" of ePTFE.

not. Finding ways to terminate the resulting product with commercially available connectors for actual sale proved even harder. With the dramatic reduction in ε_r, the ratio of outer/inner diameter (D/d) resulted in problems with respect to connectors. If you chose the inner conductor diameter as a constant, based on standard AWG wire sizes, the outer conductor outgrew everyday connectors. Conversely, holding the outer conductor diameter constant meant the inner conductor became much larger.

The attenuation per unit length of the cable dropped like a rock compared to previous constructions, so it was crucial to make it possible to produce cable assemblies with this product. Don and Roger approached connector manufacturers for help. "When you get to perhaps 100,000 units per year, then we are interested," was the response. But help did come, as one manufacturer saw the potential of the performance improvement, offering to assist. Electromagnetic simulators had not yet been invented, as the computers to support them were either still a dream or busy doing more important things. So it took a lot of cut and try for the new cable configuration to marry up to standard connector interfaces. Succeed, agonizingly, they did, and the Gore Microwave Cable Assembly was born. All cables needed a jacket, or outer protection layer, to protect against abrasion and whatever. The microporous ePTFE further needed protections against fluids. Jacketing material could assume almost any color with the addition of dye components. Black and brown were industry standard. Many colors were tried, but purple provided the best results. It was different—no one was making purple cables. So in 1976 Gore introduced its first purple microwave assembly to the world.

But this new product still had a long way to go to be accepted: "What programs are you on?" "Have you been qualified?" But there were those who saw the value and bought in to the lower loss. Westinghouse put Gore cables in the ALQ-119 and 131 pods, and NRL installed GORE™ Microwave Assemblies in a research satellite. This established Gore as space qualified. Credibility was beginning to happen.

The US Navy was charged with developing a system that could deal with a wide range of targets, both water- and air-based simultaneously with a high degree of precision and mission success. The key to this system was a computerized, passive, electronically steered phased-array radar, the SPY-1A, as the primary source of situational awareness.

The radar was to provide a 360° horizon coverage, be manufacturable, and have 20 year (minimum) lifetime under maritime conditions. Approximately 10,000 microwave cables were required to outfit each destroyer/cruiser system. It was necessary that the system be able to operate over a wide temperature range as a precaution. The ε_r and hence the electrical length vs. tem-

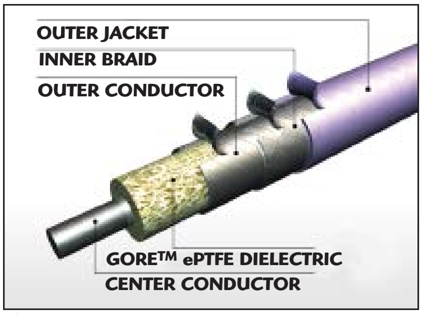

▲ *Fig. 3 Construction of Gore's purple microwave cable.*

perature characteristic of dielectrics can be a killer in phase sensitive situations. The GORE Microwave Assemblies with its ePTFE-based dielectric, and a nominally 70 percent air content, appealed to the engineers at RCA. PTFE, from a microwave perspective, exhibits a large and nonlinear change vs. temperature. Tempering the PTFE with air, as in ePTFE, proportionally reduces this temperature dependency by a factor of 3 or 4 to 1. That is why GORE Microwave Assemblies were chosen for the next generation SPY-1-B upgraded system. Required was that Gore provide a cable assembly with a given electrical length, but that the electrical length (phase vs. temperature) characteristic be reproducible from lot to lot over a long-term production cycle. This was not easy, as product process variability and improvement can be counter-productive. In other words, when you qualify good, bad or indifferent, that is where you are. Gore produces its own ePTFE from resin pellets and has complete control over the entire process. This allows for tailoring the final product based on specific needs. As a result, Gore was able to meet this challenge and provided a significant number of systems before a radical system redesign eliminated the need for flexible cables.

RF leakage, as it was known in 1961, is now characterized as shielding effectiveness (SE). It was not a big issue then. In those early days, systems were generally simple and power levels were low. But that all changed as technology evolved. Satellites grew more complex with dramatic increases in the number of channels and advances in power amplifier technology raised the ambient RF field levels. The triaxial cavity, while able to evaluate short sections of cable or a connector pair, could not predict performance of a full cable assembly, or a cascade of cables and other components. Further, there was a considerable amount of subjectivity, as the cavity had to be manually tuned for each test frequency. Multiline connectors were also difficult to characterize, as they could not conveniently be included within the cavity. Making a larger cavity reduced the upper frequency limit of the test due to higher order modes.

Crawford, Koepke, Jesch, Staeger and Bolinger at the National Bureau of Standards, now the National Institute of Standards and Technology (NIST), undertook the task of providing a test system to specifically solve these problems. The outcome was a system called the mode stirred chamber, which resembles a giant microwave oven (see ***Figure 4***). The test specimen is placed in the chamber, and a mode stirrer, not unlike a Casablanca fan, stirs the modes to ensure a complete exploration of coupled fields.

This proved to be a rigorous test, collecting radiation in all directions and configurations. It was now possible to measure the SE of a wide range of specimens from miniature connectors to entire airplanes, over the frequency range of 1 to 18 GHz. Dynamic range of 130 dB or more is possible with this system. With its own

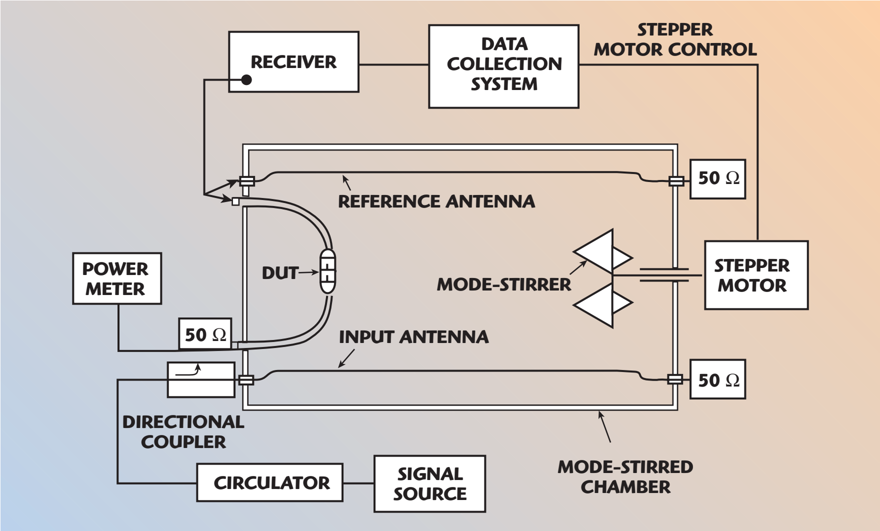

▲ *Fig. 4 Diagram of the mode-stirred SE measurement chamber.*

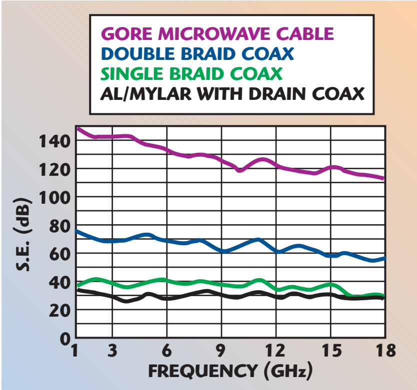

▲ *Fig. 5 Typical shielding performance using test method MIL-STD-1344, method 3008.*

mode stirred cavity, Gore was able to characterize cable assemblies to determine how best to achieve a high level of SE. From this knowledge, it was then possible to fine-tune the elements that make up the barrier to leakage of the GORE Microwave Assemblies. This included foil pitch, cross-section size and shape, and the applied tension.

SE of a new cable right out of the box is a good metric. Going a step further, what happens to a cable after it has been installed or heavily flexed? Gore engineers developed a test system that could pinpoint the source of leakage, even in long cables. With this, they are able to analyze "used" or damaged cable assemblies to determine where the barrier had weakened or outright failed. This information is used to further fine-tune the cable to produce acceptable levels of SE.

The current accepted industry practice for SE is 90 dBc per foot to 18 GHz. Gore cables routinely exceed 110 dBc regardless of length. ***Figure 5*** shows the typical shielding performance for four different coax cable types. Each type differs only in the construction of the cable's outer shield. As shown, a Gore microwave cable provides significantly better shielding than braiding or aluminized mylar approaches because of the helically wrapped foil outer shield.

Connectors are sometimes a different issue, as some are better than others. As an indication of how the needs of the microwave community have evolved over time, the 110 dBc is not always sufficient to satisfy some requirements. It is also interesting to note that the 1961 article speaks of 7.5 GHz as if it were some magic number. (The triaxial cavity is capable of 18 GHz and beyond). Today, we work at 110 GHz and find those who would have cables at 160 GHz. It is fortunate that machine shops have kept pace with the microwave industry needs, and are capable of building some of the things we need. ■

ACKNOWLEDGMENT

The author would like to thank Roger Kauffman for providing information for this article.

Reference

1. G.L. Ragan, *Microwave Transmission Circuits*, McGraw Hill Book Co. Inc., New York, NY, 1948.

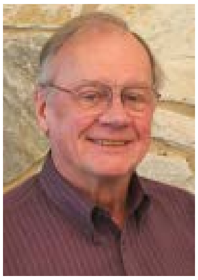

Harmon Banning, *retired Gore Associate, received his BS degree in electrical engineering from the University of Maine in 1961. He had a distinguished career that spanned over 45 years in the RF/microwave industry. He worked for General Electric Co., Andrew Alford Consulting Engineers, Weinschel Engineering Inc. and joined W.L. Gore & Associates in 1987. In November 2007, he was honored with the Automated RF Techniques Group (ARFTG) Career Award.*

FLEX TEST™ CABLES

DC to 18 GHz from $68.95 ea. (qty.1-9) IN STOCK

Strength, ruggedness, and reliability…*supercharged!* That's what you get when you choose Mini-Circuits ultra-flexible precision test cables. Engineered to be a workhorse for your day-to-day test operations, these triple shielded cable assemblies are qualified to at least 20,000 bends, employ an advanced strain relief system, and are equipped with passivated stainless steel connectors, *so you can rely on them to* ***flex, connect and disconnect over and over and over again!*** They're so rugged, each test cable is backed by our 6 month guarantee*! With low insertion loss and very good return loss, you can also rely on getting good performance over the wide DC-18 GHz band. Need them right away? Overnight shipment is available. So make Mini-Circuits your test cable connection! *Mini-Circuits…we're redefining what VALUE is all about!*

Frequency Range: DC-18 GHz, Impedance: 50 ohms

Models	Connector Type	Length (Ft.)	Inser. Loss (dB) Midband Typ.	Return Loss (dB) Midband Typ.	Price $ ea. Qty.(1-9)
Male to Male					
CBL-1.5FT-SMSM+	SMA	1.5	0.7	27	68.95
CBL-2FT-SMSM+	SMA	2	1.1	27	69.95
CBL-3FT-SMSM+	SMA	3	1.5	27	72.95
CBL-4FT-SMSM+	SMA	4	1.6	27	75.95
CBL-5FT-SMSM+	SMA	5	2.5	27	77.95
CBL-6FT-SMSM+	SMA	6	3.0	27	79.95
CBL-10FT-SMSM+	SMA	10	4.8	27	87.95
CBL-12FT-SMSM+	SMA	12	5.9	27	91.95
CBL-15FT-SMSM+	SMA	15	7.3	27	100.95
CBL-2FT-SMNM+	SMA to N-Type	2	1.1	27	99.95
CBL-3FT-SMNM+	SMA to N-Type	3	1.5	27	104.95
CBL-4FT-SMNM+	SMA to N-Type	4	1.6	27	112.95
CBL-6FT-SMNM+	SMA to N-Type	6	3.0	27	114.95
CBL-15FT-SMNM+	SMA to N-Type	15	7.3	27	156.95
CBL-2FT-NMNM+	N-Type	2	1.1	27	102.95
CBL-3FT-NMNM+	N-Type	3	1.5	27	105.95
CBL-6FT-NMNM+	N-Type	6	3.0	27	112.95
CBL-15FT-NMNM+	N-Type	15	7.3	27	164.95
CBL-20FT-NMNM+	N-Type	20	9.4	27	178.95
CBL-25FT-NMNM+	N-Type	25	11.7	27	199.95
Female to Male					
CBL-3FT-SFSM+	SMA-F to SMA-M	3	1.5	27	93.95
CBL-2FT-SFNM+	SMA-F to N-M	2	1.1	27	119.95
CBL-3FT-SFNM+	SMA-F to N-M	3	1.5	27	124.95
CBL-6FT-SFNM+	SMA-F to N-M	6	3.0	27	146.95

Custom sizes available, consult factory.

SMA Female　SMA Male　N-Type Male

RoHS COMPLIANT

6 mo. GUARANTEE

Mini-Circuits will repair or replace your test cable at its option if the connector attachment fails within* ***six* *months of shipment. This guarantee excludes cable or connector interface damage from misuse or abuse.*

Mini-Circuits®
ISO 9001 ISO 14001 CERTIFIED

ALL NEW minicircuits.com

P.O. Box 350166, Brooklyn, New York 11235-0003 (718) 934-4500 Fax (718) 332-4661 For detailed performance specs & shopping online see Mini-Circuits web site

YONI2™ Patent Pending ***The Design Engineers Search Engine*** *Provides ACTUAL Data Instantly From MINI-CIRCUITS At:* ***www.minicircuits.com***

IF/RF MICROWAVE COMPONENTS

403 Rev J

50 GHz End Launch Connector Test Boards

The description of the development of coax to grounded coplanar launches and through lines on 30 mil Rogers 4350 material.

For many years Southwest Microwave has manufactured field replaceable connectors and launch accessories where connector performance was easily verified by measuring two connectors back-to-back as a two-port device. The responsibility for packaging and board layout fell to the user to develop independently.

With the introduction and success of Southwest Microwave end launch connectors, the packaging responsibility has fallen to Southwest Microwave; the user is now only responsible for board layouts. To assure maximum performance of the Southwest Microwave end launch connectors, equally high performance test boards were needed to accurately measure the connectors.

In the pursuit of high performance test boards, it was decided to broaden the research project and begin a comprehensive study of board layout design variables and their effects on microwave performance. This evaluation on 30 mil Rogers 4350 material explores transitions of grounded coplanar waveguide (GCPWG) and microstrip lines to coaxial connectors with the use of Southwest Microwave end launch connectors. The baseline for the GCPWG portion of this study is an older board design that worked reasonably well to 45 GHz. The use of 3-D simulation was included in this evaluation.

Fig. 1 Southwest Microwave's end launch connector.

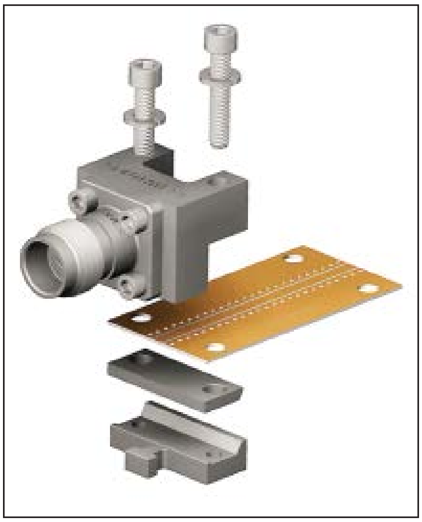

END LAUNCH CONNECTORS

The connectors used are Southwest Microwave end launch connector assemblies, model number 1492-02A-5 (see ***Figure 1***). These connectors were designed for single-layer and multi-layer boards where the top layer is the microwave layer. The 1492-02A-5 has a 2.4 mm female connector and a transition block with a 10 mil diameter circuit launch pin and a 63.5 mil diameter coaxial ground. Because they were for multi-layer boards, there is a 20 mil overhang of the ground over the board to catch the top ground of the board which is useful for single-layer GCPWG.

No soldering is needed to connect the end launch connectors to a board due to a slight interference fit between the circuit pin and the board to ensure good contact. This means that the connector can be re-used. All of the

BILL ROSAS
Southwest Microwave Inc.
Tempe, AZ

data in this study (over 30 boards) was taken with the same two connectors.

TEST EQUIPMENT AND TECHNIQUES

An Agilent 8510D network analyzer was used for all of the published measurements. The test port connectors used were 2.4 mm connectors and the frequency range for all measurements was DC to 50 GHz. Calibration was a full 12-term SOLT calibration with sliding loads. The TDR measurements were set up as low pass step in real units. All of the data was taken from the same calibration.

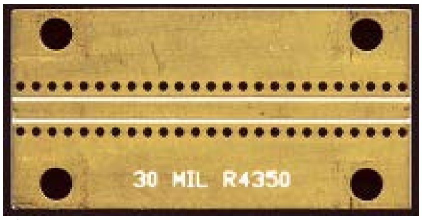

▲ *Fig. 2 The original 30 mil coplanar test board fabricated in 2003.*

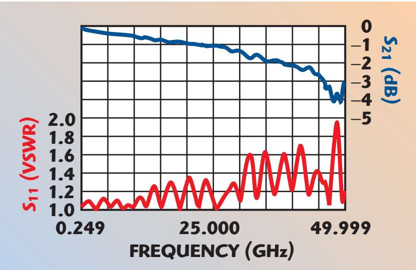

▲ *Fig. 3 Test data of the original 30 mil GCPWG test board.*

Some internal verification of data was done on an Anritsu 37297 network analyzer.

REVIEW OF ORIGINAL TEST BOARD (2003)

When the end launch connectors were first introduced in 2003, a one-inch long GCPWG test board was developed for testing (see ***Figure 2***). One of these original test boards was used in this study to establish the baseline performance of the connectors. The results of the original end launch connector test board, displayed in ***Figure 3***, shows a glitch in the loss starting at 45 GHz that is characteristic of this board.

3-D SIMULATION OF THE ORIGINAL TEST BOARD

CST MWS Model

3-D simulation models have promise to be useful tools in developing good transitions from coaxial lines to coplanar or microstrip lines. With this hope in mind models were worked out for many of the line structures and some results are shared in this article.

Simulation is used to predict results of these types of structures then changes are made and the results of that change are viewed without having to fabricate and test actual hardware. CST Microwave Studio® (CST MWS) was used for many of the simulations in this study and CST provided the simulations.

The 3-D simulation model is created by only looking at the transition blocks and the test board; the connectors are not part of the simulation (see ***Figure 4***). The biggest discontinuity in the transmission line is the transition from coax to PCB and the worst transmission line is the PCB itself. The two coaxial connectors are well matched and have very low loss, so even without them in the simulation a very good correlation to the actual performance can be achieved.

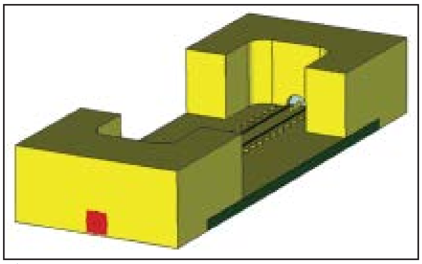

▲ *Fig. 4 The CST MWS model without connectors.*

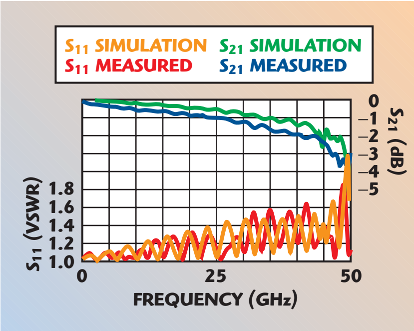

▲ *Fig. 5 Simulation of the original test board compared to actual measured data.*

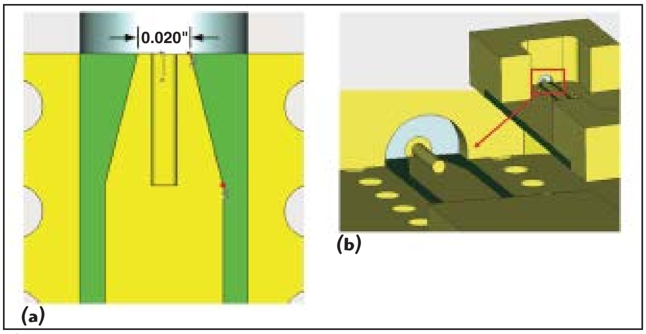

▲ *Fig. 6 Version 1 taper top view (a) and 3-D view (b) of the launch pin on the center trace.*

Simulation Results

The simulation results displayed in ***Figure 5*** show the insertion loss has a dip at 45 GHz and the VSWR slowly rises over frequency from below 1.2 to 1.6 through 45 GHz. Both of these are characteristic of the test board and show good correlation of simulated to measured.

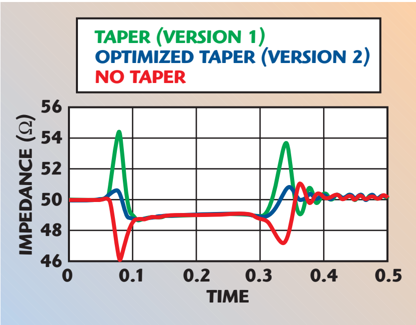

▲ *Fig. 7 TDR simulation showing the discontinuity from the pin sitting on the board (no taper shows capacitive, version 1 taper is inductive and version 2 taper is an optimized transition from connector to board).*

UNDERSTANDING THE IMPORTANCE OF THE LAUNCH TO A GCPWG

Determination of the Optimal Launch (Taper)

At the end of the board where the launch from the board's microwave transmission structure to a coaxial line occurs, there is a pin from the coax sitting on top of the board. This added metal creates an increase in capacitance that has to be addressed for optimal performance. The way to compensate for the capacitance of the pin is to add inductance to the board. This can be done in both microstrip and GCPWG by narrowing the trace. The method used here is reducing the trace in what is referred to as a taper.

This is the first study by Southwest Microwave where the taper of GCPWG is examined in detail. The traditional way a taper was determined was to match the width of the trace with the coax launch pin, then taper it out to the proper microstrip width over the distance that the pin sits on the line (see ***Figure 6***). For the model 1492-02A-5 the through pin is 0.020" so the end of the taper is 0.020" to match it. It has been shown in earlier test boards that this may be over-compensating for the capacitance, so the CST MWS 3-D model was again used to get a prediction. The result of the simulation showed this taper makes the launch inductive and the performance is actually worse than having no taper at all (see ***Figure 7***).

Optimized Taper (Version 2)

The second taper design, shown in ***Figure 8***, was developed using CST Microwave Studio's optimization routine. The taper length was kept the same, but the final dimension at the edge of the board was the variable in the optimization and it was increased to 0.033". This still adds some inductance to the board right at the launch, but it is less inductive than the first taper design. The simulation and actual data show improved results for S_{11} and the insertion loss is very smooth up to the normal 45 GHz glitch always seen (see ***Figure 9***).

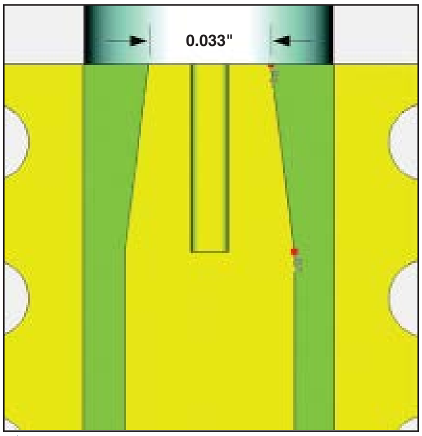

▲ *Fig. 8 Optimized taper (version 2) top view showing the launch pin sitting on the center trace with the second taper.*

IMPROVING BANDWIDTH: MYSTERY OF THE VIAS

After optimizing the match, the bandwidth was studied. It has been assumed the vias played a role in bandwidth, but there was no clear explanation of what that role was exactly.

Channelized Coplanar Waveguide

While doing research into proper via placement, a reference to channelized coplanar waveguide (CPW)[1] was found that explained the function of the vias as it related to bandwidth (see ***Figure 10***). Channelized coplanar waveguide is a GCPWG structure with lateral walls that create another waveguide mode and stops surface wave inside the structure from being created.

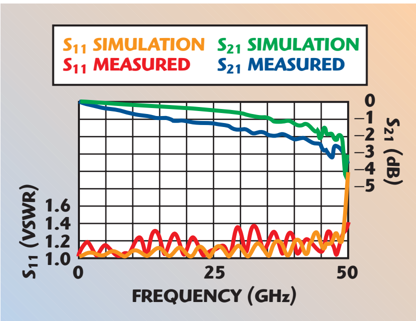

▲ *Fig. 9 Simulation of the optimized taper compared to actual measured data.*

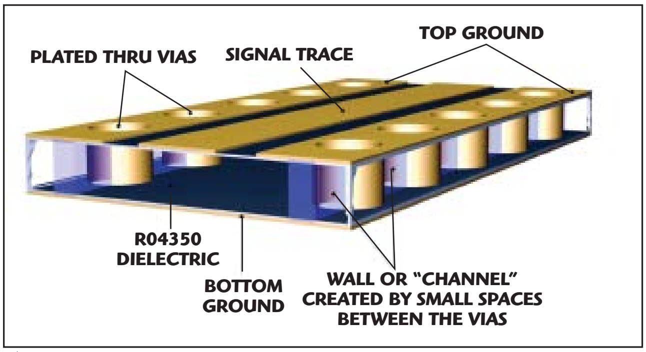

▲ *Fig. 10 3-D schematic of channelized coplanar waveguide realized by GCPWG with closely spaced vias.*

Purpose of the Vias

Once it was determined that placing lateral walls would increase the bandwidth of the circuit and that the vias were acting as a microwave wall, the spacing of the vias became more predictable. In general, microwave energy will reflect from openings less than a quarter wavelength of the signal.

The other determining factor in the high frequency performance of the vias is the spacing between the rows of the vias. The wider the spacing, the lower the cut-off frequency and the closer the spacing the higher the cut-off frequency.

Realization of Lateral Walls by Closely Spaced Vias

The illustration in Figure 10 shows the GCPWG used for these test boards. Rows of plated through vias are used to tie the top ground planes to the bottom ground plane, simulating a wall as shown in shadow between the vias. Microwave energy will not pass through spaces that are less than a quarter wavelength of the frequency, so the spacing between the vias becomes the critical dimension.

Analysis of Spacing Between Vias

The original test board shows the VSWR gently increasing over frequency through 50 GHz. This increase in VSWR is due to the match and as seen in the previous section can be addressed by introducing a taper at the launch.

The insertion loss is fairly smooth until 45 GHz. The reason for the glitch at 45 GHz is a function of the vias. The original test board has 25 vias of 0.020" in diameter and equally spaced at 0.040" centers. Since the purpose of the vias is to create a "wall," the important dimension of the vias is the space between the vias, or the dimension from the edge of one via to the edge of the next via. For this board the spacing is 0.029", which in RO4350 with a dielectric constant of 3.66 corresponds to a quarter wavelength frequency of 53 GHz. The via rows spacing is 0.112" and is also a determinant in the performance of the board. Again, closer spacing should lead to higher frequency operation.

To test this theory a series of additional boards with 3, 7 and 13 vias were made and tested. With only 3 vias on a one-inch board, the spacing between the vias is 0.460". The quarter wavelength frequency in RO4350 is 3 GHz. The board operates without any glitches to 5 GHz, so there is some correlation shown.

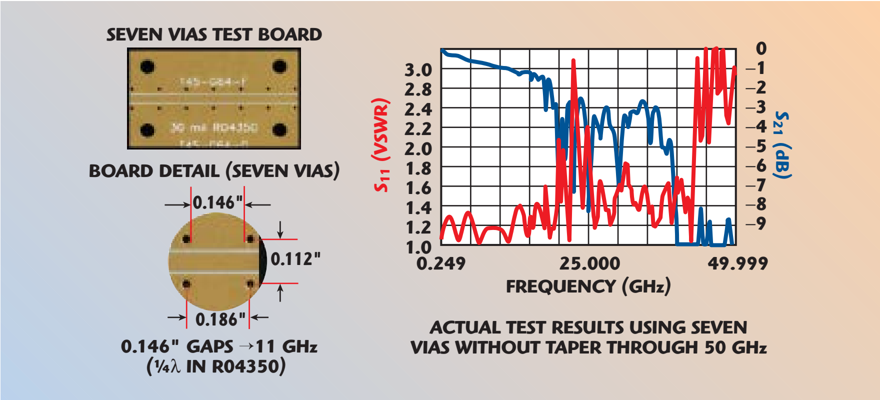

▲ *Fig. 11 The seven-via test board corresponding to a λ/4 spacing at 11 GHz and showing a first glitch at 13 GHz.*

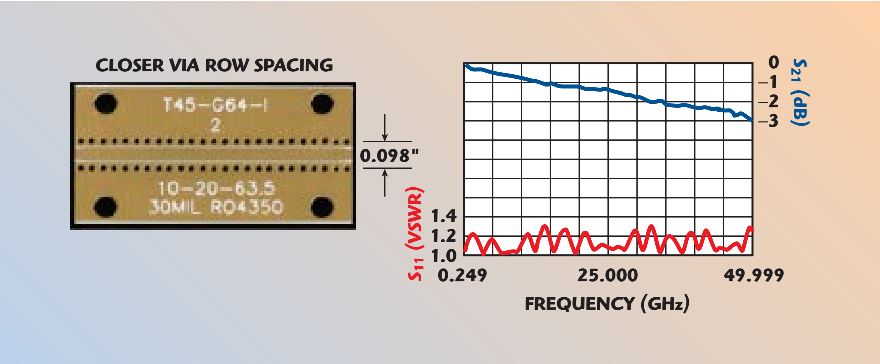

▲ *Fig. 12 Final test board including the optimized tapered trace to improve the match demonstrating that by moving the via rows closer increases the bandwidth to over 50 GHz.*

With seven vias on a one-inch board, the spacing between the vias is 0.146" (see ***Figure 11***). The quarter wavelength frequency in RO4350 is 11 GHz. The board operates without any glitches to 13 GHz, so there is more correlation shown and a clear improvement as the vias are added and the spacing between the vias is decreased.

With 13 vias on a one-inch board, the spacing between the vias is 0.0683". The quarter wavelength frequency in RO4350 is 23 GHz. The board operates without any drastic glitches to 35 GHz, so there is even more correlation shown and a clear improvement as vias are added and the spacing between the vias is decreased.

Analysis of Spacing Between Via Rows

It has been seen in the previous boards that they will work somewhat above the quarter wavelength frequency, so the original board has a via space corresponding to 53 GHz and it should work easily to 50 GHz. There is still the glitch at 45 GHz, so there must be some other factor involved.

It has been speculated that making the rows closer will increase the bandwidth of the board. To determine the effect of the row spacing a board was made where the rows were moved out to 0.126" from the original 0.112". The first glitch in insertion loss moved to below 40 GHz so a wider spacing does show a degradation in performance.

The original test board had a spacing from the centers of the rows of 0.112". A reduction of this spacing should increase the frequency response of the board. A distance of 0.098" was chosen as it was the closest spacing to the coplanar structure that could be achieved in normal board manufacturing processes.

The data from the test board with a 0.098" spacing, shown in ***Figure 12***, confirms the increased bandwidth of the board and the loss curve is smooth through 50 GHz. This final result shows that GCPWG can create boards with much higher frequency performance than what microstrip may be limited to on the same material.

CONCLUSION

This study was conducted by Southwest Microwave to evaluate grounded coplanar waveguide (GCPWG) launches and lines, top ground (coplanar) launches to microstrip lines, and microstrip lines running straight to the edge of the board on 30 mil Rogers 4350 boards. This article only includes the material related to GCPWG and has shown how to improve match and bandwidth on GCPWG. Hopefully this study, the complete version of which includes microstrip lines and an analysis of loss, has been helpful to board designers working at microwave frequencies to have a better understanding of launch and transmission line structures. Contact Southwest Microwave for more information. ■

ACKNOWLEDGMENTS

The mechanics of the layouts were done by a consultant (Petra Microwave) and the boards were fabricated by Accurate Circuit Engineering in Southern California. The material was supplied as samples by Petra Microwave® Ltd., Rogers Corp.,® CST®-Computer Simulation Technology and CST Microwave Studio® 2006. All are registered trademarks of their respective companies.

References

1. R.N. Simons, *Coplanar Waveguide Circuits, Components and Systems*, Wiley-Interscience, John Wiley & Sons Inc., New York, NY, 2001.
2. B. Rosas, "50 GHz End Launch Connector Test Boards: The Description of the Development of Coax to Grounded Coplanar Launches and Through Lines on 30 mil Rogers 4350 Material with Comparison to Microstrip," *DesignCon 2008*.

Bill Rosas *holds his BSEE degree from Arizona State University, specializing in microwaves, and his MBA degree from the University of Phoenix. He is the product engineering manager at Southwest Microwave, responsible for engineering on all standard interface connector products. He joined the company in 2003 as a senior product sales specialist. While in that position he became the acting product manager for the end launch connector product line. Creating test methods for end launch connectors led him to this ongoing study of launch structures and transmission lines. He has 15 years of experience in the microwave industry, including applications engineering positions at Rogers Corp. (high frequency capacitors) and Giga-tronics (test equipment).*

A 7-16 COMPOSITE FLANGE RECEPTACLE

The telecommunications market is dynamic, constantly evolving and requiring significant product innovation in order to meet the demands of the 21st century. To do so manufacturers must react to market needs and possess the expertise to instigate innovative processes, while also maintaining competitiveness. This is the approach taken by Radiall, which has aligned its strategy around these key issues and given priority to innovation in the development of its new 7-16 composite flange receptacle.

INTERMODULATION

The starting point for development was the fact that in modern mobile telecommunications systems it has become a basic requirement to use passive components that do not generate third-order passive intermodulation products for all pieces of equipment from the antenna to the duplexer. Many studies have been completed by research labs and connector manufacturers to identify and quantify the various sources of nonlinearity, which can be generated by a passive component.

Their findings show that the materials, plating, contact pressure at the piece-part junctions, current line deviations, contact cleanliness and contact types all have a very strong impact on the generation of passive intermodulation products.

SINGLE-PIECE DESIGN

The resulting design modifications from these studies have been implemented, year after year, on the 7-16 connector series, which has become the connector that is most frequently used when a stringent intermodulation requirement is imposed. It is a low IM 7-16 flange receptacle design in a single-piece body that utilizes silver-plating for all metal parts and features strong attachment of the insulator and center contact into the body that effectively prevents any movement. It was also seen as important to address the weak point of conventional connectors, namely the connector attachment to the equipment panel.

RADIALL
Paris, France

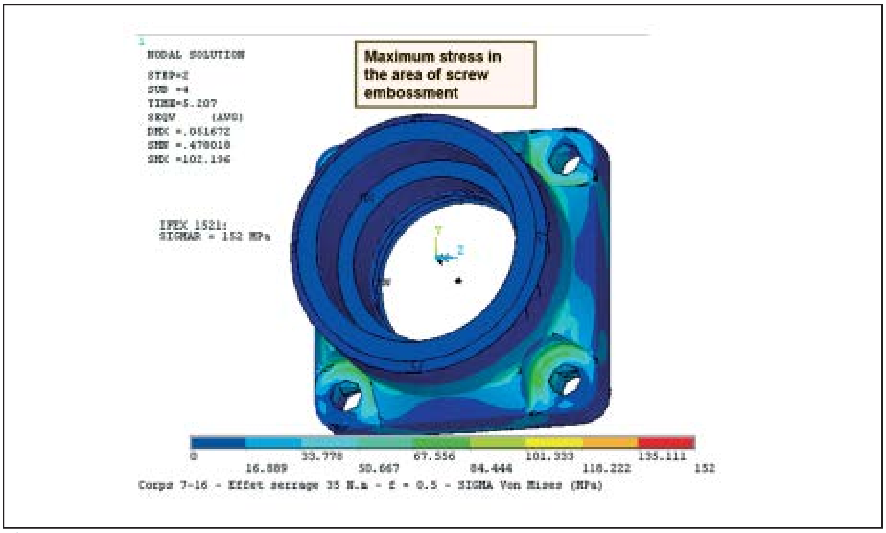

▲ *Fig. 1 Stress calculation illustrating the effect of tightening the flange screws.*

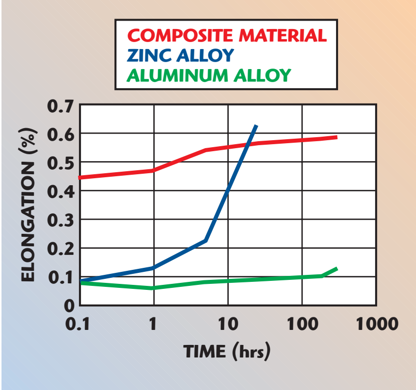

▲ *Fig. 2 Comparison of creeping behavior of different materials.*

Basically, the use of four screws to attach the flange to the equipment creates pressure distribution on the electrical contact joint that is directly dependent on the distance between the contact and the screws. In short, contact junction pressure is uneven and this irregular contact pressure is significantly amplified when screw torques are unequal. ***Figure 1*** shows a stress calculation, illustrating the effect of tightening the flange screws. In order to minimize this problem, connector manufacturers have increased the pressure by reducing the contact surface by confining it to around the coaxial line. This approach makes the problem less acute, but does not eliminate it.

NEW DESIGN

In order to fully eradicate this problem, Radiall has introduced a new receptacle concept whereby the contact pressure on the equipment side is generated by pressure applied by the 7-16 plug. Consequently, when a plug is mated to the receptacle, the tightening torque is diverted by the thread system into an axial force that is applied to the reference plane with the result being that the pressure on both contact junctions is equally distributed.

Effectively, the entire force generated by the tightening torque is efficiently transformed and used as an axial force on the contact junctions at the reference plane and panel junction. This improves the intermodulation level and its stability.

Through this concept, the receptacle body is only used as a mechanical support, which guides the reduced mass contact and no longer has an electrical function. This new degree of freedom has the added advantage of enabling the use of different materials that can be selected to offer certain features and meet specific practical needs.

MATERIAL SELECTION

In deciding on the material for the 7-16 composite flange receptacle, the main considerations were it had to be very lightweight, have high corrosion resistance and be colorable to enable color coding. Material selection was also based on:

- Material stiffness—Young's modulus
- Yield limit
- Ultimate strength
- Temperature range
- Creeping speed and stress relaxation
- Thermal dilatation coefficient
- Sensitivity to harsh outdoor environments—corrosion, UV ageing, humidity, etc.
- Flammability rating
- Density
- Price

As an example, ***Figure 2*** gives a comparison of the creeping behavior of different materials.

Taking all of these factors into consideration, an in-depth analysis revealed that the use of a composite material would meet these requirements and offer considerable advantages, including a weight reduction of more than 50 percent. Not only does the weight reduction of the components reduce the overall weight of the final module (power amplifiers, filters, etc.), but also reduces transportation costs. When the overall cost of ownership is considered, the company claims an improvement in cost at all levels, resulting in a more competitive overall solution. Components are often required to operate in harsh environments so the composite material's corrosion resistance is a key advantage for many applications.

CONCLUSION

Aimed at the telecommunications industry and based on the company's expertise in the RF field, the new 7-16 composite flange receptacle incorporates a design concept and composite materials that significantly reduce the generation of third-order passive intermodulation products. In addition, the product is easy to install and significantly reduces the total cost of ownership for customers.

Radiall,
Paris, France, +33 1 49 35 3535,
www.radiall.com.

RS No. 302

Cables & Connectors Supplement
Literature Showcase

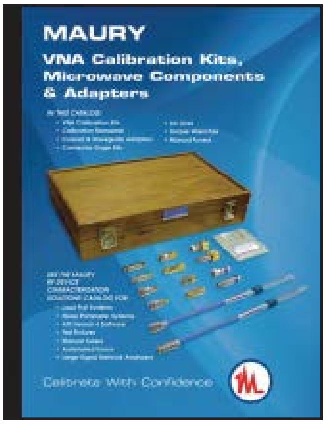

Components Catalog

Maury has a 146-page catalog covering the company's entire line of precision coaxial and waveguide VNA calibration kits, microwave components and adapters, manual tuners, torque wrenches and connector gage kits. Entries feature detailed specifications, dimensional drawings, photographs, flange diagrams, ordering information and key reference materials. The catalog provides everything engineers need to find the best components for their applications. An interactive version of the catalog is available at the company website.

Maury Microwave Corp.,
Ontario, CA (909) 987-4715, www.maurymw.com.

RS No. 325

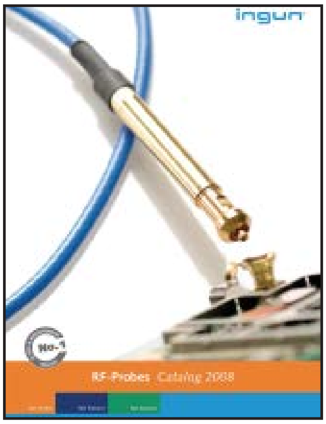

RF Test Probes

The new RF Test Probe catalog from INGUN Prüfmittelbau GmbH is a unique and time-saving reference manual and therefore a global innovation on the radio-frequency market. The plug/jack register guides you to the recommended RF test probe for your application. With just one step, engineers can find the matching solution. The catalog shows the special variants and the application versatility of INGUN RF test probes for 2, 4 and 6 GHz applications.

INGUN Prüfmittelbau GmbH,
Konstanz, Germany +49 7531 8105-62, www.ingun.com.

RS No. 326

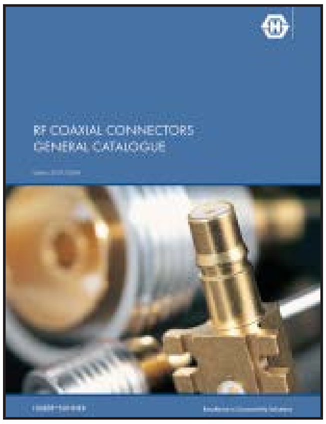

Coaxial Connectors

The 2007/2008 Huber+Suhner coaxial connectors general catalog is now available. The company is a leading supplier of RF connectors for signal (voice and data) transmissions, with many years of experience engineering and producing coaxial connectors. Standard connectors, and those designed according to customer specifications, are used in a diverse range of applications.

Huber+Suhner AG,
Herisau, Switzerland +41 71 353 4111, www.hubersuhner.com.

RS No. 327

Coaxial Cable Assemblies

MegaPhase designs and manufactures high frequency precision coaxial cable assemblies to 67 GHz for test and system applications. MegaPhase products are space qualified and have military heritage. The Warrior cable is a rugged, field proven RF antenna cable for electronic countermeasures with over 80,000 cables fielded. The VN Series Test Cable is a low-cost alternative to OEM test cables. Low loss, and phase and amplitude stability are expected from MegaPhase products. To get a full catalog, go to the MegaPhase website.

MegaPhase LLC,
Stroudsburg, PA (570) 424-8400, www.megaphase.com.

RS No. 328

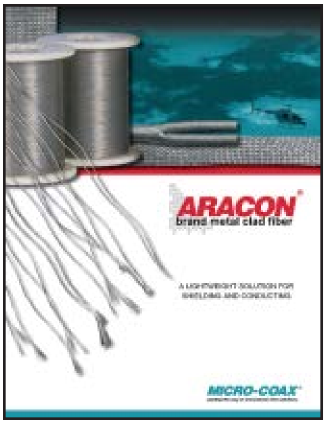

Metal-clad Fiber

Available only from Micro-Coax, ARACON® brand metal-clad fibers combine the conductivity of an outer metal coating with the strength, lightweight and flexibility of aramid fibers. Braided into an overbraid or shield, ARACON fibers offer superior performance against electromagnetic interference while yielding a 50% or greater weight savings over braided copper wire.

Micro-Coax,
Pottstown, PA (610) 495-0110, www.micro-coax.com.

RS No. 329

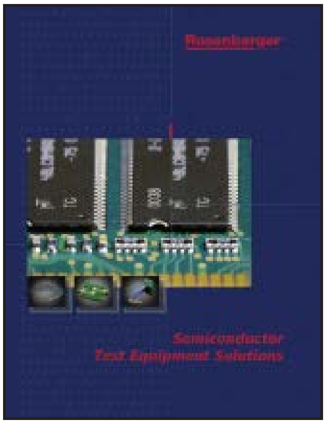

Semiconductor Test Equipment

Rosenberger's new brochure contains detailed information on its newly developed products for the semiconductor test equipment market. Test products such as microwave pogo assemblies and RF-PCB connections—for versatile applications up to 40 GHz—can be used in numerous configurations to achieve the density and frequency requirements of new chip testing devices. Rosenberger's full product range includes RF-coaxial connectors in all common worldwide standards.

Rosenberger,
Fridolfing, Germany + 49-86 84-18 0, www.rosenberger.de.

RS No. 330

CABLES & CONNECTORS SUPPLEMENT
Literature Showcase

Coaxial Surge Protectors

Spinner has completely revised its product catalog of coaxial surge protectors and now offers an extended premium choice of different protection elements for coaxial systems. It covers all relevant RF applications for which a surge protection is necessary. Spinner connector and cable assemblies are used worldwide in a large variety of communication facilities. The company offers a broad range of cost-efficient standardized products as well as specialized solutions for the most diverse applications.

Spinner GmbH,
Munich, Germany +49 89 12601-0, www.spinner.de.

RS No. 331

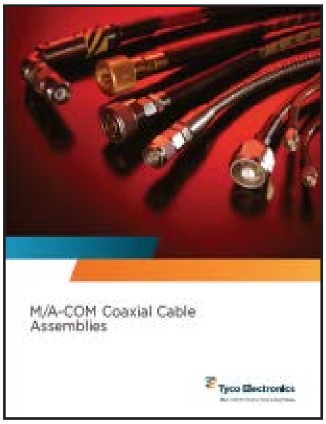

Coaxial Cable Assemblies

M/A-COM's coaxial cable assemblies catalog covers high performance products for electronic warfare, space, commercial aviation, test and special purpose applications. It includes selection guides, datasheets, insertion loss graphs, adaptors, connectors and application notes. More information is available at the company website.

Tyco Electronics, M/A-COM Products,
Lowell, MA (978) 442-5000, www.macom.com/cables.

RS No. 332

Semi-rigid Cable Products

This new data sheet features the company's Maximizer line of high performance semi-rigid cable products, available as custom assemblies, straight lengths, or coils. Options include phase stable, low loss Maximizer Gold products and low loss, RG replacement Maximizer Silver products. The data sheet includes mechanical and electrical product specifications; IL, phase vs. temperature and power handling graphs; and design considerations.

Teledyne Storm Products,
Woodridge, IL (630) 754-3361, www.stormproducts.com.

RS No. 333

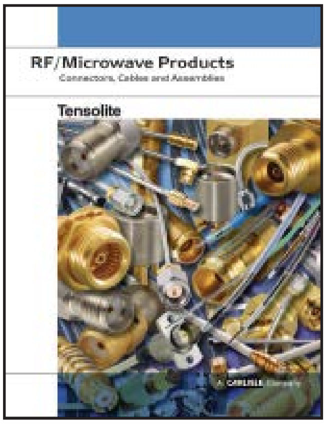

RF/Microwave Products

Tensolite's Connectors, Cables and Assemblies catalog is a reliable resource for high performance interconnect products. Renowned for quality and service, the products in this catalog display the wide range available to choose from for next generation systems. Vertical integration and extensive manufacturing capabilities ensure that quality and on-time delivery are never compromised.

Tensolite Co.,
St. Augustine, FL (904) 824-6706, www.tensolite.com.

RS No. 334

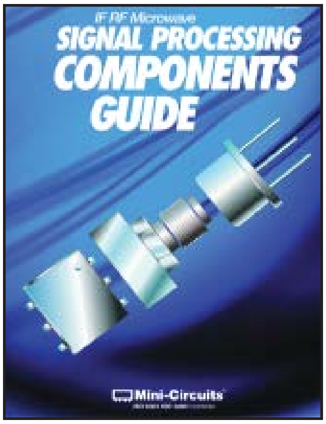

Signal Processing Components

This 144-page catalog offers comprehensive listings of RF, IF and microwave components with essential performance specifications for each product. In addition to the extensive component data, the catalog also provides a listing of Mini-Circuits' patents and the product model numbers to which they apply, as well as a complete listing of the National Stock Number (NSN) Guide for Mini-Circuits' considerable component collection.

Mini-Circuits,
Brooklyn, NY (718) 934-4500, www.minicircuits.com.

RS No. 335

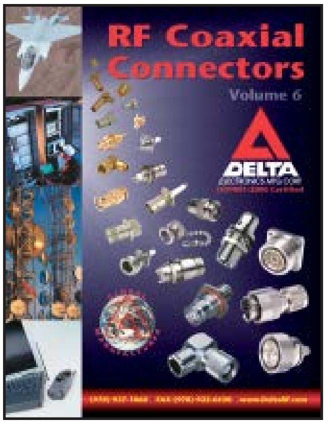

RF and Microwave Connectors

Volume 6 of Delta Electronics Manufacturing's full-line catalog contains over 200 pages of information on over 30 series of RF and microwave connectors, ranging in size from microminiature to large, high-power connectors. Along with common connector types, the catalog features many hard-to-find series, and a large selection of MIL-PRF-39012 QPL connectors and MIL-PRF-55339 qualified adapters.

Delta Electronics Manufacturing,
Beverly, MA (978) 927-1060, www.DeltaRf.com.

RS No. 336

Cables & Connectors Supplement

Advertiser Index

RS No.	Advertiser	Page No.	Phone	Fax	Web Address
1	Amphenol RF	13	800-627-7100	203-796-2032	http://mwj.hotims.com/16584-1
2	Delta Electronics Mfg. Corp.	COV 4	978-927-1060	978-922-6430	http://mwj.hotims.com/16584-2
4	ESM Cable Corporation	31	209-892-3347	209-892-3348	http://mwj.hotims.com/16584-4
5	Huber + Suhner AG	11	+41 (0)71 353 41 11	+41 (0)71 353 45 90	http://mwj.hotims.com/16584-5
6	Ingun Prufmittelbau GmbH	17	+49 7531 8105-0	+49 7531 8105-65	http://mwj.hotims.com/16584-6
7	M/A-COM, Inc.	5	800-366-2266	978-442-5350	http://mwj.hotims.com/16584-7
8	Maury Microwave Corporation	COV 2	909-987-4715	909-987-1112	http://mwj.hotims.com/16584-8
9	MegaPhase	21	877-MegaPhase		http://mwj.hotims.com/16584-9
10	Micro-Coax Components	7	800-223-2629	610-495-6656	http://mwj.hotims.com/16584-10
	Microwave Journal	26,41	800-225-9977	781-769-5037	www.mwjournal.com
11,12	Mini-Circuits	22–23,29	718-934-4500	718-332-4661	http://mwj.hotims.com/16584-11
13	RF Cable Assembly, Division of RF Industries	28	800-233-1728	858-549-6340	http://mwj.hotims.com/16584-13
14	Rosenberger	15	+49-8684-18-0	+49-8684-18-499	http://mwj.hotims.com/16584-14
3	Sabritec	25	949-250-1244	949-250-1009	http://mwj.hotims.com/16584-3
15	Santron Inc.	19	978-356-1585	978-356-1573	http://mwj.hotims.com/16584-15
16	Spectrum Elektrotechnik GmbH	39	+49-89-3548-040	+49-89-3548-0490	http://mwj.hotims.com/16584-16
17	Spinner GmbH	35	+49 89 12601-257	+49 89 12601-287	http://mwj.hotims.com/16584-17
18	SV Microwave, Inc.	3	561-840-1800	561-842-6277	http://mwj.hotims.com/16584-18
19	Teledyne Storm Products	9	630-754-3300	630-754-3500	http://mwj.hotims.com/16584-19
20	Tensolite	COV 3	800-458-9960	562-494-0955	http://mwj.hotims.com/16584-20
21	W.L. Gore & Associates, Inc.	33	800-445-GORE		http://mwj.hotims.com/16584-21
22	Winchester Electronics	27	203-741-5400	203-741-5500	http://mwj.hotims.com/16584-22

Sales Representatives

Carl Sheffres, Publisher

Ed Johnson, Associate Publisher

Ken Hernandez, Traffic Administrator

Eastern and Central Time Zones
Chuck Boyd
Northeast Reg. Sales Mgr.
(New England, Upstate NY, Eastern Canada)
685 Canton Street
Norwood, MA 02062
Tel: (781) 769-9750
FAX: (781) 769-5037
cboyd@mwjournal.com

Michael Hallman
Eastern Reg. Sales Mgr.
(Mid-Atlantic, Southeast, Midwest)
4 Valley View Court
Middletown, MD 21769
Tel: (301) 371-8830
FAX: (301) 371-8832
mhallman@mwjournal.com

Eastern and Central Time Zones
Ed Johnson
Associate Publisher
PO Box 5962
Ocala, FL 34478-5962
Tel: (352) 620-2442
FAX: (352) 620-2443
ejohnson@mwjournal.com

Pacific and Mountain Time Zones
Wynn Cook
Western Reg. Sales Mgr.
PO Box 23200
San Jose, CA 95153
Tel: (408) 224-9060
FAX: (408) 224-6106
wcook@mwjournal.com

International Sales
Richard Vaughan
International Sales Manager
46 Gillingham Street
London SW1V 1HH, England
Tel: +44 207 596 8742
FAX: +44 207 596 8749
rvaughan@horizonhouse.co.uk

Germany, Austria, and Switzerland (German-speaking)
Juergen Wissling
Wissling Marketing Services
Riedstrasse 5
72813 St. Johann-Wuertingen
Germany
Tel: +49 7122 828140
FAX: +49 7122 828145
jwissling@horizonhouse.com

Israel
Oreet Ben Yaacov
Oreet International Media
15 Kineret Street
51201 Bene-Berak, Israel
Tel: +972 3 570 6527
FAX: +972 3 570 6526
obenyaacov@horizonhouse.com

Korea
Young-Seoh Chinn
JES Media International
2nd Floor, ANA Bldg.
257-1, Myungil-Dong
Kangdong-Gu
Seoul, 134-070 Korea
Tel: +82 2 481-3411
FAX: +82 2 481-3414
yschinn@horizonhouse.com

Japan
Katsuhiro Ishii
Ace Media Service Inc.
12-6, 4-Chome,
Nishiiko, Adachi-Ku
Tokyo 121-0824, Japan
Tel: +81 3 5691 3335
FAX: +81 3 5691 3336
amskatsu@dream.com

Tensolite High Density Connectors & Assemblies

Tensolite High Density products offer numerous packaging options to optimize the ever increasing space constraints from DC to 65GHz. The **SMP** and **SSMP™** RF product lines are an excellent choice for high frequency, small form factor connectors and assemblies that provide superb isolation and performance. **HDSI®** products are ideal for low profile, micro-miniature, ribbonized, flexible assemblies that are easy to route in tight spaces. The **HDRFI™** product family of connectors and assemblies provides designers the ability to gang multiple RF contacts into a small area and reduce stubbing, especially in blind mate applications. Contact Tensolite for your high density interconnect solutions.

Visit http://mwj.hotims.com/16584-20 or use RS# 20 at www.mwjournal.com/info

RoHS COMPLIANT AVAILABLE

AS 9100 CERTIFIED

Tensolite® A Carlisle Company

For more information go to www.tensolite.com or email info@tensolite.com • Corporate HQ (800) 458-9960

HDRFI™, SSMP™ and HDSI® are trademarks of the Tensolite Company